

MPR-SAT-FE-68-4
JANUARY 25, 1969



SATURN

(NASA-TM-X-61773) RESULTS OF THE FIFTH
SATURN IB LAUNCH VEHICLE TEST FLIGHT AS-205
(APOLLO 7 MISSION) (NASA) 249 p

N90-71410

Unclas
00/15 031174+

RESULTS OF THE FIFTH SATURN IB
LAUNCH VEHICLE TEST FLIGHT

AS-205

(APOLLO 7 MISSION)

PREPARED BY
SATURN IB FLIGHT EVALUATION
WORKING GROUP



NATIONAL AERONAUTICS AND SPACE ADMINISTRATION



MPR-SAT-FE-68-4

RESULTS OF THE FIFTH SATURN IB LAUNCH VEHICLE TEST FLIGHT
AS-205

By

Saturn Flight Evaluation Working Group

George C. Marshall Space Flight Center

ABSTRACT

Saturn IB AS-205 was launched at 1102:45 EDT on October 11, 1968 from KSC Launch Complex 34, under favorable weather conditions. The vehicle lifted off on a launch azimuth of 100 deg east of north and rolled to a flight azimuth of 72 deg east of north. The actual trajectory was near nominal.

All major systems performed within design limits and close to predicted values throughout flight. No malfunctions or deviations occurred. However, a few refinements based on flight test results are being incorporated. These are discussed in detail in the body of the report.

The AS-205 test flight demonstrated successfully the performance of the orbital safing experiment which included propellant venting, LOX dump, cold helium dump, and stage/engine pneumatic supply dump. This flight also demonstrated the adequacy of the attitude control in both the manual and automatic modes and of vehicle systems to perform for extended duration in orbit.

Any questions or comments pertaining to the information contained in this report are invited, and should be directed to:

Director, George C. Marshall Space Flight Center
Marshall Space Flight Center, Alabama 35812
Attention: Chairman, Saturn Flight Evaluation Working Group
R-AERO-F (Phone 876-4575)

GEORGE C. MARSHALL SPACE FLIGHT CENTER

MPR-SAT-FE-68-4

RESULTS OF THE FIFTH SATURN IB LAUNCH VEHICLE TEST FLIGHT

AS-205

(APOLLO 7 MISSION)

SATURN IB FLIGHT EVALUATION
WORKING GROUP

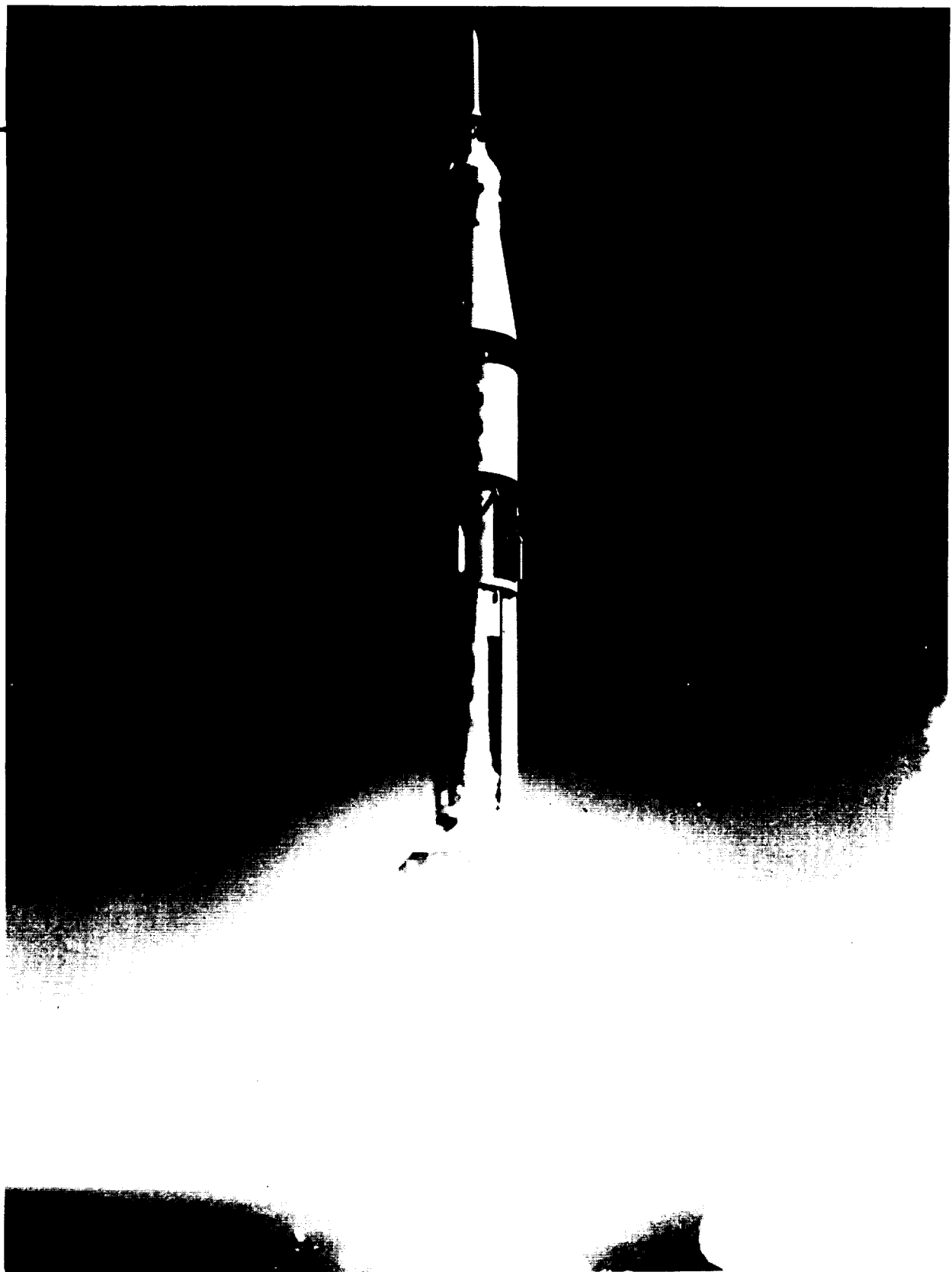


TABLE OF CONTENTS

	Page
1.0 Flight Test Summary	1
2.0 Introduction	4
3.0 Mission Description and Test Objectives	5
3.1 Mission Description	5
3.2 Primary Objectives	6
3.3 Launch Vehicle Mandatory Detailed Objectives	6
3.4 Launch Vehicle Principal Detailed Objectives	6
3.5 Launch Vehicle Secondary Detailed Test Objectives	7
3.6 Spacecraft Objectives	7
4.0 Times of Events	8
4.1 Summary	8
4.2 Sequence of Events	8
5.0 Launch Operations	17
5.1 Summary	17
5.2 Countdown	17
5.3 Propellant and Cold Helium Loading	18
5.3.1 RP-1 Loading	19
5.3.2 LOX Loading	20
5.3.3 LH ₂ Loading	20
5.3.4 Cold Helium Loading	20
5.3.5 Auxiliary Propulsion System Propellant Loading	20
5.3.6 S-IB Stage Propellant Load	21
5.3.7 S-IVB Stage Propellant Load	24
5.4 Holddown	24
6.0 Mass Characteristics	26
6.1 Summary	26
6.2 Mass Analysis	26
6.3 Center of Gravity and Moment of Inertia	27
7.0 Trajectory	39
7.1 Summary	39
7.2 Tracking Data Utilization	39
7.3 Trajectory Analysis	41

TABLE OF CONTENTS (CONT)

		Page
7.4	Orbital Tracking Data Utilization	48
7.5	Parking Orbit Trajectory	49
7.6	S-IVB Orbital Safing Experiment Trajectory	49
8.0	S-IB Propulsion	56
8.1	Summary	56
8.2	S-IB Propulsion Performance	56
	8.2.1 Stage Performance	56
	8.2.2 Individual Engine Characteristics	65
	8.2.3 LOX Seal Drain Line Temperatures	68
8.3	S-IB Propellant Usage	68
8.4	S-IB Pressurization Systems	70
	8.4.1 Fuel Pressurization System	70
	8.4.2 LOX Pressurization System	71
	8.4.3 Control Pressure System	74
9.0	S-IVB Propulsion and Associated Systems	75
9.1	Summary	75
9.2	S-IVB Propulsion Performance	75
	9.2.1 Engine Chillover	75
	9.2.2 Start Characteristics	77
	9.2.3 Mainstage Engine Analysis	78
	9.2.4 Cutoff Impulse	81
9.3	S-IVB Stage Propellant Utilization	81
	9.3.1 Propellant Mass Analysis	81
	9.3.2 PU Valve Response and Thrust Fluctuations	84
9.4	S-IVB Propellant Pressurization Systems	84
	9.4.1 Fuel Pressurization System	84
	9.4.2 LOX Pressurization System	91
9.5	S-IVB Pneumatic Systems	94
9.6	S-IVB Orbital Safing	98
	9.6.1 Safing Purpose and Events	98
	9.6.2 LH ₂ and LOX Tank Venting	98
	9.6.3 LOX Dump	102
	9.6.4 Cold Helium Dump	103
	9.6.5 Pneumatic Sphere	106
10.0	Auxiliary Propulsion System	109
10.1	Summary	109
10.2	APS Performance	109

TABLE OF CONTENTS (CONT)

	Page
10.2.1 Propellant and Pressurization Systems	109
10.2.2 APS Motor Performance	109
11.0 Hydraulic System	113
11.1 Summary	113
11.2 S-IB Hydraulic System	113
11.3 S-IVB Hydraulic System	114
12.0 Guidance and Control	115
12.1 Summary	115
12.2 System Changes and Modifications	115
12.3 Launch Vehicle Control	117
12.3.1 S-IB Stage Control Analysis	117
12.3.2 S-IVB Stage Control Analysis	119
12.3.3 Control During Orbital Coast	127
12.3.4 Control Component Analysis	133
12.4 Launch Vehicle Navigation and Guidance	133
12.4.1 Navigation and Guidance Scheme Performance Analysis	135
12.4.2 Navigation and Guidance Comparison	139
12.4.2.1 Powered Flight Comparison	139
12.4.2.2 Platform Measured Velocity Changes During Orbit	142
12.4.3 Guidance System Component Analysis	145
12.4.3.1 LVDC/LVDA Analysis	145
12.4.3.2 ST-124M Stabilized Platform Analysis	145
13.0 Separation	146
13.1 Summary	146
13.2 S-IB/S-IVB Separation	146
13.2.1 Separation Dynamics	146
13.3 LV/CSM Separation	146
14.0 Vehicle Electrical Systems	151
14.1 Summary	151
14.2 S-IB Stage Electrical System	151
14.3 S-IVB Stage Electrical System	153
14.4 Instrument Unit Electrical System	157

TABLE OF CONTENTS (CONT)

		Page
15.0	Range Safety and Command Systems Performance	161
15.1	Summary	161
15.2	Command Destruct Systems Performance	161
15.3	Instrument Unit Command System Performance	161
16.0	Emergency Detection System (EDS)	164
16.1	Summary	164
16.2	EDS Bus Voltage	164
16.3	EDS Event Times	164
16.4	Thrust OK Pressure Switches	164
16.5	EDS Rate Gyros	164
16.6	Q-Ball Differential Pressures	166
16.7	Launch Vehicle Attitude Reference Monitoring	166
17.0	Structures	167
17.1	Summary	167
17.2	Total Vehicle Loads and Moments	167
	17.2.1 Longitudinal Loads	167
	17.2.2 Bending Moments	169
	17.2.3 Body Bending Oscillations	169
17.3	S-IVB Stage Analysis	169
	17.3.1 J-2 Engine Vibrations	169
18.0	Pressure and Thermal Environment	176
18.1	Summary	176
18.2	Vehicle Pressure Environment	176
	18.2.1 S-IB Stage Base Pressures	176
	18.2.2 S-IVB Stage Internal Pressures	178
18.3	Vehicle Thermal Environment	178
	18.3.1 S-IB Stage Base Thermal Environment	178
	18.3.2 S-IVB Stage Thermal Environment	182
	18.3.3 Instrument Unit Temperatures	182
18.4	Instrument Unit Environmental Control System	182
	18.4.1 Thermal Conditioning Subsystem	187
	18.4.2 Gas Bearing Supply Subsystem	190
19.0	Aerodynamics	193
19.1	Summary	193

TABLE OF CONTENTS (CONT)

	Page
20.0 Instrumentation	194
20.1 Summary	194
20.2 Vehicle Measuring Analysis	194
20.2.1 S-IB Stage Measuring Analysis	194
20.2.2 S-IVB Stage Measuring Analysis	196
20.2.3 IU Measuring Analysis	196
20.3 Airborne Telemetry Systems	196
20.3.1 S-IB Stage	198
20.3.2 S-IVB Stage	198
20.3.3 Instrument Unit	198
20.4 RF Systems Analysis	198
20.4.1 Telemetry	200
20.4.2 Tracking	200
20.5 Optical Tracking	203
21.0 Spacecraft	204
Appendix A Configuration Differences	205
A.1 Summary	205
A.2 S-IB-5 Configuration Differences	205
A.3 S-IVB-205 Configuration Differences	207
A.4 S-IU-205 Configuration Differences	210
A.5 Payload	212
Appendix B Atmospheric Summary	215
B.1 Introduction	215
B.2 General Atmospheric Conditions at Launch Time	215
B.3 Surface Observations	215
B.4 Upper Air Measurements	215
B.5 Thermodynamic Data	219
References	
Approval	
Distribution	

LIST OF FIGURES

Figure		Page
5-1	Fuel Temperature/Density Relationship	22
6-1	Vehicle Mass, Center of Gravity, and Mass Moment of Inertia During S-IB Powered Flight	35
6-2	Vehicle Mass, Center of Gravity, and Mass Moment of Inertia During S-IVB Powered Flight	38
7-1	S-IB and S-IVB Trajectory	42
7-2	Earth-Fixed Velocity	43
7-3	Total Inertial Acceleration	45
7-4	Mach Number and Dynamic Pressure	47
7-5	AS-205 Ground Track	54
8-1	S-IB Individual Engine and Stage Thrust Buildup	59
8-2	S-IB Stage Longitudinal Thrust and Specific Impulse	60
8-3	S-IB Stage Propellant Mixture Ratio and Flowrate	62
8-4	S-IB Stage LOX and Fuel Flowrates	63
8-5	Deviation in Engine Performance Parameters	66
8-6	Fuel Tank Ullage and Helium Sphere Pressure	72
8-7	LOX Pressurization System Characteristics	73
9-1	J-2 Engine Temperature	76
9-2	S-IVB Steady State Operation	79
9-3	S-IVB Cutoff Transient	82
9-4	Second Flight Stage Best Estimate Masses	85
9-5	S-IVB-205 PU Valve Position History	87
9-6	LH ₂ and LOX Sensor Nonlinearity (Volumetric Method)	88
9-7	LH ₂ Tank Pressurization System Performance	89
9-8	LH ₂ and LOX Inlet Start Requirements	92
9-9	LOX Tank Pressurization System Performance	93
9-10	Stage Pneumatic Control and Purge System Performance	96
9-11	Engine Start Sphere Performance	97
9-12	LH ₂ and LOX Tank Ullage Performance in Orbit	101
9-13	LOX Dump Performance	104
9-14	Cold Helium Dump Performance	105
9-15	S-IVB Stage and Engine Pneumatic Supply Pressures	107
10-1	APS Propellant Remaining and Temperature	110
12-1	S-IB Stage Command Angles	120
12-2	Wind Velocity and Free Stream Angle-of-Attack	121
12-3	Pitch Control Parameters During S-IB Powered Flight	122
12-4	Pitch Attitude Control During S-IVB Powered Flight	123
12-5	Sloshing During Powered Flight	126
12-6	Pitch Attitude Control During S-IVB Alignment With Local Horizontal	128

LIST OF FIGURES (CONT)

Figure		Page
12-7	Pitch Attitude Control During LOX Dump	129
12-8	Command Angles and Vehicle Attitude During Manual Maneuvers	130
12-9	Pitch Attitude Control During S-IVB/CSM Separation	131
12-10	Command Angles and Vehicle Attitude During Navigation Update	132
12-11	Quasi-Steady-State Surface Wind Speed Envelope for Cape Kennedy	136
12-12	Liftoff Geometry LC-34	137
12-13	AS-205 Trajectory Profile and Plan Views, Liftoff through 35 Seconds of Flight	138
12-14	Guidance Platform Velocity Differences (Trajectory Minus Measured)	140
12-15	Velocity Change Due to Propulsive Vent and Passivation	144
13-1	S-IB/S-IVB Longitudinal Acceleration	147
13-2	Angular Velocities During S-IB/S-IVB Separation	148
13-3	CSM-S-IVB/IU Separation Parameters	150
14-1	S-IB Battery Current and Voltage	152
14-2	S-IVB Battery Current and Voltage-Launch Phase	155
14-3	S-IVB Battery Current and Voltage-Orbit	156
14-4	6D10 and 6D20 Battery Currents and Voltages	159
14-5	6D30 and 6D40 Battery Currents and Voltages	160
17-1	Vehicle Longitudinal Force Distribution	168
17-2	Longitudinal Load (From Strain Data at Station 23.9 m)	170
17-3	Vehicle Resultant Bending Moment	171
17-4	Vehicle Bending Modes	172
17-5	Vehicle Bending Amplitudes	173
17-6	J-2 Engine Vibration Composite Levels	175
18-1	S-IB Stage Heat Shield Loading	177
18-2	S-IB Stage Base Pressures	179
18-3	Heat Shield Inner Region Total and Radiation Heating Rates	180
18-4	Heat Shield Temperatures	181
18-5	Flame Shield Total and Radiation Heating Rates	183
18-6	ST-124 M-3 Internal Gimbal Temperature	184
18-7	LVDC Temperature	185
18-8	Component Temperatures	186
18-9	Thermal Conditioning System Performance	188
18-10	Sublimator Performance During Ascent	189

LIST OF FIGURES (CONT)

Figure		Page
18-11	ST-124 M-3 Gas Bearing GN ₂ Inlet Pressure Differential	191
20-1	AS-205 RF System Coverage	199
20-2	Orbital Telemetry Coverage	201
20-3	Orbital Radar Coverage	202
A-1	AS-205 Configuration	206
A-2	Payload	214
B-1	Scalar Wind Speed at Launch Time of AS-205	217
B-2	Wind Direction at Launch Time of AS-205	218
B-3	Pitch Wind Speed Component (W_X) at Launch Time of AS-205	220
B-4	Yaw Wind Speed Component at Launch Time of AS-205	221
B-5	Pitch (S_X) and Yaw (S_Z) Component Wind Shears	222
B-6	Relative Deviation of Temperature and Density From PAFB (63) Reference Atmosphere, AS-205	223
B-7	Relative Deviation of Pressure and Absolute Deviation of the Index of Refraction From PAFB (63) Reference Atmosphere, AS-205	223

LIST OF TABLES

Table		Page
4-I	AS-205 Event Times Summary	9
4-II	AS-205 Sequence of Events	10
5-I	AS-205 S-IB Stage Propellant Weight at Ignition Command	23
5-II	AS-205 S-IVB Stage Propellant Weight at Ignition Command	25
6-I	Flight Sequence Mass Summary	29
6-II	Vehicle Masses	30
6-III	Mass Characteristics Comparison	36
7-I	Powered Flight Data Availability	40
7-II	Cutoff Conditions	44
7-III	Significant Events	46
7-IV	Thrust Decay Velocity Gain	41
7-V	Insertion Conditions Data Utilization	50
7-VI	Summary of C-Band Orbital Tracking	51
7-VII	S-IVB Insertion Parameters	52
7-VIII	S-IVB/CSM Separation Parameters	53
7-IX	Effects of S-IVB Orbital Safing Experiments	55
8-I	Engine Start Characteristics	57
8-II	Stage Performance Parameters	61
8-III	Inflight Performance Deviation Analysis	64
8-IV	AS-205 Average Individual Engine Performance at 30 seconds	67
8-V	Propellant Usage	69
8-VI	Cutoff Probe Activation Characteristics	70
9-I	Start Transient Performance	77
9-II	S-IVB Propulsion System Performance	80
9-III	S-IVB Cutoff Transient Performance	83
9-IV	S-IVB Propellant Mass Summary	86
9-V	GH ₂ Pressurant Flowrate	90
9-VI	LOX Tank Pressurization Data Summary	94
9-VII	GH ₂ Start Bottle Parameters	95
9-VIII	Engine Control Sphere Parameters	98
9-IX	Orbital Safing Event Summary	99
9-X	Cold Helium Bottle Parameters	103
9-XI	Stage Pneumatic Sphere Parameters	106
10-I	AS-205 APS Propellant Usage	111
12-I	S-IB Maximum Control Parameters and Separation Parameters	118
12-II	Maximum Values of Critical Flight Control Parameters	125

LIST OF TABLES (CONT)

Table		Page
12-III	APS Impulse Summary	134
12-IV	Guidance Inertial Platform Velocity Comparison	141
12-V	Navigation Comparison	143
13-I	Separation Events	149
14-I	S-IB Battery Performance	153
14-II	S-IVB Battery Performance	154
14-III	IU Battery Conditions at 19.0 Hours of Flight	158
15-I	DCS Command History	162
16-I	EDS/Switch Selector Events	165
16-II	EDS Discrete Events	165
17-I	S-IVB Vibration Summary	174
20-I	Measuring Malfunctions	195
20-II	Launch Vehicle Telemetry System Description	197
B- I	Surface Observations at AS-205 Launch Time	216
B- II	Systems Used to Measure Upper Air Wind Data	216
B- III	Maximum Wind Speed in High Dynamic Pressure Region	224
B- IV	Extreme Wind Shear Values in the High Dynamic Pressure Region	226
B- V	Selected Atmospheric Observations	228

ABBREVIATIONS

Abbreviation

ABS	Air Bearing Supply System
AS	Apollo-Saturn
AGC	Automatic Gain Control
APS	Auxiliary Propulsion System
CG	Center-of-Gravity
CIF	Central Information Facility
CM	Command Module
CSM	Command Service Module
CSP	Control Signal Processor
DOM	Data Output Multiplexer
DDAS	Digital Data Acquisition System
ETR	Eastern Test Range
EDS	Emergency Detection System
EMR	Engine Mixture Ratio
ESC	Engine Start Command
ECS	Environmental Control System
ETW	Error Time Words
EBW	Exploding Bridge Wire
GFCV	GOX Flow Control Valve
GBI	Grand Bahama Island
GTI	Grand Turk Island
GSE	Ground Support Equipment
GRR	Guidance Reference Release
IECO	Inboard Engine Cutoff
IGM	Iterative Guidance Mode
LC	Launch Complex
LES	Launch Escape System
LET	Launch Escape Tower
LVDA	Launch Vehicle Data Adapter
LVDC	Launch Vehicle Digital Computer
MOV	Main Oxidizer Valve
MILA	Merritt Island Launch Area
NPSP	Net Positive Suction Pressure
OECO	Outboard Engine Cutoff
PTCS	Propellant Tanking Computer System
PU	Propellant Utilization
PCM	Pulse Code Modulation
RCS	Reaction Control System
RMS	Root Mean Square
SSB	Single Side Band
SLA	Spacecraft LEM Adapter
SMC	Steering Misalignment Correction Term
SS	Switch Selector
TM	Telemetry
F/M	Thrust/Mass

CONVERSION FACTORS TO
INTERNATIONAL SYSTEM OF UNITS OF 1960

Parameter	Multiply	By	To Obtain
acceleration	ft/s ²	3.048x10 ⁻¹ (exact)	m/s ²
area	in ²	6.4516x10 ⁻⁴ (exact)	m ²
barometer pressure	mb	1.00x10 ⁻² (exact)	N/cm ²
density	lbm/ft ³	1.6018463x10 ¹	kg/m ³
energy	Btu	1.0543503x10 ³ (thermal chem.)	watt-s
flow Rate	mass	lb s/ft	4.5359237x10 ⁻¹ (exact)
	volume	gpm	6.30901064x10 ⁻⁵
force	lb	4.448221615	N (Newton)
heating rate	Btu/ft ² -s	1.1348931 (thermal chemical)	watt/cm ²
impulse	lb-s	4.448221615	N-s
length	ft	3.048x10 ⁻¹ (exact)	m
	in	2.54x10 ⁻² (exact)	m
mass	lb s ² /ft	4.5359237x10 ⁻¹ (exact)	kg
moment	lb-ft	1.355817948	N-m
	lb-in	1.12984829x10 ⁻¹	N-m
moment of inertia	lb-ft-s ²	1.355817948	kg-m ²
power	Btu/hr	2.9287508x10 ⁻⁴	kw
pressure	lb/in ²	6.894757293x10 ⁻¹	N/cm ²
	lb/ft ²	4.788025898x10 ⁻³	N/cm ²
specific weight	lb/ft ³	1.57087468x10 ²	N/m ³
temperature	°F+459.67	5.55555556x10 ⁻¹	°K
	°C+273.15	1.00	°K
velocity	ft/s	3.048x10 ⁻¹ (exact)	m/s
	knot*	5.144444444x10 ⁻¹	m/s
volume	ft ³	2.8316846592x10 ⁻² (exact)	m ³
	gallon **	3.785411784x10 ⁻³ (exact)	m ³

Note: $g_0 = 9.80665 \text{ m/s}^2$ (exact)

* knot (International)

** gallon (U.S. Liquid)

MPR-SAT-FE-68-4

1.0 FLIGHT TEST SUMMARY

Saturn IB Space Vehicle AS-205, fifth of a series of Saturn IB vehicles, was launched at 1102:45 EDT on October 11, 1968, and placed the CSM 101 spacecraft in earth orbit. This flight test was the first in a series of Saturn IB operational vehicles and the first Saturn IB vehicle to be manned. The primary objectives of the AS-205 mission were to demonstrate CSM/crew performance, demonstrate crew/space-vehicle/mission support facilities performance during manned CSM missions, and demonstrate CSM rendezvous capability. Other important objectives were to demonstrate orbital operation of the attitude control system, demonstrate S-IVB orbital safing capability, evaluate ASI line modification, evaluate S-IVB/IU system lifetime capabilities, and demonstrate CSM manned launch vehicle orbital attitude control.

AS-205 was launched from Launch Complex 34 at Cape Kennedy, Florida, on a launch azimuth of 100 degrees east of north. After launch, the vehicle rolled into a flight azimuth of 72 degrees east of north as programmed.

The actual trajectory of AS-205 was very close to nominal. The total space-fixed velocity was 3.4 m/s lower than nominal at S-IB outboard engine cutoff and 0.4 m/s lower than nominal at S-IVB cutoff. At S-IVB guidance cutoff, the altitude was 0.2 km lower than nominal and the surface range was 1.1 km greater than nominal.

The S-IVB /IU/CSM was inserted into orbit at 626.75 sec, 1.95 sec later than nominal. The apogee altitude was 4.6 km higher than nominal and the perigee altitude was 0.2 km higher than nominal. At S-IVB/CSM-101 separation, the total space-fixed velocity was 7.6 m/s lower than nominal.

The S-IB stage propulsion system performed satisfactorily throughout flight. The stage thrust, mass loss rate, and specific impulse were 0.06%, 0.06%, and 0.002% higher than predicted, respectively. Inboard engine cutoff occurred 0.36 sec later than predicted, and outboard engine cutoff occurred 1.04 sec later than predicted, or 3.68 sec following inboard engine cutoff. Outboard engine cutoff resulted from LOX starvation as predicted.

The S-IVB stage propulsion system performance was satisfactory throughout flight. On the basis of flight simulation, the average thrust, mass loss rate, and specific impulse were 0.14% higher, 0.11% lower, and 0.24% higher than predicted, respectively. The propellant utilization system (PU) operated in open loop configuration and provided an average propellant mixture ratio of 5.5 to 1 during high thrust and 4.45 to 1 during low thrust. The PU valve was commanded to the low thrust position at 455.77 seconds.

All portions of the orbital safing operation were performed successfully. In order to adequately safe the LH₂ tank, four additional commanded vents were required to supplement the programmed vent sequence.

The Auxiliary Propulsion System (APS) functioned properly to provide roll control during S-IVB powered flight and pitch, yaw, and roll control following S-IVB cutoff. Modules I and II lifetimes were in excess of 15 hours and 30 minutes.

The performance of the guidance and control systems was excellent. Because the uprange surface winds imparted a negative range velocity to the vehicle, causing a delay in the velocity accumulation, the range accelerometer exhibited five consecutive zero-changes at approximately 15 to 18 sec after liftoff, causing the use of one prestored backup acceleration value. The resulting range velocity error was 0.1 m/s. The range accelerometer reading accurately reflected vehicle acceleration. The boost navigation and guidance scheme was executed properly, and terminal parameters were well within acceptable limits. All orbital operations were nominal.

The control system functioned properly. The maximum values observed for the control parameters, near the maximum dynamic pressure regions, were attitude errors of 1.7 deg in pitch, -0.7 deg in yaw, and -0.4 deg in roll; and angle-of-attack of -1.2 deg in pitch and 1.1 deg in yaw. Control system transients were all within the capability of the system. The vehicle commands and response during astronaut manual control correlated well with the scheduled timelines and expected vehicle response.

S-IB/S-IVB separation was accomplished as planned. The longitudinal acceleration traces indicated that the retro rockets provided more thrust than experienced on AS-204.

LV/CSM separation occurred at 10502.4 sec by command from the spacecraft. The separation was accomplished as planned.

The electrical systems on AS-205 operated satisfactorily during the entire flight. Battery lifetimes for the S-IVB stage and IU more than met the mission requirements.

The Digital Command System (DCS) performed satisfactorily. Of the 24 commands sent, two commands from Carnarvon and one from Hawaii were not issued properly to obtain the desired DCS response. No commands transmitted during flight were rejected because of onboard equipment malfunction.

The Emergency Detection System (EDS) was flown with the manual abort loop closed since this was a manned flight. The system functioned properly. All abort parameters remained well below abort limits.

Structural analysis of AS-205 indicates that all structural components performed satisfactorily. There were no structural loads of sufficiently high magnitude to threaten the structural integrity of the launch vehicle.

The mission profile for the AS-205 flight was such that the structural and component thermal environment was well within the design requirements. The S-IB stage base indicated a slightly more severe environment than observed previously. The environmental control system maintained acceptable operating conditions for components mounted in the IU and S-IVB forward skirt. The Gas Bearing Supply System performed satisfactorily, maintaining the proper regulated pressure and temperature to the ST-124M-3 inertial platform assembly.

The measurement evaluation on AS-205 revealed that 99.42% of the 691 measurements, active at liftoff, performed satisfactorily. A total of 4 measurements failed during flight. Performance of the telemetry and RF systems was satisfactory.

Camera coverage was excellent. The reliability based on 94 engineering sequential cameras was 95.74 percent.

2.0 INTRODUCTION

This report presents the results of the engineering evaluation of AS-205, the fifth Saturn IB vehicle flight-tested. The evaluation is centered on the performance of the major vehicle systems, with special emphasis on deviations from nominal.

This report is published by the Saturn Flight Evaluation Working Group - composed of representatives of Marshall Space Flight Center, John F. Kennedy Space Center, and MSFC's prime contractors - and in cooperation with the Manned Spacecraft Center. Contributions to the evaluation have been made by:

George C. Marshall Space Flight Center

Research and Development Operations

Aero-Astrodynamics Laboratory

Astrionics Laboratory

Computation Laboratory

Propulsion and Vehicle Engineering Laboratory

Industrial Operations

John F. Kennedy Space Center

Manned Spacecraft Center

Chrysler Corporation Space Division

McDonnell Douglas Astronautics Corporation

International Business Machines Corporation

Rocketdyne Division of North American Rockwell

The official MSFC position is represented by this report. This report will not be updated unless continued analysis or new evidence warrants additional revisions. Final stage evaluation reports will, however, be published by the stage contractors.

3.0 MISSION DESCRIPTION AND TEST OBJECTIVES

3.1 MISSION DESCRIPTION

The AS-205 mission was the first manned mission of the Apollo/Saturn IB series. The planned duration of space flight was 10 days, 18 hours and 59 minutes. The space vehicle was launched from Complex 34 at Cape Kennedy, Florida. The vehicle was launched on an azimuth of 100° east of north. After approximately 10 seconds of flight, the S-IB began a pitch and roll program designed to achieve a flight azimuth of 72° east of north. The first stage provided continuous thrust for 140.64 seconds, when the inboard engines were cut off. The four outboard engines cut off 3.68 seconds following the inboard engines.

The S-IB stage separated from the S-IVB/IU/CSM at approximately 146 seconds. This was followed by ignition of the S-IVB stage at approximately 147 seconds; jettisoning of the ullage motors at approximately 158 seconds; jettisoning of the launch escape tower at approximately 167 seconds; and guidance initiation at approximately 171 seconds.

The S-IVB stage was flown at a nominal mixture ratio of 5.5 to 1 until approximately 456 seconds, when it was commanded to shift to a 4.45 to 1 mixture ratio. The S-IVB continued in this flight mode until commanded to cut off by the guidance computers, when the vehicle had reached the proper conditions for orbital insertion.

At S-IVB guidance cutoff command, plus 10 seconds, the vehicle was inserted into an earth parking orbit of approximately 222 by 282 km. Shortly after insertion, the S-IVB attitude control system executed maneuvers to place the longitudinal axis of the vehicle along the velocity vector and, subsequently, maintained the attitude in an orbital rate mode.

At 1 hour: 34 min and 29 sec after liftoff over the U. S., the IU automatically initiated the S-IVB orbital safing sequence which dumped the liquid oxygen through the J-2 engine, LH₂ was vented through the LH₂ tank vent system. Venting of the cold helium spheres was initiated at 1 hour: 42 min: 29 sec, terminated at 2 hours: 30 min: 17 sec, reinitiated at 4 hours: 30 min: 17 sec, and completed at 4 hours: 5 min: 17 sec. The S-IVB stage control sphere helium dump was initiated at 3 hours: 17 min: 34 sec. This dump was terminated approximately 2,000 seconds early, at 4 hours: 7 min: 2 sec to maintain helium for subsequent unprogrammed LH₂ tank vent valve operations. This procedure ensured a safe S-IVB stage for CSM simulated transposition and docking and for rendezvous, which occurred approximately one day later.

Approximately two and one-half hours after liftoff, over Carnarvon, the crew exercised the manual S-IVB/IU orbital attitude control capability. This consisted of a three minute test of the closed loop spacecraft/launch vehicle control system by performing manual pitch, yaw, and roll maneuvers. After completion of the test, the crew switched attitude control back to the automatic launch vehicle system which resumed with the normal attitude timeline.

Approximately two hours and 55 minutes after liftoff, spacecraft separation occurred over Hawaii by a manual signal given by the crew. The crew performed simulated transposition and docking maneuver with the spacecraft and took pictures of the SLA panels in the deployed position.

The next major event involving the launch vehicle occurred at approximately 26 hours and 25 minutes after liftoff, when the crew initiated a rendezvous with the S-IVB/IU. The rendezvous required approximately 3 hours and 14 minutes and was completed at 29 hours and 39 minutes after liftoff. This simulated a LM rescue capability by the CSM. At this time the S-IVB/IU was tumbling.

3.2 PRIMARY OBJECTIVES

All primary test objectives were achieved and are as follows:

1. Demonstrate CSM/crew performance.
2. Demonstrate crew/space-vehicle/mission support facilities performance during manned CSM mission.
3. Demonstrate CSM rendezvous capability.

3.3 LAUNCH VEHICLE MANDATORY DETAILED OBJECTIVES

There were no launch vehicle mandatory detailed objectives on AS-205.

3.4 LAUNCH VEHICLE PRINCIPLE DETAILED OBJECTIVES

1. Demonstrate the adequacy of the launch vehicle attitude control system for orbital operation.
2. Demonstrate S-IVB orbital safing capability.
3. Evaluate S-IVB J-2 engine ASI line modification.

3.5 LAUNCH VEHICLE SECONDARY DETAILED TEST OBJECTIVES

1. Evaluate the S-IVB/IU orbital coast lifetime capability.
2. Demonstrate CSM manned launch vehicle orbital attitude control.

3.6 SPACECRAFT OBJECTIVES

The spacecraft detailed mission objectives are presented in the Mission Requirements "C" Type Mission CSM Operations.

4.0 TIMES OF EVENTS

4.1 SUMMARY

Table 4-I presents a summary of event times, obtained from the performance analysis of launch vehicle AS-205. Event times generally were quite close to predicted.

4.2 SEQUENCE OF EVENTS

Range zero was 1502:45 UT and liftoff occurred 0.36 sec later or at 1502:45.36 UT. Guidance Reference Release (GRR) would be expected at -4.83 sec range time (time from range zero). Guidance Reference Release actually occurred at -4.97 seconds. First motion of the vehicle occurred at 0.17 sec range time.

Switch selectors in the S-IB stage, S-IVB stage, and Instrument Unit provided programmed event sequencing for the vehicle. The Launch Vehicle Digital Computer (LVDC) provided programmed input to the appropriate switch selector. If a switch selector malfunction had occurred, a complement address would have been sent to the switch selector, thereby providing redundancy. The analysis indicated that no output resulted from complement addresses to the switch selector; hence, the operation was normal.

Table 4-II lists the switch selector event times. The nominal time bases in range time were established as follows:

Liftoff (Time Base 1) = 0.36 sec

Start of Time Base 2 = 137.49 sec

Outboard Engine Cutoff (Time Base 3) = 144.32 sec

Start of Time Base 4 = 617.00

AS-205 EVENT TIMES SUMMARY

Event	Range Time (sec)	
	Actual	Act-Pred
First Motion	0.17	-
Liftoff	0.36	-
Start Pitch	10.31	-0.05
Start Roll	10.31	-0.05
End Roll	38.46	0.10
Enable Engines EDS Cutoff	40.32	-0.04
Stop Pitch	134.26	-0.40
Low Level Sense (LLS)	137.49	0.41
IECO	140.64	0.36
OECO	144.32	1.04
S-IB/S-IVB Separation	145.58	1.00
S-IVB Start Command	146.97	0.99
Ullage Rockets Jettison	157.58	1.00
Launch Escape Tower Jettison	166.54	3.26
Start IGM	170.93	2.65
Engine Mixture Ratio Change Detected	455.77	1.01
S-IVB Cutoff (Guidance Signal)	616.75	1.95
Initiate LOX Dump	5668.95	1.95
Initiate Cold Helium Dump	6148.95	1.95
Completion of LOX Dump	6389.95	1.95
Termination of Cold Helium Dump	9016.95	1.95
CSM Separation	10502.40	7.23
Start Stage Control Sphere Helium Dump	11853.95	1.95
Restart Cold Helium Dump	16216.96	1.96
Completion of Stage Control Sphere Helium Dump	14821.27	-2061.03
Completion of Cold Helium Dump	17416.95	1.95

TABLE 4-II
AS-205 SEQUENCE OF EVENTS

FUNCTION	STAGE	TIME FROM BASE (SEC)		RANGE TIME (SEC)	
		ACTUAL	PREDICTED	ACTUAL	PREDICTED
Guidance Reference Release (GRR)	*	-5.33	-5.20	-4.97	--
Initiated S-IB Mainstage Ignition Sequence	*	-3.35	-3.30	-2.99	--
First Motion	*	-0.19	-0.20	0.17	--
Liftoff - Start of Time Base #1 (T ₁) (IU Umb. Disc.)		--	0.0	0.36	--
Sensor Bias On	IU	4.95	5.0	5.31	5.36
Multiple Engine Cutoff Enable	S-IB	9.95	10.0	10.31	10.36
Initiate Pitch Maneuver	*	9.95	10.0	10.31	10.36
Initiate Roll Maneuver	*	9.95	10.0	10.31	10.36
Telemeter Calibration On	S-IB	19.96	20.0	20.32	20.36
Telemeter Calibration Off	S-IB	24.96	25.0	25.32	25.36
Telemetry Calibrator In-Flight Calibrate On	IU	26.96	27.0	27.32	27.36
LOX Tank Relief Control Valve Enable	S-IB	29.75	29.8	30.11	30.16
Telemetry Calibrator In-Flight Calibrate Off	IU	31.96	32.0	32.32	32.36
End Roll	*	38.10	38.0	38.46	38.36
Launch Vehicle Engines EDS Cutoff Enable	IU	39.96	40.0	40.32	40.36
Maximum Dynamic Pressure (Max Q)	*	75.14	74.80	75.50	75.16
Cooling System Electrical Assembly Power Off	IU	74.95	75.0	75.31	75.36
Telemetry Calibrator In-Flight Calibrator On	IU	90.45	90.2	90.51	90.56
Telemetry Calibrator In-Flight Calibrate Off	IU	95.15	95.2	95.51	95.56
Flight Control Computer Switch Point No. 1	IU	99.96	100.0	100.32	100.36
Flight Control Computer Switch Point No. 2	IU	100.15	100.2	100.51	100.56
Telemeter Calibration On	S-IB	119.75	119.8	120.11	120.16
Flight Control Computer Switch Point No. 3	IU	119.95	120.0	120.31	120.36
IU Control Accelerometer Power Off	IU	120.17	120.2	120.53	120.56
Telemeter Calibration Off	S-IB	124.75	124.8	125.11	125.16
TM Calibrate On	S-IVB	127.66	127.7	128.02	128.06
TM Calibrate Off	S-IVB	128.65	128.7	129.01	129.06
Excessive Rate (P, Y, R) Auto-Abort Inhibit Enable	IU	132.55	132.6	132.91	132.96
Excessive Rate (P, Y, R) Auto-Abort Inhibit and Switch Rate Gyros SC Indication "A"	IU	132.75	132.8	133.11	133.16
S-IB Two Engines Out Auto-Abort Inhibit Enable	IU	132.97	133.0	133.33	133.36
S-IB Two Engines Out Auto-Abort Inhibit	IU	133.15	133.2	133.51	133.56
Propellant Level Sensors Enable	S-IB	133.65	133.7	134.01	134.06
Tilt Arrest	*	133.90	134.3	134.26	134.66

*Not Switch Selector Event

TABLE 4-II (CONT)

FUNCTION	STAGE	TIME FROM BASE (SEC)		RANGE TIME (SEC)	
		ACTUAL	PREDICTED	ACTUAL	PREDICTED
<u>S-IB Propellant Level Sensor Actuation - Time Base #2 (T₂)</u>	S-IB	--	0.0	137.49	137.08
Excess Rate (Roll) Auto-Abort Inhibit Enable	IU	0.15	0.2	137.64	137.28
Excess Rate (Roll) Auto-Abort Inhibit and Switch Rate Gyros SC Indication "B"	IU	0.37	0.4	137.86	137.48
Inboard Engines Cutoff	S-IB	3.15	3.2	140.64	140.28
Auto-Abort Enable Relays Reset	IU	3.37	3.4	140.86	140.48
Charge Ullage Ignition EBW Firing Units	S-IVB	3.55	3.6	141.04	140.68
Q-Ball Power Off	IU	3.96	4.0	141.45	141.08
Prevalves Open	S-IVB	4.46	4.5	141.95	141.58
LOX Depletion Cutoff Enable	S-IB	4.65	4.7	142.14	141.78
Fuel Depletion Cutoff Enable	S-IB	5.67	5.7	143.16	142.78
<u>S-IB Outboard Engines Cutoff Signal - Time Base #3 (T₃)</u>	S-IB	--	0.0	144.32	143.28
LOX Tank Flight Pressurization Switch Enable	S-IVB	0.17	0.2	144.49	143.48
Engine Cutoff Signal Off	S-IVB	0.35	0.4	144.67	143.68
Ullage Rockets Ignition	S-IVB	1.05	1.1	145.37	144.38
S-IB/S-IVB Separation On	S-IB	1.26	1.3	145.58	144.58
Flight Control Computer S-IVB Burn Mode On "A"	IU	1.45	1.5	145.77	144.78
Flight Control Computer S-IVB Burn Mode On "B"	IU	**1.65	1.7	**145.97	144.98
Engine Ready Bypass On	S-IVB	**1.85	1.9	**146.17	145.18
LH ₂ Chilldown Pump Off	S-IVB	**2.05	2.1	**146.37	145.38
LOX Chilldown Pump Off	S-IVB	2.26	2.3	146.58	145.58
S-IVB Engine Out Indication "A" Enable	IU	2.35	2.4	146.67	145.68
S-IVB Engine Out Indication "B" Enable	IU	2.56	2.6	146.88	145.88
Engine Ignition Sequence Start	S-IVB	**2.65	2.7	**146.97	145.98
Engine Ignition Sequence Start Relay Reset	S-IVB	**3.15	3.2	**147.47	146.48
Fuel Injection Temperature OK Bypass	S-IVB	**3.65	3.7	**147.97	146.98
Ullage Burn Out	*		5.05		148.33
LH ₂ Tank Pressurization Control Switch Enable	S-IVB	5.25	5.3	149.57	148.58
90% J-2 Thrust Level	*	5.88	6.3	150.20	149.58
P. U. Mixture Ratio 5.5 On	S-IVB	8.65	8.7	152.97	151.98
Charge Ullage Jettison EBW Firing Units	S-IVB	10.15	10.2	154.47	153.48
Ullage Rockets Jettison	S-IVB	13.26	13.3	157.58	156.58
Fuel Injection Temperature OK Bypass Reset	S-IVB	13.65	13.7	157.97	156.98

*Not Switch Selector Event

**Data Dropout, Computed Values Used

TABLE 4-II (CONT)

FUNCTION	STAGE	TIME FROM BASE (SEC)		RANGE TIME (SEC)	
		ACTUAL	PREDICTED	ACTUAL	PREDICTED
Ullage EBW Firing Units Charge Relays Reset	S-IVB	19.25	19.3	163.57	162.58
Ullage Rockets Ignition and Jettison Relays Reset	S-IVB	19.45	19.5	163.77	162.78
Jettison Launch Escape Tower	*	22.22	20.0	166.54	163.28
Heat Exchanger Bypass Value Enable On	S-IVB	23.95	24.0	168.27	167.28
Command Active Guidance Initiation	*	26.61	25.0	170.93	168.28
Telemetry Calibrator In-Flight Calibrate On	IU	25.35	25.4	169.67	168.68
Telemetry Calibrator In-Flight Calibrate Off	IU	30.35	30.4	174.67	173.68
Water Coolant Valve Open	IU	36.95	37.0	181.27	180.28
Flight Control Computer Switch Point No. 4	IU	41.95	42.0	186.27	185.28
Flight Control Computer Switch Point No. 5	IU	203.65	203.7	347.97	346.98
Telemetry Calibrator In-Flight Calibrate On	IU	205.37	205.4	349.69	348.68
Telemetry Calibrator In-Flight Calibrate Off	IU	210.35	210.4	354.67	353.68
LH ₂ Tank Pressurization Control Switch Disable	S-IVB	302.85	302.9	447.17	446.18
P. U. Mixture Ratio 5.5 Off	S-IVB	311.26	311.3	455.58	454.58
P. U. Mixture Ratio 4.5 On	S-IVB	311.45	311.5	455.77	454.78
Telemetry Calibrator In-Flight Calibrate On	IU	355.35	355.4	499.67	498.68
Telemetry Calibrator In-Flight Calibrate Off	IU	360.37	360.4	504.69	503.68
Guidance Cutoff Signal	*	472.43	471.52	616.75	614.80
Propellant Depletion Cutoff Arm	S-IVB		471.6		614.88
<u>Start of Time Base #4 (T₄)</u>	S-IVB	--	0.0	617.00	615.00
LH ₂ Tank Vent Valve Open	S-IVB	0.37	0.4	617.37	615.40
Passivation "B" Enable	S-IVB	0.47	0.5	617.47	615.50
LH ₂ Tank Passivation Valve Open Enable	S-IVB	0.56	0.6	617.56	615.60
LOX Tank Flight Pressurization Shutoff Valves Close	S-IVB	0.77	0.8	617.77	615.80
Passivation "A" Enable	S-IVB	0.95	1.0	617.95	616.00
LOX Tank Flight Pressurization Switch Disable	S-IVB	1.15	1.2	618.15	616.20
Propellant Depletion Cutoff Disarm	S-IVB	1.75	1.8	618.75	616.80
P. U. Mixture Ratio 4.5 Off	S-IVB	2.15	2.2	619.15	617.20
LH ₂ Tank Passivation Valve Open Disable	S-IVB	2.65	2.7	619.65	617.70
Flight Control Computer S-IVB Burn Mode Off "A"	IU	3.45	3.5	620.45	618.50
Flight Control Computer S-IVB Burn Mode Off "B"	IU	3.66	3.7	620.66	618.70
Auxiliary Hydraulic Pump Flight Mode Off	S-IVB	3.87	3.9	620.87	618.90
Rate Measurements Switch	IU	5.95	6.0	622.95	621.00
Orbital Insertion (S-IVB Guidance Cutoff Sig. + 10 sec)	*	9.75	9.8	626.75	624.80

*Not Switch Selector Event

TABLE 4-II (CONT)

FUNCTION	STAGE	TIME FROM BASE (SEC)		RANGE TIME (SEC)	
		ACTUAL	PREDICTED	ACTUAL	PREDICTED
LOX Tank Vent Valve Open	S-IVB	30.17	30.2	647.17	645.20
LOX Tank Vent Valve Close	S-IVB	60.17	60.2	677.17	675.20
LOX Tank Vent Valve Boost Close On	S-IVB	63.16	63.2	680.16	678.20
LOX Tank Vent Valve Boost Close Off	S-IVB	65.17	65.2	682.17	680.20
P. U. Inverter and DC Power Off	S-IVB	239.95	240.0	856.95	855.00
LH ₂ Tank Vent Valve Close	S-IVB	**1260.35	1260.4	**1877.35	1875.40
LH ₂ Tank Vent Valve Boost Close On	S-IVB	**1263.35	1263.4	**1880.35	1878.40
LH ₂ Tank Vent Valve Boost Close Off	S-IVB	**1265.35	1265.4	**1882.35	1880.40
LH ₂ Tank Vent Valve Open	S-IVB	2629.95	2630.0	3246.95	3245.00
Auxiliary Hydraulic Pump Flight Mode On	S-IVB	2709.95	2710.0	3326.95	3325.00
Auxiliary Hydraulic Pump Flight Mode Off	S-IVB	2757.95	2758.0	3374.95	3373.00
LH ₂ Tank Vent Valve Close	S-IVB	2929.95	2930.0	3546.95	3545.00
LH ₂ Tank Vent Valve Boost Close On	S-IVB	2932.95	2933.0	3549.95	3548.00
LH ₂ Tank Vent Valve Boost Close Off	S-IVB	2934.95	2935.0	3551.95	3550.00
P. U. Inverter and DC Power On	S-IVB	**4451.95	4452.0	**5068.95	5067.00
Auxiliary Hydraulic Pump Flight Mode On	S-IVB	5029.95	5030.0	5646.95	5645.00
Engine Mainstage Control Valve Open On	S-IVB	5051.75	5051.8	5668.75	5666.80
Engine Helium Control Valve Open On (Initiate LOX Dump)	S-IVB	5051.95	5052.0	5668.95	5667.00
LOX Tank NPV Valve Open On	S-IVB	5061.95	5062.0	5678.95	5677.00
LOX Tank NPV Valve Open Off	S-IVB	5063.95	5064.0	5680.95	5679.00
LH ₂ Tank Vent Valve Open	S-IVB	5065.95	5066.0	5682.95	5681.00
LOX Tank Flight Pressurization Shutoff Valves Open (Initiate Cold Helium Dump)	S-IVB	5531.95	5532.0	6148.95	6147.00
LH ₂ Tank Vent Valve Close	S-IVB	5665.95	5666.0	6282.95	6281.00
LH ₂ Tank Vent Valve Boost Close On	S-IVB	5668.95	5669.0	6285.95	6284.00
LH ₂ Tank Vent Valve Boost Close Off	S-IVB	5670.95	5671.0	6287.95	6286.00
Engine Mainstage Control Valve Open Off	S-IVB	5771.95	5772.0	6388.95	6387.00
Engine Helium Control Valve Open Off (Completion of LOX Dump)	S-IVB	5772.95	5773.0	6389.95	6388.00
Auxiliary Hydraulic Pump Flight Mode Off	S-IVB	5774.95	5775.0	6391.95	6390.00
P. U. Inverter and DC Power Off	S-IVB	5784.95	5785.0	6401.95	6400.00
Passivation "A" Disable	S-IVB	5799.95	5800.0	6416.95	6415.00
Passivation "B" Disable	S-IVB	5800.15	5800.2	6417.15	6415.20
LOX Tank Flight Pressurization Shutoff Valves Close (Termination of cold Helium Dump)	S-IVB	8399.95	8400.0	9016.95	9015.00

**Data Dropout, Computed Values Used

TABLE 4-II (CONT)

FUNCTION	STAGE	TIME FROM BASE (SEC)		RANGE TIME (SEC)	
		ACTUAL	PREDICTED	ACTUAL	PREDICTED
Begin Manual Control of S-IVB Attitude from CSM	*	8431.80	8380.17	9048.80	8995.17
End Manual Control of S-IVB Attitude from CSM	*	8607.80	8560.17	9224.80	9175.17
Nominal CSM Physical Separation	*	9885.40	9880.17	10502.40	10495.17
LOX and LH ₂ Pump Seal Purge on (Start Stage Control Sphere Helium Dump)	S-IVB	11236.95	11237.0	11853.95	11852.00
LOX Tank Flight Pressurization Shutoff Valves Open (Restart Cold Helium Dump)	S-IVB	15599.96	15600.0	16216.96	16215.00
LOX and LH ₂ Pump Seal Purge Off (Completion of Stage Control Sphere Helium Dump)	S-IVB	14204.27	16267.3	**14821.27	16882.30
LOX Tank Flight Pressurization Shutoff Valves Close (Completion of Cold Helium Dump)	S-IVB	16799.95	16800.0	17416.95	17415.00
<u>Water coolant Valve Switching</u>					
Water Coolant Valve Closed	IU	338.05	Variable	482.37	Variable
Water Coolant Valve Open	IU	# 1065.50	Variable	# 1682.5	Variable
Water Coolant Valve Closed	IU	# 1366.00	Variable	# 1983.0	Variable
Water Coolant Valve Open	IU	# 7377.50	Variable	# 7994.5	Variable
Water Coolant Valve Closed	IU	# 7678.50	Variable	# 8295.5	Variable
Water Coolant Valve Closed	IU	#12793.50	Variable	#13410.5	Variable
Water Coolant Valve Closed	IU	18199.08	Variable	18816.08	Variable
<u>Special Sequence for Vehicle Telemetry Calibration</u>					
Telemetry Calibrator In-Flight Calibrate On	IU	43.67	--	660.67	Acq. + 60.0
TM Calibrate On	S-IVB	46.67	--	663.67	Acq. + 63.0
TM Calibrate Off	S-IVB	47.67	--	665.67	Acq. + 64.0
Telemetry Calibrator In-Flight Calibrate Off	IU	48.67	--	665.67	Acq. + 65.0
Telemetry Calibrator In-Flight Calibrate On	IU	2599.02	--	3216.02	--
TM Calibrate On	S-IVB	2602.02	--	3219.02	--
TM Calibrate Off	S-IVB	2603.02	--	3220.02	--
Telemetry Calibrator In-Flight Calibrate Off	IU	2604.02	--	3221.02	--
Telemetry Calibrator In-Flight Calibrate On	IU	4839.00	--	5456.00	--
TM Calibrate On	S-IVB	4842.00	--	5459.00	--
TM Calibrate Off	S-IVB	4843.00	--	5460.00	--
Telemetry Calibrator In-Flight Calibrate Off	IU	4844.00	--	5461.00	--
Telemetry Calibrator In-Flight Calibrate On	IU	6182.96	--	6799.96	--
TM Calibrate On	S-IVB	6185.96	--	6802.96	--

*Not Switch Selector Event

**Early Completion Initiated by Ground Command, Switch Selector Functioned Properly at 16, 884.25 Seconds.

Data Accurate to ± 0.5 Second.

TABLE 4-II (CONT)

FUNCTION	STAGE	TIME FROM BASE (SEC)		RANGE TIME (SEC)	
		ACTUAL	PREDICTED	ACTUAL	PREDICTED
TM Calibrate Off	S-IVB	6186.96	--	6803.96	--
Telemetry Calibrator In-Flight Calibrate Off	IU	6187.96	--	6804.96	--
Telemetry Calibrator In-Flight Calibrate On	IU	8279.02	--	8896.02	--
TM Calibrate On	S-IVB	8282.02	--	8899.02	--
TM Calibrate Off	S-IVB	8283.02	--	8900.02	--
Telemetry Calibrator In-Flight Calibrate Off	IU	8284.02	--	8901.02	--
Telemetry Calibrator In-Flight Calibrate On	IU	9839.01	--	10456.01	--
TM Calibrate On	S-IVB	9842.01	--	10459.01	--
TM Calibrate Off	S-IVB	9843.01	--	10460.01	--
Telemetry Calibrator In-Flight Calibrate Off	IU	9844.01	--	10461.01	--
Telemetry Calibrator In-Flight Calibrate On	IU	10510.99	--	11127.99	--
TM Calibrate On	S-IVB	10513.99	--	11130.99	--
TM Calibrate Off	S-IVB	10514.99	--	11131.99	--
Telemetry Calibrator In-Flight Calibrate Off	IU	10515.99	--	11132.99	--
Telemetry Calibrator In-Flight Calibrate On	IU	12079.05	--	12696.05	--
TM Calibrate On	S-IVB	12082.05	--	12699.05	--
TM Calibrate Off	S-IVB	12083.06	--	12700.06	--
Telemetry Calibrator In-Flight Calibrate Off	IU	12084.05	--	12701.05	--
Telemetry Calibrator In-Flight Calibrate On	IU	*13950.9	--	*14567.9	--
TM Calibrate On	S-IVB	13953.95	--	14570.95	--
TM Calibrate Off	S-IVB	13954.96	--	14571.96	--
Telemetry Calibrator In-Flight Calibrate Off	IU	*13955.9	--	*14572.9	--
Telemetry Calibrator In-Flight Calibrate On	IU	16190.98	--	16807.98	--
TM Calibrate On	S-IVB	16193.98	--	16810.98	--
TM Calibrate Off	S-IVB	16194.98	--	16811.98	--
Telemetry Calibrator In-Flight Calibrate Off	IU	16195.98	--	16812.98	--
Telemetry Calibrator In-Flight Calibrate On	IU	19739.43	--	20356.43	--
TM Calibrate On	S-IVB	19742.42	--	20359.42	--
TM Calibrate Off	S-IVB	19743.42	--	20360.42	--
Telemetry Calibrator In-Flight Calibrate Off	IU	19744.43	--	20361.43	--
<u>Events Initiated by Ground Command</u>					
LH ₂ Tank Vent Valve Open	S-IVB	10737.48	--	11354.48	--
LH ₂ Tank Vent Valve Close	S-IVB	11139.11	--	11756.11	--

* Data dropout, computed values used (event verified in registers)

TABLE 4-II (CONT)

FUNCTION	STAGE	TIME FROM BASE (SEC)		RANGE TIME (SEC)	
		ACTUAL	PREDICTED	ACTUAL	PREDICTED
LH ₂ Tank Vent Valve Boost Close On	S-IVB	11140.00	--	11757.00	--
LH ₂ Tank Vent Valve Boost Close Off	S-IVB	11146.35	--	11763.35	--
LH ₂ Tank Vent Valve Open	S-IVB	14130.27	--	14747.27	--
LH ₂ Tank Vent Valve Close	S-IVB	14391.43	--	15068.43	--
LH ₂ Tank Vent Valve Boost Close On	S-IVB	14392.24	--	15009.24	--
LH ₂ Tank Vent Valve Boost Close Off	S-IVB	14398.60	--	15015.69	--
LH ₂ Tank Vent Valve Open	S-IVB	16418.85	--	17035.85	--
LH ₂ Tank Vent Valve Close	S-IVB	16724.73	--	17341.73	--
LH ₂ Tank Vent Valve Boost Close On	S-IVB	16725.63	--	17342.63	--
LH ₂ Tank Vent Valve Boost Close Off	S-IVB	16731.58	--	17348.58	--
LH ₂ Tank Vent Valve Open	S-IVB	17921.99	--	18538.99	--
LH ₂ Tank Vent Valve Close	S-IVB	18067.65	--	18684.65	--
LH ₂ Tank Vent Valve Boost Close On	S-IVB	18068.43	--	18685.43	--
LH ₂ Tank Vent Valve Boost Close Off	S-IVB		--		--

5.0 LAUNCH OPERATIONS

5.1 SUMMARY

Apollo/Saturn vehicle AS-205, the fifth vehicle to be flown in the Saturn IB series, was launched from Kennedy Space Center Launch Complex 34. At launch time, the temperature was 300.9°K (82°F), visibility was greater than 16km (10 mi) with a few scattered clouds in the area, and surface winds were from the east (near 90°), at the launch site. The surface winds were nearly twice the peak values recorded during previous Saturn IB launches, but their magnitudes were below the launch vehicle limits.

The initial count was picked up at T-4 days and 5 hours at 1500 EDT on October 6, 1968. Three scheduled holds of 6 hours, 3 hours, and 6 hours were called. The terminal count was started, at the finish of the third scheduled hold, at T-6 hours (0500 EDT) on October 11, 1968. At T-6 minutes and 15 seconds, a 2 minute and 45 second hold was required to allow S-IVB thrust chamber chilldown to be completed. There was no other significant problem that caused delay. Launch occurred at 1102:45 EDT.

In general, the ground systems performance was satisfactory although several problems were encountered. All redline requirements were met and launch damage to the facilities was nominal.

5.2 COUNTDOWN

The AS-205 countdown was started at T-4 days and 5 hours (T-101 hours) at 1500 EDT on October 6, 1968. The three holds scheduled in the countdown plan were called. A 6 hour hold at T-3 days and a 3 hour hold at T-1 day and 9 hours were scheduled, as requested for the spacecraft, to cover any spacecraft problems. Another 6 hour hold was scheduled at T-6 hours primarily for launch crew rest before the final count. The final count was started at T-6 hours at 0500 EDT on October 11, 1968 with an expected launch time of 1100 EDT. The count proceeded on schedule with no major problem until T-6 minutes and 15 seconds when it appeared that the J-2 engine thrust chamber would not reach the desired chilldown level for liftoff. A hold was called which lasted 2 minutes and 45 seconds. This hold time was sufficient to allow chilldown and the count was continued without any recycling required. Post launch analysis determined that chilldown would have been accomplished without the hold and the ground support equipment was functioning normally. However, to be certain, in real-time, of meeting redline requirements was difficult since this was the first launch utilizing a ten-minute thrust chamber chilldown and

the first S-IVB launch using the 175°K (315°R) redline limit, 16.7°K (30°R) colder than the redline limit for AS-502, at the start of automatic sequence. A hold was deemed advisable. Launch occurred at 1102:45 EDT.

Although no major problems were encountered, the following problems occurred during countdown but caused no delay:

1. Prior to LOX loading, the Hazard Gas Monitor System indicated approximately 2 percent oxygen content in the S-IB engine compartment. Since this system functioned as expected during the countdown demonstration test (CDDT) and the other readings in more contained areas were nominal, the reading was attributed to the high wind velocity in the relatively open compartment. Therefore, the background level for S-IB was taken as 2 percent and any reading above this value would have been considered real. However, no increase was seen throughout the launch.

2. During the transformation from replenish to line drain on the RP-1 system, the automatic RP-1 positive bus D442 on the LCC RP-1 power panel blew a fuse. The manual system was operative and the remaining functions were conducted manually.

3. When power was applied during the last 6 hour hold, the automatic and manual propellant tanking computer system (PTCS) mass readout indicated a shift in RP-1 percent mass from that obtained for final RP-1 loading on October 5, 1968. The delta P manometer indication did not shift. Therefore, the decision was made to use the delta P indication for replenish and final level adjust.

4. The F1 fuel tank temperature measurement (XC-179-F1) was much higher than the other three fuel tank temperature measurements. This caused the decision to be made to eliminate this reading from the averaging for T-0 fuel density prediction.

5. During power transfer test at T-30 minutes, the flight control computer inverter detector in the IU switched from the primary to secondary (spare) inverter. The unit was restored to the primary inverter and the power transfer test was re-run. The problem did not repeat and the countdown proceeded. This switching was caused by a voltage transient during the transfer. This event was similar to that which occurred during the AS-204 countdown.

5.3 PROPELLANT AND COLD HELIUM LOADING

In loading the S-IB stage, the Propellant Tanking Computer System (PTCS) measures the pressure difference between sensing lines in the stage propellant systems. The differential pressure required to tank the LOX and fuel, together with PTCS reference values, are obtained from a propellant loading table.

5.3.1 RP-1 LOADING

RP-1 loading was not conducted on AS-205 prior to or during CDDT as had been done on previous vehicles. Actual loading was started at 2240 EDT on October 4, 1968 and flight mass of 100.10% was reached at 0003 EDT on October 5, 1968. At this time, the tanks were pressurized to 6.9 N/cm² gauge (10 psig), and stage leak checks were made. During this period, the PTCS manometer reading dropped at a rate of approximately 1.2 percent/minute although the system is isolated by solenoid valves in the pressure sensing lines. This caused considerable concern about the accuracy of the level indication. Leak checks were performed on the system, but no leaks were found. The system was repressurized to 6.9 N/cm² gauge (10 psig) and the indications functioned normally. Transfer line drain was conducted and then autoreplenish was conducted to 2% ullage based on an average tank temperature of 301.3°K (82.6°F), giving a PTCS thumbwheel setting of 8878. Next, a drain level adjust to 3% ullage was conducted based on an average temperature of 301.0°K (82.2°F), giving a PTCS thumbwheel setting of 8785. The system was left in this configuration until countdown.

During countdown, a problem was encountered two days prior to launch when the RP-1 level could not be accurately determined. Another test was run on the manometer system. This time the manometers were used to leak test the hi-sense line. A pinhole leak was found and a section of the tube was replaced on the 24.4 m (80 ft) tower level. A comparison PTCS reading was taken which compared with the original reading, indicating that the leak was not causing any reading error.

During the last 6 hour hold prior to the terminal count, when power was applied to the PTCS, the automatic and manual mass readouts indicated a shift in RP-1 percent mass from that obtained for final RP-1 loading on October 5, 1968. The delta P manometer indication did not shift. This indicated a problem in the delta P to percent mass conversion equipment. The automatic readout shifted from approximately 100.01% to 100.12% and remained continuously at this level. The manual readout shifted erratically from 99.99% to 99.22%.

At T-3 hours and 10 minutes, the S-IB fuel tanks were replenished to a 2% ullage level to assure that the final fuel adjustment would be a drain sequence. As the countdown progressed, the fuel temperature chilled down as expected until T-2 hours and 23 minutes. At that time, the fuel temperature in tank F1 (measurement XC-179-F1) stopped decreasing. For several subsequent sample points, the temperature appeared to increase. The decision was then made to disregard the temperature in tank F1 and base the average fuel temperature on the remaining three tanks for T-0 fuel density prediction.

At approximately T-28 minutes, the final fuel adjustment was made. The delta P manometer was assumed to be correct and used for the final adjustment. Final RP-1 levels as indicated by the PTCS computer were: Manometer delta P 12.147 N/cm² diff (17.618 psid), Automatic Mass Readout 100.12% with thumbwheel setting at 8748, and Manual Mass Readout 99.99% with thumbwheel setting at 8748. F2, 3, and 4 fuel tank temperature average was 294.0°K (69.5°F); and F1 fuel tank temperature, which was deleted from averaging, was 298.2°K (77.1°F).

5.3.2 LOX LOADING

The LOX system performed normally during dual loading operations and maintained flight mass to the S-IB and S-IVB stages until start of automatic sequence. Fill command was initiated at T-5 hours and 56 minutes (0504 EDT) in the final countdown. The S-IB stage reached the replenish mode at 0602 EDT and the S-IVB stage at 0607 EDT. No problems were encountered. The LOX crew was cleared to the pad and four tankers were off-loaded, adding 53.0 m³ (14,000 gallons) to the storage tank. LOX boiloff of S-IB and S-IVB was replenished, using approximately 165.0 m³ (43,600 gallons), by the autoreplenish system satisfactorily until LOX tank pressurization for launch.

5.3.3 LH₂ LOADING

S-IVB LH₂ loading was initiated at T-4 hours and 34 minutes (0626 EDT) in the final countdown with chilldown of the heat exchanger. Slow fill rate was 0.019 m³/sec (300 gpm) until 5% level was reached at 0654 EDT and fast fill was initiated. Flow continued without any problems, and 96% LH₂ mass was reached at 0721 EDT. Slow fill from 96% to 100% was terminated at 0724 EDT. At this time, approximately 189.3 m³ (50,000 gallons) of the initial 477.0 m³ (126,000 gallons) of LH₂ remained in the storage tank. At approximately T-3 hours, the crew transferred LH₂ from four tankers to the storage tank. Approximately 90.8 m³ (24,000 gallons) were lost due to boiloff and pressurization.

5.3.4 COLD HELIUM LOADING

The cold helium spheres were pressurized to approximately 655 ± 34 N/cm² (950 ± 50 psi) at T-14 hours. Prior to LOX load the spheres were pressurized to 1034 N/cm² (1500 psi). At 92% LH₂ mass, the pressure was increased to 2137 N/cm² (3100 psi).

5.3.5 AUXILIARY PROPULSION SYSTEM PROPELLANT LOADING

The auxiliary propulsion system (APS) fuel and oxidizer loading was accomplished on October 4, 1968. Fuel loading was 24.9 cm (9.8 in) and 24.82 cm (9.77 in) for Modules I and II fuel tanks, respectively. Oxidizer tanks for both Modules I and II were loaded to 24.9 cm (9.8 in).

5.3.6 S-IB STAGE PROPELLANT LOAD

The propellant loading criteria for the S-IB-5 stage were based on environmental conditions expected during October. The propellant loading table provided a LOX weight and tanking differential pressure based on this criteria and a nominal LOX tank ullage volume of 1.5 percent. The loading table contained fuel tanking weights and differential pressures for fuel densities from 790.671 kg/m^3 at 309.8°K (49.360 lbm/ft^3 at 98°F) to 814.058 kg/m^3 at 276.5°K (50.820 lbm/ft^3 at 38°F). The fuel temperature was monitored during the launch countdown and at T-28 minutes a final fuel temperature was projected to ignition. The final fuel density was obtained using the projected temperature. Figure 5-1 shows the temperature-density relationship of the fuel used for constructing the propellant loading tables and was taken from the Complex 34 fuel storage tanks on March 14, 1968.

During the first part of August 1968, 43.911 m^3 (11,600 gallons) of RP-1 were added to the Complex 34 storage tanks. On August 23 a new fuel sample was taken and another temperature density analysis was made. The relationship is also shown in Figure 5-1. The difference between the first and second density curves is about 0.384 kg/m^3 (0.024 lbm/ft^3), the latest sample being more dense. Because of the small change in density and lack of time before launch, it was decided to use the propellant loading table based on the first density sample, and to reconstruct the loads based on the second sample.

The decision to disregard the temperature in tank F1 and base the average fuel temperature at T-28 minutes on the remaining three tanks resulted in a difference of about 1.1°K (2°F) in temperature averages. The final fuel temperature projected to stage ignition was 294.0°K (69.5°F). There remains some question whether the tank F1 measurement was actually valid. This analysis assumes that it was not. Fuel residuals tend to agree with this conclusion.

Due to the problem in the delta P to percent mass conversion equipment, the delta P manometer was assumed to be correct and used for the final adjustment. The final reading was 12.1464 N/cm^2 diff (17.617 psid). The closest value in the propellant loading table is 12.1469 N/cm^2 diff (17.6176 psid) and corresponds to a mass of $125,421.9 \text{ kg}$ ($276,508 \text{ lbm}$). The S-IB stage propellant tanking weights are shown in Table 5-I.

In Table 5-I, the predicted values were used in the operational flight trajectory (Reference 1). These values were based on a nominal LOX density of 1129.41 kg/m^3 (70.507 lbm/ft^3) and a nominal fuel density of 800.76 kg/m^3 (49.990 lbm/ft^3) for a September launch. The loading system values are based

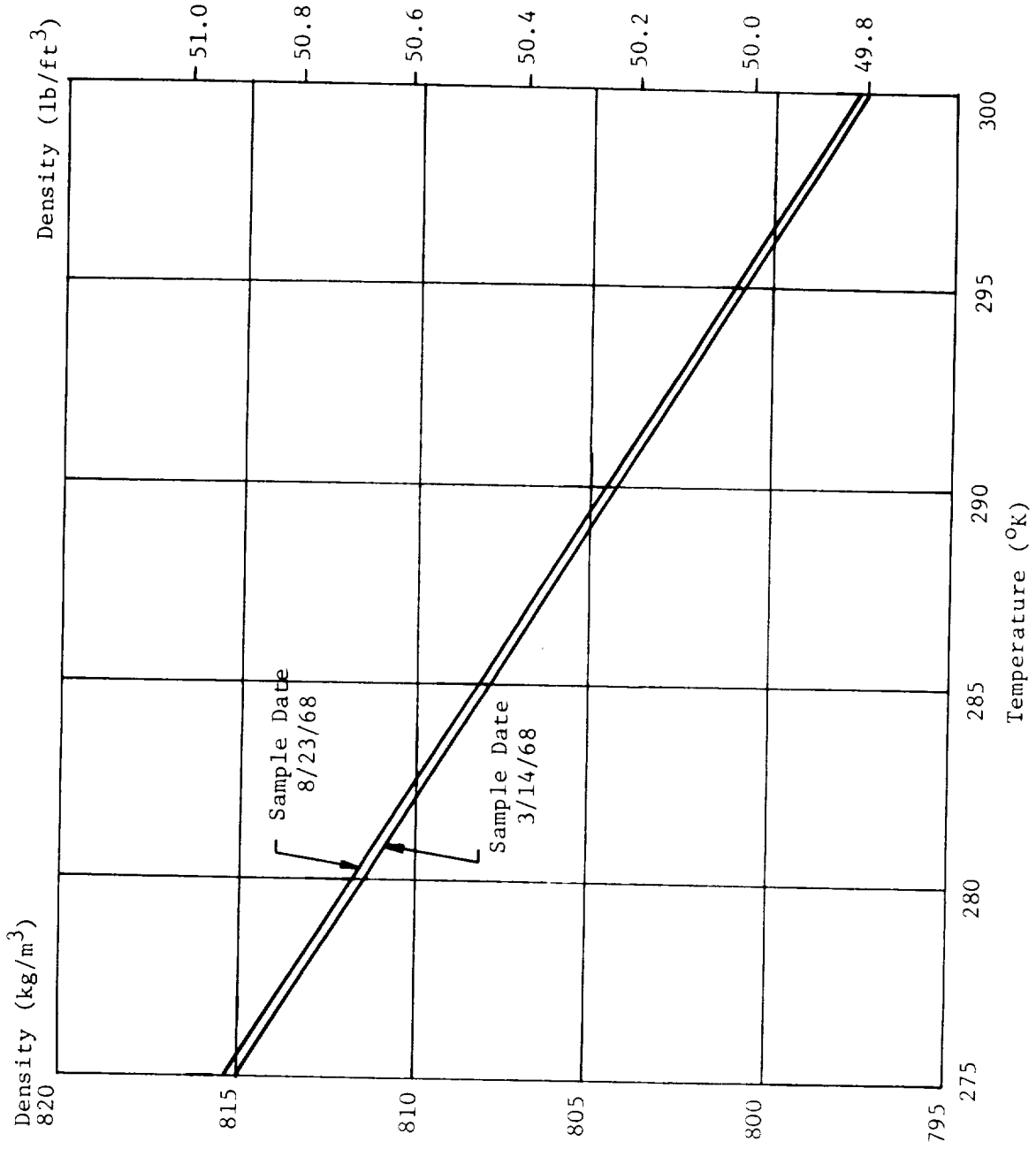


FIGURE 5-1 FUEL TEMPERATURE/DENSITY RELATIONSHIP

TABLE 5-1

AS-205 S-1B STAGE PROPELLANT WEIGHTS AT IGNITION COMMAND

PROPELLANT	UNITS	WEIGHT REQUIREMENTS				WEIGHT INDICATIONS	
		PREDICTED FOR SEPT LAUNCH	PREDICTED FOR OCT LAUNCH	FOR IGNITION	LOADING SYSTEM	BEST ESTIMATE	
LOX	kg	286,468.1	286,549.7	286,549.7	286,549.7	286,352.9	
	lbm	631,554	631,734	631,734	631,734	631,300	
Fuel	kg	125,213.3	125,583.3	125,331.7	125,331.7	125,599.7	
	lbm	276,048	276,864	276,309	276,309	276,900	
Total	kg	411,681.4	412,133.0	411,881.4	411,881.4	411,952.6	
	lbm	907,602	908,598	908,043	908,043	908,200	

on pressure values determined immediately prior to propellant system pressurization. These values were based on a nominal LOX density of 1129.81 kg/m³ (70.532 lbm/ft³) and a fuel density of 802.28 kg/m³ (50.085 lbm/ft³) determined immediately prior to ignition and based on densities after the fuel storage tanks were replenished. The loading system values compare favorably with loads and densities expected for an October launch as documented in Reference 2. This document predicted the required LOX load at 286,549.7 kg (631,734 lbm) based on a nominal LOX density of 1130.12 kg/m³ (70.551 lbm/ft³) and the required fuel load at 125,583.3 kg (276,864 lbm) based on a nominal fuel density of 802.68 kg/m³ (50.11 lbm/ft³) prior to vent closure. The best estimate values are based on discrete probe data in conjunction with engine transient consumption rates in the Mark IV reconstruction. The reconstructed average LOX density at ignition, based on the average LOX pump inlet temperature throughout the flight, was 1127.01 kg/m³ (70.357 lbm/ft³). The LOX pump inlet temperature monitored during the flight indicated that the temperature of the LOX at ignition was 0.54°K (0.97°F) warmer than predicted. Most of the difference can be attributed to the higher than predicted surface winds. The reconstructed average fuel density at ignition, based on tank F2, F3, and F4 measurements, was 802.28 kg/m³ (50.085 lbm/ft³).

The propellant discrete level instrumentation for this stage consisted of three probes in each of tanks 0C, 01, and 03 and fifteen probes in each of tanks F1 and F3. The propellant levels in the other tanks were approximated by using data from the instrumented tanks. Because probe 1 failed in tank 03, tank 01 flow rate was used as representative of the initial LOX flow for all outboard LOX tanks.

5.3.7 S-IVB STAGE PROPELLANT LOAD

Table 5-II presents the S-IVB propellant load at S-IB ignition command. The best estimate includes loading determined from the PU system, engine analysis, and trajectory reconstruction.

5.4 HOLDDOWN

No known problems occurred during holddown. All functions occurred at nominal times. The ground systems overall performance during countdown was satisfactory and all redline requirements were met.

Post launch inspection revealed that launch damage to the facilities was nominal. Damage to the short cable mast II, the engine service platform, and the water quench line area of holddown arm III was attributed to engine gimbaling to offset wind loads during liftoff.

TABLE 5-II

AS-205 S-IVB STAGE PROPELLANT WEIGHTS AT S-IB IGNITION COMMAND

PROPELLANT	UNITS	WEIGHT REQUIREMENTS	WEIGHT INDICATIONS		WEIGHT DEVIATIONS	
		PREDICTED PRIOR TO LAUNCH	LOADING SYSTEM	BEST ESTIMATE	LOADING SYSTEM MINUS PREDICTED	BEST EST MINUS PREDICTED
LOX	kg	87,667.2	87,761.1	87,693.0	93.9	25.8
	lbm	193,273	193,480	193,330	207	57
	%				0.10	0.03
Fuel	kg	17,983.1	18,077.0	18,102.4	93.9	119.3
	lbm	39,646	39,853	39,909	207	263
	%				0.52	0.66
Total	kg	105,650.3	105,838.1	105,795.4	187.8	145.1
	lbm	232,919	233,333	233,239	414	320
	%				0.18	0.14

6.0 MASS CHARACTERISTICS

6.1 SUMMARY

Postflight analysis indicated that vehicle mass characteristics were generally in agreement with predicted data. Weight deviations during powered flight were less than 0.4% of predicted. Vehicle weight deviations of 450.3 kg (993 lbm) higher at first motion and 676.4 kg (1.491 lbm) lower at S-IB outboard cutoff signal were noted. Vehicle weight was 19.9 kg (44 lbm) and 33.0 kg (73 lbm) greater than predicted at S-IVB engine start and cutoff commands, respectively. Longitudinal center of gravity travel during first flight stage operation was essentially as predicted. A maximum deviation of 0.07 meter (2.6 in) forward was noted at outboard engine cutoff signal. Deviations during second flight stage operation ranged from 0.02 meter (0.6 in) aft at start command to 0.04 meter (1.5 in) aft at cutoff signal. Examination of post-flight vehicle moment of inertia data indicated deviations from predicted of only 1% or less throughout powered flight.

6.2 MASS ANALYSIS

Postflight mass characteristics are determined and compared to the final predicted mass characteristics (Reference 3) which were used in the generation of the final operational trajectory (Reference 1). The postflight mass characteristics were determined from an analysis of actual and reconstructed data from ground ignition through 5 hr: 11 min: 26 sec of launch vehicle flight. Dry weights of the S-IB stage, S-IVB stage, and vehicle instrument unit were based on an evaluation of the Weight and Balance Log Books (MSFC Form 998). Payload data were obtained from the Manned Spacecraft Center. S-IB stage propellant loading and utilization were evaluated from the S-IB propulsion system performance reconstruction. S-IVB propellant and service item loading and utilization were evaluated from a composite of Propulsion Utilization (PU) system, engine flow integral, reconstruction, and level sensor residuals.

Deviations in the dry weights of the S-IB stage, S-IVB stage and vehicle instrument unit were within the predicted three sigma limits. The weight of S-IB/S-IVB interstage exceeded the upper limit by 34.5 kg (76 lbm), while the Spacecraft and LES totaled 10.9 kg (24 lbm) under the lower limit. Since these deviations were compensating, the total weight of the vehicle before the loading of any propellants and usable load items into the S-IB and S-IVB stages was only 41.3 kg (91 lbm) lower than predicted.

At first motion the vehicle weight was 586,392.8 kg (1,292,775 lbm) which was 450.3 kg (993 lbm) more than predicted. This increase is primarily a result of higher RP-1 and LH₂ loadings in the S-IB and S-IVB stages. Predicted data is based on the September launch S-IB stage propulsion prediction. Additionally, S-IB stage oxidizer weight was lower than predicted due to relatively high surface winds experienced during the launch period. Mainstage mass losses were higher than predicted due to a mixture ratio shift brought about by the relatively low oxidizer density which resulted in the consumption of a substantial portion of the fuel bias (RP-1) loading. Low S-IB stage propellant residuals are responsible for 676.4 kg (1,491 lbm) and 612.4 kg (1,350 lbm) lower than predicted weight deviations, which were noted for the outboard engine cutoff and separation events, respectively.

Vehicle weights were essentially as predicted during second flight stage operation. The higher S-IVB LH₂ load was offset by a lighter than predicted spacecraft weight. Deviations of only 19.9 kg (44 lbm) and 33.0 kg (73 lbm) for the engine start and cutoff events were noted. Vehicle weight at guidance cutoff signal was 30,767.1 kg (67,830 lbm).

Vehicle mass history comparison at significant events is presented in Table 6-I. Detailed vehicle masses are tabulated in Tables 6-IIa and 6-IIb for the vehicle during S-IB stage powered flight, Tables 6-IIc and 6-IId for the vehicle during S-IVB stage powered flight, and Tables 6-IIe for the vehicle during orbital flight. Graphical representations of these data, center-of-gravity, and mass moment of inertia histories, with respect to time, are illustrated in Figures 6-1 and 6-2 for the S-IB stage and S-IVB stage powered flight, respectively.

6.3 CENTER OF GRAVITY AND MOMENT OF INERTIA

Comparison of the longitudinal center of gravity with the predicted data indicated small deviations ranging from zero to 0.07 meter (2.6 in). The maximum deviation occurred at outboard cutoff signal resulting from low propellant residuals. Mass moments of inertia deviations during S-IB stage powered flight were minor with the maximum deviation noted of only 1%.

Longitudinal center of gravity travel during S-IVB stage powered flight closely approximated the predicted values. The location at engine cutoff command was 0.04 meter (1.5 in) aft, reflecting the lighter spacecraft weight. Mass moments of inertia were essentially as predicted.

Weight, center of gravity, and moment of inertia data for the individual stages and the vehicle at significant events are presented in Tables 6-IIIa and 6-IIIb.

Weight data presented in this section are of masses under acceleration of one standard g. The sign convention used herein conforms to the Project Apollo mass properties coordinate system (Reference 4).

TABLE 6-I
FLIGHT SEQUENCE MASS SUMMARY
SATURN IB AS-205

MASS HISTORY	ACTUAL		PREDICTED	
	kg	lbm	kg	lbm
S-IB Stage	450,830.9	993,912	450,503.9	993,191
S-IB/S-IVB Interstage	2,995.5	6,604	2,938.3	6,478
S-IVB Stage	116,356.9	256,403	116,158.2	256,084
Vehicle Instrument Unit	1,933.6	4,263	1,941.4	4,280
Spacecraft	16,528.0	36,438	16,601.5	36,600
Launch Escape System	4,025.2	8,874	4,076.0	8,986
First Flight Stage at Ground Ignition	592,670.1	1,306,614	592,219.3	1,305,670
S-IB Thrust Buildup Propellant	-6,277.3	-13,839	-6,276.8	-13,838
First Flight Stage at First Motion	586,392.8	1,292,775	585,942.5	1,291,782
S-IB Main Stage Propellant	-399,543.6	-880,843	-398,463.2	-878,461
S-IB Stage Frost	-453.6	-1,000	-453.6	-1,000
S-IVB Stage Frost	-88.5	-191	-85.4	-180
S-IB Stage Engine Seal Purge (GN ₂)	-2.7	-6	-2.7	-6
S-IB Stage Gear Box Consumption (RP-1)	-327.5	-722	-326.1	-719
S-IB Stage Fuel Lubricant (Oronite)	-12.3	-27	-12.3	-27
S-IB Stage Inboard Engine Thrust Decay	-977.9	-2,156	-976.1	-2,152
First Flight Stage at Outboard Cutoff Signal	184,986.7	407,826	185,663.1	409,317
S-IB Outboard Thrust Decay to Sep. Command	-661.8	-1,459	-730.8	-1,611
S-IVB Ullage Rocket Propellant	-4.1	-9	0.0	0
S-IVB Frost	-0.9	-2	0.0	0
First Flight Stage at Separation Command	184,319.9	406,356	184,932.3	407,706
S-IB Stage at Separation Command	-42,574.2	-93,860	-43,262.3	-95,377
S-IB/S-IVB Interstage	-2,995.5	-6,604	-2,938.3	-6,478
S-IVB Separation and Ullage Components	-15.4	-34	-16.3	-36
S-IVB Ullage Rocket Propellant	-30.4	-67	-32.2	-71
S-IVB Frost	-1.3	-3	0.0	0
Second Flight Stage at Ignition Command	138,703.1	305,788	138,683.2	305,744
S-IVB Thrust Buildup Propellant	-159.7	-352	-234.6	-517
S-IVB Ullage Rocket Propellant	-45.8	-101	-47.6	-105
S-IVB GH ₂ Start Tank	-1.8	-4	-1.8	-4
Second Flight Stage at 90% Thrust	138,495.8	305,331	138,399.2	305,118
S-IVB Main Stage Propellant	-103,602.8	-228,405	-103,489.3	-228,155
S-IVB Ullage Rocket Cases	-98.9	-218	-97.1	-214
S-IVB Auxilliary Propellant (APS)	-1.8	-4	-2.7	-6
Launch Escape System	-4,025.2	-8,874	-4,076.0	-8,986
Second Flight Stage at Cutoff Command	30,767.1	67,830	30,734.1	67,757
S-IVB Thrust Decay Propellant	-73.0	-161	-63.5	-140
Second Flight Stage at Insertion	30,694.1	67,669	30,670.6	67,617

TABLE 6-IIa VEHICLE MASSES (KILOGRAMS)

FIRST FLIGHT STAGE

EVENT	GROUND IGNITION		FIRST MOTION		INBOARD ENGINE CUTOFF SIGNAL		OUTBOARD ENGINE CUTOFF SIGNAL		SEPARATION SIGNAL	
	PRED	ACTUAL	PRED	ACTUAL	PRED	ACTUAL	PRED	ACTUAL	PRED	ACTUAL
RANGE TIME (SEC)	-2.94	-2.99	0.17	0.17	140.28	140.64	143.28	144.32	144.58	145.58
S-IB Stage, Dry	38,283.6	38,342.2	38,283.6	38,342.2	38,283.6	38,342.2	38,283.6	38,342.2	38,283.6	38,342.2
LOX in Tanks	282,759.5	282,633.4	277,677.5	277,571.7	953.5	1,421.1	0.0	0.0	0.0	0.0
LOX Below Tanks	3,708.6	3,719.4	3,914.0	3,898.2	3,863.7	3,847.9	1,625.2	1,465.6	1,373.0	1,267.3
LOX Tank Ullage Gas	15.4	12.7	37.2	34.4	1,210.2	1,211.5	1,225.2	1,228.8	1,224.5	1,229.2
Fuel in Tanks	123,038.3	123,420.7	121,196.3	121,584.1	2,085.6	1,715.5	419.6	0.0	34.5	0.0
Fuel Below Tanks	2,175.0	2,179.0	2,595.0	2,599.5	2,594.6	2,599.5	2,384.6	2,144.5	2,289.8	1,680.6
Fuel Tank Ullage Gas	2.7	2.7	3.6	3.6	27.2	26.7	27.2	27.2	27.2	27.2
Nitrogen	6.8	6.8	6.8	6.8	4.1	4.1	4.1	4.1	4.1	4.1
Helium - Fuel Pressurant	32.7	32.7	31.8	31.8	8.2	8.2	8.2	8.2	8.2	8.2
Hydraulic Oil	12.7	12.7	12.7	12.7	12.7	12.7	12.7	12.7	12.7	12.7
Oronite	15.0	15.0	15.0	15.0	2.7	2.7	2.7	2.7	2.7	2.7
Frost	453.6	453.6	453.6	453.6	-	-	-	-	-	-
Total: S-IB Stage	450,503.9	450,830.9	444,227.1	444,553.6	49,046.1	49,192.6	43,993.1	43,236.0	43,262.3	42,574.2
S-IB/S-IVB Interstage, Dry	2,456.6	2,514.3	2,456.6	2,514.3	2,456.6	2,514.3	2,456.6	2,514.3	2,456.6	2,514.3
Retro Rocket Propellant	481.7	481.2	481.7	481.2	481.7	481.2	481.7	481.2	481.7	481.2
Total: First Vehicle Stage	453,442.2	453,826.4	447,165.4	447,549.1	51,984.4	52,188.1	46,931.4	46,231.5	46,200.6	45,569.7
S-IVB Stage	116,158.2	116,356.9	116,158.2	116,356.9	116,112.8	116,270.7	116,112.8	116,268.4	116,112.8	116,263.4
Vehicle Instrument Unit	1,941.4	1,933.6	1,941.4	1,933.6	1,941.4	1,933.6	1,941.4	1,933.6	1,941.4	1,933.6
Spacecraft and LES	20,677.5	20,553.2	20,677.5	20,553.2	20,677.5	20,553.2	20,677.5	20,553.2	20,677.5	20,553.2
Total: First Flight Stage	592,219.3	592,670.1	585,942.5	586,399.8	190,716.1	190,945.6	185,663.1	184,986.7	184,932.3	184,319.9

TABLE 6-IIb VEHICLE MASSES (POUNDS)

FIRST FLIGHT STAGE

EVENT	GROUND IGNITION		FIRST MOTION		INBOARD ENGINE CUTOFF SIGNAL		OUTBOARD ENGINE CUTOFF SIGNAL		SEPARATION SIGNAL	
	PRED	ACTUAL	PRED	ACTUAL	PRED	ACTUAL	PRED	ACTUAL	PRED	ACTUAL
RANGE TIME (SEC)	-2.94	-2.99	0.17	0.17	140.28	140.64	143.28	144.32	144.58	145.58
S-IB Stage, Dry	84,401	84,530	84,401	84,530	84,401	84,530	84,401	84,530	84,401	84,530
LOX in Tanks	623,378	623,100	612,174	611,941	2,102	3,133	0	0	0	0
LOX Below Tanks	8,176	8,200	8,629	8,594	8,518	8,483	3,583	3,231	3,027	2,794
LOX Tank Ullage Gas	34	28	82	76	2,668	2,671	2,701	2,709	2,704	2,710
Fuel in Tanks	271,253	272,096	267,192	268,047	4,598	3,782	925	0	76	0
Fuel Below Tanks	4,795	4,804	5,721	5,731	5,720	5,731	5,257	4,728	5,048	3,705
Fuel Tank Ullage Gas	6	6	8	8	60	59	60	60	60	60
Nitrogen	15	15	15	15	9	9	9	9	9	9
Helium - Fuel Pressurant	72	72	70	70	18	18	18	18	18	18
Hydraulic Oil	28	28	28	28	28	28	28	28	28	28
Oronite	33	33	33	33	6	7	6	6	6	6
Frost	1,000	1,000	1,000	1,000	-	-	-	-	-	-
Total:S-IB Stage	993,191	993,912	979,353	980,073	108,128	108,451	96,988	95,319	95,377	93,860
S-IB/S-IVB Interstage, Dry	5,416	5,543	5,416	5,543	5,416	5,543	5,416	5,543	5,416	5,543
Retro Rocket Propellant	1,062	1,061	1,062	1,061	1,062	1,061	1,062	1,061	1,062	1,061
Total:First Vehicle Stage	999,669	1,000,516	985,831	986,677	114,606	115,055	103,466	101,923	101,855	100,464
S-IVB Stage	256,085	256,523	256,085	256,523	255,985	256,333	255,985	256,284	255,985	256,317
Vehicle Instrument Unit	4,280	4,263	4,280	4,263	4,280	4,263	4,280	4,263	4,280	4,263
Spacecraft and LRS	45,586	45,312	45,586	45,312	45,586	45,312	45,586	45,312	45,586	45,312
Total:First Flight Stage	1,305,620	1,306,614	1,291,782	1,292,775	420,457	420,963	409,317	407,826	407,706	406,356

TABLE 6-IIc VEHICLE MASSÉS (KILOGRAMS)

SECOND FLIGHT STAGE

EVENT	S-IB STAGE GROUND IGNITION		J-2 ENGINE START COMMAND		90% THRUST LEVEL		J-2 ENGINE CUTOFF COMMAND		ORBITAL INSERTION	
	Pred	Actual	Pred	Actual	Pred	Actual	Pred	Actual	Pred	Actual
RANGE TIME (SEC)	-2.94	-2.99	145.98	146.97	149.68	150.20	621.80	616.75	621.80	626.75
S-IVB Stage	9,937.7	9,911.9	9,937.7	9,911.9	9,937.7	9,911.9	9,937.7	9,911.9	9,937.7	9,911.9
Separation Package	16.3	15.4	-	-	-	-	-	-	-	-
Ullage Rocket Cases	97.1	98.9	97.1	98.9	97.1	98.9	-	-	-	-
Ullage Rocket Grain	79.8	80.3	47.6	45.8	-	-	-	-	-	-
LOX in Tank	87,500.7	87,526.5	87,500.7	87,526.5	87,304.7	87,274.4	576.1	550.6	539.3	509.8
LOX Below Tank	166.5	166.5	166.5	166.5	180.1	180.1	180.1	180.1	166.5	166.5
LOX Tank Ullage Gas	16.3	15.0	16.3	15.0	17.2	15.4	166.5	124.7	166.5	141.7
LH2 in Tank	17,961.4	18,080.7	17,961.4	18,080.7	17,904.2	18,037.1	911.7	1,108.6	903.1	1,094.9
LH2 Below Tank	21.8	21.8	21.8	21.8	26.3	26.3	26.3	26.3	21.8	21.8
LH2 Tank Ullage Gas	76.6	62.6	76.6	62.6	76.6	63.5	228.1	194.6	194.6	194.6
Cold Helium - Bottles	149.7	152.4	149.7	152.4	149.2	151.9	80.3	78.0	80.3	77.6
APS Propellant	59.9	61.2	59.9	61.2	59.9	61.2	57.1	59.4	57.1	59.4
GH2 - Start Tank	2.2	2.2	2.2	2.2	5	5	5	5	5	5
Service Items	26.8	25.4	26.8	25.4	26.8	25.4	26.8	25.4	26.8	25.4
Frost	45.4	45.4	-	45.4	-	45.4	-	45.4	-	45.4
Total: S-IVB Stage	116,158.2	116,356.9	116,064.3	116,216.3	115,780.3	116,009.3	12,191.2	13,000.2	12,177.7	12,694.1
Launch Escape System	4,076.0	4,025.2	4,076.0	4,025.2	4,076.0	4,025.2	-	-	-	-
Spacecraft	16,601.5	16,528.0	16,601.5	16,528.0	16,601.5	16,528.0	16,601.5	16,528.0	16,601.5	16,528.0
Instrument Unit	1,941.4	1,933.6	1,941.4	1,933.6	1,941.4	1,933.6	1,941.4	1,933.6	1,941.4	1,933.6
Total: Second Flight Stage	138,777.1	138,843.7	138,663.2	138,703.1	138,399.2	138,495.2	30,734.1	30,767.1	30,670.6	30,694.1

TABLE 6-11d VEHICLE MASSES (POUNDS)

SECOND FLIGHT STAGE

EVENT	S-1B STAGE GROUND IGNITION		J-2 ENGINE START COMMAND		90% THRUST LEVEL		J-2 ENGINE CUTOFF COMMAND		ORBITAL INSERTION	
	Pred	Actual	Pred	Actual	Pred	Actual	Pred	Actual	Pred	Actual
RANGE TIME (SEC)	-2.94	-2.99	145.98	146.97	149.58	150.20	614.50	616.75	624.80	626.75
S-1VB Stage	21,909	21,852	21,909	21,852	21,909	21,852	21,909	21,852	21,909	21,852
Separation Package	36	34	-	-	-	-	-	-	-	-
Ullage Rocket Cases	214	218	214	218	214	218	-	-	-	-
Ullage Rocket Grain	176	177	105	101	-	-	-	-	-	-
LOX in Tank	192,906	192,963	192,906	192,963	192,474	192,664	1,270	1,214	1,189	1,154
LOX Below Tank	367	367	367	367	397	397	397	397	367	367
LOX Tank Ullage Gas	36	33	36	33	38	34	367	275	367	275
LH2 in Tank	39,598	39,861	39,598	39,861	39,472	39,764	2,010	2,444	1,991	2,421
LH2 Below Tank	48	48	48	48	58	58	58	58	48	48
LH2 Tank Ullage Gas	169	138	169	138	169	140	503	429	503	429
Cold Helium - Bottles	330	336	330	336	329	335	177	172	177	171
APS Propellant	132	135	132	135	132	133	126	131	126	131
GH2 - Start Tank	5	5	5	5	1	1	1	1	1	1
Service Items	59	56	59	56	59	56	59	56	59	56
Frost	100	100	-	100	-	100	-	100	-	100
Total: S-1VB Stage	256,085	256,513	255,878	256,213	255,252	255,711	26,877	27,129	26,737	26,468
Launch Escape System	8,986	8,874	8,986	8,874	8,986	8,874	-	-	-	-
Spacecraft	36,600	36,438	36,600	36,438	36,600	36,438	36,600	36,438	36,600	36,438
Instrument Unit	4,280	4,263	4,280	4,263	4,280	4,263	4,280	4,263	4,280	4,263
Total: Second Flight Stage	305,951	306,098	305,744	305,788	305,118	305,311	67,757	67,830	67,617	67,669

TABLE 6-IIe VEHICLE MASSES
ORBITAL VEHICLE

EVENT	START LOX DUMP		END LOX DUMP		CSM SEPARATION		END PASSIVATION	
	kg	lbm	kg	lbm	kg	lbm	kg	lbm
RANGE TIME (sec)	5,668.95		6,389.95		10,502.40		18,685.43	
RANGE TIME (hr:min:sec)	1:34:28.95		1:46:29.95		2:55:2.40		5:11:25.43	
MASSES	kg	lbm	kg	lbm	kg	lbm	kg	lbm
S-IVB Stage	9,911.9	21,852	9,911.9	21,852	9,911.9	21,852	9,911.9	21,852
Separation Package	-	-	-	-	-	-	-	-
Ullage Rocket Cases	-	-	-	-	-	-	-	-
Ullage Rocket Grain	-	-	-	-	-	-	-	-
LOX in Tank	282.1	622	-	-	-	-	-	-
LOX Below Tank	166.5	367	-	-	-	-	-	-
LOX Tank Ullage Gas	305.3	673	-	-	-	-	-	-
LH ₂ in Tank	677.7	1,494	96.2	212	-	-	-	-
LH ₂ Below Tank	21.8	48	579.2	1,277	234.9	518	-	-
LH ₂ Tank Ullage Gas	187.3	413	21.8	48	21.8	48	-	-
Cold Helium - Bottles	77.5	171	104.8	231	449.0	990	14.9	33
APS Propellant	55.3	122	71.7	158	7.3	16	1.4	3
GH ₂ - Start Tank	0.5	1	53.9	119	44.5	98	31.3	69
Service Items	25.4	56	-	-	-	-	-	-
Frost	45.4	100	25.4	56	25.4	56	25.4	56
Total: S-IVB Stage	11,756.7	25,919	10,910.3	24,053	10,740.2	23,678	10,030.3	22,113
Launch Escape System	-	-	-	-	-	-	-	-
Command Module	5,604.6	12,356	5,604.6	12,356	-	-	-	-
Service Module	4,800.8	10,584	4,800.8	10,584	-	-	-	-
SM Oxidizer	2,677.6	5,903	2,677.6	5,903	-	-	-	-
SM Fuel	1,656.5	3,652	1,656.5	3,652	-	-	-	-
SLA Ring	41.3	91	41.3	91	-	-	-	-
Adapter (SLA)	1,747.2	3,852	1,747.2	3,852	1,747.2	3,852	1,747.2	3,852
Instrument Unit	1,933.6	4,263	1,933.6	4,263	1,933.6	4,263	1,933.6	4,263
Total: Orbital Vehicle	30,218.3	66,620	29,371.9	64,754	14,421.0	31,793	13,711.1	30,228

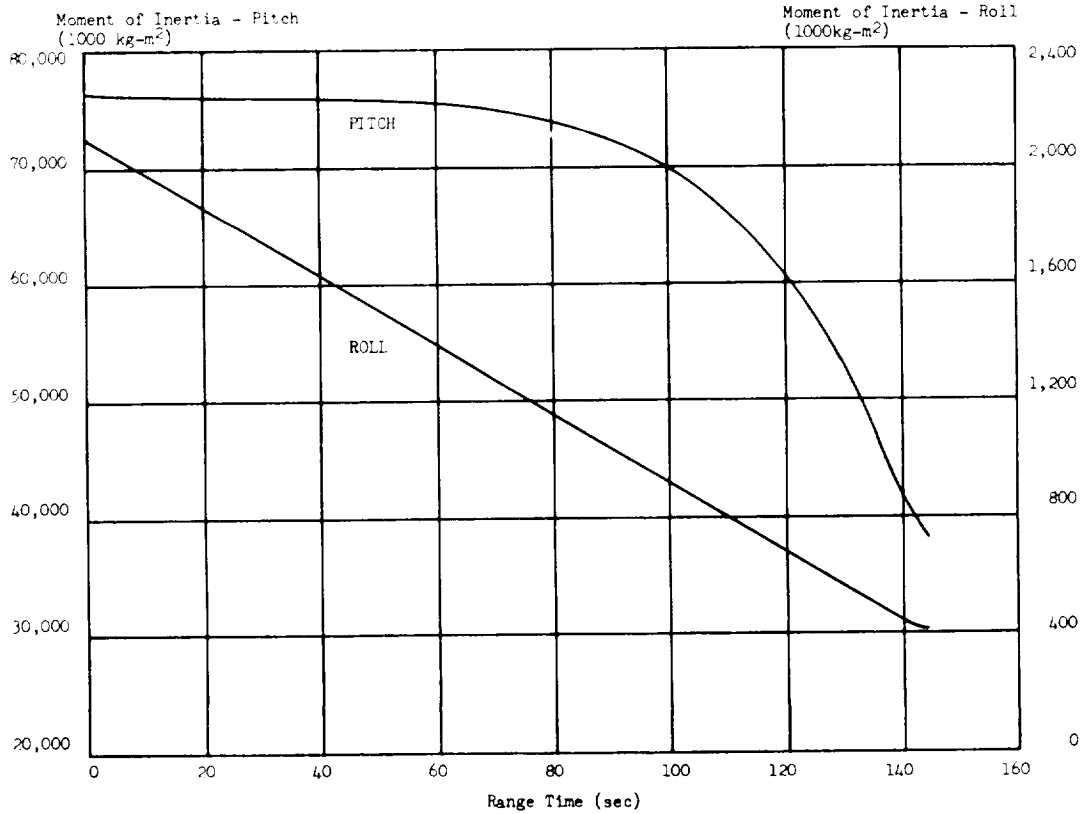
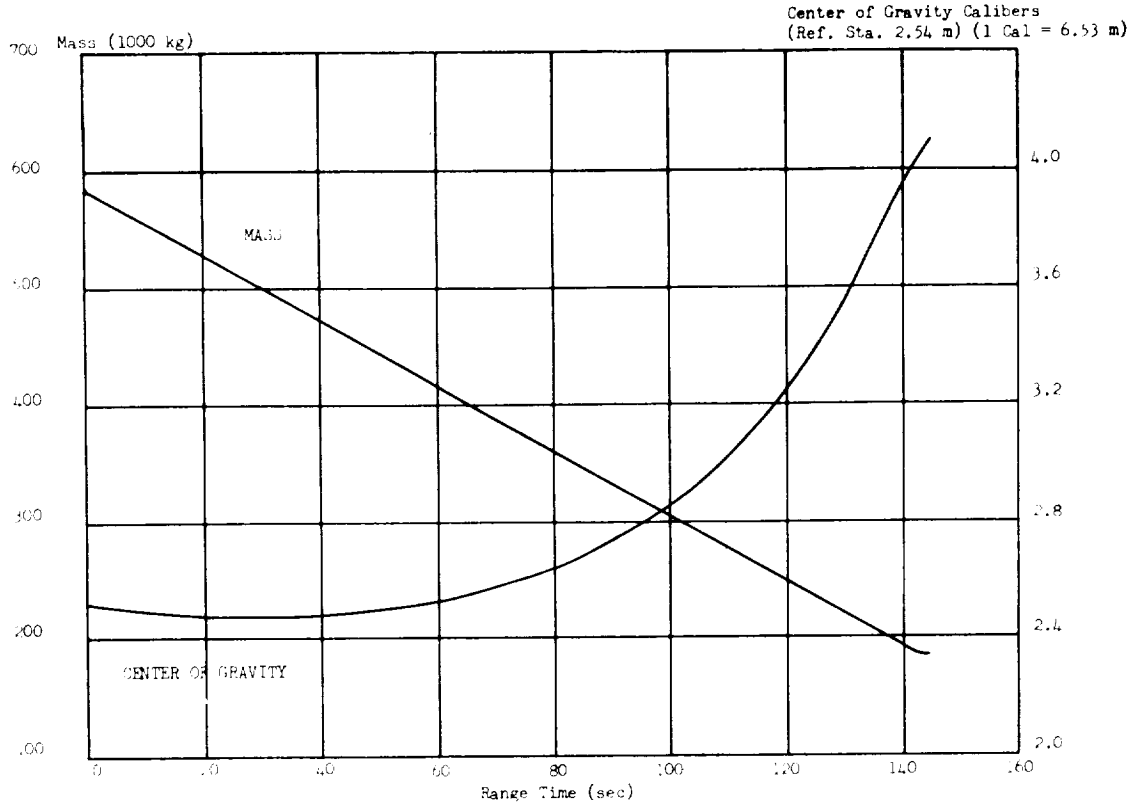


FIGURE 6-1 VEHICLE MASS, CENTER OF GRAVITY, AND MASS MOMENT OF INERTIA DURING S-IB STAGE POWERED FLIGHT

TABLE 6-IIIa
MASS CHARACTERISTICS COMPARISON

EVENTS	MASS		LONGITUDINAL C.G. STATION		RADIAL C.G.		ROLL MOMENT OF INERTIA		PITCH MOMENT OF INERTIA		YAW MOMENT OF INERTIA	
	KILOGRAMS POUNDS	% DEV.	METERS INCHES	ACT-PRED	METERS INCHES	ACT-PRED	Kg-M ²	% DEV.	Kg-M ²	% DEV.	Kg-M ²	% DEV.
S-IB Stage, Dry	Pred	38,283.6 84,401	8.65 340.6	0.00	0.01 0.4	0.00	224,788	0.15	2,599,223	0.15	2,599,223	0.15
	Actual	38,342.2 84,530	8.66 341.0	0.4	0.4 0.4	0.0	225,131		2,603,195		2,603,105	
S-IB/S-IVB Interstage (Includes Retro Rocket Propellant)	Pred	2,938.3 6,478	26.66 1,049.8	0.02	0.06 2.3	0.00	32,450	0.77	22,987	2.17	23,418	0.58
	Actual	2,995.5 6,604	26.68 1,050.5	0.7	0.06 2.3	0.0	32,701		23,485		23,554	
S-IVB Stage, Dry (Includes Ullage Rocket Cases Separation Package)	Pred	10,051.1 22,159	33.06 1,301.6	0.02	0.23 9.0	-0.00	73,785	-0.02	267,516	0.13	267,251	0.37
	Actual	10,026.2 22,104	33.08 1,302.4	0.8	0.23 8.9	-0.1	73,770		267,875		268,245	
Vehicle Instrument Unit	Pred	1,941.4 4,280	42.78 1,684.3	-0.01	0.35 13.8	-0.01	18,888	-0.96	10,326	-1.63	8,904	-0.39
	Actual	1,933.6 4,263	42.77 1,684.0	-0.3	0.34 13.5	-0.3	18,706		10,158		8,869	
Spacecraft (Includes IES)	Pred	20,677.5 45,586	55.63 2,190.3	-0.03	0.11 4.3	0.01	39,609	-0.96	542,170	-1.53	547,074	-1.79
	Actual	20,553.2 45,312	55.60 2,189.0	-1.3	0.12 4.6	0.3	39,228		533,873		537,274	
First Flight Stage at Ground Ignition	Pred	592,219.3 1,303,620	19.00 748.2	-0.00	0.01 0.2	0.00	2,142,360	0.12	76,949,230	-0.37	76,953,230	-0.41
	Actual	592,670.1 1,306,614	19.00 748.0	-0.2	0.01 0.3	0.1	2,144,951		76,663,470		76,639,823	
First Flight Stage at First Motion	Pred	585,942.5 1,291,782	18.95 745.9	-0.01	0.01 0.2	0.00	2,108,765	0.12	77,020,510	-0.35	77,024,700	-0.39
	Actual	586,392.8 1,292,775	18.94 745.8	-0.1	0.01 0.3	0.1	2,111,258		76,748,548		76,724,584	

TABLE 6-IIIB
MASS CHARACTERISTICS COMPARISON

EVENTS	MASS		LONGITUDINAL C.G. STATION		RADIAL C.G.		ROLL MOMENT OF INERTIA		PITCH MOMENT OF INERTIA		YAW MOMENT OF INERTIA	
	KILOGRAMS POUNDS	% DEV	METERS INCHES	ACT-PRED	METERS INCHES	ACT-PRED	Kg-M ²	% DEV	Kg-M ²	% DEV	Kg-M ²	% DEV
First Flight Stage at Inboard Engine Cutoff Signal	Pred	190,716.1 420,457	0.12	28.55 1,124.0	-0.05	0.02 0.8	0.00	444,938	41,651,610	0.29	41,655,340	0.23
	Actual	190,945.6 420,963		28.50 1,122.2	-1.8	0.02 0.8	0.0	444,608	41,774,512		41,751,257	
First Flight Stage at Outboard Engine Cutoff Signal	Pred	185,663.1 409,317	-0.36	29.17 1,148.5	0.07	0.02 0.8	0.00	423,478	38,933,070	-0.94	38,936,870	-1.01
	Actual	184,986.7 407,826		29.24 1,151.1	2.6	0.02 0.8	0.0	419,275	38,555,778		38,544,757	
First Flight Stage at Separation Command	Pred	184,932.3 407,706	-0.33	29.27 1,152.2	0.06	0.02 0.8	0.00	419,654	38,508,330	-0.84	38,512,280	-0.97
	Actual	184,319.9 406,356		29.33 1,154.6	2.4	0.02 0.8	0.0	416,113	38,146,629		38,138,522	
S-IB and Interstage at Separation	Pred	46,200.6 101,855	-1.37	9.63 379.2	0.03	0.01 0.5	-0.00	283,335	3,667,562	1.08	3,667,900	0.74
	Actual	45,569.7 100,464		9.66 380.5	1.3	0.01 0.4	-0.1	279,818	3,707,013		3,694,967	
Second Flight Stage at Engine Start Command	Pred	138,683.2 305,744	0.01	35.81 1,409.8	-0.02	0.02 0.9	0.00	135,797	11,085,120	-0.74	11,088,650	-0.73
	Actual	138,703.1 305,788		35.79 1,409.2	-0.6	0.02 0.9	0.0	135,859	11,003,403		11,007,205	
Second Flight Stage at Cutoff Command	Pred	30,734.1 67,457	0.11	44.74 1,761.3	-0.04	0.10 4.0	0.00	132,267	3,564,858	-0.07	3,567,806	-0.07
	Actual	30,767.1 67,850		44.70 1,759.8	-1.5	0.10 4.0	0.0	132,236	3,562,197		3,565,432	

NOTE: Percent Deviation = (Deviation ÷ Predicted) x 100

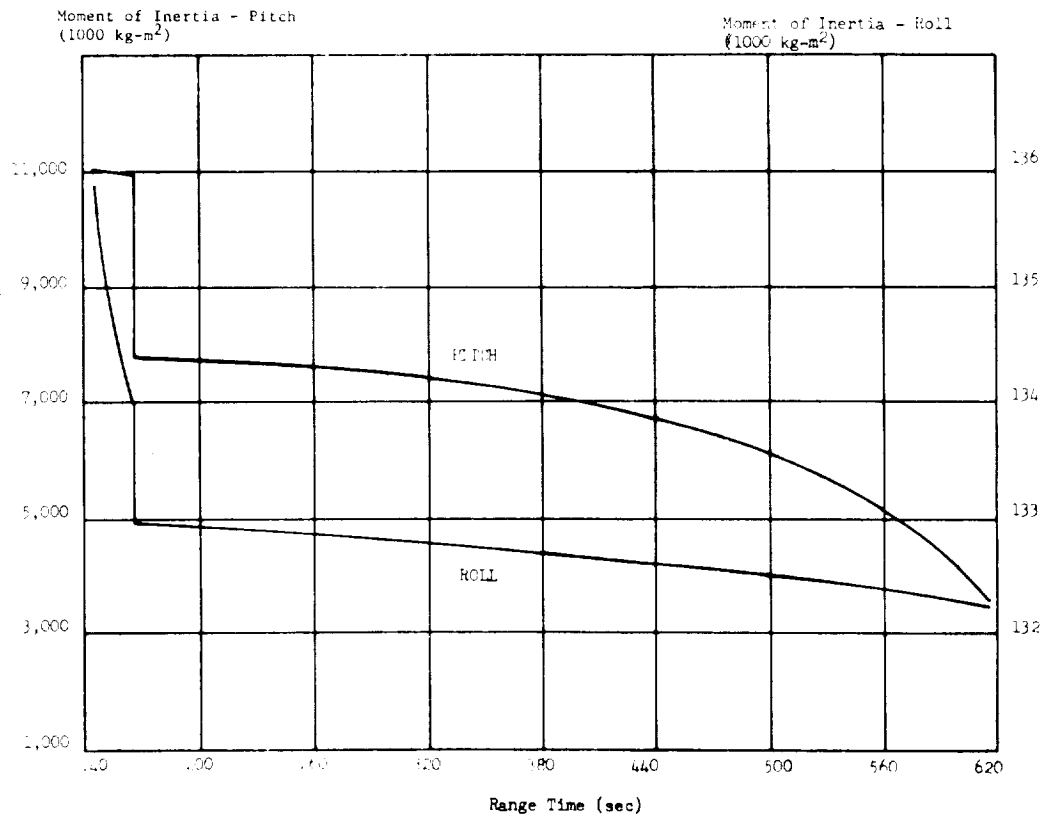
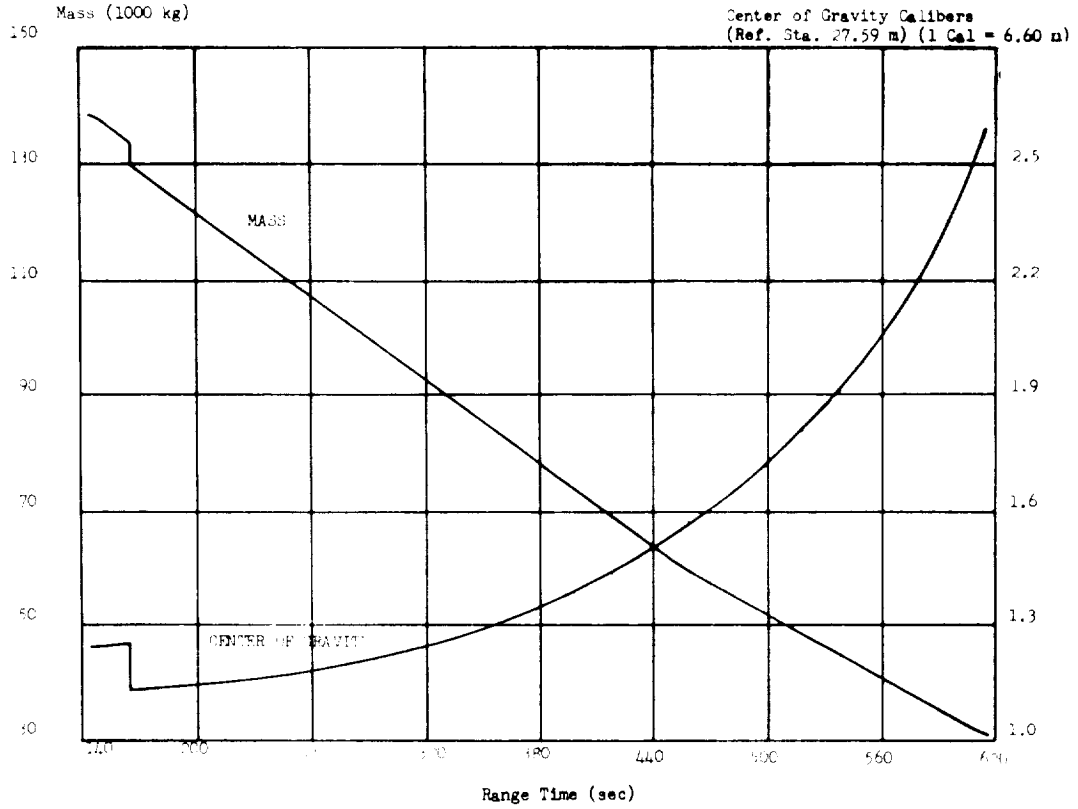


FIGURE 6-2 VEHICLE MASS, CENTER OF GRAVITY, AND MASS MOMENT OF INERTIA DURING S-1VB STAGE POWERED FLIGHT

7.0 TRAJECTORY

7.1 SUMMARY

The actual flight trajectory of the AS-205 vehicle was very close to nominal. Launch azimuth, from pad 34, was 100 deg east of north. After approximately 10 sec of vertical rise, the vehicle began a roll maneuver to the flight azimuth of 72 deg east of north. Also at 10 sec, the downrange pitch maneuver was initiated. Total space-fixed velocity was 3.4 m/s lower than nominal at OECO and 0.4 m/s lower than nominal at S-IVB cutoff. At S-IVB cutoff, the altitude and surface range were 0.2 km higher than nominal and 1.1 km greater than nominal, respectively.

The probable impact of the spent S-IB booster stage was determined from a theoretical free flight trajectory, utilizing a tumbling drag coefficient. Assuming the booster remained intact during re-entry, the impact occurred at 560.2 sec at a ground range of 490.8 km.

Orbital insertion (S-IVB cutoff plus 10 sec) occurred at 626.75 sec, which was 1.95 sec later than nominal. The space-fixed velocity at insertion was 1.2 m/s greater than nominal. The flight path angle, relative to the local horizontal, was 0.007 deg above nominal. The S-IVB/CSM-101 apogee altitude was 4.6 km higher than nominal and perigee was 0.2 km higher than nominal.

The parking orbit portion of the trajectory, from insertion to S-IVB/CSM-101 separation, was close to nominal. Separation of the Command Service Module from the S-IVB/IU occurred at 10,502.4 sec, by command from the spacecraft, 7.2 sec later than nominal. During the parking orbit, an S-IVB safing experiment was conducted by dumping remaining propellants. The orbital effects of this propellant dump are presented.

7.2 TRACKING DATA UTILIZATION

Tracking data from C-band radars, covering the major portion of the powered flight, were available for establishing the postflight trajectory. Also used in determining the postflight trajectory were telemetered guidance data and measured meteorological data.

The initial launch phase trajectory (from first motion to 28 sec) was established by a least squares curve fit of the initial tracking data. From 28 sec to orbit insertion (626.75 sec), the trajectory was established by a composite fit of all tracking data available, utilizing the guidance velocity data as the generating parameters for fit of the tracking data through an 18-term guidance error model.

The tracking sources available during powered flight are shown in Table 7-1 .

TABLE 7-1
POWERED FLIGHT DATA AVAILABILITY

DATA SOURCE	RADAR	TRACKING INTERVAL (SEC)
Patrick	0.18	20 to 593
Cape	1.16	0 to 499 599 to 603
Merritt Island	19.18	11 to 606
Grand Bahamas	3.18	96 to 584
Grand Turk	7.18	211 to 685
Bermuda	67.18 67.16	250 to 689 250 to 689

7.3 TRAJECTORY ANALYSIS

The actual flight trajectory was very close to nominal during the launch vehicle powered flight. Altitude, surface range, and cross range for the powered flight phase are presented in Figure 7-1. The total earth-fixed velocity is shown in Figure 7-2. The nominal values are shown in these figures where there is sufficient deviation from the actual to make them distinguishable. Comparisons of the actual and nominal parameters at the three cutoff events are shown in Table 7-II. Figure 7-3 presents the total inertial acceleration. The nominal values used for this comparison are taken from Reference 1.

The combined burn time of the S-IB and S-IVB stages was 1.95 sec longer than predicted. Of this 1.95 sec, the S-IB stage was responsible for 1.04 sec and the S-IVB stage for 0.91 second. Trajectory parameters at significant events are presented in Table 7-III.

The S-IB stage OECO was issued by the LVDC at 144.32 sec as a result of LOX depletion; the S-IVB cutoff signal was issued by the guidance computer, when end conditions were satisfied, at 616.75 seconds. The magnitude of incremental velocity imparted to the vehicle as a result of thrust decay impulse are given in Table 7-IV.

TABLE 7-IV
THRUST DECAY VELOCITY GAIN

Event	Actual (m/s)	Nominal (m/s)
OECO	4.1	6.1
S-IVB CO	6.4	5.2

Mach number and dynamic pressure are shown in Figure 7-4. These parameters were calculated using measured meteorological data to an altitude of 90 km. Above this altitude, the U. S. Standard Reference Atmosphere was used.

A theoretical free-flight trajectory was computed for the discarded S-IB stage, using initial conditions at S-IB/S-IVB separation. The trajectory was integrated from separation, assuming nominal retrorocket performance and outboard engine thrust decay. Tracking data were not available to confirm the results obtained.

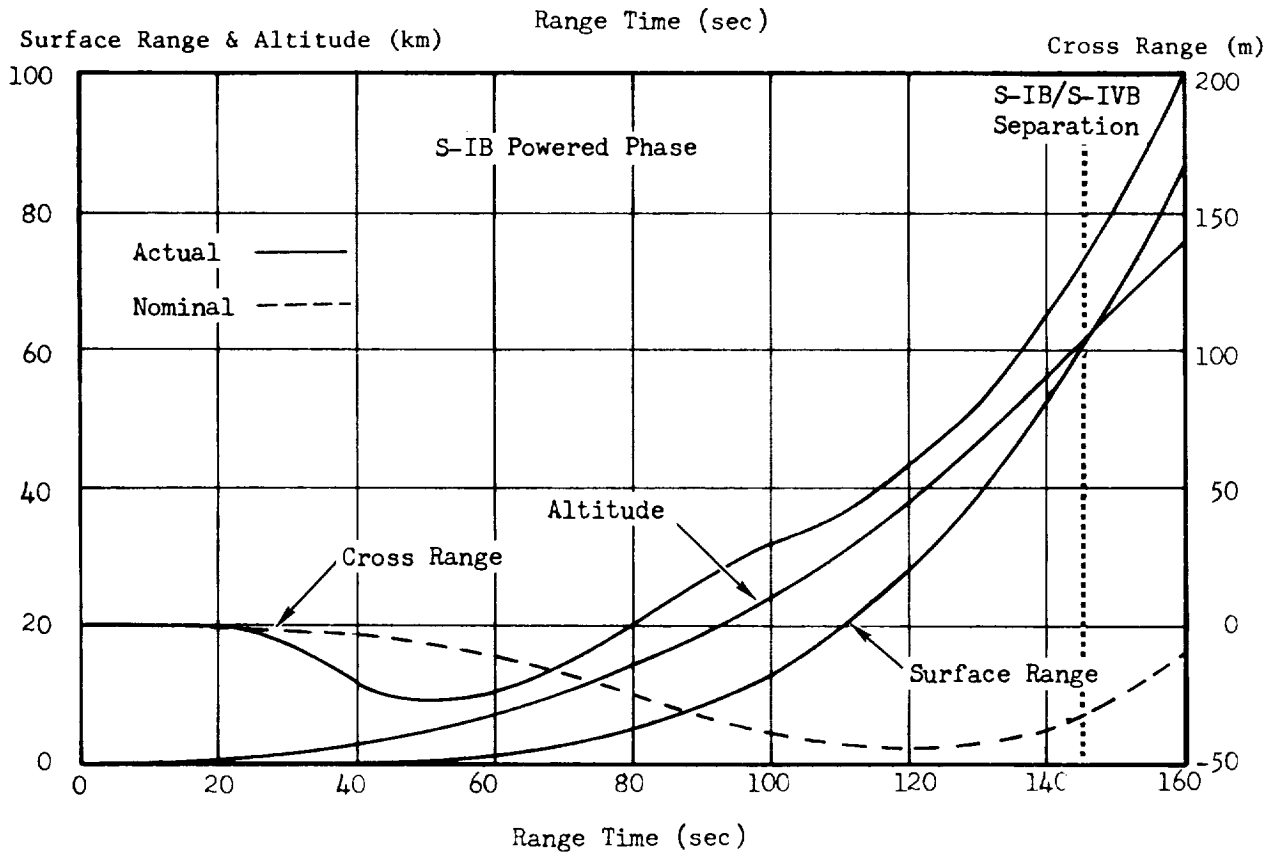
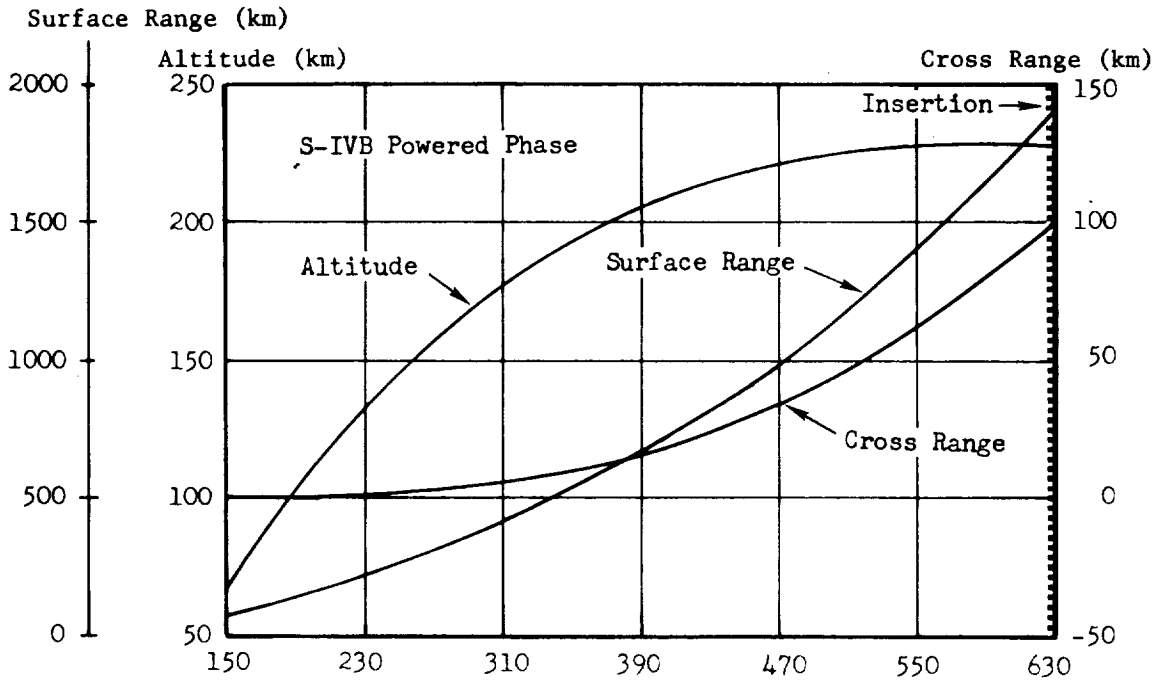


FIGURE 7-1 S-IB AND S-IVB TRAJECTORY

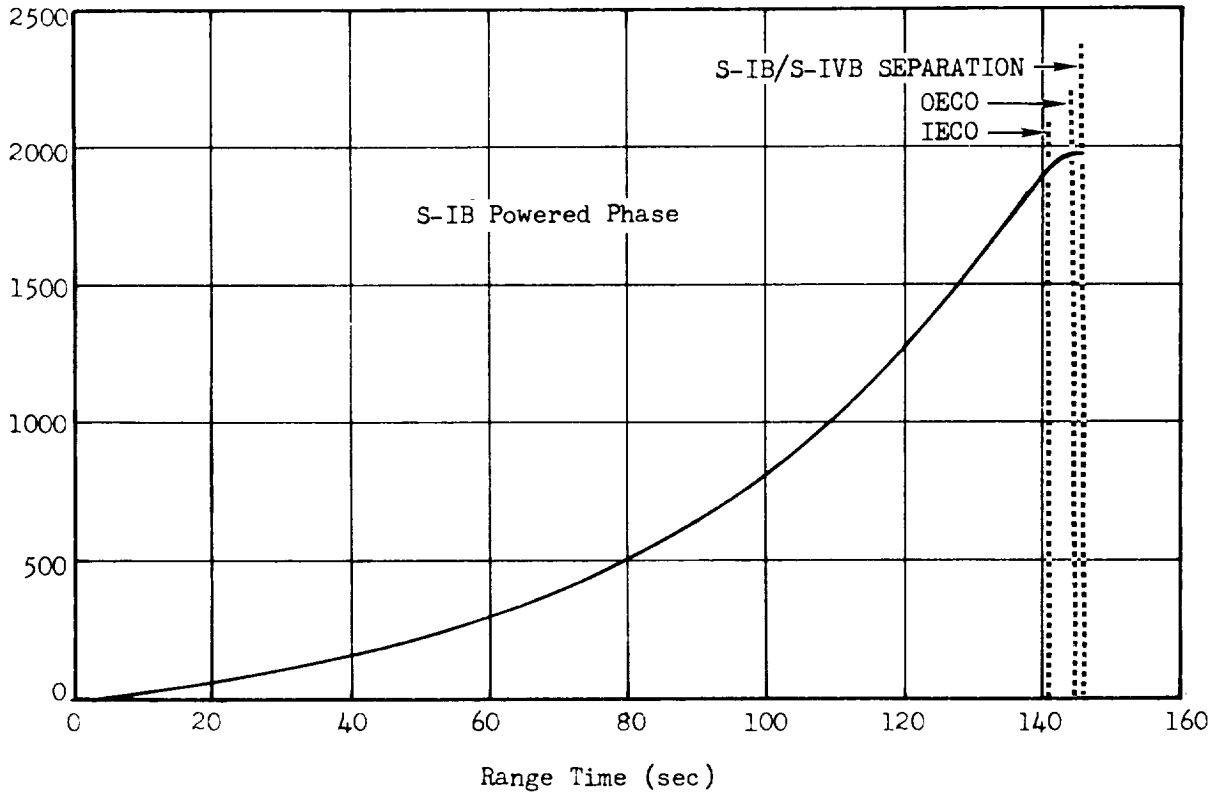
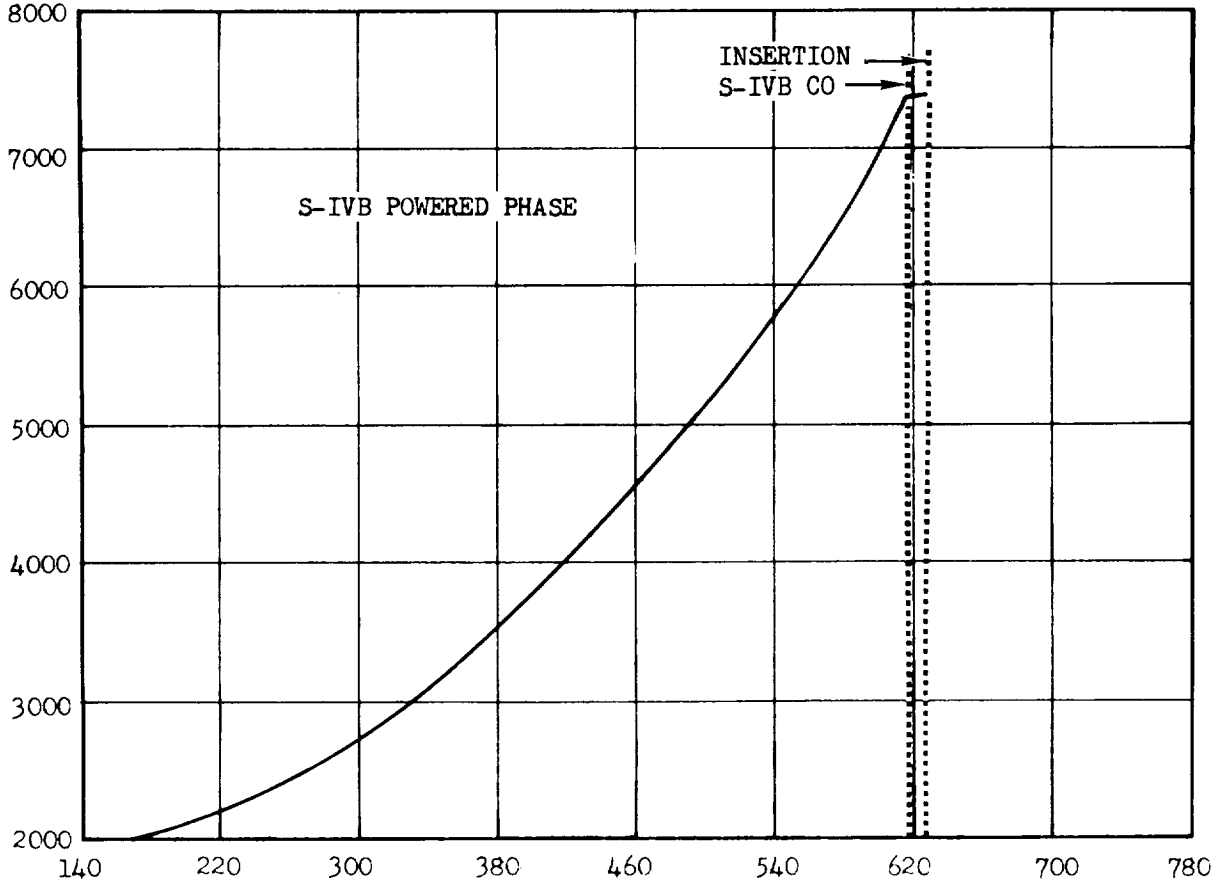


FIGURE 7-2 EARTH-FIXED VELOCITY

TABLE 7-II
CUTOFF CONDITIONS

Parameter	IECO			OECO			S-IVB CO		
	Actual	Nominal	Act-Nom	Actual	Nominal	Act-Nom	Actual	Nominal	Act-Nom
Range Time (sec)	140.64	140.28	0.36	144.32	143.28	1.04	616.75	614.80	1.95
Altitude (km)	56.72	57.41	-0.69	60.52	60.55	-0.03	228.1	227.9	0.2
Range (km)	54.05	54.74	-0.69	60.04	59.65	0.39	1821.1	1820.0	1.1
Cross Range Y_E (km)	0.11	-0.04	0.15	0.13	-0.03	0.16	92.7	92.9	-0.2
Cross Range Velocity (m/s)	3.9	0.7	3.2	4.3	1.0	3.3	539.8	539.9	-0.1
Earth-Fixed Velocity Vector Elevation (deg)	32.52	32.69	-0.17	31.69	32.02	-0.33	0.00	-0.01	0.01
Earth-Fixed Velocity Vector Azimuth (deg)	72.29	72.18	0.11	72.33	72.22	0.11	85.68	85.67	0.01
Space-Fixed Velocity (m/s)	2253.8	2267.8	-14.0	2321.6	2325.0	-3.4	7780.3	7780.7	-0.4
Total Inertial Acceleration (m/s)	40.53	41.94	-1.41	20.36	18.94	1.42	25.05	25.24	-0.19

Earth-Fixed Velocity Accuracy
 OECO ± 0.4 m/s
 S-IVB CO ± 0.7 m/s

Altitude Accuracy
 OECO ± 30 m
 S-IVB CO ± 100 m

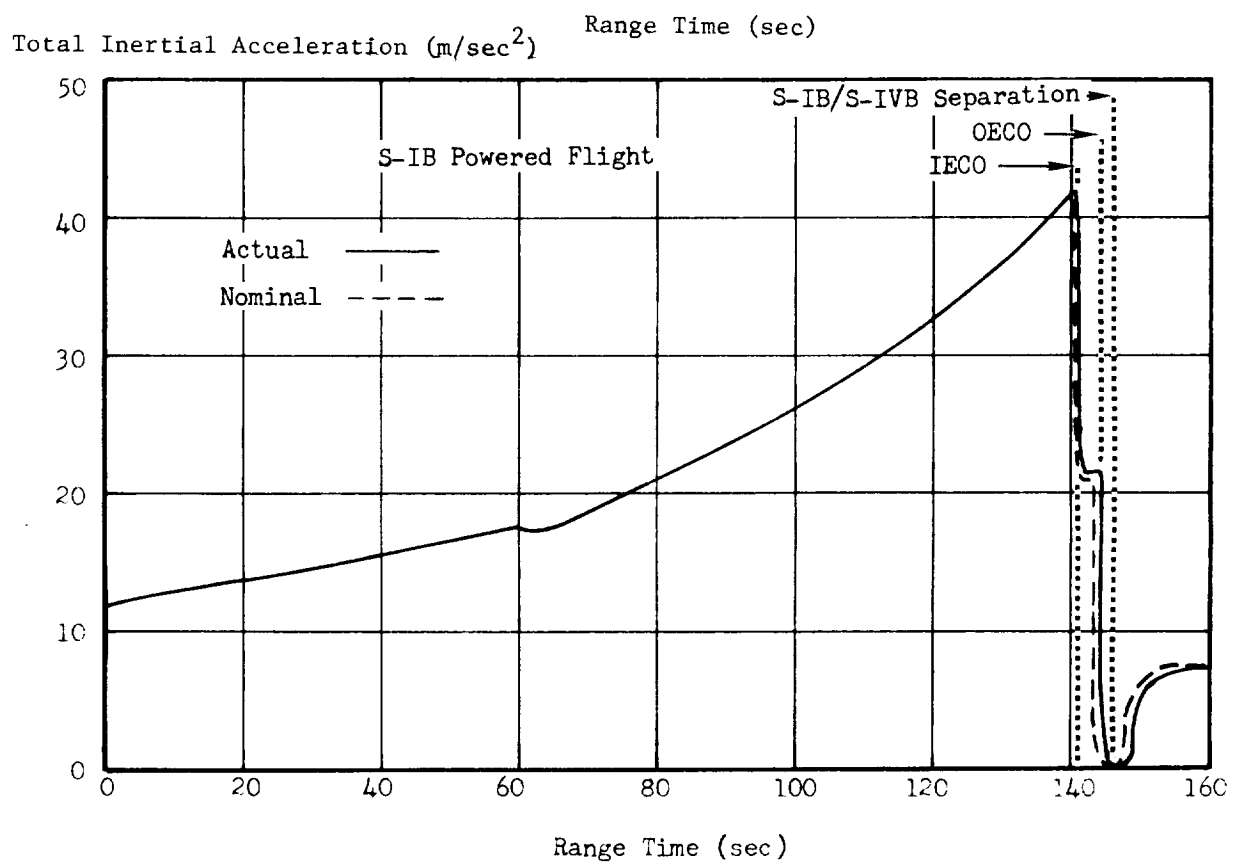
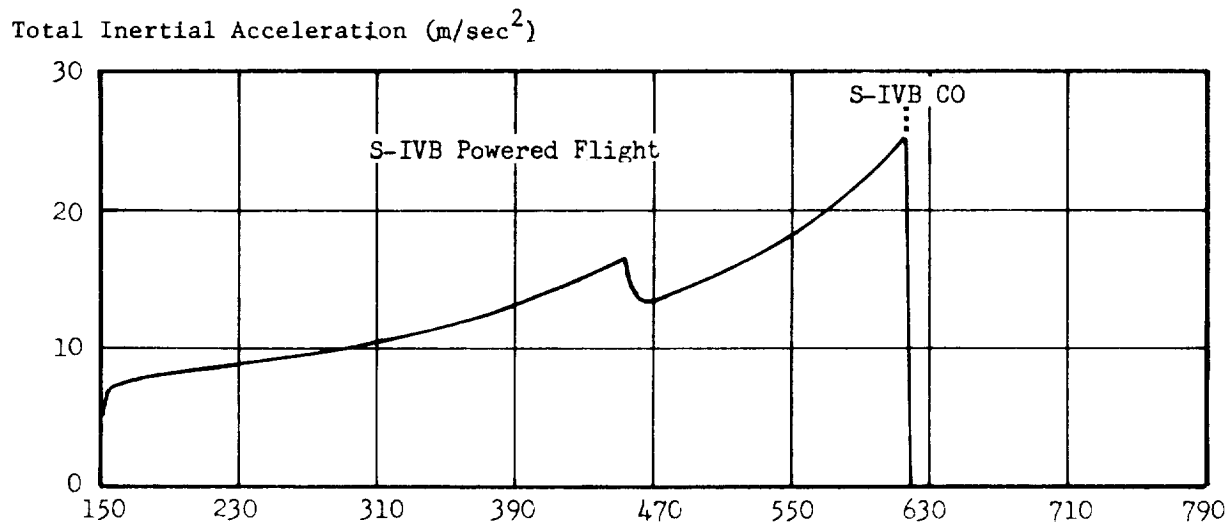


FIGURE 7-3 TOTAL INERTIAL ACCELERATION

TABLE 7-III
SIGNIFICANT EVENTS

EVENTS	PARAMETER	ACTUAL	NOMINAL	ACT-NOM
First Motion	Range Time (sec) Total Inertial Acceleration (m/s^2)	0.17 11.86	0.17 11.93	0.00 -0.07
Mach 1	Range Time (sec) Altitude (km)	62.15 7.63	61.55 7.65	0.60 -0.02
Maximum Dynamic Pressure	Range Time (sec) Dynamic Pressure (N/cm^2) Altitude (km)	75.5 3.20 12.16	75.0 3.16 12.32	0.5 0.04 -0.16
Maximum Total Inertial Acceleration (S-IB Stage)	Range Time (sec) Acceleration (m/s^2)	140.10 41.99	140.38 42.00	-0.28 -0.01
Maximum Earth-Fixed Velocity (S-IB Stage)	Range Time (sec) Velocity (m/s)	144.6 1978.2	143.6 1981.7	1.0 -3.5
Maximum Total Inertial Acceleration (S-IVB Stage)	Range Time (sec) Acceleration (m/s^2)	616.86 25.06	614.90 25.26	1.96 -0.20
Maximum Earth-Fixed Velocity (S-IVB Stage)	Range Time (sec) Velocity (m/s)	619.3 7378.8	616.6 7377.6	2.7 1.2

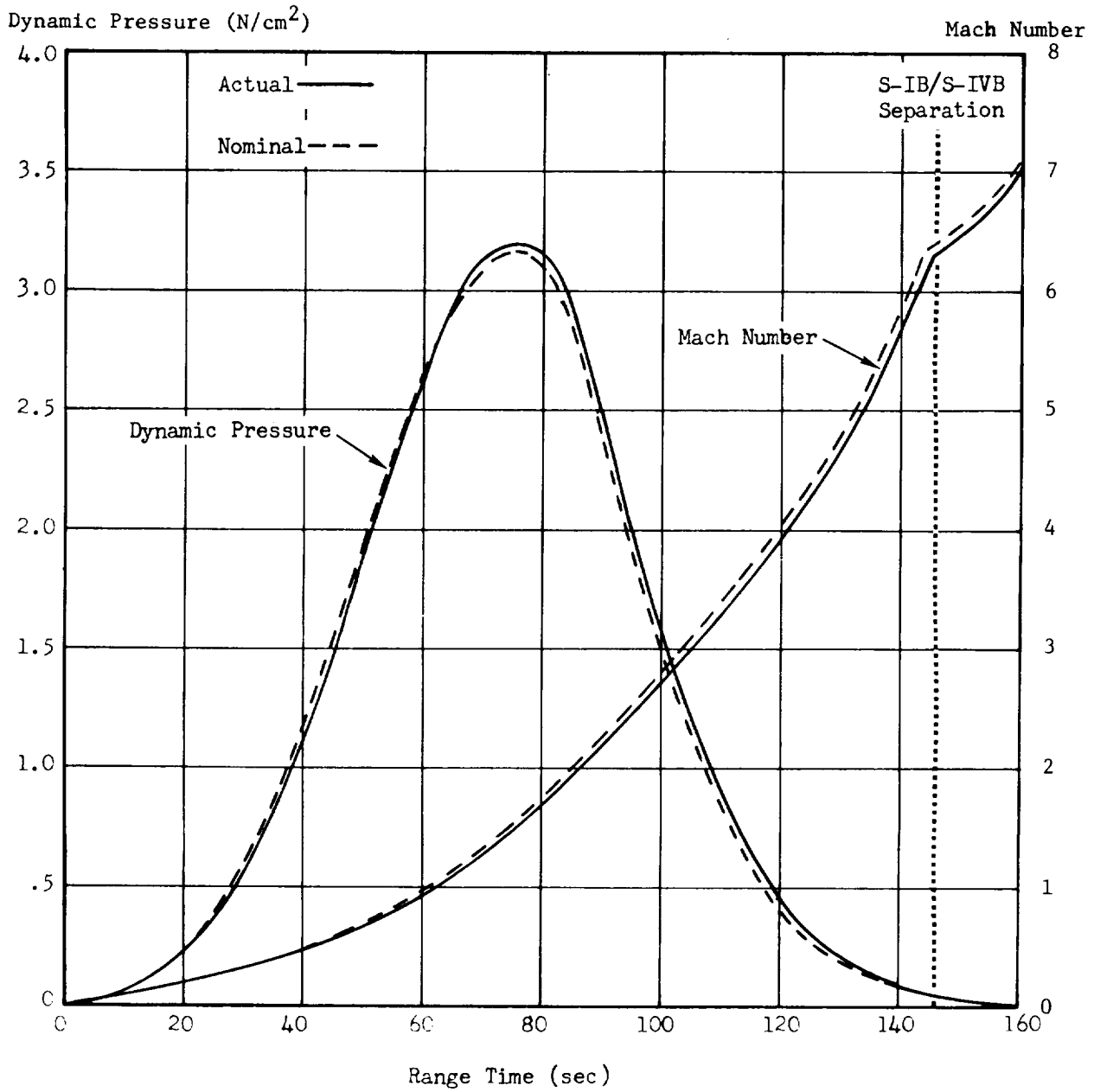


FIGURE 7-4 MACH NUMBER AND DYNAMIC PRESSURE

The free flight trajectory utilizing the tumbling drag coefficient data was considered as the actual trajectory for the S-IB booster stage. Tracking on previous flights has proven this method to be a close approximation. The impact point from this free-flight trajectory, provided the S-IB stage remained intact, was 75.72 deg west longitude and 29.76 deg north latitude. This is 490.8 km down range and occurred at 560.2 seconds.

The S-IVB/IU impacted at 81.6 deg east longitude and 8.9 deg south latitude, as indicated by Goddard impact data. Impact occurred at 162 hr: 27 min: 15 sec after launch (Rev. 108), on October 18, 1968.

The preflight predicted lifetime of the S-IVB stage based on a nominal passivation was 9.0 days with $\pm 2 \sigma$ error bounds of 12.3 and 6.8 days, respectively. At the end of the second revolution, an estimation of the orbital lifetime was made based on an Antigua vector at 1835 U.T. This estimated lifetime was 8.9 days nominal and 12.9 and 5.6 days as the $\pm 2 \sigma$ error bounds of this estimate.

The S-IVB was estimated to have actually impacted 162 hours, 27 minutes, 15 seconds after launch or an actual orbital lifetime of 6.77 days. Two reasons appear to explain the difference between the predicted lifetimes and the actual lifetime. Either the lifetime estimates made are very inaccurate (over 30 percent error in nominal prediction compared to actual lifetime) or significant venting took place to perturb the orbit of the S-IVB prior to loss of attitude control. To ascertain which of these two would best explain these differences, an orbit determination was made using C-Band tracking data on October 12, 1968. The orbital vector at 1146:56 U.T. on October 12th was utilized in determining an orbital lifetime prediction. This prediction yielded a nominal lifetime of 6.88 days with $\pm 2 \sigma$ error bounds of 8.16 and 6.11 days. This prediction is in error by less than 2 percent (comparing nominal predicted lifetime to the actual lifetime). It is therefore evident that some force, which probably is venting did perturb the orbit of the S-IVB and would explain the differences between the actual and predicted orbital decay and lifetime of the S-IVB stage. However, with the data available during this period, it is impossible to determine exactly when this venting occurred or its magnitude.

7.4 ORBITAL TRACKING DATA UTILIZATION

The orbital insertion conditions were determined by adjusting the estimated insertion parameters to fit the orbital tracking data in accordance with the respective weights assigned to the tracking data. The most reasonable solutions had a spread of ± 150 meters in position components and ± 1 m/s in velocity components. The best solutions were reached using revolution 1; Bermuda (FPS-16), Carnarvon, California, Merritt Island, and Patrick data.

The data utilized in the Orbital Correction Program to establish the insertion point are presented in Table 7-V. Orbital C-band radar tracking data are shown in Table 7-VI.

7.5 PARKING ORBIT TRAJECTORY

The parking orbit trajectory originates at S-IVB/CSM orbital insertion (626.75 sec) and continues until S-IVB/CSM separation (10502.4 sec). The trajectory parameters at orbital insertion were established by the best estimate trajectory in conjunction with the Orbital Correction Program. The trajectory parameters for orbital insertion and S-IVB/CSM separation, as obtained from the Orbital Correction Program, are presented in Tables 7-VII and 7-VIII. The orbital ground track is presented in Figure 7-5.

7.6 S-IVB ORBITAL SAFING EXPERIMENT TRAJECTORY

The programmed S-IVB propellant dump was initiated at 1 hr: 34 min: 28.95 sec (5668.95 sec) range time and was terminated at 1 hr: 46 min: 29.95 sec (6389.95 sec) range time. The orbital parameters at these times were calculated from the integrated trajectory, utilizing the telemetered guidance velocity data to determine the acceleration during the dump. A trajectory was also initiated at the start of the propellant dump and integrated through the dump period, assuming no acceleration due to dumping. This provides a theoretical calculated orbit, which would have occurred with no propellant dumping, as a basis for comparison. The orbital parameters at 1 hr: 46 min: 29.95 sec (6389.95 sec) from the theoretical trajectory are tabulated in Table 7-IX under the no-dump column. These parameters are compared to the parameters computed with the actual accelerations to determine the effects of the propellant dump on the orbit. The apogee and perigee of the S-IVB orbital phase were increased due to the safing experiment by 21.2 km and 0.4 km, respectively. The total space-fixed velocity was increased by 3.7 m/s due to the propellant dumping or safing experiment.

TABLE 7-v
INSERTION CONDITIONS DATA UTILIZATION

STATION	PARAMETER	NO. OF DATA POINTS	RMS ERROR
Bermuda (FPS-16)	Azimuth	29	0.006
	Elevation	28	0.013
	Range	29	5m
Carnarvon	Azimuth	50	0.003
	Elevation	50	0.008
	Range	52	6m
California	Azimuth	47	0.018
	Elevation	45	0.017
	Range	47	8m
Merrit Island	Azimuth	68	0.009
	Elevation	67	0.014
	Range	68	18m
Patrick	Azimuth	48	0.005
	Elevation	49	0.009
	Range	49	21m

TABLE 7-VI
SUMMARY OF C-BAND ORBITAL TRACKING

STATION	TYPE OF RADAR	REVOLUTION				
		1	2	3	4	5
Antigua	FPQ-6			X		
Ascension	TPQ-18			X		
Bermuda	FPS-16	X	X	X		
Bermuda	FPQ-6	X	X	X		
California	FPS-16	X	X	X	X	
Carnarvon	FPQ-6	X	X	X		
Hawaii	FPS-16		X			
Merritt Island	TPQ-18	X	X	X		
Patrick	FPQ-6	X	X			
Pretoria	MPS-25		X	X		
Tananarive	FPS-16			X	X	X
White Sands	FPS-16M	X		X		

TABLE 7-VII
S-IVB INSERTION PARAMETERS

PARAMETER	ACTUAL	NOMINAL	ACT-NOM
Range Time (sec)	626.75	624.80	1.95
Space-Fixed Velocity (m/s)	7788.6	7787.4	1.2
Altitude (km)	228.1	228.0	0.1
Range (km)	1892.3	1891.2	1.1
Cross Range, Y_E (km)	98.1	98.4	-0.3
Cross Range Velocity, Y_E (m/s)	544.9	544.9	0.0
Flight Path Angle (deg)	0.005	-0.002	0.007
Apogee (km)	282.1	277.5	4.6
Perigee (km)	222.3	222.1	0.2

TABLE 7-VIII
S-IVB/CSM SEPARATION PARAMETERS

PARAMETER	ACTUAL	NOMINAL	ACT-NOM
Range Time (sec)	10502.4	10495.17	7.23
Altitude (km)	246.8	240.2	6.6
Space-Fixed Velocity (m/s)	7772.3	7779.9	-7.6
Flight Path Angle (deg)	-0.30	-0.28	-0.02
Heading Angle (deg)	60.87	60.87	0.0

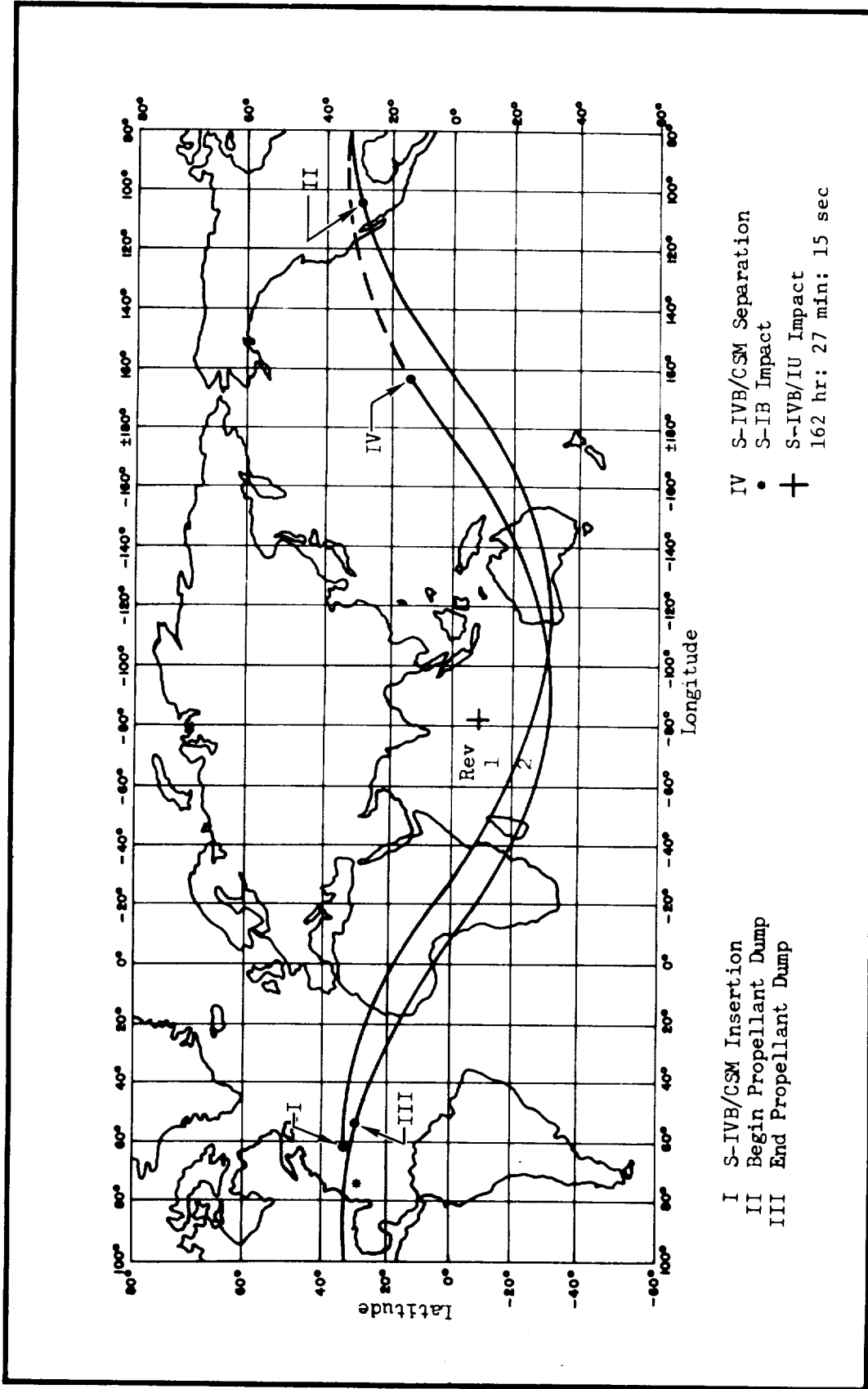


Figure 7-5 AS-205 GROUND TRACK

TABLE 7-IX
EFFECTS OF S-IVB ORBITAL SAFING EXPERIMENTS

PARAMETER	UNITS	BEFORE PROPELLANT DUMP	AFTER PROPELLANT DUMP	NO DUMP (THEORETICAL ORBIT)	ORBITAL EFFECTS (DUMP - NO DUMP)
Range Time	sec	5668.95	6389.95	6389.95	-----
Period	min	89.625	89.833	89.614	0.219
Apogee	km	289.2	309.2	288.0	21.2
	mm	156.1	167.0	155.5	11.5
Perigee	km	222.6	223.1	222.7	0.4
	mm	120.2	120.5	120.2	0.3
Space-Fixed Velocity	m/s	7788.2	7789.9	7786.2	3.7
	ft/s	25551.7	25557.3	25545.3	12.0
Flight Path Angle	deg	-.0954	.1745	.1216	0.0529
Inclination	deg	31.6172	31.6136	31.6135	0.0001
Eccentricity	-	0.0050	0.0065	0.0049	0.0016

8.0 S-IB PROPULSION

8.1 SUMMARY

The S-IB propulsion and associated systems performed satisfactorily throughout flight, providing the proper thrust, specific impulse, and propellant flowrates to fulfill the stage objectives. On the basis of engine analysis; the stage thrust, propellant flowrate, and specific impulse averaged 0.06%, 0.06%, and 0.002% higher than predicted, respectively. All eight engines ignited satisfactorily with the proper sequencing between starting pairs. Inboard Engine Cutoff (IECO) occurred at 140.64 sec, 0.36 sec later than predicted. Outboard Engine Cutoff (OECO) occurred at 144.32 sec, 1.04 sec later than predicted. OECO was initiated 3.68 sec after IECO by deactivation of the thrust OK pressure switches due to LOX starvation.

The propellant utilization system functioned as expected. The consumption ratio was low during flight and was responsible for the utilization of approximately 204.1 kg (450 lbm) of the fuel residual at OECO.

8.2 S-IB PROPULSION PERFORMANCE

The S-IB stage propulsion system flight performance was determined by reconstruction of the flight with the Mark IV computer program. The Mark IV program is a mathematical model of the Saturn IB stage propulsion system, utilizing a table of influence coefficients to determine engine performance. Input data were obtained from telemetry flight measurements, and from calculated propellant loads and residuals. A program option, RPM match, was used to arrive at engine power levels and propellant flowrates. When flight results are compared to pre-launch predictions, the prediction is that value given for an October launch month in Reference 15.

8.2.1 STAGE PERFORMANCE

All eight H-1 engines ignited satisfactorily. The automatic ignition sequence, which schedules the engines to start in pairs with a 100 millisecond (ms) delay between each pair, began with ignition command at -2.988 seconds. The recorded individual engine ignition signals are shown in the top portion of Table 8-I. In the bottom portion of Table 8-I, thrust chamber ignition and main propellant ignition (P_c prime) times are shown referenced to the individual engine's ignition signal. The nominal times from 200 K H-1 engines in cluster firings are also shown.

Table 8-I. Engine Start Characteristics

Engine Position	Time from Ignition Command to Engine Ignition Signal (ms)	
	Actual	Programmed
5 and 7	13	10
6 and 8	112	110
2 and 4	212	210
1 and 3	313	310

Engine Position	Time from Engine Ignition Signal (ms)	
	Thrust Chamber Ignition	Pc Prime
5	570	878
7	530	869
6	540	875
8	544	879
2	545	884
4	519	881
1	535	893
3	545	872
Average	541	879
Nominal *	575.5	899.4

* Nominal from cluster tests of S-IB-1 through S-IB-5.

Individual engine thrust buildup and stage thrust buildup are presented in Figure 8-1. The stage thrust shown is the sum of the individual engine thrusts and does not account for engine cant angles.

S-IB stage performance throughout flight was satisfactory. Figure 8-2 shows inflight stage longitudinal thrust and specific impulse determined from analysis of engine measurements. Stage inflight performance parameters, averaged from first motion to IECO, are shown in Table 8-II. With the exception of the LOX density deviation, the prediction/reconstruction discrepancies were the smallest ever observed. S-IB stage propellant mixture ratio and flowrate are shown in Figure 8-3. Stage LOX and fuel flowrates are shown in Figure 8-4.

Several factors contributed to the small discrepancies noted in Table 8-II. These factors and their effect on the stage parameters are tabulated in Table 8-III.

Table 8-III shows that the largest deviations from predicted performance were due to LOX temperature and engine tag data. The LOX temperature was about 0.56° K (1° F) warmer than predicted, primarily due to the very high surface winds (20 knots). High surface winds increase the heat transfer rate to the LOX. The warmer than predicted LOX temperature lowered the thrust, specific impulse, and mixture ratio. However, the effects on thrust and specific impulse were almost entirely nullified by the higher than predicted engine tag data and other parameters listed in Table 8-III. The effect of the deviations on the mixture ratio was the prime factor contributing to time base 2 (TB₂) initiation by a fuel low-level sensor.

The overall differences in engine performance from predicted, attributed to engine tag data, were some of the smallest ever experienced. Engine performance was not predicted to be the same as either Rocketdyne or stage test data. Average data from the Rocketdyne single engine acceptance data were empirically changed in accordance with the deviations from Rocketdyne test data experienced in the flights of S-IB-1, S-IB-2, S-IB-3, and S-IB-4.

The cutoff sequence on the S-IB stage began at 137.49 sec with the actuation of a fuel low-level cutoff probe. Inboard Engine Cutoff (IECO) was initiated 3.15 sec later by the Launch Vehicle Digital Computer (LVDC) at 140.64 seconds. IECO occurred 0.36 sec later than predicted.

Thrust decay on each inboard engine was normal. The total inboard engine cutoff impulse was 1,140,960 N-s (256,498 lbf-s).

Outboard engine cutoff (OECO) occurred at 144.32 sec due to the deactivation of the thrust OK pressure switches of all four outboard engines. It was expected that OECO would be initiated by thrust OK pressure switch (TOPS) deactuation when LOX

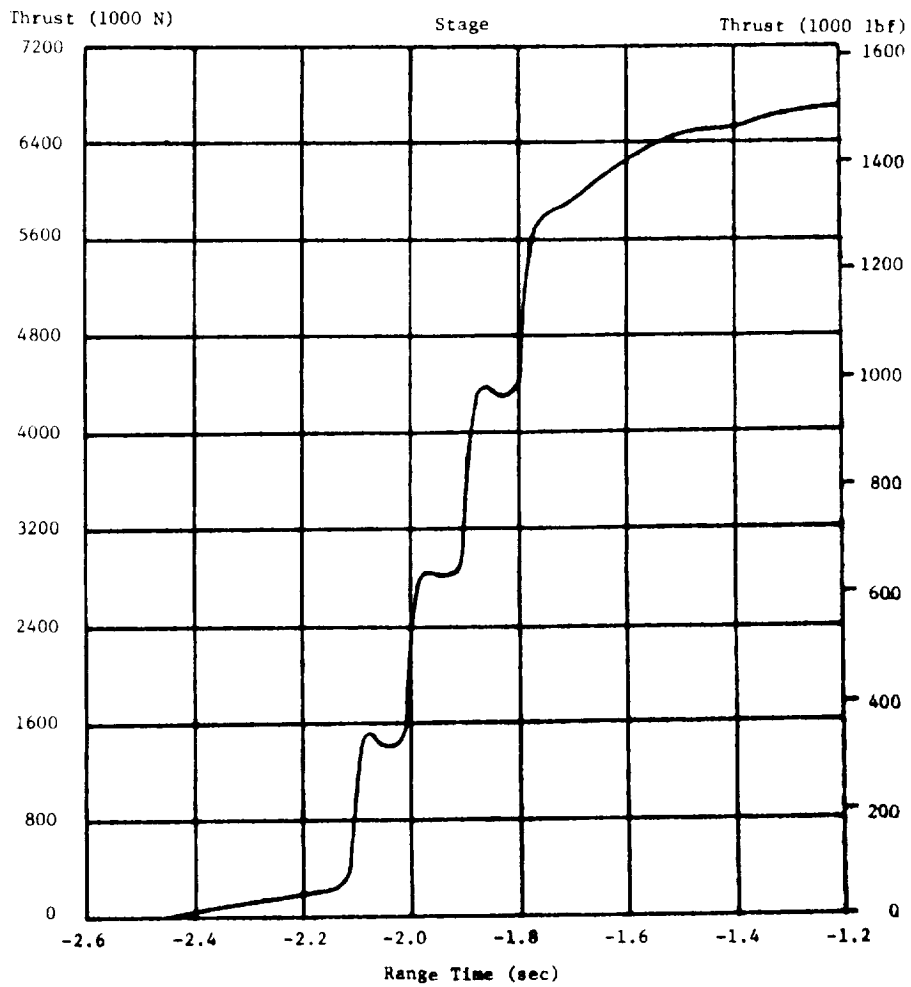
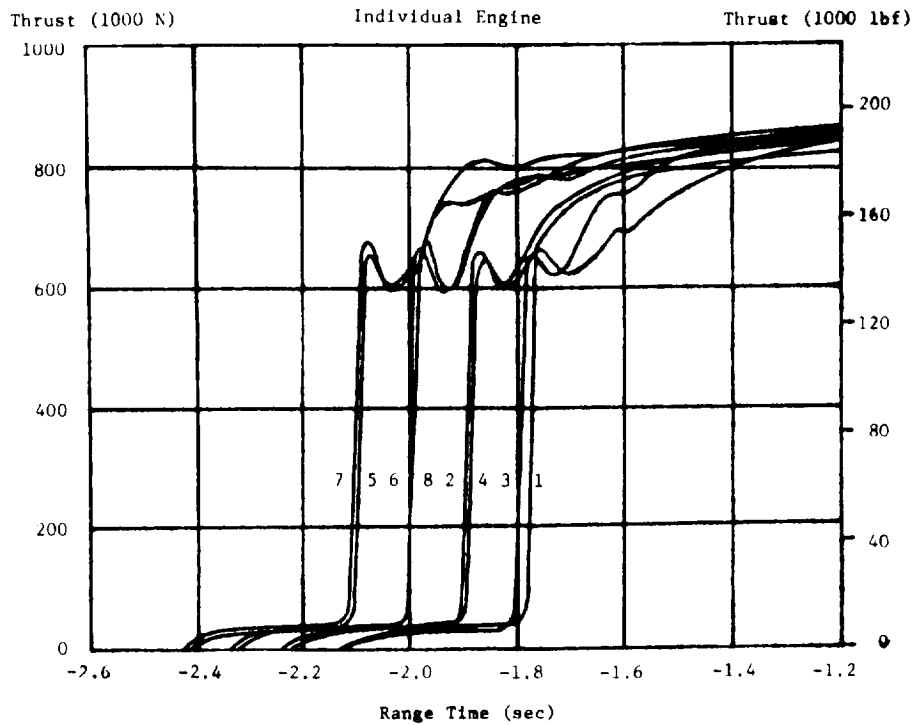


FIGURE 8-1 S-1B INDIVIDUAL ENGINE AND STAGE THRUST BUILDUP

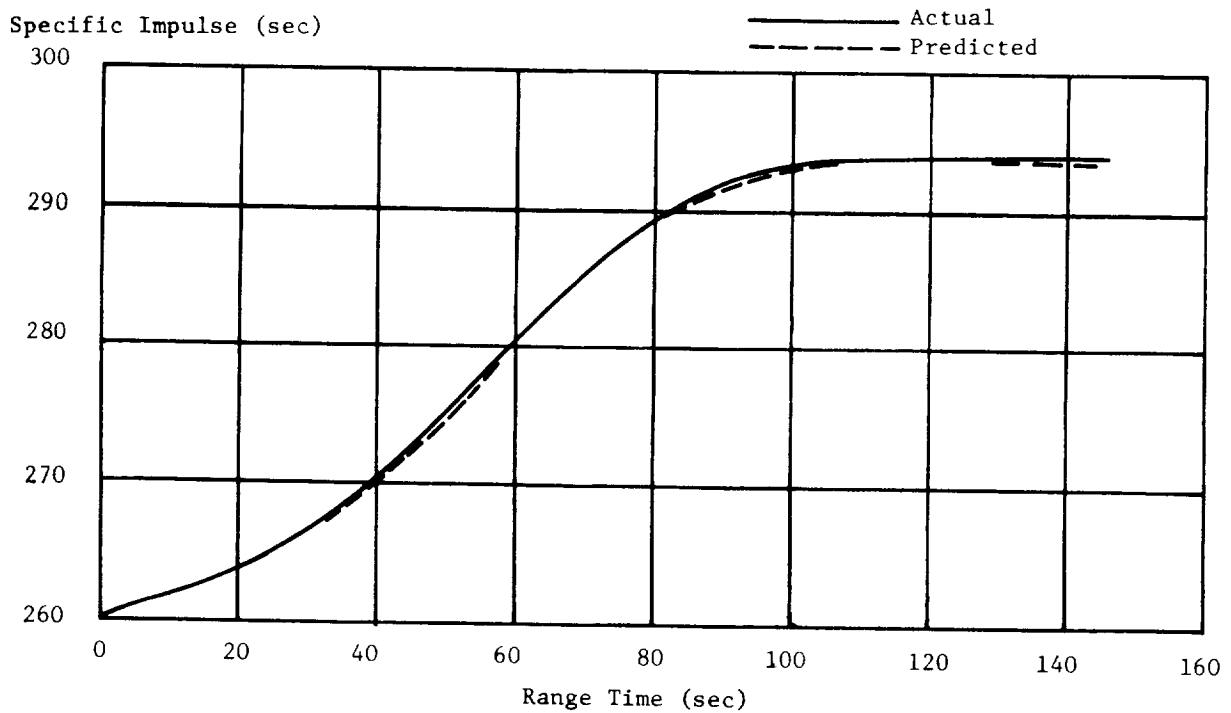
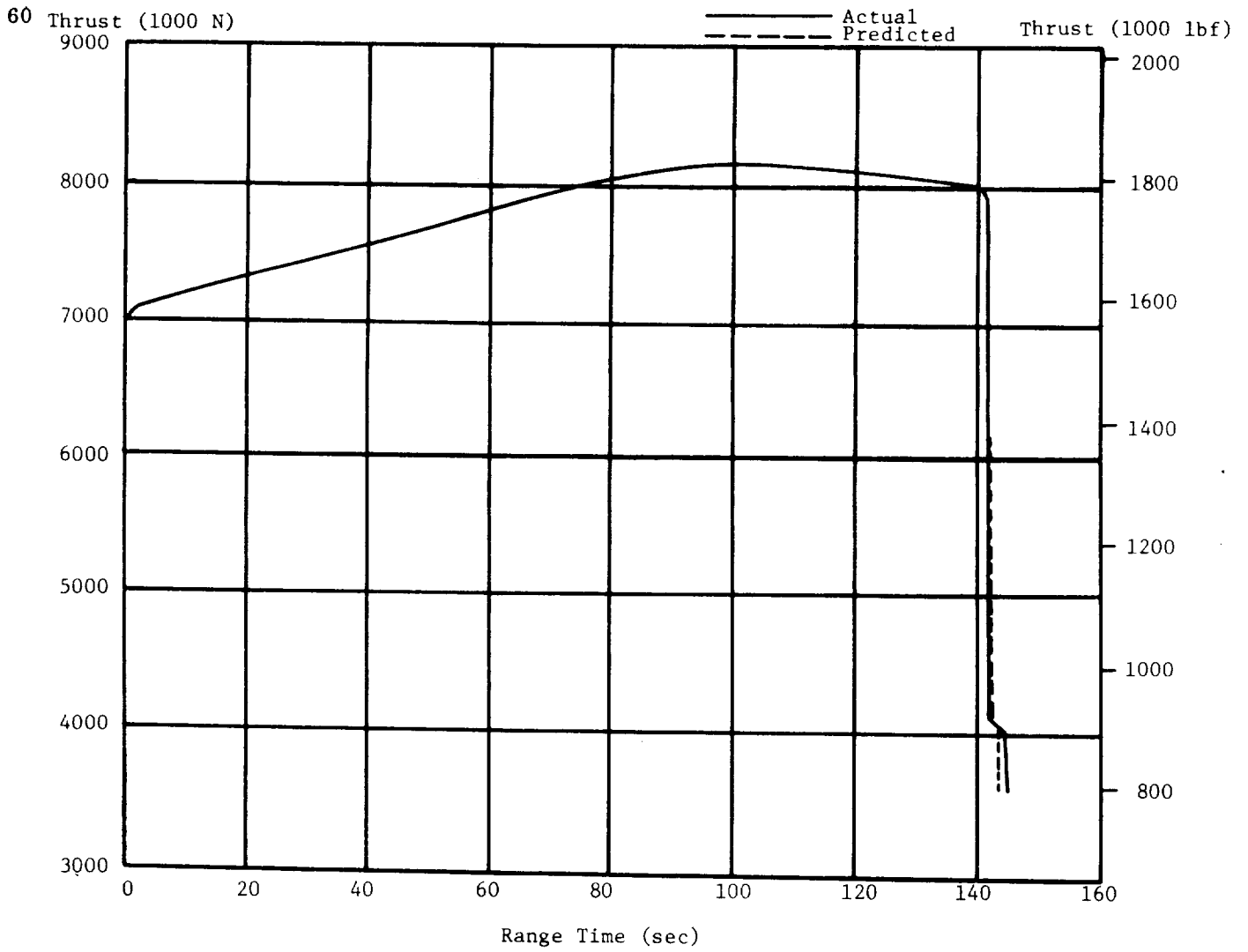


FIGURE 8-2 S-IB STAGE LONGITUDINAL THRUST AND SPECIFIC IMPULSE

Table 8-II. Stage Performance Parameters
(Overall Flight Average)

Parameter	Predicted	Actual	Deviation	% Deviation
Thrust (N) (LBF)	7,755,030.	7,759,478	4448.	+0.06
	1,743,400	1,744,400	1000.	
Specific Impulse (sec)	281.484	281.491	+0.007	+0.002
LOX Flowrate (kg/s) (lbm/s)	1,960.02	1,957.66	-2.35	-0.12
	4,321.10	4,315.91	-5.19	
Fuel Flowrate (kg/s) (lbm/s)	849.35	853.25	3.90	+0.46
	1,872.50	1,881.09	8.59	
Total Flowrate (kg/s) (lbm/s)	2,809.37	2,810.91	1.54	+0.06
	6,193.60	6,197.00	3.40	
Stage Mixture Ratio (LOX/Fuel)	2.3076	2.2943	-0.0133	-0.58

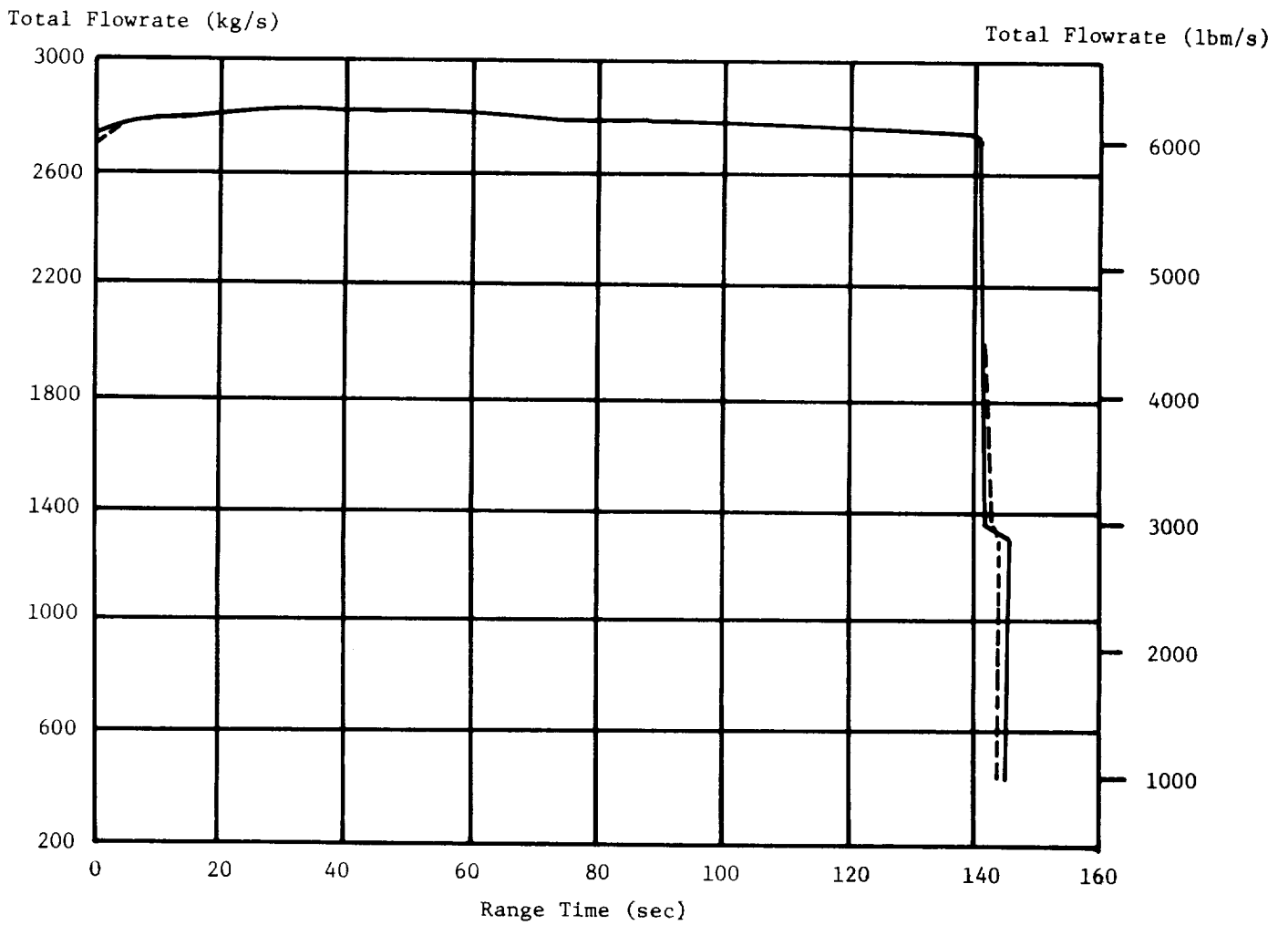
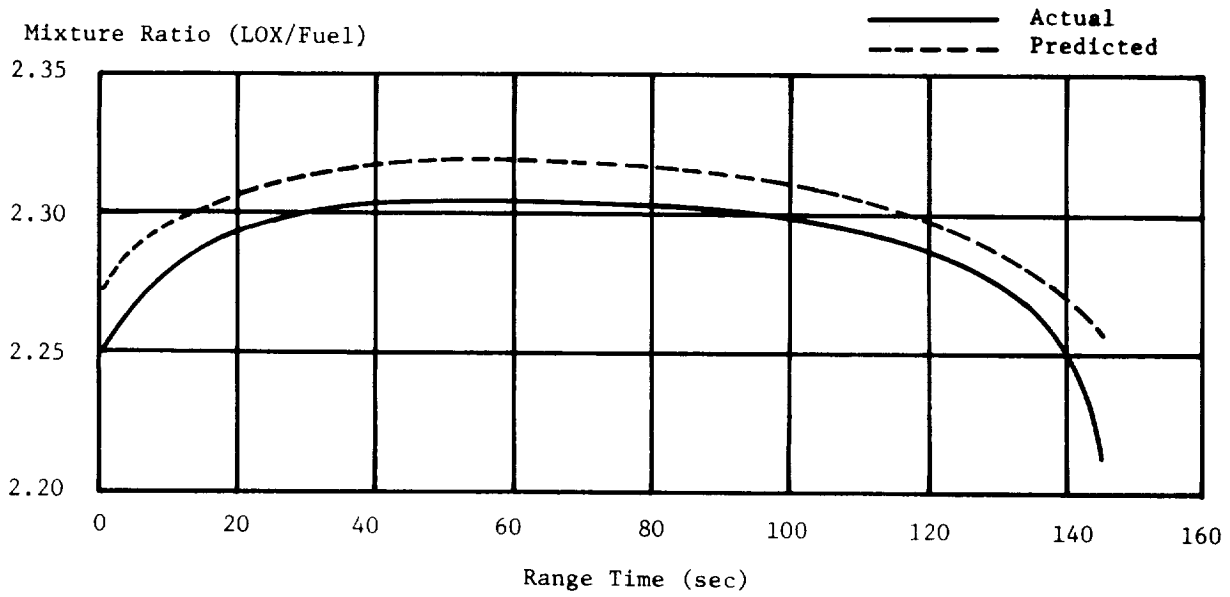


FIGURE 8-3 S-IB STAGE PROPELLANT MIXTURE RATIO AND FLOWRATE

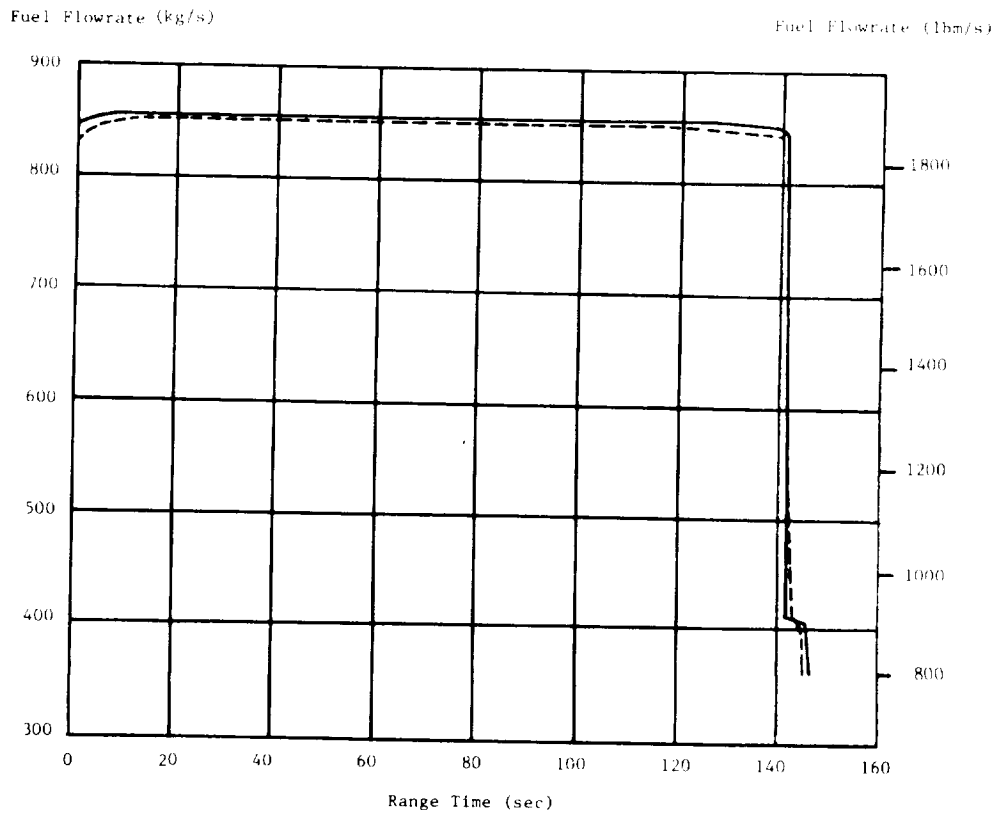
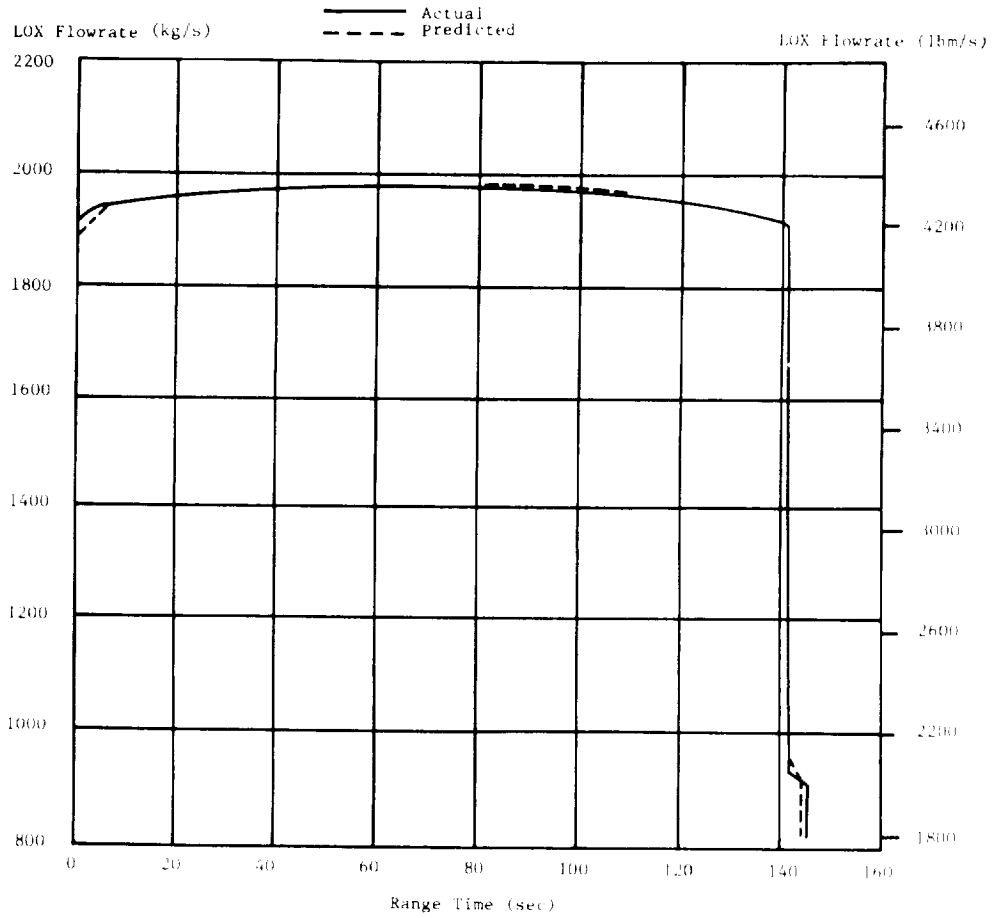


FIGURE 8-4 S-1B STAGE LOX AND FUEL FLOWRATES

Table 8-III. Inflight Performance Deviation Analysis

PARAMETER	Deviation from Predicted	Percent Deviation From Predicted		
		Thrust	Specific Impulse	Mixture Ratio
LOX Pump Inlet Temperature	+0.56 ^o K (+1.0 ^o F)	-0.44	-0.09	-0.40
Fuel Temperature & Density	+1.32 ^o K (+2.37 ^o F) -0.40 kg/m ³ (-0.025 lbm/ft ³)	+0.11	+0.02	+0.03
LOX Pump Inlet Pressure	+0.56 N/cm ² (+0.811 psi)	+0.12	-0.02	+0.10
Fuel Pump Inlet Pressure	+0.77 N/cm ² (+1.111 psi)	-0.05	+0.02	-0.12
Engine Tag Data	-	+0.27	+0.04	-0.24
Misc. Effects	-	+0.05	-0.008	+0.05
Observed Deviation		+0.06	+0.002	-0.56

starvation occurred. The expected time differential between IECO and OECO was 3.0 sec, with an actual time differential of 3.68 seconds. The longer-than-predicted time differential resulted from the significantly lower-than-predicted mixture ratio due primarily to the warm LOX. This caused a fuel level sensor actuation starting TB₂ instead of a LOX level sensor actuation as predicted. It also caused a larger than predicted amount of LOX to be onboard at IECO. This LOX had to be consumed during the four outboard engines burn to achieve a LOX starvation initiation of time base 3 (TB₃). This mode of TB₂ initiation can result in as much as 4 sec of four-engine burn before initiation of TB₃. In this extreme case, TB₃ can begin with actuation of the fuel depletion sensors.

It is estimated that the fuel level at the end of outboard engine thrust decay was at or slightly below the fuel depletion probes. Total cutoff impulse for the outboard engine was 718,228 N-s (161,464 lbf-s).

8.2.2 INDIVIDUAL ENGINE CHARACTERISTICS

The performance of all eight engines was satisfactory. Thrust levels for all engines averaged 551 N (124 lbf) or 0.06% higher than predicted for each engine. The average deviation from predicted specific impulse was +0.007 sec, or +0.002% higher than predicted. Figure 8-5 shows the average deviation from predicted thrust and specific impulse for engines 1 through 8 between first motion and IECO.

Individual engine flight performance data from the Mark IV Reconstruction Program were reduced to Sea Level and Standard Turbopump inlet conditions to permit comparison of flight performance with predicted and preflight test data. The reduction of engine data to Sea Level Standard conditions isolates performance variations due to engine characteristics from those attributable to engine inlet and environmental conditions.

The following discussion applies to the sea level performance at 30 seconds. This is the time period for which sea level performance is normally presented, and the flight prediction is based on test data obtained at this point. Analysis of post-flight data, along with static test data, indicated a pronounced increase in sea level performance occurring during the first 30 sec of flight, with a less pronounced increase occurring between this time and cutoff. The increase in sea level performance during the first 30 sec has been attributed to non-equilibrium engine operation and has been satisfactorily accounted for in the prediction. Sea level thrust, specific impulse, and mixture ratio are compared with predicted values at a time slice of 30 sec in Table 8-IV.

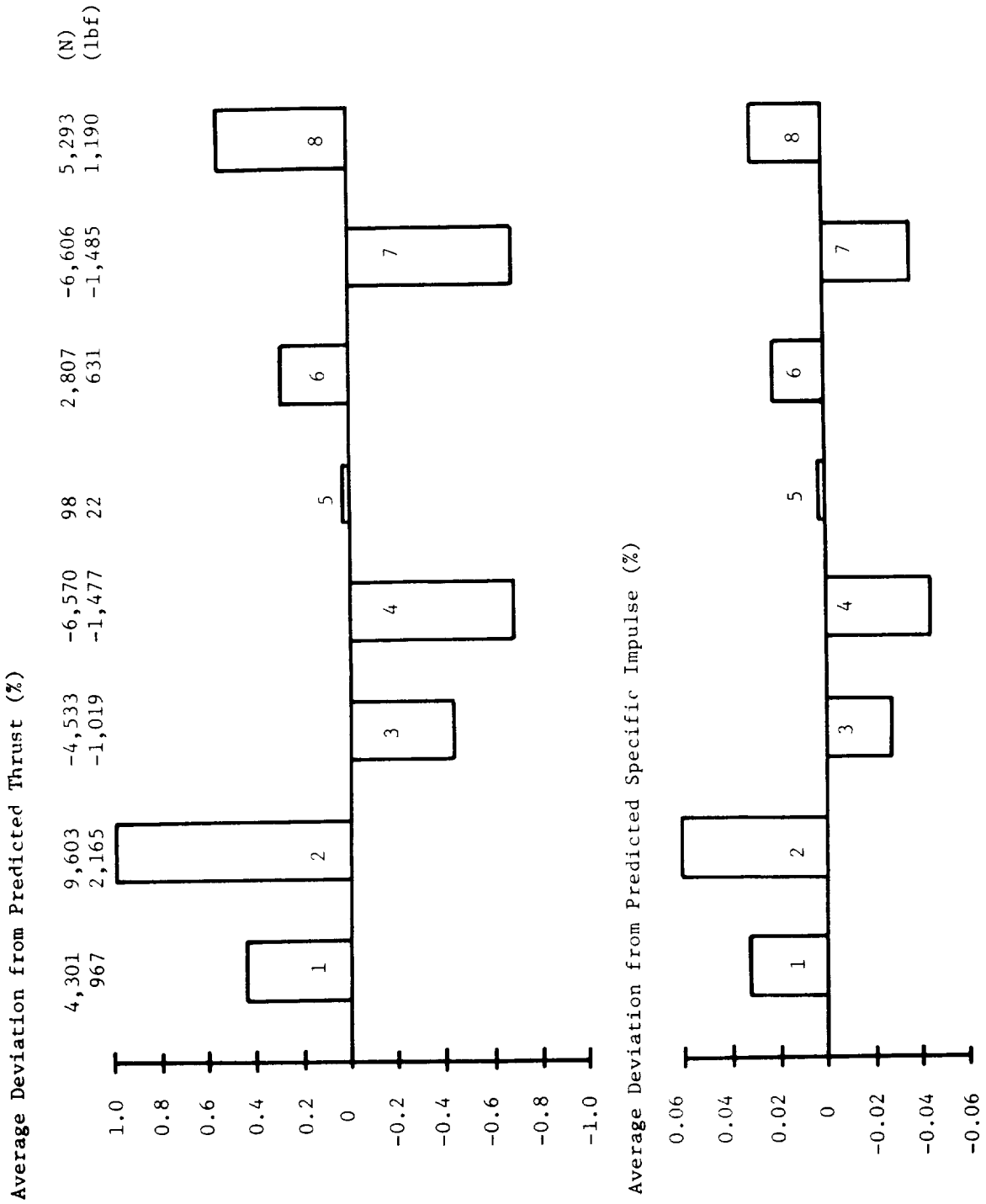


FIGURE 8-5 DEVIATION IN ENGINE PERFORMANCE PARAMETERS (FLIGHT TIME AVERAGE)

Table 8-IV. AS-205 Average Individual Engine Performance at 30 Seconds

Sea Level Parameters	Units	Actual	Predicted	Actual-Predicted	% Deviation
Engine Thrust	N	887,629	885,232	2398	0.27
Mixture Ratio	lbf LOX/Fuel	199,547 2.2476	199,008 2.2531	539 -0.0055	-0.24
Specific Impulse	sec	262.21	262.10	0.11	0.04

8.2.3 LOX SEAL DRAIN LINE TEMPERATURES

For the first time, flight telemetry measurements were made of the temperature inside the primary LOX seal drain line of each engine. The added instrumentation was necessary to prevent liftoff with a leaking turbopump LOX shaft seal. A similar occurrence during the static test of S-IB-11 caused a gear-case explosion. Because the leak, by nature, would occur quickly, the output of all 24 elements (3 elements on each of 8 engines) was supervised and electrically programmed to cause engine cutoff and prevent liftoff if 2 of the 3 thermocouple elements on any engine indicated a LOX seal leak. The criterion was established that a drain line temperature colder than 116.5°K (-250°F) indicated LOX presence in the line and, therefore, an unacceptable LOX leak.

Prior to the AS-205 launch, the data taken during the static test of S-IB-12 furnished the only valid data sample of drain line temperature history. Drain line temperatures had been measured in previous static tests but never with the tri-element sensor, bellows-type LOX shaft seal combination. The average pre-ignition temperature based upon the static test data was 161.8°K (-168.5°F). This compares with 173.0°K (-148.3°F) average at -10.0 sec on AS-205.

The inflight LOX drain line temperatures generally bore little resemblance to the static test temperature data taken from S-IB-12. All temperatures show a rise at engine ignition of approximately 11.7°K (21°F), the smallest being 7.8°K (14°F) and the largest 22.2°K (40°F). Of special interest is the fact that all drain line temperatures except engine 4 show a definite cooling trend between 90 and 100 sec which varies in rate and magnitude. No environmental conditions occurred at this time which could be connected with the cooling trend.

In spite of the unexpected temperatures, it appears no failures of the LOX shaft seal occurred. The temperature variations may be the result of the flight environment of acceleration and trajectory, and will be compared with future flight temperatures.

8.3 S-IB PROPELLANT USAGE

Propellant usage is expressed as the ratio of propellant consumed to propellant loaded, and is an indication of the propulsion system performance and the capability of the propellant loading system to load the correct propellant weights. Predicted and actual percentages (by weight) of loaded propellants utilized during the flight are shown in table 8-V.

Table 8-V. Propellant Usage

Propellant	Predicted (%)	Actual (%)
Total	99.14	99.32
Fuel	98.24	98.75
LOX	99.53	99.56

The planned mode of OEEO was by LOX starvation. The LOX and fuel level cutoff probe heights and flight sequence settings were adjusted to yield a 3.2 sec time interval between any cutoff probe actuation and IEEO, and a planned time interval between IEEO and OEEO of 3.0 seconds. OEEO was to be initiated by the deactuation of two of the three thrust OK pressure switches on any outboard engine as a result of LOX starvation. It was assumed that approximately 0.284 m³ (75 gallons) of LOX in the outboard suction lines was usable. The backup timer (flight sequencer) was set to initiate OEEO 10.1 sec after level sensor actuation. To prevent fuel starvation, fuel depletion cutoff probes were located in the F2 and F4 container sumps. The center LOX tank sump orifice was 48.3 ± 0.013 cm (19.0 ± 0.005 in) in diameter. Center LOX tank level was predicted to be 7.6 cm (3.0 in) higher than the LOX level in the outboard tanks at IEEO.

The fuel bias for S-IB-5 was 453.6 kg (1000lbm). This was included in the predicted residual and was available for consumption prior to IEEO. An additional 388.6 kg (850 lbm) of the predicted residual was available for consumption prior to OEEO if a significantly lower than predicted consumption ratio was experienced. A low consumption ratio during the flight was responsible for the utilization of approximately 204.1 kg (450 lbm) of the additional 388.6 kg (850 lbm) of fuel.

Data used in evaluating the S-IB propellant usage consisted of two discrete probe racks of 15 probes each in F1 and F3; three discrete probe racks of 3 probes each 0C, 01, and 03; cutoff level sensors in 02, 04, F2, and F4; and fuel depletion probes in the F2 and F4 sumps. The first discrete probe in LOX tank 03 failed to actuate, and data from the thirteenth discrete probe in fuel tank F3 was lost due to either inflight calibration or probe failure.

The cutoff sequence of S-IB-5 was initiated by a signal from the cutoff level sensor in either fuel tank F2 or F4 at 137.48 seconds. (Actuation of sensors was simultaneous within measurement limits.) The LVDC initiated TB₂ 0.01 sec later

at 137.49 seconds. The IECO signal was received 3.15 sec later at 140.64 seconds. OECO occurred 3.68 sec after IECO at 144.32 sec due to LOX starvation. Fuel depletion probes actuated only after retrorocket ignition.

Based on discrete and cutoff sensor probe data, the liquid levels in the fuel tanks were nearly equal and approximately 45.7 cm (18 in) above theoretical tank bottom at IECO. This level represents 4315 kg (9,513 lbm) of fuel onboard. At that time, 5268.9 kg (11,616 lbm) of LOX remained onboard. Corresponding LOX liquid height in the center tank was approximately 38.1 cm (15 in), and the average height in the outboard tanks 29.2 cm (11.5 in) above theoretical tank bottom. Propellants remaining above the main valves after outboard engine thrust decay were reconstructed as 1247 kg (2,750 lbm) of LOX and 1565 kg (3,450 lbm) of fuel. Predicted values for these quantities were 1356 kg (2,989 lbm) of LOX and 2208 kg (4,867 lbm) of fuel. The reconstructed fuel residual of 1565 kg (3,450 lbm) represents a liquid level below the position of the fuel depletion sensors; however, since the sensors did not actuate, it is probable that the actual weight of the fuel residual was higher than 1565 kg (3,450 lbm). No continuous liquid level measurements were available on S-IB-5; so no rigorous attempt was made to determine exact liquid level versus time after IECO.

The cutoff probe signal times and setting heights from theoretical tank bottom are shown below.

Table 8-VI. Cutoff Probe Activation Characteristics

Container	Height		Activation Time (sec)
	(cm)	(in)	
02	69.80	27.48	137.81
04	69.80	27.48	137.81
F2	84.77	33.375	137.48
F4	84.77	33.375	137.48

8.4 S-IB PRESSURIZATION SYSTEMS

8.4.1 FUEL PRESSURIZATION SYSTEM

The fuel tank pressurization system performed satisfactorily during the entire flight. The helium blowdown system used on this flight was identical to that used on S-IB-3, which included the 0.55 m³ (19.28 ft³) titanium spheres, lightweight tanks,

and fuel vent valves. The measured absolute ullage pressure is compared with the predicted pressure in the upper portion of Figure 8-6. Measured ullage pressure compared favorably to the predicted pressure and never exceeded a difference of 1.4 N/cm^2 (2.0 psi). The Digital Events Evaluator (DEE) showed that fuel vent valves 1 and 2 were closed at the beginning of the pressurization sequence and remained closed throughout the flight, as planned.

The helium sphere pressure is shown in the lower portion of Figure 8-6, along with the predicted curve. Initial sphere pressure, which can vary from 1,941 to $2,206 \text{ N/cm}^2$ (2,815 to 3,200 psi), is the most significant factor affecting ullage pressure. Telemetry data shows it to have been approximately $1,999 \text{ N/cm}^2$ (2,900 psi) at ignition, which was slightly lower than the initial predicted value.

Discrete probe data revealed that the behavior of the fuel tank liquid levels during flight was very similar to that seen on AS-204. The maximum recorded difference between the levels in tanks F1 and F3 was 12.7 cm (5.0 in) at 11 seconds. The levels converged to equal heights at approximately 120 seconds.

The 3.93% ullage volume was pressurized to 22.3 N/cm^2 (32.3 psi) in 2.912 seconds. Between the initial pressurization time and ignition, one more pressurizing cycle was necessary because of system cooldown.

8.4.2 LOX PRESSURIZATION SYSTEM

The LOX tank pressurization system performed satisfactorily during the AS-205 flight. The system configuration was the same as that flown on S-IB-4.

Pressurization of the LOX tanks provides increased structural rigidity and adequate LOX pump inlet pressures. Prelaunch prepressurization was achieved with helium from a ground source. From vehicle ignition command to liftoff, helium bypass flow was used to augment normal prepressurization flow. This maintained adequate pump inlet pressure during engine start.

The LOX tank pressurizing switch, which had an actuation range of $39.8 \pm 0.6 \text{ N/cm}^2$ (57.7 ± 0.8 psi), actuated at 39.3 N/cm^2 (57.0 psi) for all six prepressurizing cycles. Dropout occurred at 38.6 N/cm^2 (56.0 psi) for all cycles. Initial pressurization was started at -102.93 sec and continued for 53.787 seconds. Orifice bypass flow was initiated at -2.357 seconds. The reconstructed LOX tank ullage volume prior to vent closure was 3.41 m^3 (901 gal) or 1.34%.

In the upper portion of Figure 8-7, center LOX tank pressure during flight is compared with the predicted LOX tank pressure derived from static test and postflight data. The slight oscillation at about 9 sec was due to the GOX flow control valve (GFCV) response to the tank pressure drop during the ignition transient.

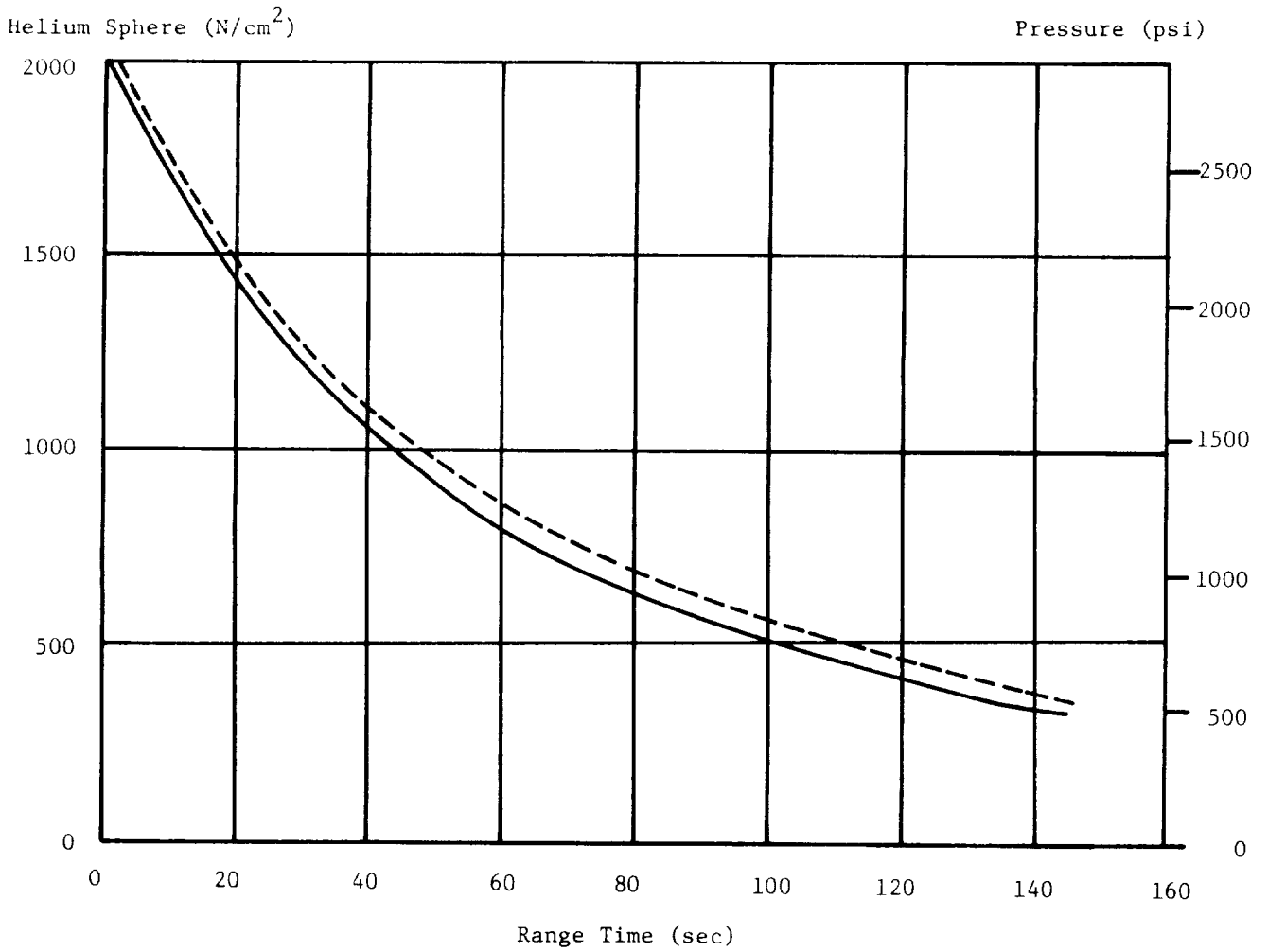
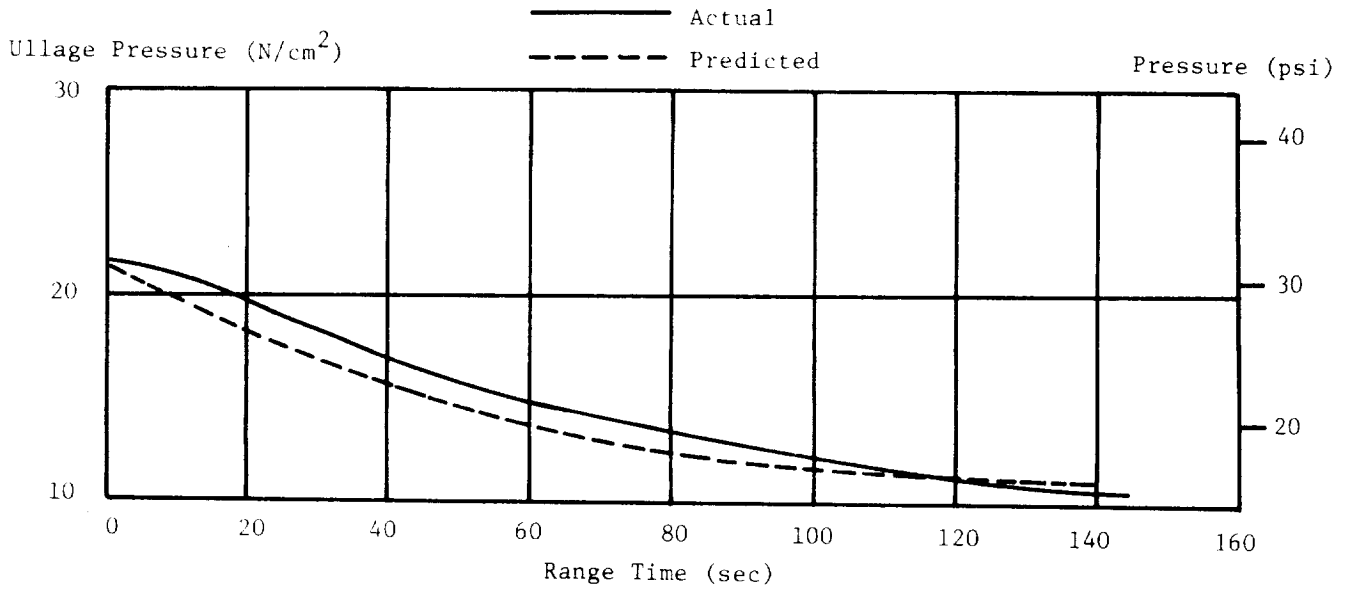


FIGURE 8-6 FUEL TANK ULLAGE AND HELIUM SPHERE PRESSURES

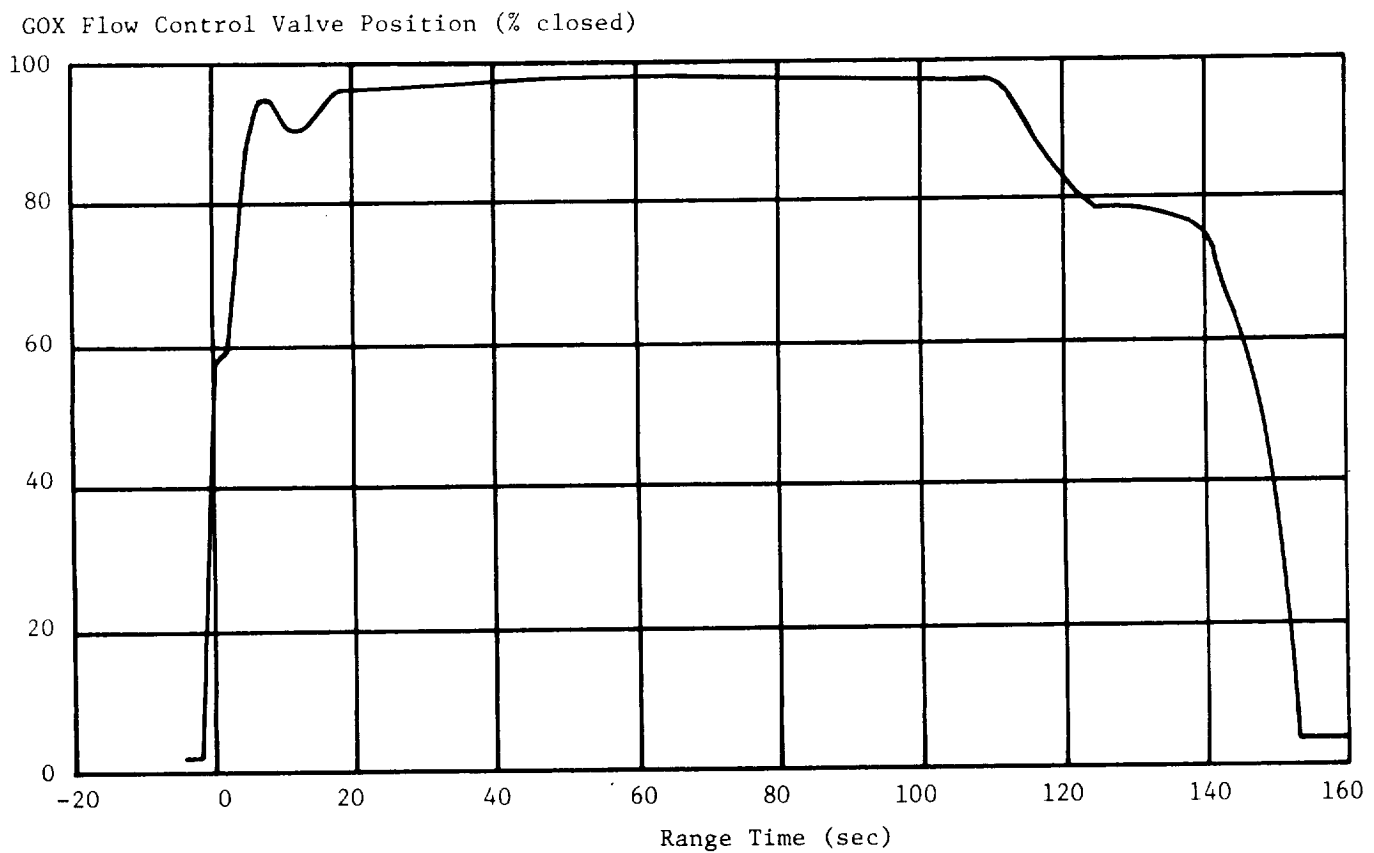
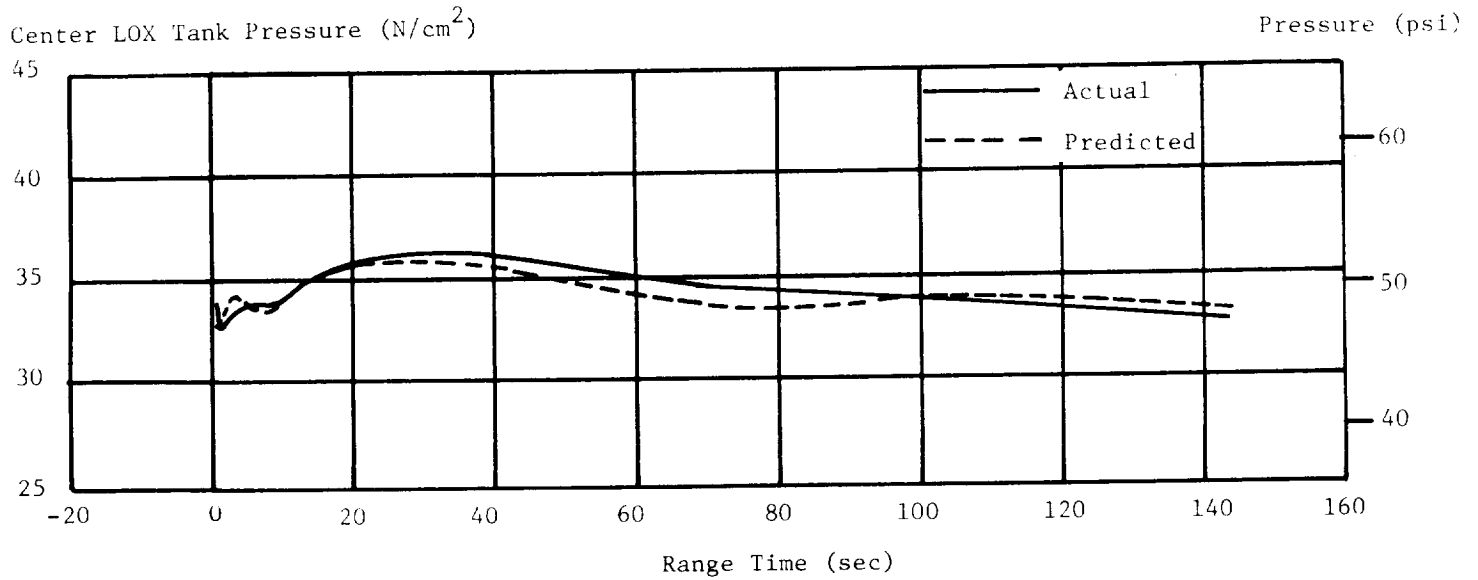


FIGURE 8-7 LOX PRESSURIZATION SYSTEM CHARACTERISTICS

The maximum pressure of approximately 36.2 N/cm^2 (52.5 psi) occurred at 33 sec, with tank pressure gradually decaying to 33.1 N/cm^2 (48 psi) at IECO.

The GFCV started to close at ignition and, after the normal hesitations during start transient, reached the full closed position at approximately 17 seconds. The valve appeared to continue closing after 17 sec due to a suspected calibration or measurement shift (lower portion of Figure 8-7). At 17 sec, the center tank ullage pressure was 35.5 N/cm^2 (51.5 psi), well above the GFCV nominal pressure setting of 34.5 N/cm^2 (50.0 psi), where the valve should have been closed.

The GFCV remained in the closed position until 108 sec when decreased LOX tank pressure caused it to start opening. At IECO, the valve was approximately 74% closed. Predicted GFCV positions are not given because the valve was removed after static test for refurbishment, invalidating the basis for the prediction. The pressure and temperature upstream of the GFCV were as expected and indicated nominal GOX flowrate.

8.4.3 CONTROL PRESSURE SYSTEM

The S-IB control pressure system was essentially the same configuration as used on the S-IB-4 stage. GN_2 , at a regulated pressure of 517 N/cm^2 (750 psi), was supplied to pressurize the eight H-1 engine turbopump gearboxes and to purge the LOX pump seals and two radiation calorimeters. Regulated pressure was also available to operate one LOX vent and relief valve and was used to close the LOX and fuel prevalues at IECO and OECO.

System performance was satisfactory throughout the flight. The flight sphere pressure history always remained within the acceptable limits. The regulated pressure decayed from 523 to 520 N/cm^2 (759 to 754 psi) during the flight.

9.0 S-IVB PROPULSION AND ASSOCIATED SYSTEMS

9.1 SUMMARY

The performance of the S-IVB stage propulsion system was satisfactory throughout flight. All average steady state performance values were within 0.24% of predicted.

On the basis of flight simulation, the overall average S-IVB thrust, mass loss rate, and specific impulse were 0.14% higher, 0.11% lower, and 0.24% higher than predicted, respectively. S-IVB guidance cutoff occurred at 616.75 sec, 1.95 sec later than predicted.

The PU system operated in the open loop configuration and provided an average propellant mixture ratio of 5.5 to 1 during the high thrust period and 4.45 to 1 during the low thrust period. The PU valve was commanded to the low thrust position (nominally 4.5 EMR) at 308.80 sec after J-2 start command (455.77 sec). Propellant loading by the PU system was satisfactory.

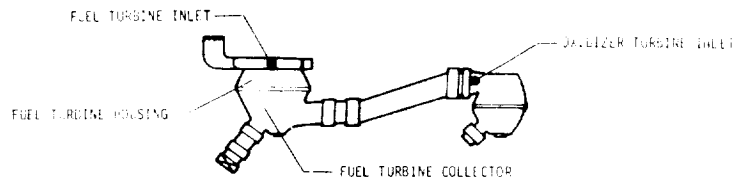
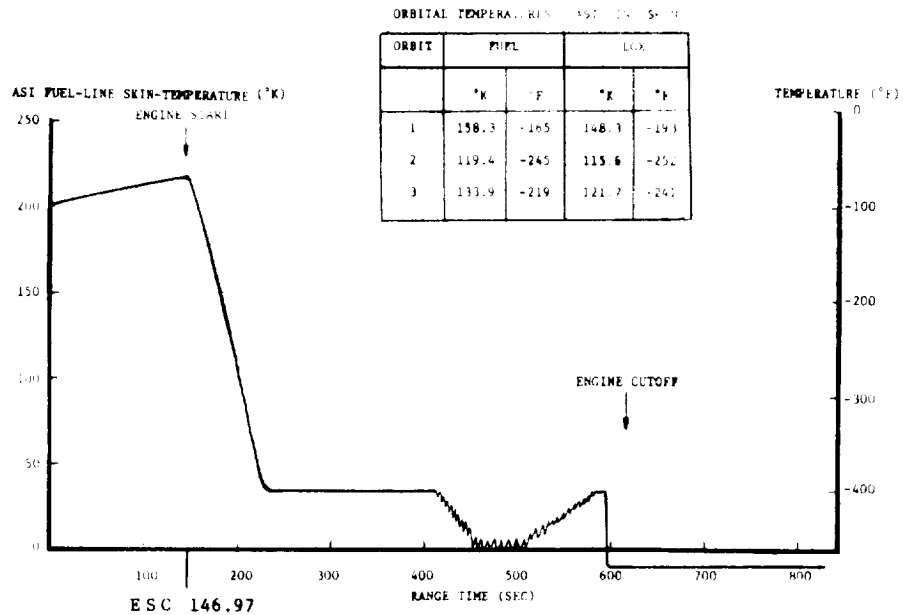
All portions of the orbital safing operation were performed successfully. In order to adequately safe the LH₂ tank, four additional ground commanded vents were required to supplement the programmed vent sequence.

The LOX turbine inlet temperatures in orbit were very close to expected.

9.2 S-IVB PROPULSION PERFORMANCE

9.2.1 ENGINE CHILLDOWN

Thrust chamber chilldown was initiated at -10 minutes. The thrust chamber jacket temperature response was slightly slower than expected, and it appeared that a flow restriction may have occurred in the ground support equipment (GSE). The GSE heat exchanger crossover valve was closed for 50 sec and reopened to verify flow through both coils of the heat exchanger. This procedure reduced the rate of chilldown, and raised doubts that the temperature requirement would be met at Initiation of Automatic Countdown Sequence (IAS). To avoid calling a hold after IAS, which would have caused a countdown recycle to -15 min, a hold was called out at -6 min 15 sec. After 165 sec, the chilldown progress was satisfactory, and the countdown was resumed. When chilldown was terminated at liftoff (lower left-hand portion of Figure 9-1), the temperature was 143°K (-203°F or 257°R),



CROSSOVER DUCT MEASUREMENT LOCATIONS

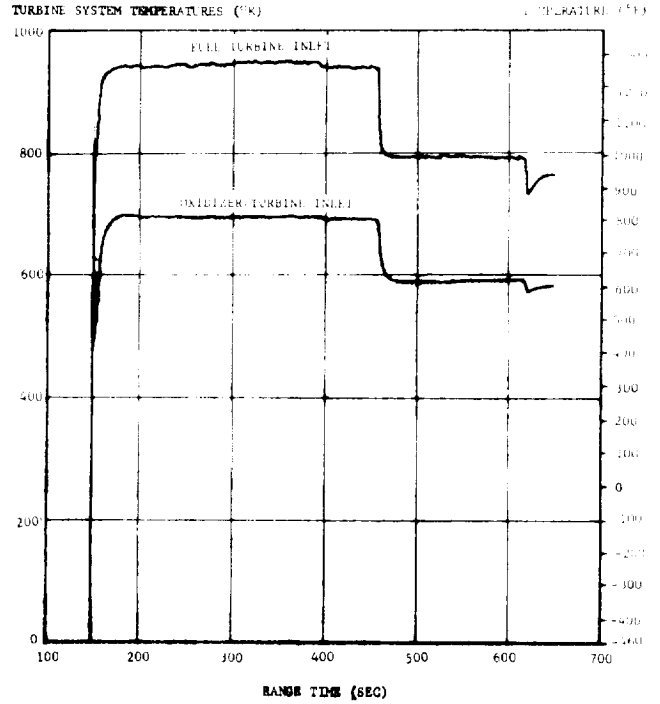
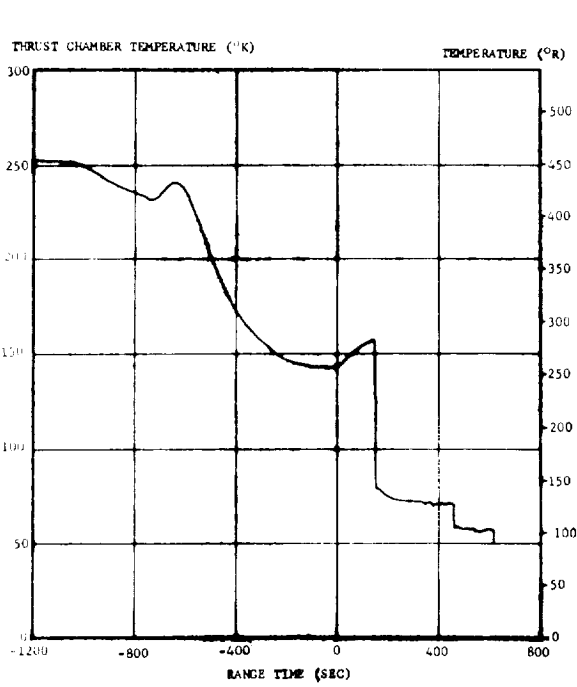


FIGURE 9-1 J-2 ENGINE TEMPERATURES

which was below the redline maximum temperature of 153°K (-185°F). At S-IVB engine start command (ESC), the temperature was 157°K (-177°F), which was within the requirement of $133 \pm 28^{\circ}\text{K}$ ($-220 \pm 50^{\circ}\text{F}$).

The J-2 engine fuel turbine system temperatures were close to the expected range and are shown in the lower right-hand portion of Figure 9-1.

9.2.2 START CHARACTERISTICS

ESC occurred at 146.97 sec, 0.99 sec later than predicted. The engine start transient was satisfactory and slightly faster than predicted. The thrust buildup was within the limits set by the engine manufacturer and was consistent with predicted performance. During the start transient, minor thrust instability was reflected in some of the pressure data and in the main LOX valve position data. The instability was within testing experience limits and was not considered to be a problem. The PU valve was at the proper null setting during the start transient. The faster thrust buildup resulted in less total impulse during the start transient (to 90% performance level) compared to predicted. Table 9-1 briefly summarizes the start transient performance.

Performance of the GH₂ start sphere is discussed in paragraph 9.5.

TABLE 9-1 START TRANSIENT PERFORMANCE

PARAMETER	FLIGHT	PREDICTED
Time from STDV to 90% thrust (sec)*	2.25	2.66**
Time from ESC to 90% thrust (sec)	3.23	3.60
Total Impulse to 90% thrust (N-sec)	658,394	873,377**
(lbf-sec)	148,013	196,343**

* 90% thrust is defined as chamber pressure of 426 N/cm² (618 psi).
STDV - Start tank discharge valve initiation.

** Predicted based on acceptance test data.

9.2.3 MAINSTAGE ENGINE ANALYSIS

Two separate analyses were employed in reconstructing S-IVB J-2 engine performance. The first method, engine analysis, employed telemetered engine and stage data to compute longitudinal thrust, specific impulse, and propellant mass flowrate. In the second method, flight simulation, a five-degree-of-freedom trajectory simulation was utilized to fit engine analysis results to the trajectory. The flight performance values and the deviations from predicted are summarized in Table 9-II.

Thrust, specific impulse, total flowrate, and engine mixture ratio during J-2 engine steady-state performance, based upon engine analysis, are depicted in Figure 9-2. On the basis of engine analysis, the overall average S-IVB stage thrust, mass loss rate, and specific impulse were 0.50%, 0.37%, and 0.13% lower than predicted, respectively. These performance levels were satisfactory.

A five-degree-of-freedom trajectory simulation program was employed to adjust the S-IVB propulsion performance analysis results generated by the engine analysis. Using a differential correction procedure, this simulation determined adjustments to the engine analysis thrust and mass flow histories to yield a simulated trajectory which matched the observed mass point trajectory closely. These results were obtained by a hunting procedure adjustment to the engine analysis. Adjustments to thrust were -0.15% and +0.85% at the high and low thrust periods, respectively. Adjustments to the mass loss rate were +0.07% and -1.23% at the high and low thrust periods, respectively. Adjustments to the overall average thrust and mass loss rate were +0.64% and +0.27%, respectively.

On the basis of flight simulation, the overall S-IVB thrust, mass loss rate, and specific impulse were 0.14% higher, 0.11% lower, and 0.24% higher than predicted, respectively.

A negative shift in engine performance was observed to occur at ESC +244 sec (391 sec). A similar shift occurred during the S-IVB-205 acceptance test. The magnitude of the shift reduced the chamber pressure by 4.1 N/cm² (6 psi), reduced the fuel turbine inlet temperature by 8.3° K (15° F), and reduced the LOX injector pressure by 3.4 N/cm² (5 psi).

Unlike the acceptance-test shift which recovered after 10 sec, the shift during flight did not recover but persisted throughout the high engine mixture ratio (EMR) period. These negative shifts have been associated with a positive shift in gas generator LOX feedline resistance. (See Reference 5.)

▽ S-IVB ESC (146.97 SEC)

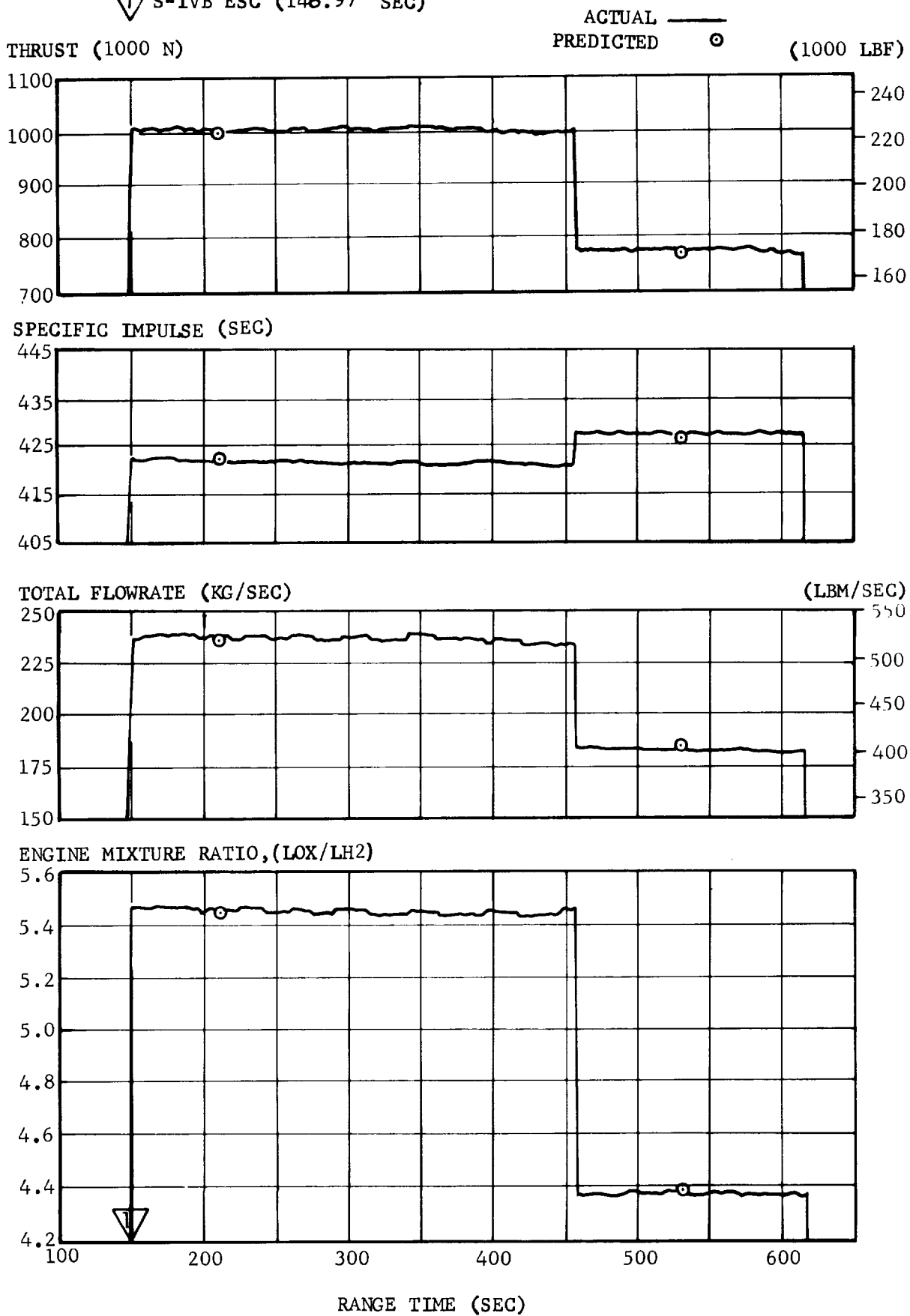


TABLE 9-II
S-IVB PROPELLSION SYSTEM PERFORMANCE

Parameters	Units	PREDICTED			ENGINE ANALYSIS			FLIGHT SIMULATION					
		High Mixture Ratio	Low Mixture Ratio	Flight Average	ACTUAL			% DEVIATION FROM PREDICTED					
					High MR	Low MR	Flt Avg	High MR	Low MR	Flt Avg	High MR	Low MR	Flt Avg
Long Vehicle Thrust	N	1,005,383	783,274	929,024	1,009,902	769,231	924,498	1,008,421	775,792	930,310	0.30	-0.46	0.14
Vehicle Mass Loss Rate	lbf	226,019	176,087	208,853	227,035	172,930	207,802	226,702	174,405	209,142	0.45	-1.79	-0.50
Vehicle Mass Loss Rate	kg/sec	242.20	185.03	222.55	242.8	183.4	221.7	243.0	182.8	222.3	0.25	-0.86	-0.37
	lbm/sec	533.97	407.92	490.63	535.3	404.4	488.8	535.7	402.9	490.1	0.32	-1.23	-0.11
Longitudinal Vehicle Specific Impulse	sec	423.28	431.67	425.68	424.1	427.6	425.1	423.2	411.9	426.7	0.20	-0.94	-0.13
											-0.02	0.28	0.24

MR - Mixture Ratio

The engine performance influence coefficient program was used to reconstruct the engine performance shift. The reconstructed performance shift closely duplicated the observed thrust-shift of 6672 N (1500 lbf). This shift was well within the acceptable $\pm 3\%$ rated thrust variation range.

Instrumentation added to the ASI system as a result of the failure on S-IVB-502 mission indicated normal operation of this system. The LOX supply line skin temperature decayed from 222^oK (-60^oF) at ESC to a stable level of 97^oK (-285^oF) at ESC +30 sec (177 sec). The LH₂ supply line temperature (upper portion of Figure 9-1) dropped from 222^oK (-60^oF) to 33^oK (-400^oF) in the same time span before becoming invalid. At ESC +268 sec (415 sec), the LH₂ line temperature showed a sudden unsteady temperature decrease from a steady 31^oK (-405^oF). This indication is unreasonable and is not supported by any other data. It has been attributed to an instrumentation failure.

9.2.4 CUTOFF IMPULSE

The engine cutoff transient indicated that the time between engine cutoff command (ECC) and thrust decrease to 5% of rated thrust or 50,042 N (11,250 lbf) was within the maximum allowable time of 800 milliseconds (Figure 9-3). The cutoff impulse to zero thrust was 207,492 N-s (46,646 lbf-s) and was higher than the predicted cutoff impulse of 205,041 N-s (46,095 lbf-s). This resulted because the main oxidizer valve (MOV) began to close later and therefore remained open longer than expected. This probably resulted from a colder MOV actuator temperature during flight.

Table 9-III summarizes S-IVB cutoff transient performance. The total impulse, as determined from engine data, agrees closely with the cutoff impulse based on guidance data.

9.3 S-IVB STAGE PROPELLANT UTILIZATION

9.3.1 PROPELLANT MASS ANALYSIS

The propellant utilization system successfully accomplished the requirements associated with propellant loading. The best estimate values were 0.03% higher LOX and 0.66% higher LH₂ than predicted. The deviations were well within the required $\pm 1.12\%$ loading accuracy.

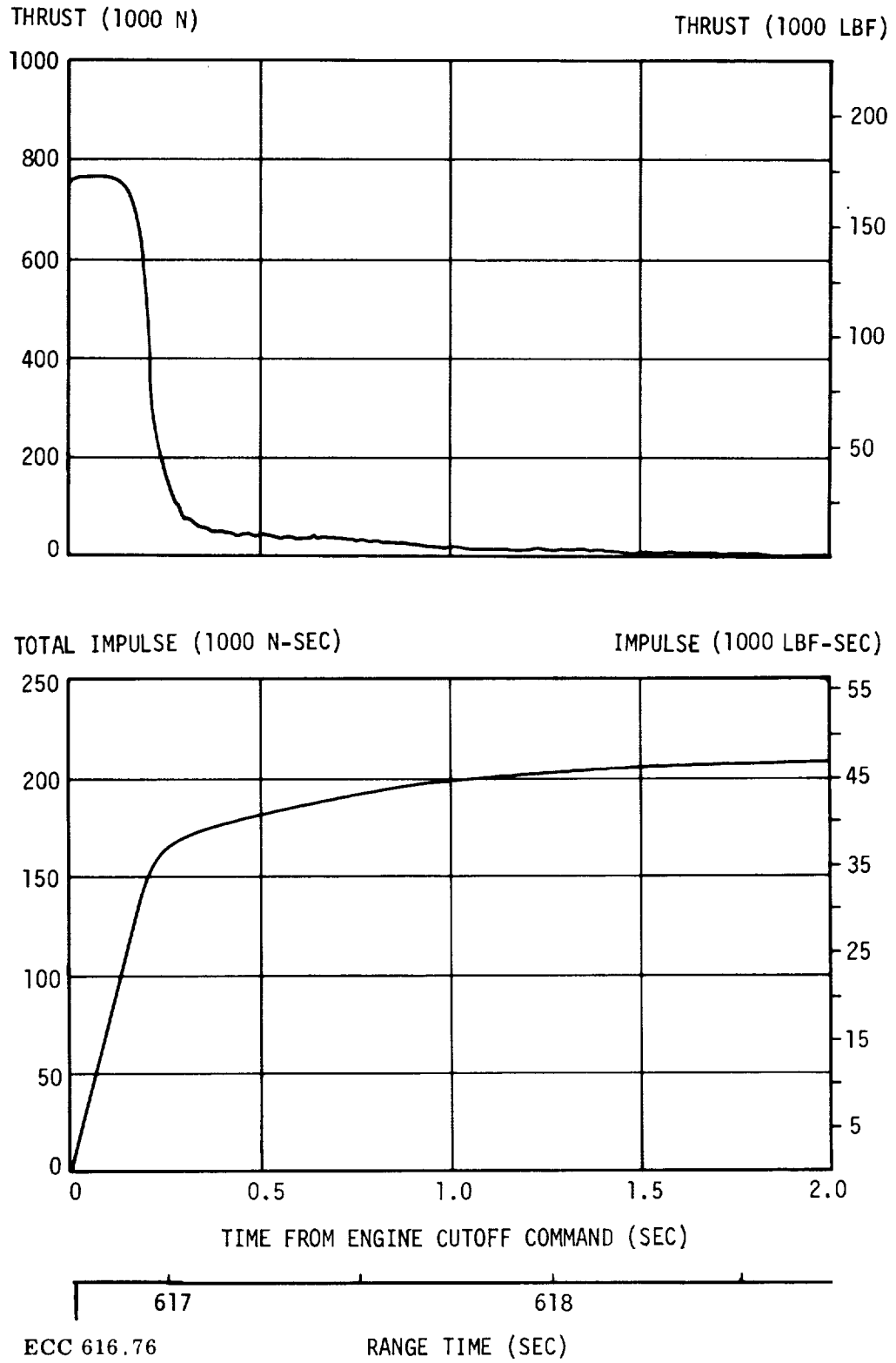


FIGURE 9-3. S-IVB CUTOFF TRANSIENT

TABLE 9-III S-IVB CUTOFF TRANSIENT PERFORMANCE

Parameter	Predicted	Acceptance Test		Flight	
		Stage	Engine	Engine Data	Guidance Data
Total Cutoff Impulse (N-s)	205,041	193,409*	176,158*	207,492	196,545
(lbf-s)	46,095	43,480*	39,602*	46,646	44,185
Velocity Increase (m/s)	5.2	--	--	6.75	6.4
(ft/s)	17.06	--	--	22.13	21.0

*Cutoff impulse to 5 percent thrust.

Figure 9-4 presents the second-flight-stage best-estimate ignition and cutoff masses. At ESC, the mass was 138,703 kg (305,788 lbm); and at ECC, 30,767 kg (67,830 lbm).

A comparison of propellant mass values at critical flight events, as determined by various analyses, is presented in Table 9-IV.

Extrapolation of propellant residuals to depletion indicated that a LOX depletion would have occurred 3.46 sec after velocity cutoff with a usable LH₂ residual of 674 kg (1,486 lbm). 472 kg (1,040 lbm) of usable residual resulted from the intentional LH₂ bias. The extrapolated residual yielded a PU system efficiency of 99.82 percent.

9.3.2 PU VALVE RESPONSE AND THRUST FLUCTUATIONS

The PU valve position history is illustrated in Figure 9-5. LOX and LH₂ probe mismatch are presented in Figure 9-6.

The PU system operated in an open loop mode. It was commanded to the 5.5 EMR high thrust position (nominally 5.5 EMR) at 152.97 sec (TB 3 + 8.65 sec) and was commanded to the 4.45 EMR low thrust position (nominally 4.5 EMR) at 455.77 sec (TB 3 + 3.1145 sec) as planned. It remained at the low thrust position until engine cutoff. There was no anomalous valve activity nor any unacceptable thrust fluctuation during the burn period.

9.4 S-IVB PROPELLANT PRESSURIZATION SYSTEMS

9.4.1 FUEL PRESSURIZATION SYSTEM

The fuel pressurization system performance was satisfactory throughout flight, supplying LH₂ to the engine pump inlet within the specified operating limits by maintaining the NPSP above the allowable minimum throughout S-IVB powered flight. Fuel pressurization control and step pressurization modes were normal and within predicted limits.

The LH₂ pressurization command was received at approximately -113 seconds. The LH₂ tank-pressurized signal was received 18 sec later, when the LH₂ tank ullage pressure reached 21.0 N/cm² (30.4 psi). However, the ullage pressure continued to increase until it reached relief conditions of 22.1 N/cm² (32.1 psi) at approximately -20 seconds (upper portion of Figure 9-7). Data indicates that, just after liftoff, the ullage pressure decayed slightly below the relief level until approximately 60 sec. At 60 sec, the tank began relieving and continued relieving until S-IVB ESC.

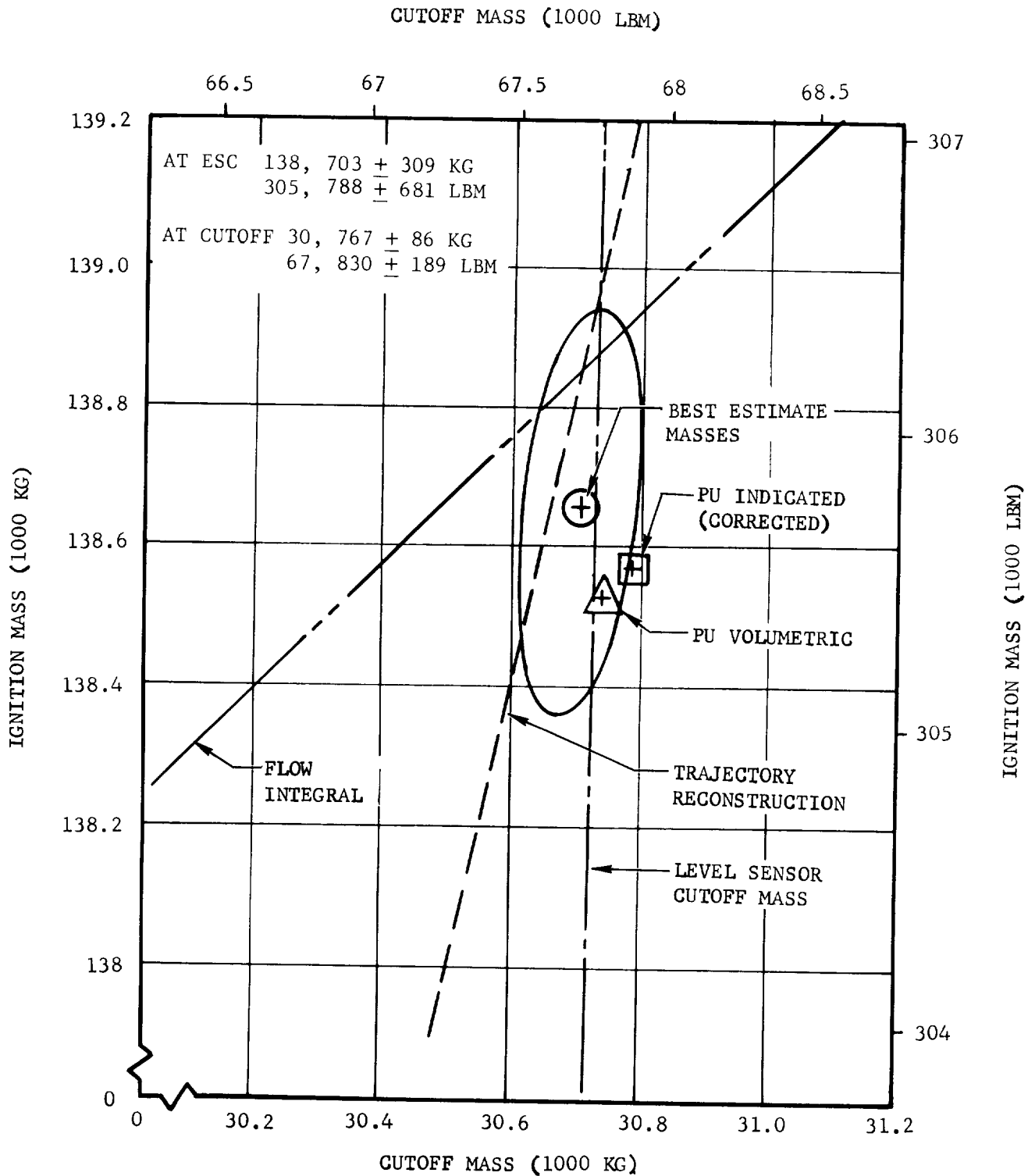


FIGURE 9-4 SECOND FLIGHT STAGE BEST ESTIMATE MASSES

TABLE 9-IV S-IVB PROPELLANT MASS SUMMARY

Events	Units	Predicted		PU System		PU Volumetric		Engine Flow Integral (2)		Best Estimate (3)	
		LOX	LH ₂	LOX	LH ₂	LOX	LH ₂	LOX	LH ₂	LOX	LH ₂
S-IB Liftoff	kg	87,667	17,983	87,761	18,077	87,620	18,174	87,524	17,946	87,693	18,102
	lbm	193,273	39,646	193,480	39,853	193,170	40,066	192,955	39,563	193,330	39,909
S-IVB ESC	kg	87,667	17,983	87,694	18,026	87,549	18,121	87,524	17,946	87,693	18,102
	lbm	193,273	39,647	193,330	39,740	193,010	39,950	192,955	39,563	193,330	39,909
PU Valve Cutback	kg	25,055	6,495	24,957	6,627	25,077	6,611	24,987	6,560	24,974	6,536
	lbm	55,235	14,319	55,020	14,610	55,285	14,575	55,087	14,461	55,058	14,410
Residuals Above Main Propellant Valves at ECC	kg	742	933	733	1,173	733	1,130	751	1,136	731	1,135
	lbm	1,636	2,057	1,615	2,585	1,615	2,492	1,656	2,505	1,611	2,502

(1) PU system indicated mass corrected for inflight tank geometry variations and center-of-gravity offset.

(2) Composite of engine analysis programs.

(3) Composite of PU system, PU volumetric, engine flow integral, trajectory reconstruction, and level sensor residuals.

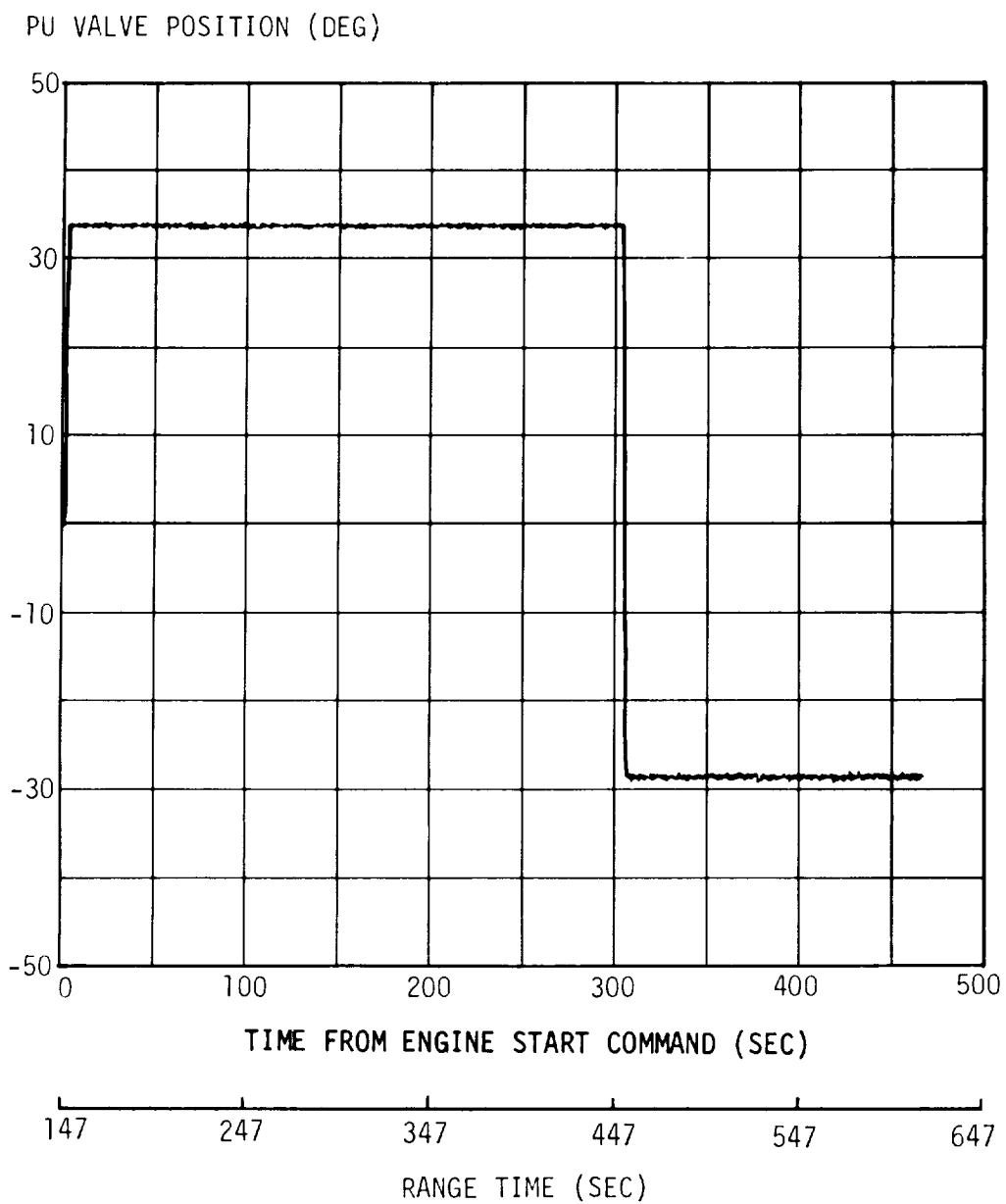


FIGURE 9-5 S-IVB-205 PU VALVE POSITION HISTORY

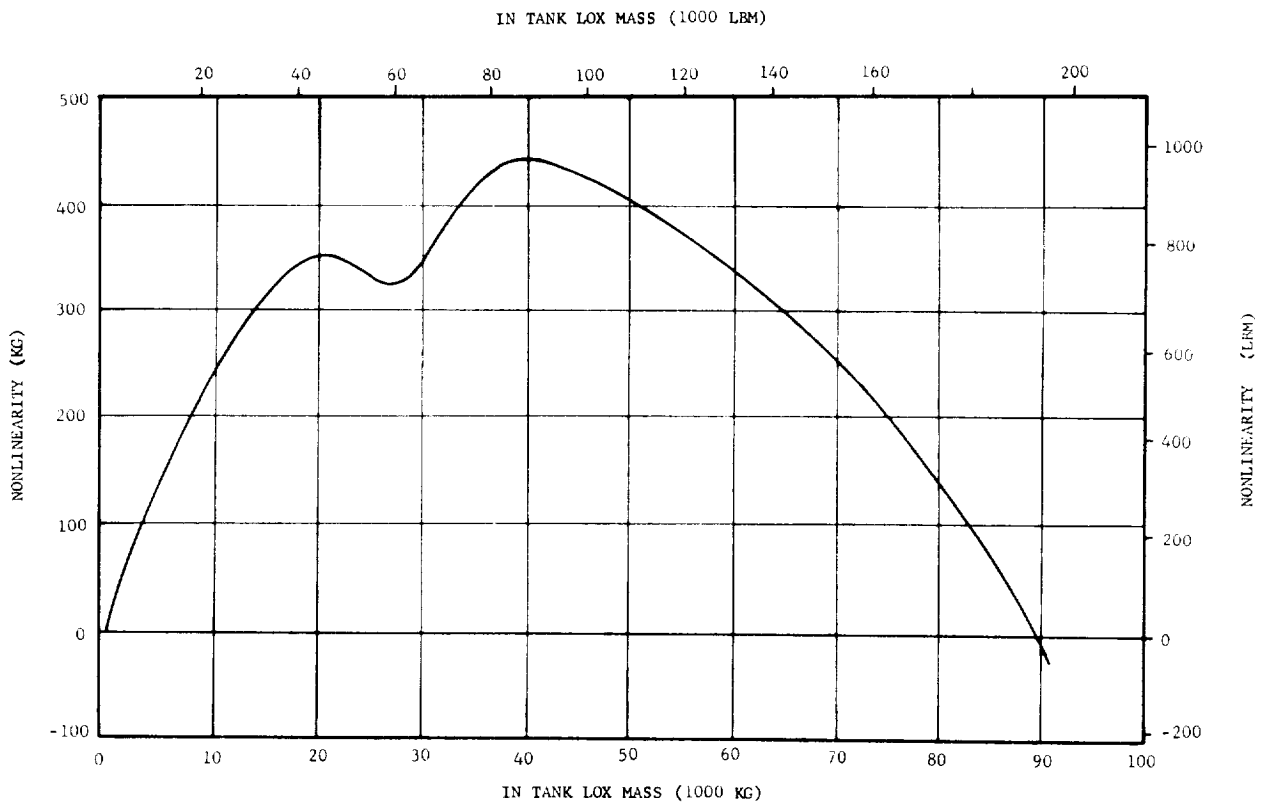
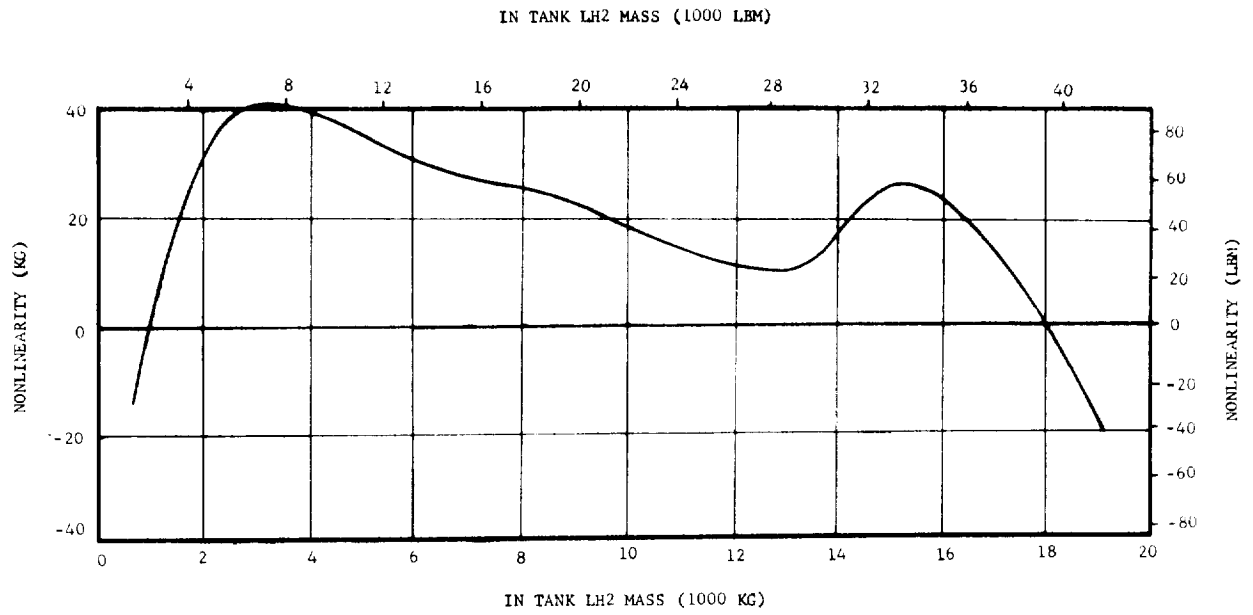


FIGURE 9-6 LH₂ AND LOX SENSOR NONLINEARITY (VOLUMETRIC METHOD)

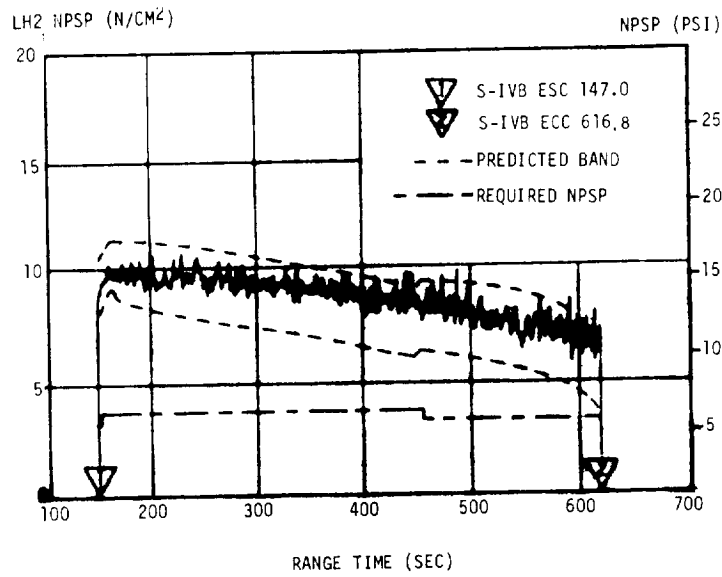
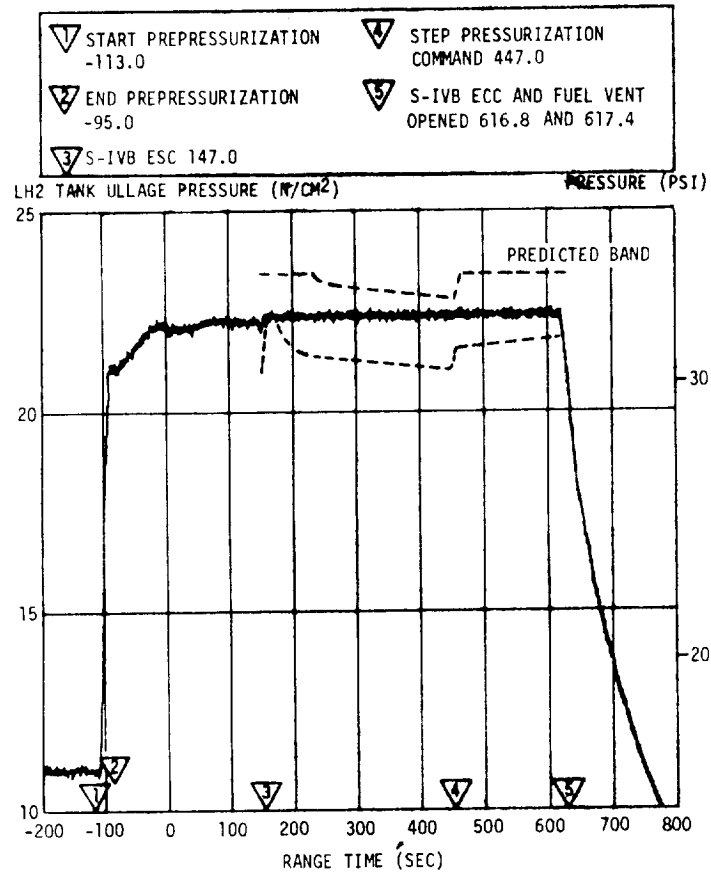


FIGURE 9-7 LH₂ TANK PRESSURIZATION SYSTEM PERFORMANCE

The control and step pressurization flow passages remained open until 2.7 sec after S-IVB ESC to compensate for the initial low pressurant supply pressure. At ESC, the ullage pressure dropped slightly; but, by the time the flow passages were closed, the ullage pressure was again relieving at 22.2 N/cm² (32.2 psi). The venting continued during the remaining S-IVB burn, maintaining a constant pressure of 22.2 to 22.3 N/cm² (32.2 to 32.3 psi). This fell within the predicted band (upper portion of Figure 9-7).

Step pressurization was initiated automatically and was performed satisfactorily at S-IVB ESC + 300 sec (447 sec) to provide adequate LH₂ pump NPSP until S-IVB ECC. At step pressurization command, both the control and step-pressurization orifices were opened to permit additional pressurant flow into the LH₂ tank.

The pressure transducer response in the LH₂ pressurization module inlet was unrealistic and inconsistent with other system parameters after approximately ESC + 200 sec (347 sec). System performance was determined to be in close agreement with predictions, even though pressure levels from the transducer were indeterminate after about 347 seconds. Table 9-V shows the GH₂ pressurant flow-rate history.

TABLE 9-V GH₂ PRESSURANT FLOWRATE

Before Step Pressurization		After Step Pressurization		Total Pressurant From ESC to ECC
Predicted	Actual	Predicted	Actual	
kg/s (lbm/s)	kg/s (lbm/s)	kg/s (lbm/s)	kg/s (lbm/s)	kg (lbm)
0.28 (0.62)	0.29 (0.64)	0.39 (0.87)	0.39 (0.87)	158 (349)

A meaningful ullage collapse factor could not be determined because of the continuous venting during powered flight.

LH₂ Supply Condition

The LH₂ pump inlet NPSP was calculated from the pump inlet temperature and total pressure. The NPSP was within the predicted band (lower portion of Figure 9-7). The LH₂ system recirculation chilldown was adequate. At S-IVB ESC, the LH₂ pump

inlet static pressure and temperature were 22.6 N/cm^2 (32.8 psi) and 21.1°K (-421.7°F), respectively. This was well within engine start requirements (upper portion of Figure 9-8).

9.4.2 LOX PRESSURIZATION SYSTEM

The LOX pressurization system performance was satisfactory throughout the flight, supplying LOX to the engine pump inlet within the specified operating limits. Prepressurization and pressurization control were normal and within predicted limits.

LOX tank pressurization was initiated at -163 sec, and increased the LOX tank ullage pressure from 10.5 N/cm^2 (15.3 psi) to 26.8 N/cm^2 (38.9 psi) within 16 sec (upper portion of Figure 9-9). As a result of ullage chilldown, two makeup cycles were required prior to liftoff to maintain the LOX tank ullage pressure above the control pressure switch minimum of 25.7 N/cm^2 (37.3 psi). The ambient helium purges of the ullage pressure sense line and of the tank vent-and-relief valve caused a gradual rise in ullage pressure until -1 second.

The modified LOX tank pressurization system, utilized for the first time during the S-IVB 506N acceptance test, was also employed during the S-IVB-205 flight. The cold helium shutoff valves were opened 2.5 sec prior to S-IVB ESC, and the heat exchanger control valve was programmed to the open position during cold helium lead and during the first 21 sec of S-IVB engine burn. On previous flights, the shutoff valves were not opened until 0.2 sec prior to start-tank-discharge-valve command, and the control valve was maintained closed by the pressure switch until the ullage pressure had dropped below the lower switch setting. The resulting high initial flowrate on S-IVB-205 completely eliminated the usual LOX ullage pressure dip. This modified pressurization sequence is planned for all future flights.

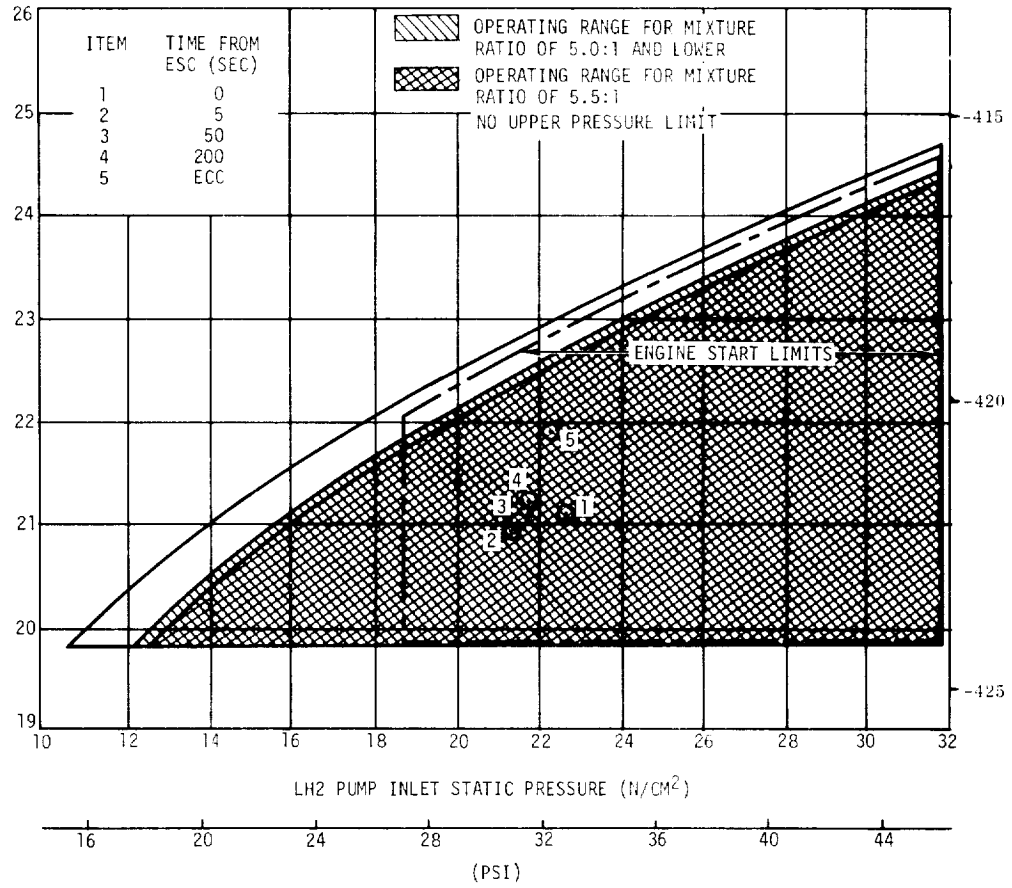
During S-IVB powered flight (middle portion of Figure 9-9), the ullage pressure cycled seven times and remained between 25.7 and 27.0 N/cm^2 (37.3 and 39.2 psi).

The calculated helium mass utilized during S-IVB powered flight was 72 kg (159 lbm), based upon flow integrations. Mass calculations, using bottle calculated pressures, agree reasonably well with flow integration calculations. Using bottle conditions, the helium mass loaded was 158 kg (349 lbm).

The J-2 engine heat exchanger outlet temperatures were higher than those recorded during S-IVB-205 acceptance testing. This difference was caused by the absence of atmospheric convective heat transfer loss through the uninsulated part of the pressurization line during flight, and by differences between the actual and predicted engine mixture ratio. Heat exchanger and LOX tank pressurant data are summarized in Table 9-VI.

LH₂ PUMP INLET TEMPERATURE (°K)

TEMPERATURE (°F)



LOX PUMP INLET TEMPERATURE (°K)

TEMPERATURE (°F)

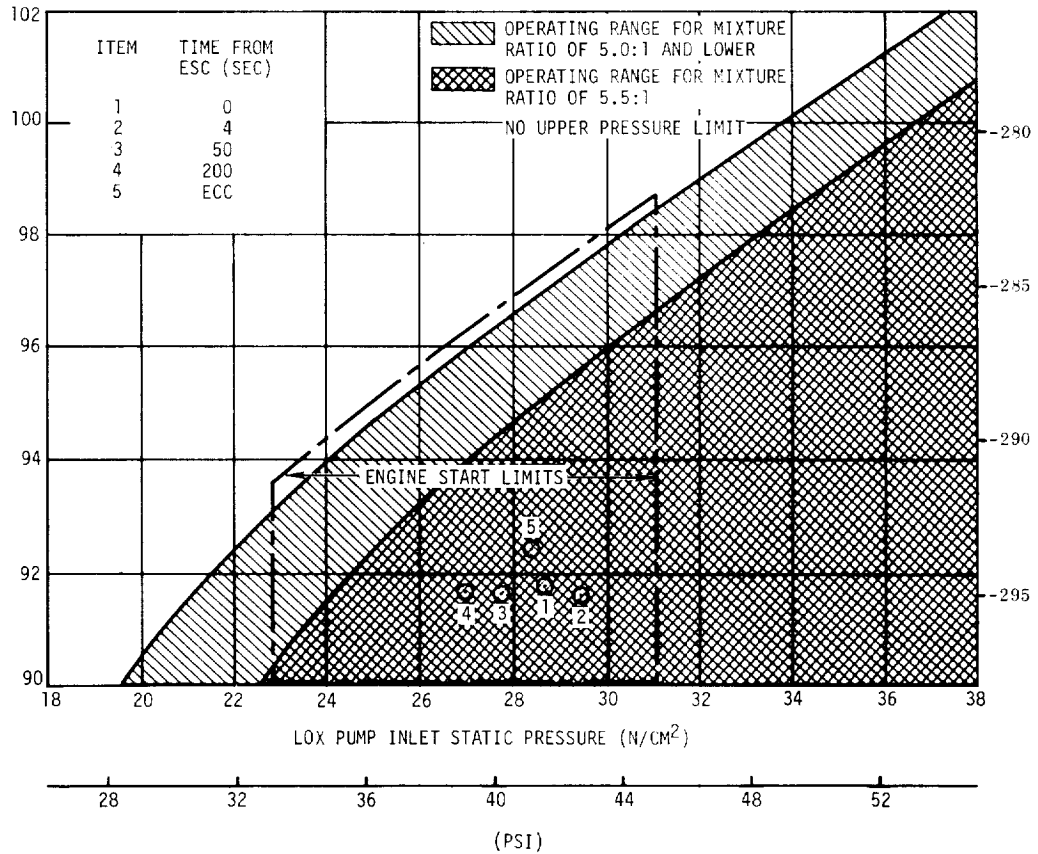


FIGURE 9-8 LH₂ AND LOX INLET START REQUIREMENTS

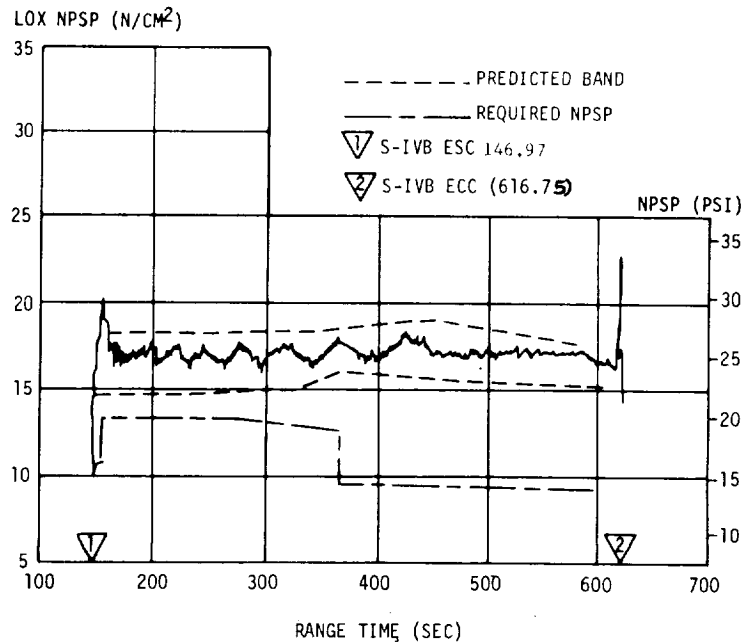
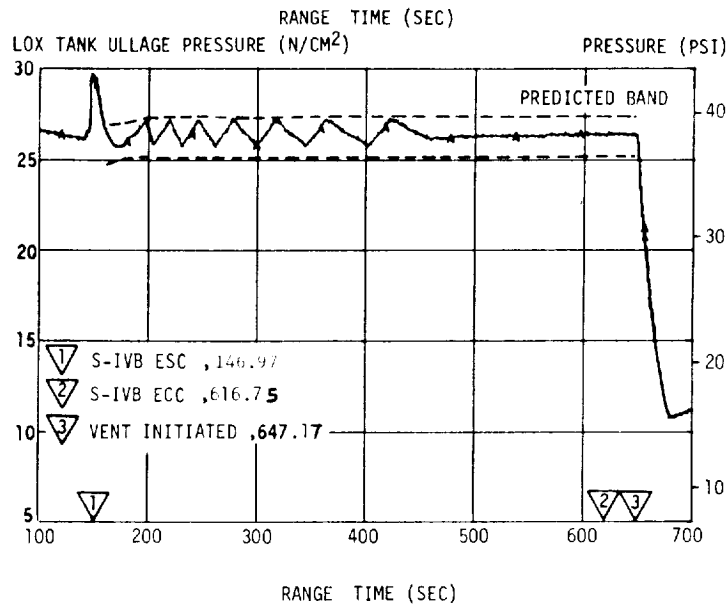
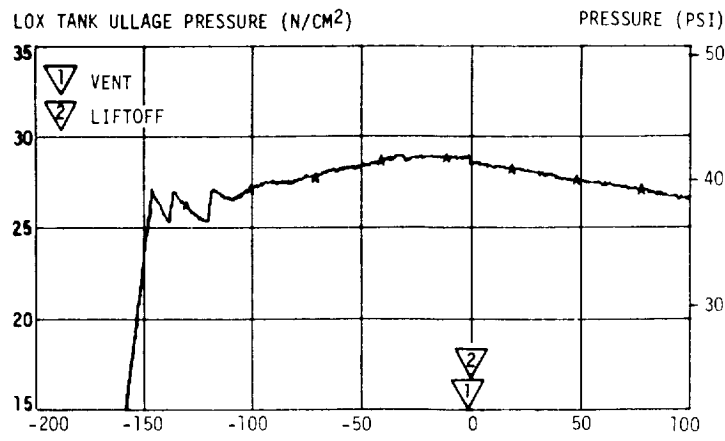


FIGURE 9-9 LOX TANK PRESSURIZATION SYSTEM PERFORMANCE

TABLE 9-VI LOX TANK PRESSURIZATION DATA SUMMARY

Time	Heat Exchanger Temperature	Helium Flowrate through the Heat Exchanger	LOX Tank Pressurant Total Flowrate **
	$^{\circ}\text{K}$ ($^{\circ}\text{F}$)	kg/s (lbm/s)	kg/s (lbm/s)
End Start Transient	533 (500)	-	-
Overcontrol Operation	*549 (528)	0.091 (0.20)	0.17 to 0.20 (0.37 to 0.45)
Undercontrol Operation	*578 (580)	0.034 (0.075)	0.11 to 0.15 (0.25 to 0.33)

* Throughout high EMR portion of the S-IVB burn.

** Variation is normal: bypass orifice inlet temperatures change as they follow the heat exchanger temperature.

After S-IVB ECC (616.76 sec)*, the ullage pressure remained momentarily at 26.1 N/cm^2 (37.8 psi) until the programmed LOX vent at 647.17 seconds. The pressure had decayed to about 11 N/cm^2 (16 psi) when the LOX vent valve was commanded closed at 677.17 seconds.

LOX Supply Conditions

The NPSP, calculated at LOX pump inlet, was 16.8 N/cm^2 (24.4 psi) at S-IVB ESC (lower portion of Figure 9-9). The NPSP was near the predicted, and was greater than required by engine specifications.

The LOX system chilldown circulation was satisfactory. The LOX pump inlet static pressure and temperature were well within the start requirements (lower portion of Figure 9-8).

9.5 S-IVB PNEUMATIC SYSTEMS

The following three S-IVB pneumatic systems performed satisfactorily: (1) stage pneumatic control and purge system, (2) GH_2 start tank system, and (3) engine pneumatic control system.

*Cutoff signal received at J-2 engine.

Stage Pneumatic Supply

The pneumatic control and purge system performed satisfactorily throughout flight. The helium supply to the system was adequate for both pneumatic valve control and purging. The regulated pressure was maintained within acceptable limits, and all components functioned normally.

Figure 9-10 shows the stage pneumatic sphere pressure and regulator discharge pressure. The normal pressure rise occurred during S-IVB powered flight due to the thermal input to the sphere. In contrast to AS-204, the stage pneumatic sphere temperature measurement was deleted from the AS-205 flight. As a result, temperature measurements and mass calculations are not available.

All stage pneumatic control valves responded properly throughout the count-down and flight. The stage pneumatic helium regulator operated satisfactorily and maintained an output pressure of 331 to 390 N/cm² (480 to 565 psi).

GH₂ Start Bottle

Chilldown and loading of the engine GH₂ start bottle were accomplished satisfactorily. The warmup rate after the sphere was pressurized, until liftoff, was 0.02°K/min (0.04°F/min). The total GH₂ mass utilized was 1.70 kg (3.75 lbm).

Figure 9-11 shows the GH₂ start bottle performance. Fuel pump spin-up, as the result of GH₂ discharge from the start tank, was completed by ESC + 1.89 sec (148.86 seconds). The GH₂ start bottle was not recharged during the S-IVB burn, as is reflected in Figure 9-11. Table 9-VII shows the mass, temperature, and pressure in the start bottle at significant time points.

TABLE 9-VII GH₂ START BOTTLE PARAMETERS

Time	Mass kg (lbm)	Temperature		Pressure	
		Required	^o K (^o F) Actual	Required	² N/cm (psi) Actual
Liftoff	1.58 (3.49)	89 to 178 (-300 to -140)	151 (-189)	838 to 965 (1215 to 1400)	881 (1278)
ESC	-	89 to 177 (-300 to -141)	152 (-187)	-	891 (1293)
After Bottle Blowdown	0.282 (0.622)	-	111 (-261)	-	109 (158)

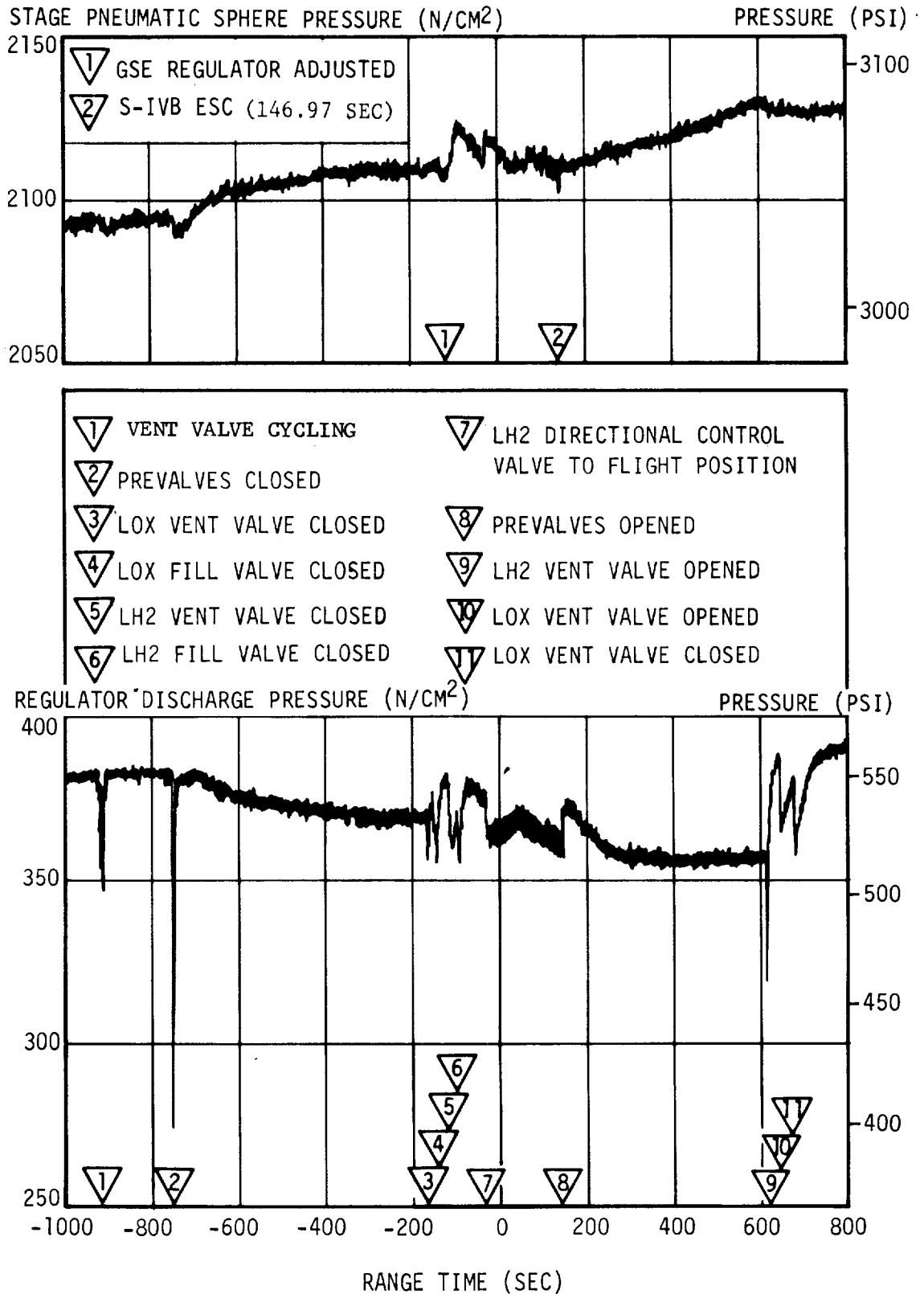


FIGURE 9-10 Stage Pneumatic Control and Purge System Performance

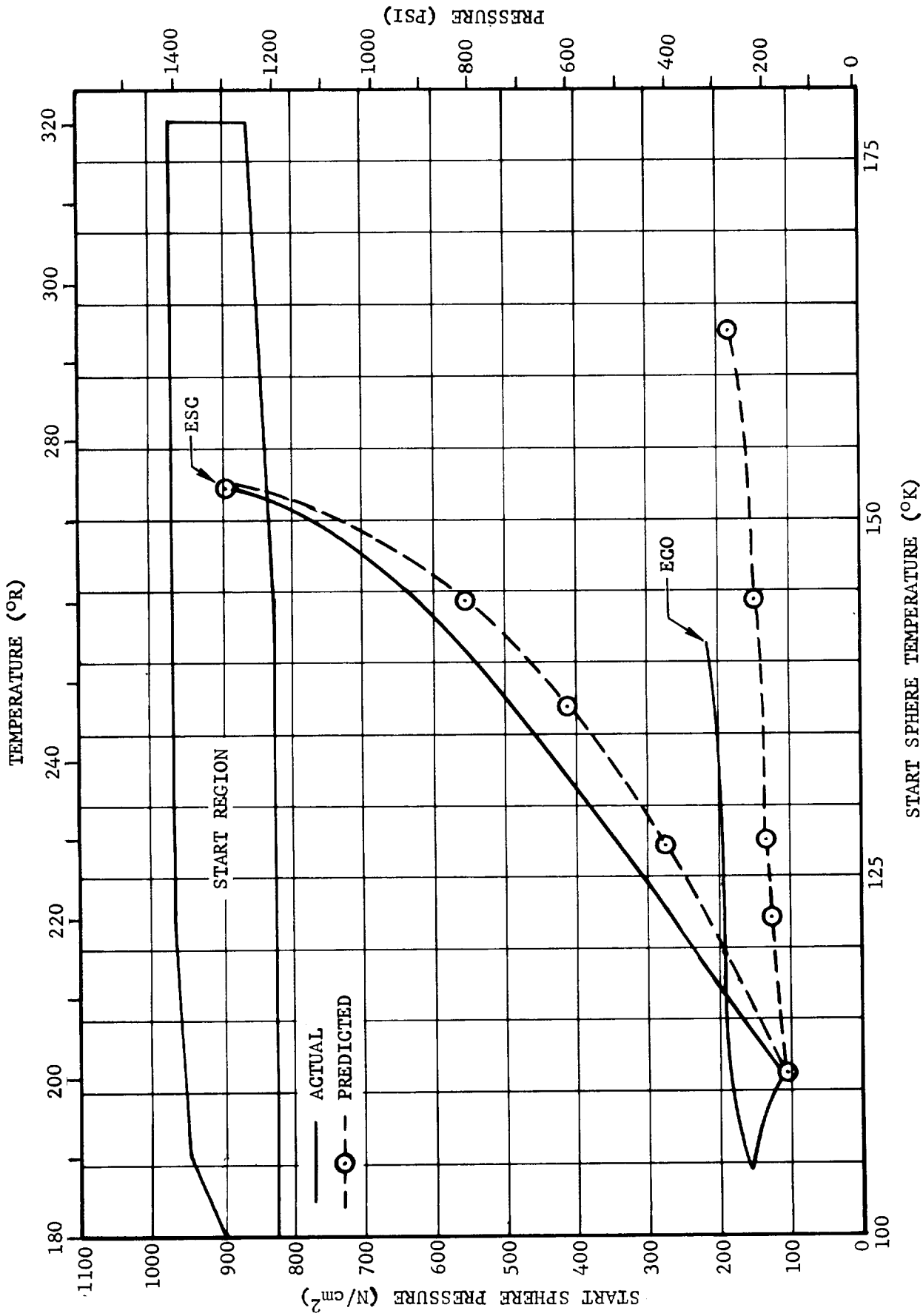


FIGURE 9-11 ENGINE START SPHERE PERFORMANCE

Engine Control Sphere

The helium control system for the J-2 engine performed satisfactorily during mainstage operation. The engine pneumatic control sphere conditioning was satisfactory. The mass consumed to engine cutoff was 0.18 kg (0.40 lbm). The mass, temperature, and pressure data for significant time points are presented in Table 9-VIII.

TABLE 9-VIII ENGINE CONTROL SPHERE PARAMETERS

Event	Mass kg (lbm)	Temperature °K (°F)		Pressure N/cm ² (psi)	
		Required	Actual	Required	Actual
ESC	0.93 (2.07)	144 to 178 (-200 to -140)	158 (-176)	1,931 to 2,379 (2,800 to 3,450)	2,268 (3,290)
ECC	0.75 (1.67)	--	141 (-207)	--	1,589 (2,305)

9.6 S-IVB ORBITAL SAFING

9.6.1 SAFING PURPOSE AND EVENTS

The purpose of safing the S-IVB stage was to lower the pressure in the propellant tanks and high-pressure bottles to a level permitting safe spacecraft/S-IVB rendezvous and safe spacecraft simulated docking maneuvers.

The manner and sequencing in which safing was performed is presented in Table 9-IX.

9.6.2 LH₂ AND LOX TANK VENTING

The LH₂ tank vent-and-relief valve and the mechanically latched passivation valve performed adequately and responded satisfactorily to all preprogrammed and commanded vents; however, the preprogrammed vent sequence for these valves was not adequate to safe the tank under the orbital conditions experienced. The tank safing sequence was supplemented by 4 additional ground commanded vents, resulting in elimination of the liquid residual of 1129 kg (2488 lbm) by approximately 18,750 seconds.

TABLE 9-IX ORBITAL SAFING EVENTS SUMMARY

Event	Duration (sec)	Time Started		Time Completed	
		(sec)	hrs:min:secs	(sec)	hrs:min:secs
LH ₂ Tank Vent 1	1259.99*	617.37	00:10:17.37	1,877.36*	00:31:17.36*
LH ₂ Tank Passivation Valve Open		617.56	00:10:17.56	EOM	
LOX Tank Vent	30.00	647.17	00:10:47.17	677.17	00:11:17.17
LH ₂ Tank Vent 2	300.00	3,246.95	00:54:06.95	3,546.95	00:59:06.95
LOX Dump	721.00	5,668.95	01:34:28.95	6,389.95	01:46:29.95
LOX Tank NPV Valve Open		5,678.95	01:34:38.95	EOM	
LH ₂ Tank Vent 3	600.00	5,682.95	01:34:42.95	6,282.95	01:44:42.95
Cold Helium Dump 1	2868.00	6,148.95	01:42:28.95	9,016.95	02:30:16.95
LH ₂ Tank Vent 4	400.63	11,354.48	03:09:14.48	11,756.11	03:15:56.11
Stage Control Sphere Helium Dump	2967.32	11,853.95	03:17:33.95	14,821.27**	04:07:01.27**
LH ₂ Tank Vent 5	261.16	14,747.27	04:05:47.27	15,008.43	04:10:08.43
Cold Helium Dump 2	1199.99	16,216.96	04:30:16.96	17,416.95	04:50:16.95
LH ₂ Tank Vent 6	305.88	17,035.85	04:43:55.85	17,341.73	04:49:01.73
LH ₂ Tank Vent 7	146.44	18,538.99	05:08:58.99	18,685.43	05:11:15.43

EOM - End of Mission

*Approximate time due to data dropout

**Early dump termination by ground command

The three preprogrammed vents through the vent and relief valve, in combination with the passivation valve which was opened at ECC, controlled the tank ullage pressure approximately as had been predicted until about 9,000 seconds (upper portion of Figure 9-12). The pressure continued to rise after this time, however; and, at 11,354.48 sec the vent-and-relief valve was commanded open. By this action, the mission rule which prohibits a common bulkhead delta pressure in excess of 14 N/cm^2 (20 psi) was observed.

It is currently believed that the continuing pressure rise in the LH_2 tank, subsequent to the preprogrammed third vent (6,282.95 sec), was due to the lack of venting of liquid hydrogen from the tank. This is contrary to the two-phase flow (liquid and gas) which had been anticipated. The lack of liquid entrainment resulted in a much lower rate of LH_2 residual depletion. Additionally, the rate of ullage pressure rise subsequent to 6282.95 sec is higher than would have been anticipated, due to a higher than expected orbital heat transfer into the ullage gas. Preliminary calculations also indicate that the rate of heat transfer into the ullage gas was greater than the anticipated rate of 8,786 watts (30,000 BTU/hr) by a factor of approximately 2. In view of the continuing and excessive self-pressurization, four more vents through the vent-and-relief valve were commanded in order to maintain a safe LH_2 tank pressure level. At approximately 18,750 sec, little if any liquid remained in the tank. Subsequent pressure variations were caused by ullage heating and continuing gas flow through the passivation valve.

The LH_2 ullage pressure rise rate was temporarily increased at approximately 9,000 sec by the astronaut-controlled attitude maneuvering and at approximately 10,400 sec by disturbances induced at spacecraft separation and retrograde maneuver. The pressure rise rate increases during these events because the disturbances to the liquid residual increases the surface area of the liquid that is exposed to the tank wall and ullage. Therefore boiloff increases, which increases the ullage pressure rise rate.

Analysis of the available data, assuming no liquid entrainment in the gas flow from the vent system, indicates that the total mass flow is in close agreement with the total liquid and ullage mass in the tank at ECC. Additionally, the temperature history at the vent nozzles, both in level and profile, is indicative of 100% gas flow. A calculation of the enthalpy of the hydrogen flowing from the vents also supports the probability that virtually all the liquid inside the tank was boiled off.

The prediction for LH_2 tank safing on the S-IVB-205 stage was strongly influenced by the safing experiment performed on the S-IVB-204 stage, with an assumed residual of 1179 kg (2600 lbm). In retrospect, the AS-204 data does not appear to provide a representative model; predictions based solely on theoretical considerations, not influenced by AS-204, would have been much closer to observed

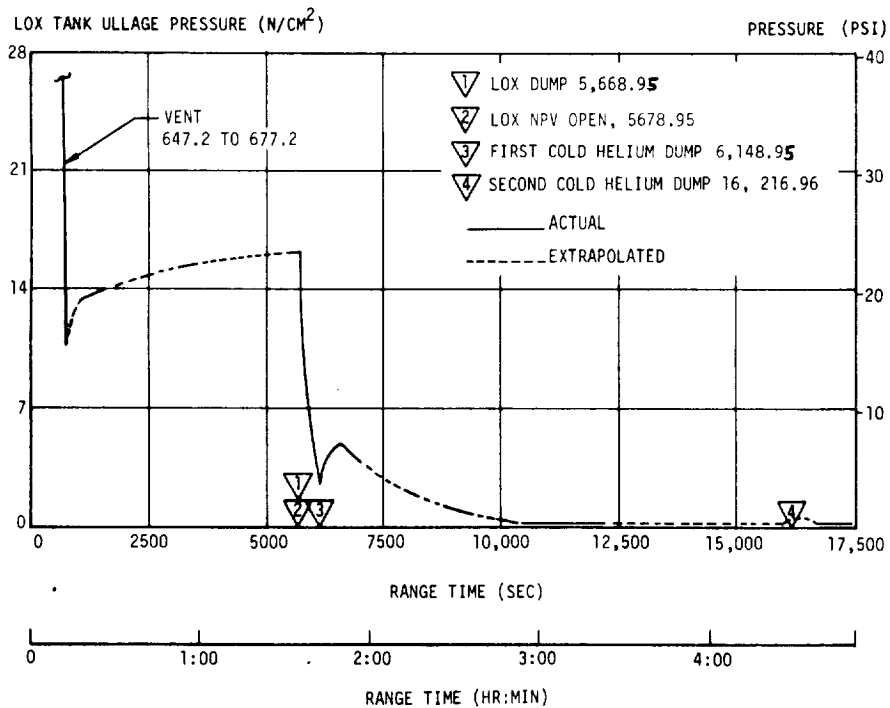
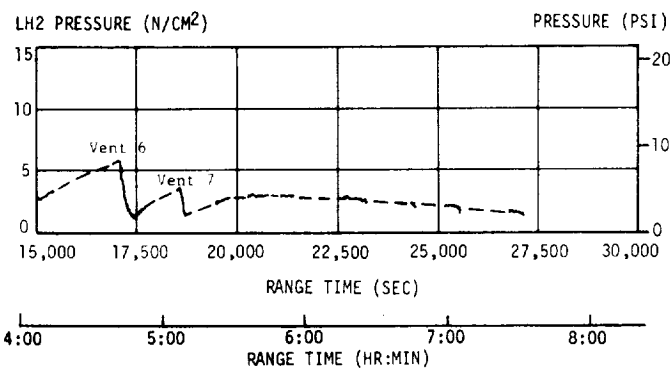
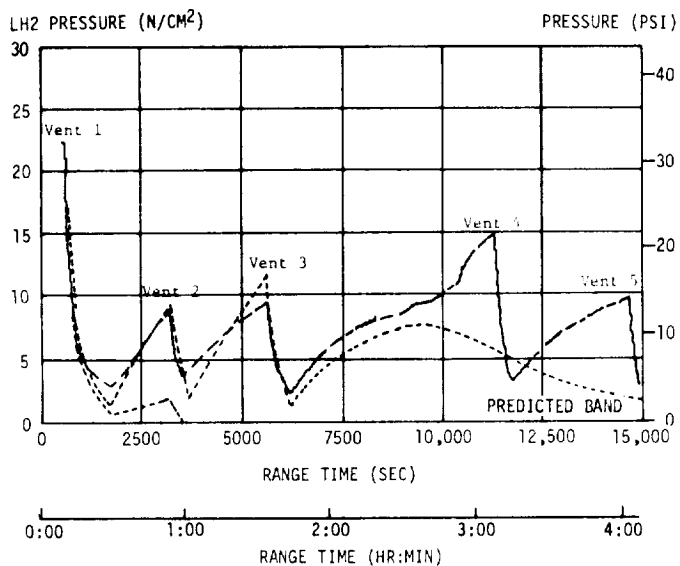


FIGURE 9-12 LH₂ AND LOX TANK ULLAGE PERFORMANCE IN ORBIT

performance. It is currently believed that the difference in entrainment is a result of liquid positioning in the tank. On the AS-205 mission, the liquid mass was located away from the vent inlet; whereas, on AS-204, the liquid was positioned near the forward end of the tank. Possible cause of the different positioning of the liquid may be the reduced drag experienced by the AS-205 vehicle during the first 10,000 sec of orbit as a result of the 16 km (30 nm) higher orbit. The drag experienced in the higher orbit is less by a factor of 2 to 4.

The lower drag on AS-205 would be less likely to move the liquid to the forward end of the tank and consequently there is less likelihood that liquid would be entrained in the venting gases.

The slight residual thrust caused by the J-2 main oxidizer valve not closing completely at the end of LOX dump (6389.95 sec) tended to maintain the LH₂ in a settled position. Additionally, after spacecraft separation (10,502.40 sec) and the subsequent maneuver to retrograde attitude, orbital drag would tend further to settle the liquid at the bottom of this tank.

The lack of liquid entrainment and the higher than anticipated ullage heating contributed to the excessive pressure rise rates observed during orbital coast.

Subsequent stages on which a safing operation is to be performed will have the larger size latching vent-and-relief valve, which will tend to eliminate problems of the nature experienced on this mission.

LOX Tank Venting

The LOX tank orbital venting operations were satisfactorily accomplished. A 30 sec propulsive vent was programmed 30.4 sec after cutoff, and the ullage pressure was lowered from 26 N/cm² (38 psi) to 10 N/cm² (15 psi). The pressure had increased to 16.3 N/cm² (23.6 psi) by the time of LOX dump initiation (lower portion of Figure 9-12). At 5678.95 sec (about 10 sec after LOX dump initiation), the LOX tank passivation valve (non-propulsive) was opened to ensure adequate venting for the cold helium dump. The valve remained open for the duration of the mission, as planned.

9.6.3 LOX DUMP

The LOX tank dump was accomplished satisfactorily. The dump was initiated at 5668.95 seconds. Approximately 33 sec after dump initiation, the ullage pressure began decreasing, indicating that gas ingestion had begun. Due to the small liquid residual remaining in the tank at the start of LOX dump, a steady state liquid flow

condition was not reached. Calculations, based upon propulsion data, indicate that, of the remaining LOX residual, approximately 485 kg (1070 lbf) was completely dumped within 130 seconds. Ullage gases continued to be dumped until the tank pressure decayed to 0 N/cm². During this time, the stage cold helium dump contributed a small additional impulse.

The LOX dump essentially ended at 6341 sec (commanded to close at 6,389.95 sec) when the main oxidizer valve (MOV) closed to the 15% open position, due to the depletion of the engine pneumatic helium. This partially open condition was expected, since pneumatic pressure is required to fully close the MOV. The maximum LOX dump thrust of 1979 N (445 lbf) occurred at 5702 seconds. The total impulse to the end of LOX dump resulted in a velocity increase of 6.6 m/sec (21.7 ft/sec). A small residual thrust, developed through the partially open MOV, was maintained until the tank pressure reached 0 N/cm². The residual thrust decayed from 1.1 N (2.5 lbf) at MOV partial closure to 0 N when the LOX tank ullage pressure reached 0 N/cm² (approximately 10,500 sec), providing an additional impulse of 13,789 N-sec (3,100 lbf-sec). Figure 9-13 shows the ullage pressure, thrust, and mass in the LOX tank during the first 130 sec of the dump.

9.6.4 COLD HELIUM DUMP

Cold helium dump was performed in two distinct periods, 6,148.95 sec to 9,016.95 sec and 16,216.96 sec to 17,416.95 seconds. The LOX tank ullage pressure and helium mass dumped during the first dump are shown in Figure 9-14. All data indicate that safing of the cold helium bottles was accomplished successfully. Table 9-X shows the mass, temperature, and pressure in the cold helium bottles at significant times during the first dump.

A projected analysis of the second cold helium dump indicates that the mass dumped was negligible, but that end conditions were satisfactory. The LOX tank ullage pressure during the second dump is shown in the lower portion of Figure 9-12.

TABLE 9-X COLD HELIUM BOTTLE PARAMETERS

Event	Temperature °K (°F)	Pressure N/cm ² (psi)	Mass kg (lbf)
ECC	23.3 to 26.7 (-418 to -412)	771 (1,118)	84.4 (186)
Initiation of Dump	20.0 to 22.2 (-424 to -420)	517 (750)	84.4 (186)
Termination of Dump	23.3 to 38.9 (-418 to -390)	34 (50)	7.3 (16)

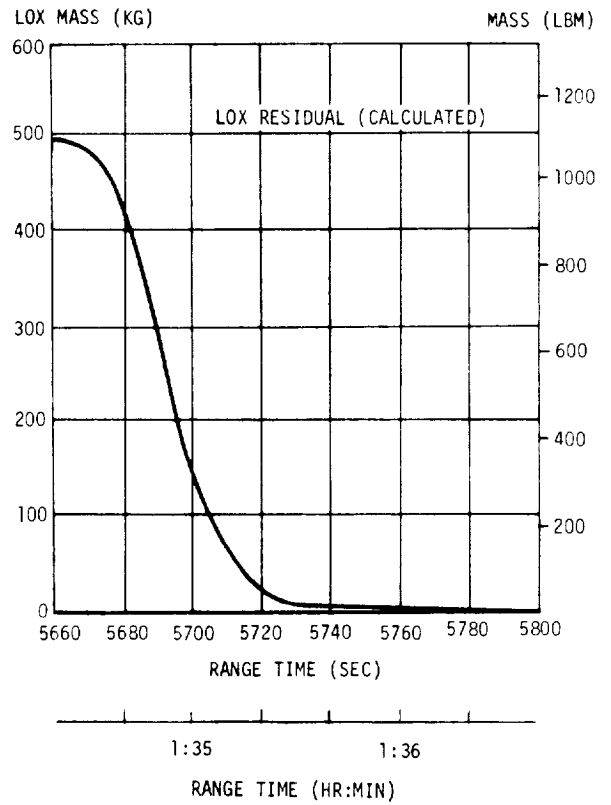
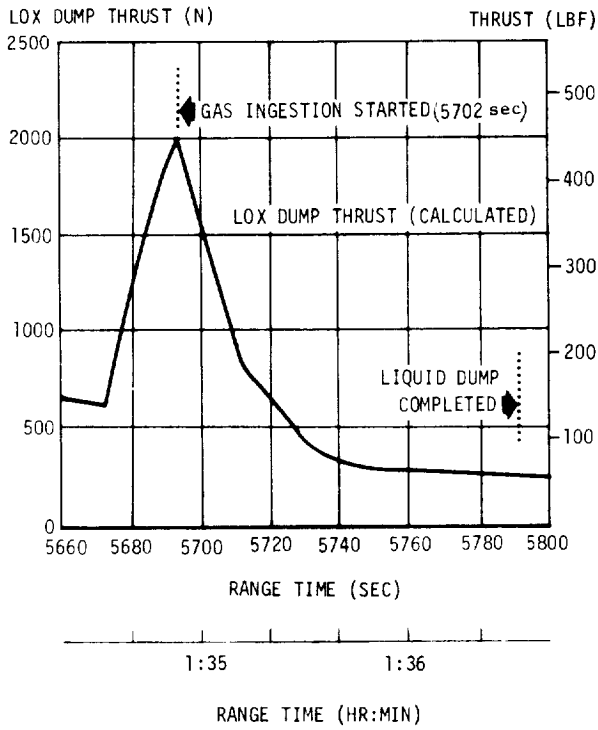
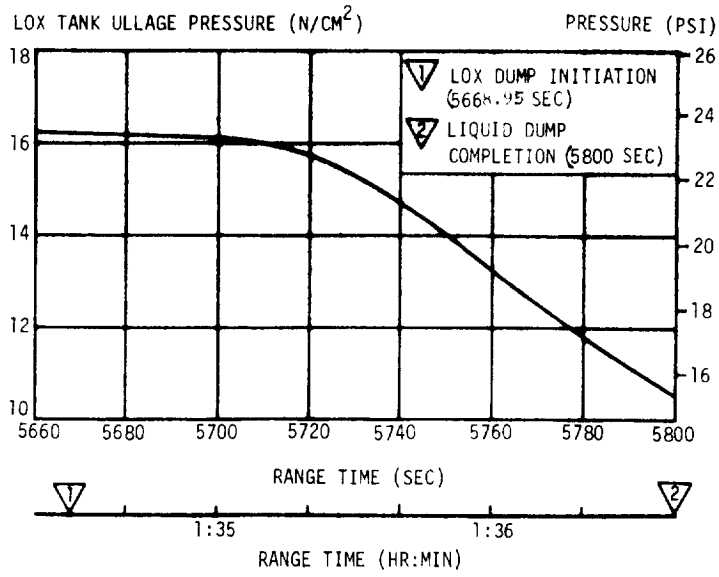


Figure 9-13. LOX Dump Performance

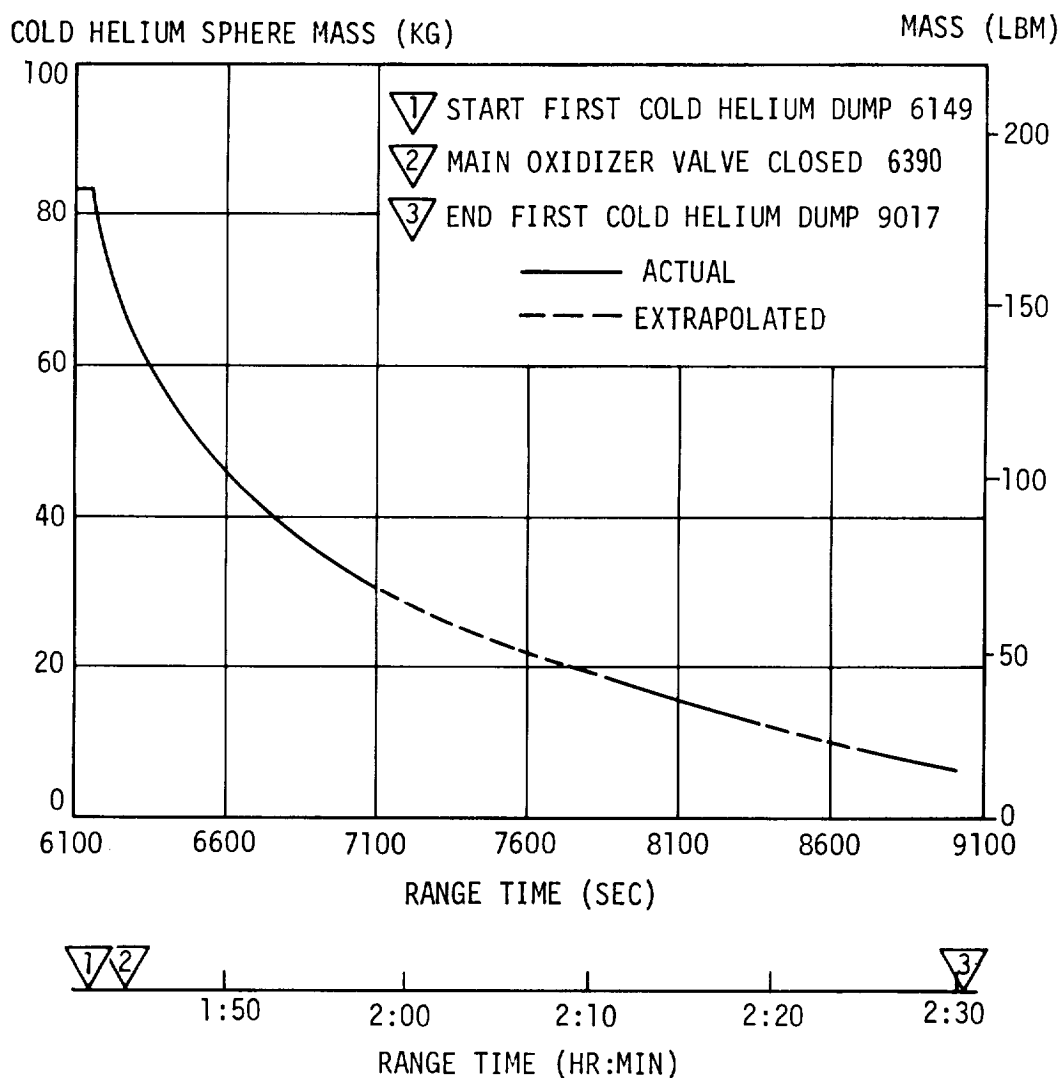
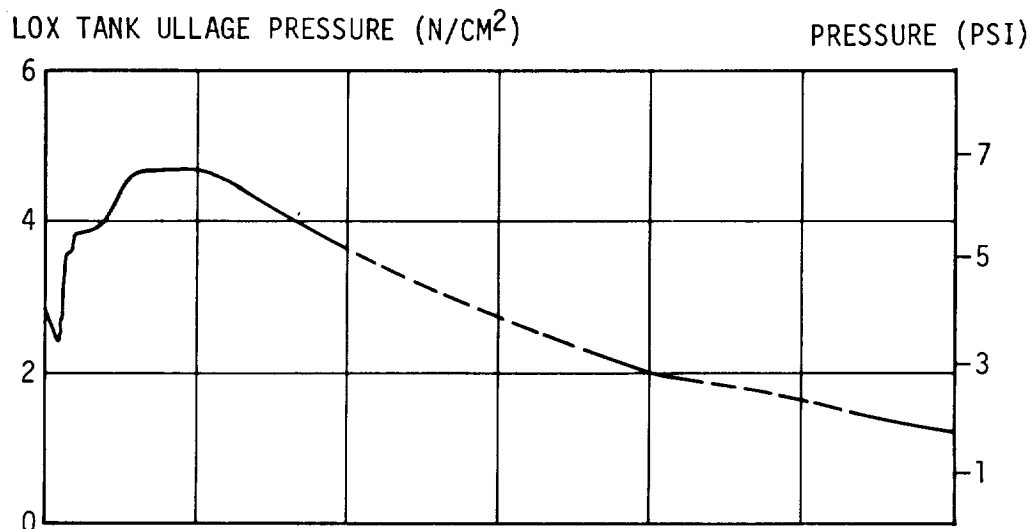


FIGURE 9-14 COLD HELIUM DUMP PERFORMANCE

9.6.5 PNEUMATIC SPHERE

Stage Pneumatic Sphere (Ambient Helium)

The stage pneumatic helium usage during orbit was negligible. The pressure in the sphere increased slightly due to warmup as indicated in Table 9-XI. The sphere was safed by activating the J-2 engine turbopump seal purges, and allowing the helium to vent through the pump. As indicated in the left-hand portion of Figure 9-15, the sphere pressure stayed within the predicted band, although the rate of pressure decay was more rapid than had been anticipated. This was the result of a blowdown which was polytropic in nature rather than isothermal as had been expected.

The purge was terminated at 14,821.27 sec by ground command, 2,061.03 sec earlier than programmed, with the sphere pressure at 1034 N/cm² (1500 psi), in order to save the remaining helium for control of the LH₂ tank vent-and-relief valve. Safing, however, was adequately accomplished.

TABLE 9-XI STAGE PNEUMATIC SPHERE PARAMETERS

Event	Pressure N/cm (psi)
ECC	2130 (3090)
Initiation of Sphere Safing	2206 (3200)
Termination of Sphere Safing	1034 (1500)

GH₂ Start Bottle

No safing of the start sphere was needed, since it was not repressurized during the burn. A backup pressure measurement, added to S-IVB-205, agreed very closely with the still existing, previously used measurement, thus increasing confidence that the previous measurement is valid in orbit.

Engine Control Sphere

The engine control sphere safing was satisfactorily accomplished by dumping through the main-fuel-valve-closed vent and holding the main oxidizer valve in the

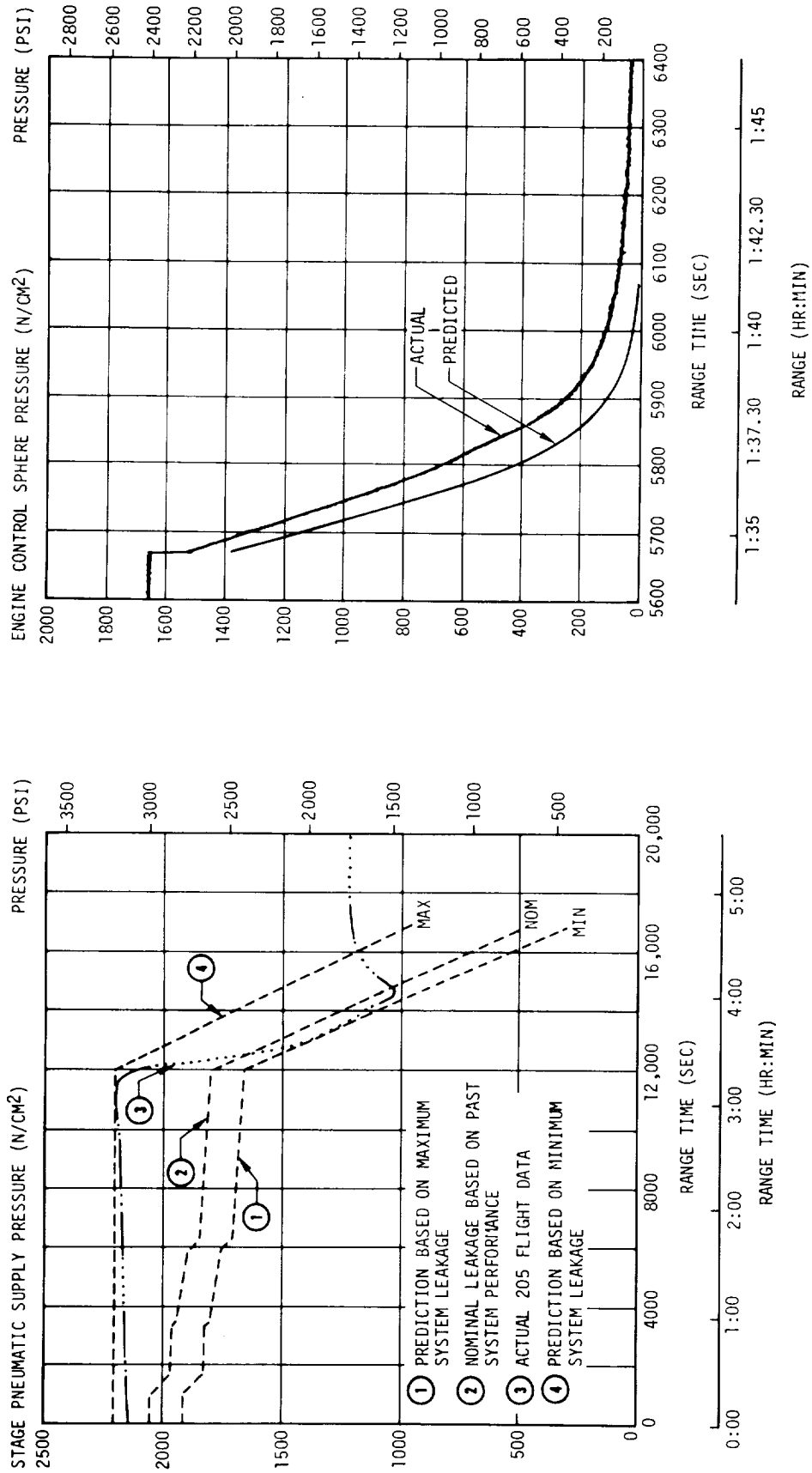


FIGURE 9-15 S-IVB STAGE AND ENGINE PNEUMATIC SUPPLY PRESSURES

open position. At LOX dump initiation (5668.95 sec), the sphere pressure was approximately 138 N/cm^2 (200 psi) higher than predicted (right-hand portion of Figure 9-15). Because of the higher initial pressure, the sphere pressure decay rate was slightly higher than predicted. There was no significant pressure recovery subsequently to the dump.

10.0 AUXILIARY PROPULSION SYSTEM

10.1 SUMMARY

The performance of each motor in the two Auxiliary Propulsion System (APS) modules was as expected. The average specific impulses of Modules 1 and 2 during powered flight were 213 and 216 sec, respectively.

The APS functioned properly to provide roll control during S-IVB powered flight and to provide pitch, yaw, and roll control following S-IVB engine cutoff. Of the available propellants, 2.3% was required for roll control during S-IVB powered flight. Modules 1 and 2 lifetimes were in excess of 15 hr 30 min.

10.2 APS PERFORMANCE

10.2.1 PROPELLANT AND PRESSURIZATION SYSTEMS

Modules 1 and 2 oxidizer and fuel systems operated properly. The temperatures of propellants remaining in each module during the flight are included in the lower portion of Figure 10-1. The propellant masses consumed during the major phases of flight are tabulated in Table 10-1 and shown in the upper portion of Figure 10-1.

APS helium pressurization systems functioned satisfactorily throughout the flight.

10.2.2 APS MOTOR PERFORMANCE

APS motor performance was satisfactory throughout the flight. It is evident from the coincidence of the APS motor pulses and flight events that the APS firings were of satisfactory frequency and duration. The longest pulse recorded was 1.140 sec on the pitch motor of Module 2 during the pitch-up maneuver under manual control.

After the propellant supply pressures decreased to the nominal orbital level (regulator at vacuum reference), the APS motor chamber pressures were in the 62 to 69 N/cm² (90 to 100 psi) range. The chamber pressure traces exhibited normal start, transient, and cutoff characteristics. Of the available propellants, 2.3% was required for roll control during S-IVB powered flight. This is 0.6 kg (1.3 lbm) from each module and is close to the predicted usage for this period. Roll control required 42 pulses each from engines I_{II} and III_{IV} and 5 pulses each from engines I_{IV} and III_{II}. The specific impulse during this period was 213 sec for Module 1

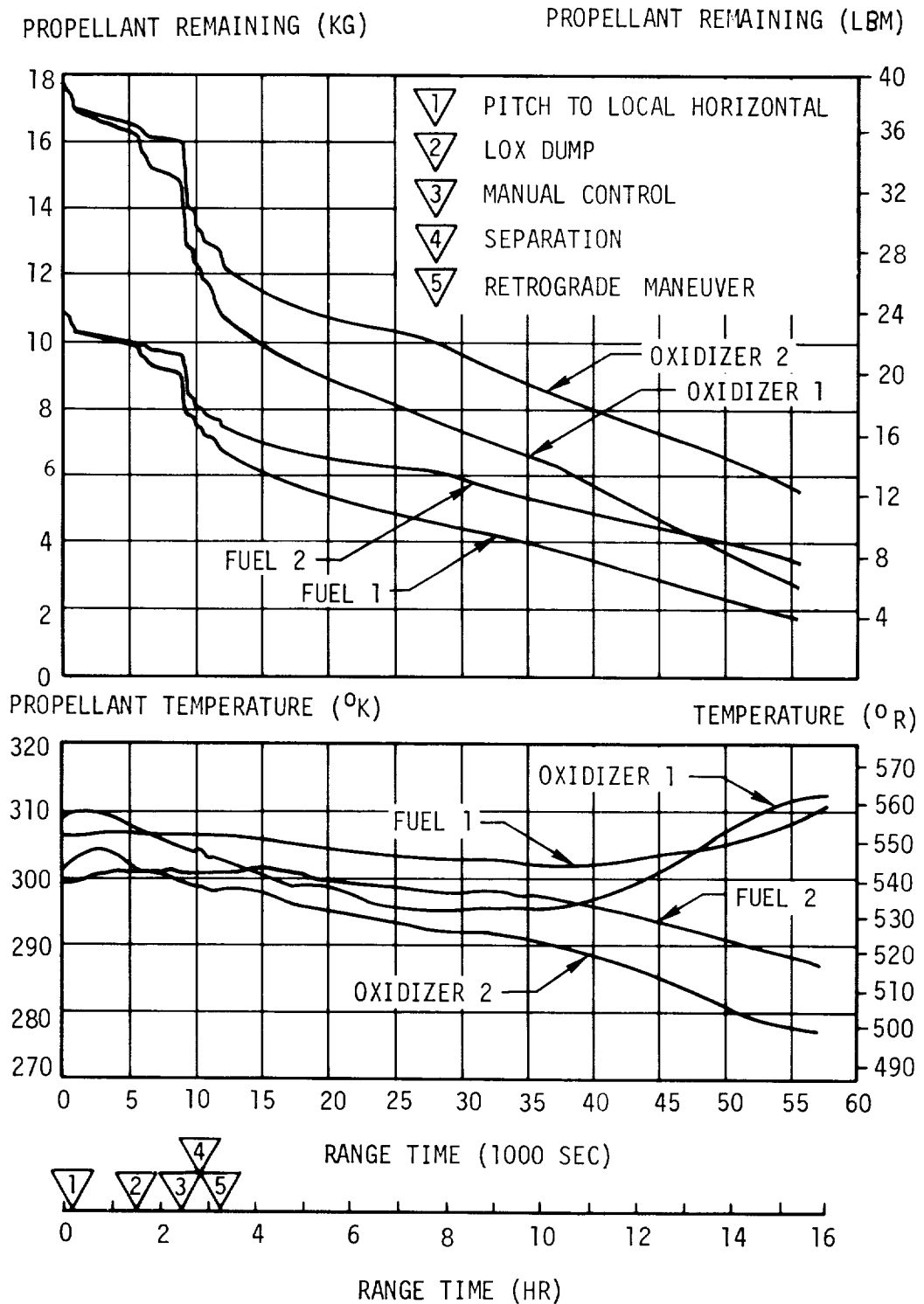


FIGURE 10-1. APS PROPELLANT REMAINING AND TEMPERATURE

TABLE 10-I AS-205 APS PROPELLANT USAGE

Events	MODULE 1				MODULE 2			
	Oxid Quant Used	% of Ox Used	Fuel Quant Used	% of Fuel Used	Oxid Quant Used	% of Ox Used	Fuel Quant Used	% of Fuel Used
Roll Control During S-IVB Powered Flight	0.4 kg (0.9 lbm)	2.3%	0.2 kg (0.5 lbm)	2.1%	0.4 kg (0.9 lbm)	2.3%	0.2 kg (0.5 lbm)	2.1%
Coast Period from End of Powered Flight Until Start of LOX Dump	1.4 kg (3.1 lbm)	7.9%	0.9 kg (2.0 lbm)	8.4%	0.9 kg (1.9 lbm)	4.9%	0.5 kg (1.2 lbm)	5.0%
LOX Dump	0.8 kg (1.7 lbm)	4.4%	0.5 kg (1.0 lbm)	4.2%	0.3 kg (0.7 lbm)	1.8%	0.2 kg (0.4 lbm)	1.7%
Coast Period from LOX Dump to Start of Manual Control	0.3 kg (0.6 lbm)	1.5%	0.2 kg (0.5 lbm)	2.1%	0.1 kg (0.3 lbm)	0.8%	0.1 kg (0.1 lbm)	0.4%
Astronaut Manual Control	2.2 kg (4.8 lbm)	12.3%	1.3 kg (2.8 lbm)	11.7%	2.1 kg (4.7 lbm)	12.1%	1.3 kg (2.9 lbm)	12.1%
Coast Period From Manual Control Thru Retrograde	1.9 kg (4.2 lbm)	10.8%	1.1 kg (2.4 lbm)	10.0%	1.6 kg (3.5 lbm)	9.0%	1.0 kg (2.1 lbm)	8.8%
Coast Period From the End of Retrograde to Liftoff +55,780 sec	8.1 kg (17.8 lbm)	45.6%	4.9 kg (10.9 lbm)	45.6%	6.7 kg (14.8 lbm)	38.0%	4.0 kg (8.8 lbm)	36.8%
TOTAL	15.1 kg (33.1 lbm)	84.8%	9.1 kg (20.1 lbm)	84.1%	12.1 kg (26.8 lbm)	68.7%	7.3 kg (16.0 lbm)	66.9%

EMR Average Module 1 = 1.65
EMR Average Module 2 = 1.68

NOTE: All the propellant was depleted by liftoff + 58,800 sec. This is at Canary Island 11th Orbit.

and 216 sec for Module 2. These values are as expected for minimum impulse bits. The Modules 1 and 2 total impulse for various events throughout the flight is presented in Table 12-III(APS Event Summary in Section 12). The average engine mixture ratio (EMR) of Module 1 was 1.65; and of Module 2, 1.68.

11.0 HYDRAULIC SYSTEM

11.1 SUMMARY

The vehicle's hydraulic systems performed satisfactorily throughout powered flight and during the orbital control mode. Pressure, oil levels, and temperatures remained within acceptable limits.

11.2 S-IB HYDRAULIC SYSTEM

The four outboard H-1 engines are gimbal-mounted to the S-IB stage thrust structure. Controlled positioning of these engines by means of hydraulic actuators provides thrust vectoring for vehicle attitude control. The force required for actuator movement is provided by four independent closed-loop hydraulic systems.

The system pressures were satisfactory during the flight and were similar to those of the S-IB-4 flight. Engine 1 pressure was approximately 137.9 N/cm^2 (200 psi) lower than the other three pressures during prelaunch and flight. Analysis of the system pressures (static firing, prelaunch, and flight), the reservoir fluid levels, and previous high pressure transducer discrepancies, shows that the indicated pressure of engine 1 was low because some turns of the high pressure transducer potentiometer were shorted together. Oil level and temperature data show that the hydraulic system on engine 1 functioned satisfactorily. At range zero, the system pressures ranged from 2223.6 to 2240.8 N/cm^2 gauge (3225 to 3250 psig) on engines 2 through 4. The pressure decreased approximately 24.1 N/cm^2 (35 psi) on each engine during flight. This normal pressure decrease was due to the main pump temperature increase during the flight.

Reservoir oil levels were also similar to those of the S-IB-4 flight. There was a rise of approximately 2% in each level from 0 to 114 sec, indicating about 7.8°K (14°F) rise in each hydraulic system's average oil temperature (not reservoir oil temperature). The indicated reservoir oil level of engine 2 fluctuated from 10 sec until the end of the flight. The cause of these fluctuations was attributed to transducer "noise." Analysis of the pressure and temperature data shows that the hydraulic system on engine 2 functioned satisfactorily.

The reservoir oil temperatures were satisfactory during flight. Temperatures for S-IB-5 at lift-off averaged 329.3°K (133°F) as compared to an average 333.7°K (141°F) for the four S-IB-4 hydraulic systems. The average temperature decrease during the flight was 9.4°K (17°F) for S-IB-5 as compared to a decrease of 10.6°K (19°F) for the four S-IB-4 hydraulic systems. The reservoir oil temperature of

engine 2 hydraulic system increased approximately 1.1°K (2°F) between 88 and 91 seconds. Similar temperature increases were noted on all four S-IB-1 systems and three of the S-IB-2 systems. The maximum flowrate during the flight occurred at approximately 87 sec on all four hydraulic systems. The temperature increase on engine 2 probably was caused by interchange of actuator return oil, which is warmer than the fluid in the reservoir, with fluid in the bottom of the reservoir. Normally, the bulk of the actuator return oil returns directly to the main pump without entering the reservoir; consequently, the reservoir oil temperature decreases during flight.

11.3 S-IVB STAGE HYDRAULIC SYSTEM

The S-IVB hydraulic system performed satisfactorily throughout the flight. Thermal expansion of oil was not sufficient to cause overboard venting. System internal leakage of $0.0022\text{ m}^3/\text{min}$ (0.59 gpm) was within the allowable range of 0.0015 to $0.0030\text{ m}^3/\text{min}$ (0.4 to 0.8 gpm).

The auxiliary pump discharge pressure setting was slightly higher than that of the main engine-driven pump. The auxiliary pump provided the system internal leakage flow during burn. Reservoir fluid level rose from 17% at liftoff to 25% at the end of engine burn due to increased oil temperature. After flight-mode-off command, when pump pressure had decreased to zero, the accumulator oil volume was forced back into the reservoir by the accumulator gas precharge, bringing the reservoir level up to 92%. The main (engine-driven) hydraulic pump extracted 2 horsepower during engine burn mode.

After S-IVB ECC, the main pump inlet oil temperature continued to rise because of the transfer of heat from the LOX turbine housing to the pump manifold. Inlet temperature peaked at 349.8°K (170°F) at 2250 seconds.

There was one programmed thermal cycle of the auxiliary pump during orbital coast. The auxiliary pump was turned on for 48 sec in order to circulate system fluid and distribute the higher temperature fluid in the reservoir throughout the system lines.

The auxiliary hydraulic pump was activated prior to the LOX dump experiment to center the engine. After the auxiliary hydraulic pump start, the inlet oil temperature dropped approximately to the reservoir temperature level. The reservoir oil temperature gradually increased as the hydraulic pump warmed the oil. No appreciable temperature change of the accumulator gas was noticed during the LOX dump experiment. The reservoir oil level dropped to 33% after pump start as 0.0015 m^3 (92 in^3) of oil was pumped into the accumulator. When the pump stopped, the reservoir was refilled to the 93% level.

12.0 GUIDANCE AND CONTROL

12.1 SUMMARY

The performance of the guidance and control system was excellent. The range (Z) accelerometer exhibited five consecutive zero-changes (i.e., changes between successive readings of one count or less) causing the use, at approximately 18 sec after liftoff, of one prestored backup acceleration value. The resulting Z velocity error of 0.1 m/sec was insignificant. The boost navigation and guidance schemes were executed properly and terminal parameters were well within acceptable limits. All orbital operations were nominal.

The control system functioned properly. Near the maximum dynamic pressure region, the maximum values observed for the control parameters were attitude errors of 1.7 deg in pitch, -0.7 deg in yaw, and -0.4 deg in roll; and angle-of-attack of -1.2 deg in pitch, and 1.1 deg in yaw. Control system transients occurred at S-IB/S-IVB separation, guidance initiation, artificial tau and chi bar guidance modes, chi freeze, and J-2 engine cutoff. These transients were expected and well within the capabilities of the control system. As experienced on previous flights, a steady state roll torque required roll control APS firings throughout S-IVB powered flight. The roll torque created a roll attitude error of approximately 0.6 degrees. During orbit, disturbances were noted during the 30 sec propulsive LOX vent shortly after cutoff, but control was normal during this period and also during LOX dump. The vehicle commands and responses, during the three minute astronaut manual control interface exercise, correlated well with the scheduled timeline and expected vehicle responses. Control during launch vehicle/spacecraft separation was nominal, and control of the launch vehicle continued normal until APS propellant depletion. The control system experienced an extended lifetime compared to previous flights due to a higher orbit resulting in lower aerodynamic disturbances.

12.2 SYSTEM CHANGES AND MODIFICATIONS

The navigation, guidance, and control system was the same as those flown on previous Saturn IB vehicles except for minor component changes to improve reliability and to permit astronaut control of the launch vehicle from the spacecraft (see Appendix A). The flight program was basically similar to the one used in the AS-204 LVDC but contained the following differences.

The accelerometer reasonableness test was revised by replacing the reasonableness test constant (RTC) with the product of the RTC multiplied by the time length of the computation cycle.

The initial gimbal angle reasonableness test constants were changed from 1.0 deg to 1.4 deg for the fine resolvers and from 4.0 deg to 18.5 deg for the coarse resolvers. Thereafter during flight, the RTC remained 0.4 deg for the fine resolvers and 0.6 deg for the coarse resolvers and during orbit, the RTC remained 1.0 deg for the fine resolvers and 2.0 deg for the coarse resolvers.

S-IVB propellant mixture ratio shift (PMRS) was caused by a switch selector command rather than by the propellant utilization system in the S-IVB stage.

During orbital flight, the minor loop was cycled twice each second rather than once. The APS thrusters were used for attitude control during orbital safing, rather than switching the flight control computer (FCC) to burn mode and gimbaling the engine. During periods of vehicle attitude control by the CSM crew, the LVDA/LVDC did not provide attitude correction command inputs to the FCC. Any offset in vehicle attitude at the end of spacecraft control was removed by the control system.

Telemetry station acquisition and loss were based on comparisons of vehicle and station positions rather than elapsed time. A telemetry calibration switch selector command was issued 60 sec after each station acquisition. Compressed data no longer included analog quantities provided by the computer interface unit.

The digital command system was inhibited during boost. The system capabilities included the provision for disabling environmental control system (ECS) water control valve logic. The logic temperature test was begun 480 sec after lift-off, preceded by the water valve opening at 180 sec after liftoff.

The orbital guidance routine, initiated 15.2 sec after time base 4 (T4), controlled the computation of the commanded platform gimbal angles during orbit. The predicted orbital attitude time line was as follows:

	<u>Maneuver</u>	<u>Time</u>
1.	Maintain cutoff inertial attitude for 20 sec after initiation of time base 4.	T4 + 0
2.	Begin orbital safing sequence by enabling J-2 engine dump. Maintain vehicle attitude.	T4 + 1
3.	Initiate maneuver to align the S-IVB/CSM along the local horizontal (CSM forward, position I down) and maintain with respect to local reference.	T4 + 20

	<u>Maneuver</u>	<u>Time</u>
4.	Begin manual control of S-IVB attitude from the spacecraft. Maneuvers in roll, pitch, and yaw will be based on maximum commandable rates of 0.3 deg/sec in pitch and yaw, and 0.5 deg/sec in roll.	GRR + 9000
5.	End manual control of S-IVB attitude from the spacecraft. The IU will return to its programed timeline whenever the spacecraft relinquishes attitude control.	GRR + 9180
6.	Initiate maneuver to pitch nose down 20 deg from the local horizontal (position I down) and maintain orbital rate.	GRR + 9780
7.	Initiate inertial attitude hold using gimbal angles at the specified initiation time. Maintain inertial attitude.	GRR + 10275
8.	Nominal CSM physical separation.	GRR + 10500
9.	Initiate maneuver to align the S-IVB/IU along the local horizontal, tail leading and roll to position I up. Maintain orbital rate.	GRR + 11820

12.3 LAUNCH VEHICLE FLIGHT CONTROL

Launch vehicle flight control parameters were nominal in the pitch, yaw, and roll planes during powered flight and during orbital coast. Graphical presentations of control data are made mostly for the pitch plane only, the plane of primary interest and as illustration of the nominal conditions. Detailed analyses, including plots of control parameters for the yaw and roll planes, are presented in the vehicle stage reports. (See References 6, 7, and 8.)

12.3.1 S-IB STAGE CONTROL ANALYSIS

The S-IB stage control system performed satisfactorily in the pitch, yaw, and roll planes. Table 12-I presents the control parameters maximum values in the high dynamic pressure region and values at S-IB/S-IVB separation. These maximum values are considered nominal and the values at separation are within the design limits of 1 deg attitude error and 1 deg/sec angular rate for S-IVB stage capture control analysis.

TABLE 12-1 S-IB MAXIMUM CONTROL PARAMETERS AND SEPARATION PARAMETERS

S-IB STAGE SEPARATION PARAMETERS

Parameter	Units	Pitch	Yaw	Roll
Attitude Error	deg	0.1	-0.1	0.6
Attitude Rate	deg/sec	0.0	0.0	0.3
Actuator Position	deg	0.1	0.0	0.2

S-IB MAXIMUM CONTROL PARAMETERS IN THE HIGH DYNAMIC PRESSURE REGION AND DURING ROLL MANEUVER

Parameters	Units	Pitch Plane		Yaw Plane	
		Magnitude	Range Time (sec)	Magnitude	Range Time (sec)
Attitude Error	deg	1.7	77.8	-0.7	86.2
Angle-of-Attack (Q-ball)	deg	-1.2	74.7	1.1	79.2
Angular Rate	deg/sec	-0.9	64.2	0.4	87.0
Normal Acceleration at IU	m/sec ²	-0.5	75.0	-0.4	91.4
Average Actuator Position	deg	0.6	84.3	1.0	86.1
Angle-of-Attack Dynamic Pressure Product	deg-N/cm ²	3.8	74.7	3.5	79.2
Roll Plane					
		During Roll Maneuver		After Roll Maneuver	
		Magnitude	Range Time (sec)	Magnitude	Range Time (sec)
Attitude Error	deg	-1.5	12.7	-0.4	84.3
Angular Rate	deg/sec	1.2	29.0	0.3	60.0
Engine Deflection	deg	-0.2	12.3	-0.1	84.3

Figure 12-1 shows the vehicle attitudes in roll and pitch compared to the commanded attitudes. The commanded attitudes started and stopped at the proper times and were properly executed by the control system.

The Q-ball free stream angle-of-attack and measured wind velocity in pitch are given in Figure 12-2 along with the resultant angle-of-attack, the vector sum of the pitch and yaw angles-of-attack. Comparison of Q-ball angles-of-attack with the FPS-16 calculated and the simulation angles-of-attack indicated an apparent Q-ball misalignment of -0.4 deg in yaw. The winds that are presented were taken from the final meteorological data tape.

Figure 12-3 shows the pitch plane control parameters; attitude error, angular rate, normal acceleration, and average actuator position. Comparison of telemetered attitude error and actuator position with the simulation values indicates an apparent engine misalignment of -0.05 deg for eight engines (or -0.10 deg for four engines, etc.). This is within the 3 sigma value for mechanical engine misalignment only. (See Reference 9.)

The yaw and roll control parameters were nominal and compared well with the simulation. Both the pitch and yaw accelerometers have their power turned off at 120 sec, so their readings past that time are not valid. All control parameters in pitch, yaw, and roll were digitally filtered with a 1 Hz low-pass filter.

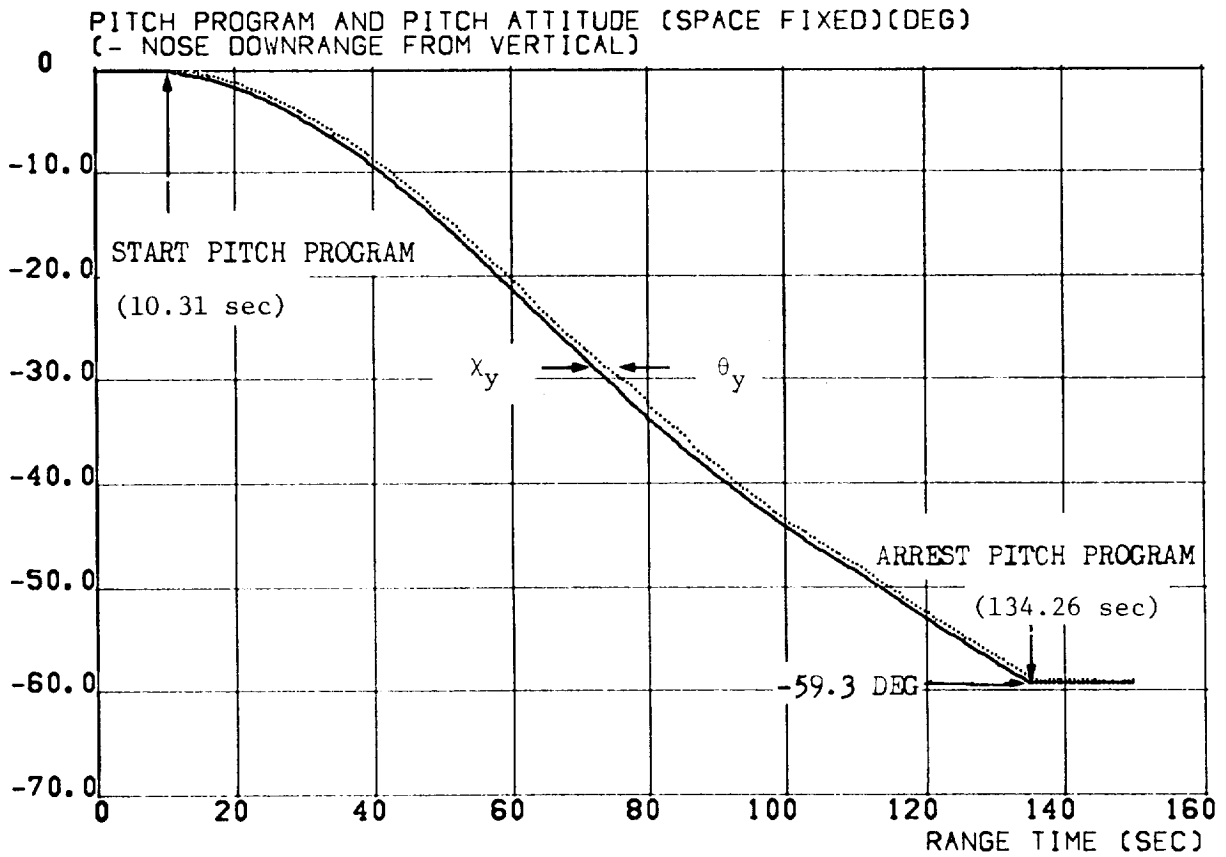
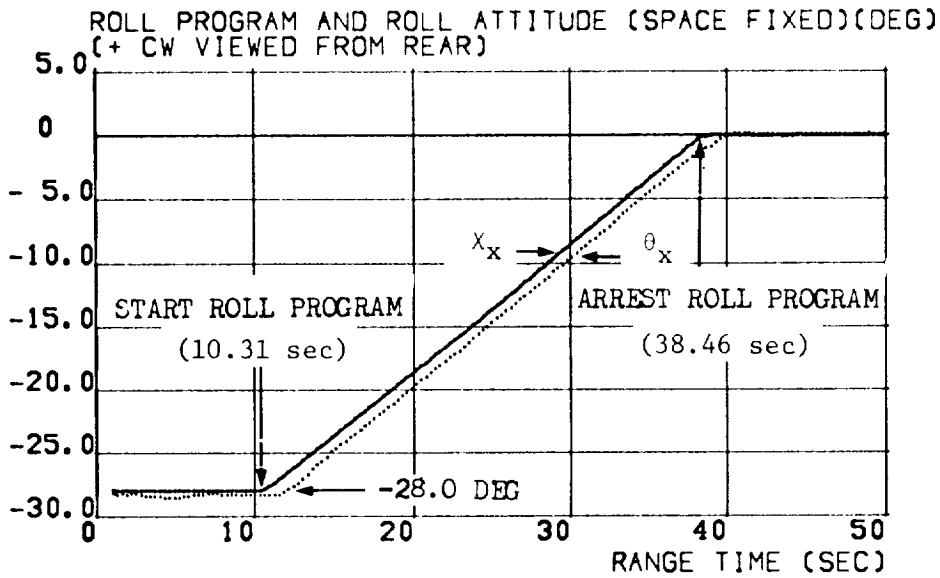
12.3.2 S-IVB STAGE CONTROL ANALYSIS

The S-IVB thrust vector control system provided satisfactory control in the pitch and yaw planes during powered flight. The auxiliary propulsion system (APS) provided satisfactory roll control during powered flight and satisfactory pitch, yaw, and roll control during orbital coast.

During S-IVB powered flight, control system transients were experienced at S-IB/S-IVB separation, guidance initiation, artificial tau and chi bar guidance modes, chi freeze, and J-2 engine cutoff. These transients were expected and were well within the capabilities of the system.

The S-IVB attitude control system responses to guidance commands for the pitch axis during powered flight are presented in Figure 12-4. Significant events related to control system operation are indicated on the figure.

As experienced on previous flights, a steady state roll torque, approximately 20.3 N-m (15 lbf-ft) clockwise looking forward, required roll control APS firings throughout powered flight. This roll torque was considerably less than the maximum steady state roll torque previously experienced on AS-502, 54.2 N-m (40 lbf-ft). The steady state roll torque experienced on AS-204 was 36.6 N-m (27 lbf-ft).



θ VEHICLE ATTITUDE

X COMMAND ATTITUDE

FIGURE 12-1 S-1B STAGE COMMAND ANGLES

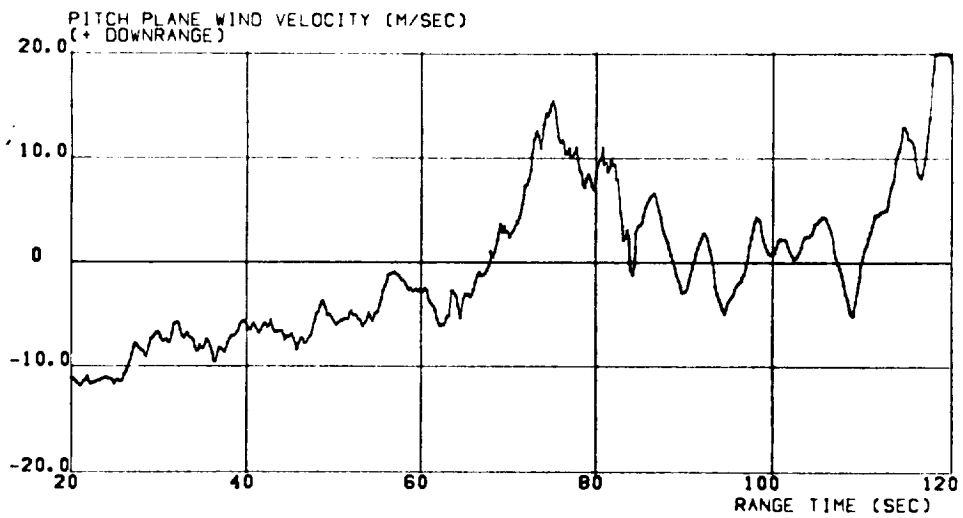
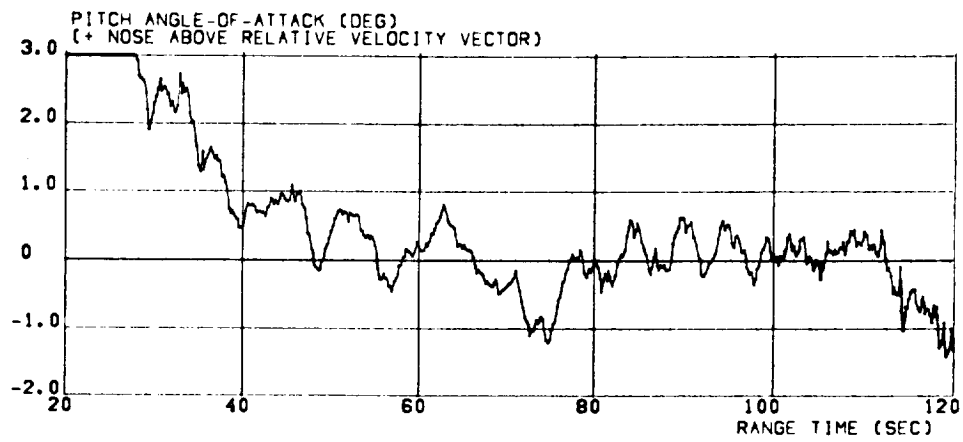
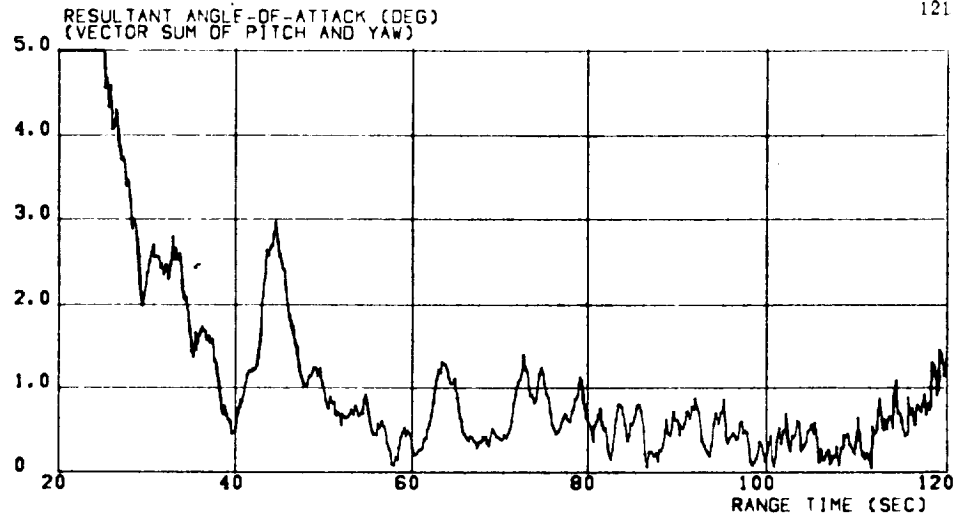


FIGURE 12-2 WIND VELOCITY AND FREE STREAM ANGLE-OF-ATTACK

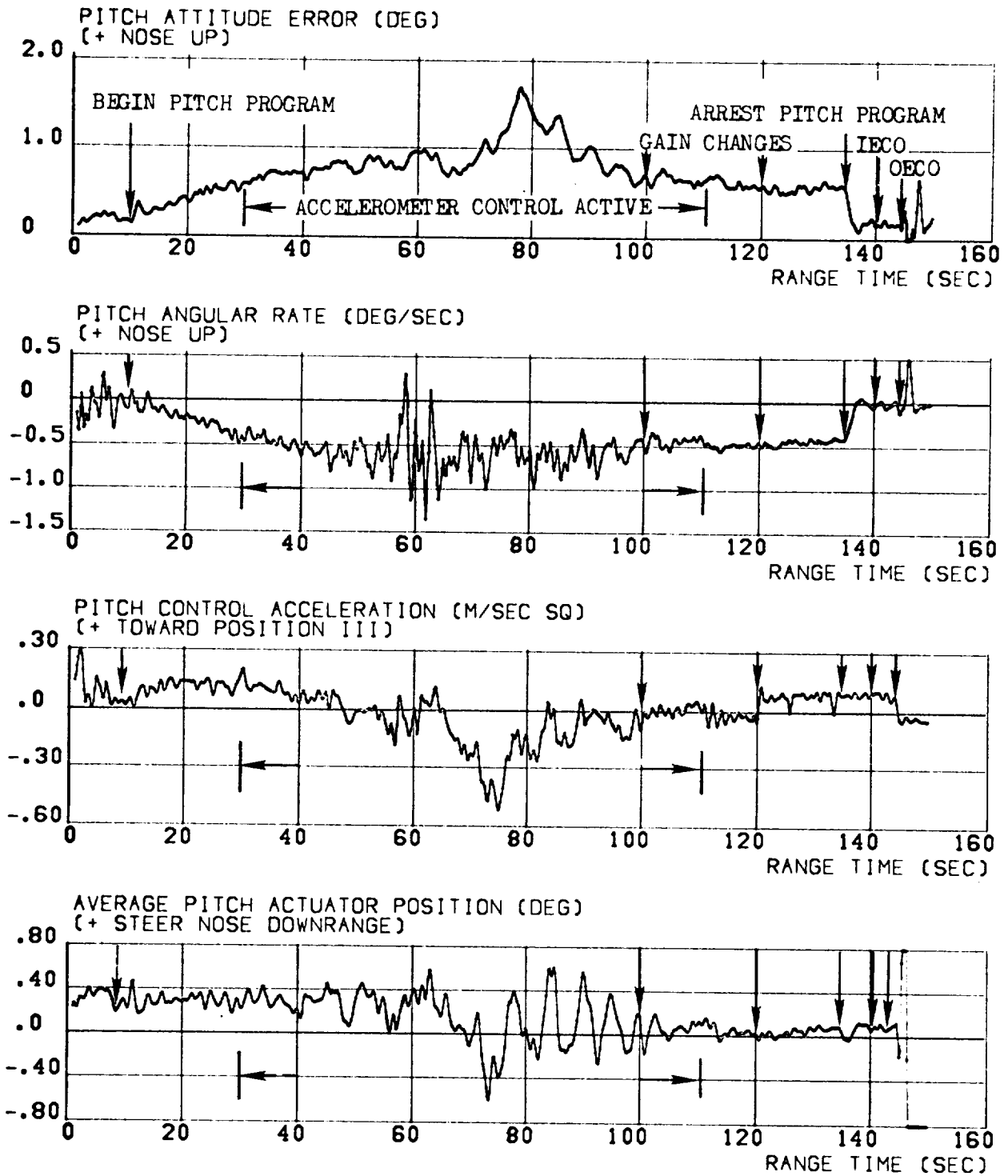


FIGURE 12-3 PITCH CONTROL PARAMETERS DURING S-IB POWERED FLIGHT

- ▽ 1 S-IB/S-IVB SEPARATION, S-IVB ENGINE START, FLIGHT CONTROL COMPUTER BURN MODE ON
- ▽ 2 INITIATE ITERATIVE GUIDANCE MODE
- ▽ 3 INITIATE ARTIFICIAL TAU MODE
- ▽ 4 INITIATE CHI BAR GUIDANCE
- ▽ 5 INITIATE CHI FREEZE
- ▽ 6 S-IVB ENGINE CUTOFF, FLIGHT CONTROL COMPUTER BURN MODE OFF

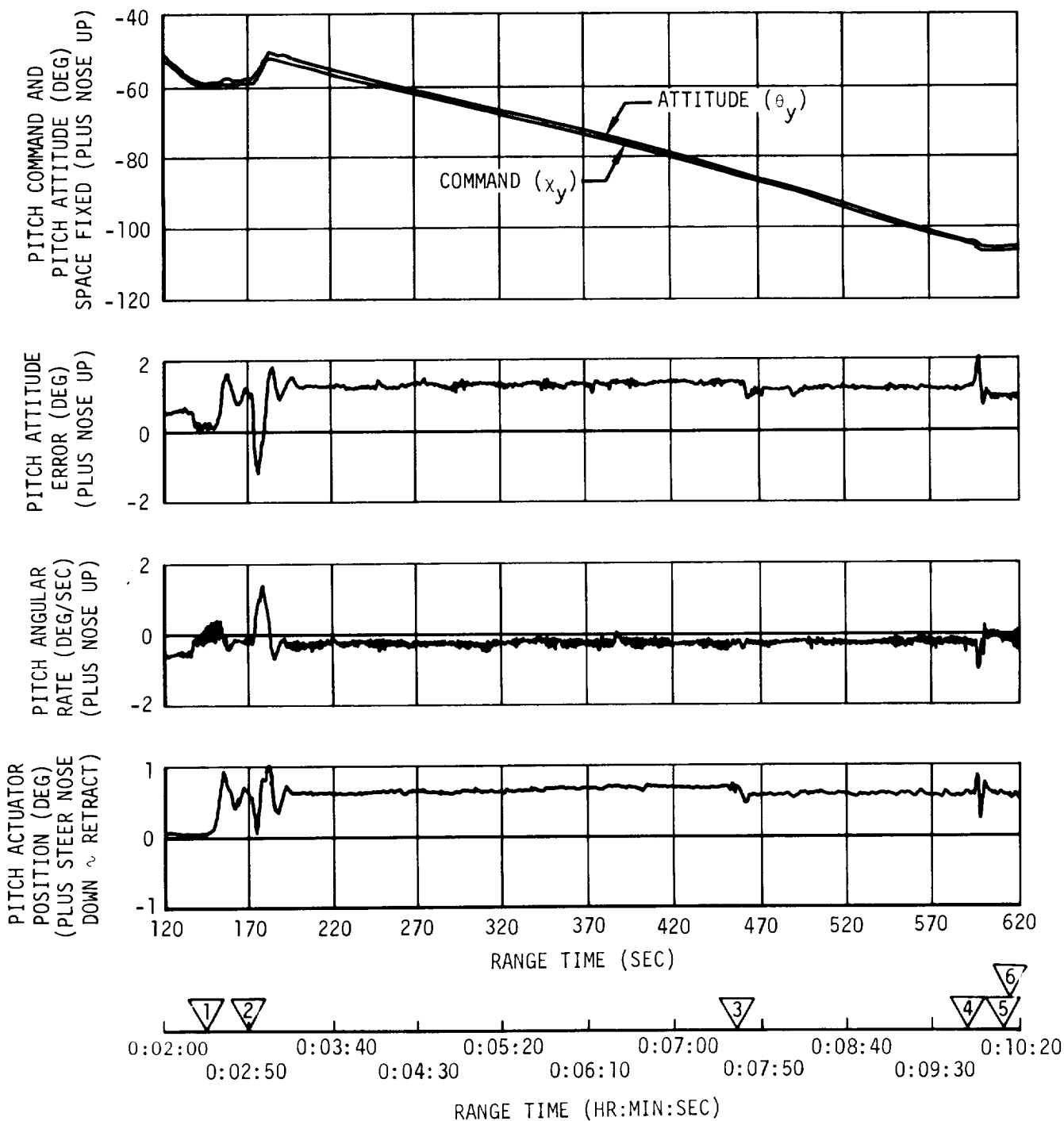


FIGURE 12-4 PITCH ATTITUDE CONTROL DURING S-IVB POWERED FLIGHT

Sinusoidal variations were detected on both hydraulic actuators throughout S-IVB powered flight. The variations were approximately 0.05 deg peak to peak amplitude with a frequency of 0.4 Hz. The frequency corresponds closely with the telemetered LH₂ slosh frequency; therefore, the LH₂ slosh mass was assumed to be the driving force. Similar actuator oscillations have been evidenced on previous Saturn flights. Actuator oscillations of 0.1 deg peak to peak between 0.4 and 0.8 Hz were observed on AS-201. The propellant sloshing did not have a significant effect on the control system operation.

A sudden shift in the pitch and yaw actuator positions and attitude errors was noted following the programmed propellant mixture ratio shift (PMRS) at approximately 456 seconds. The shift in actuator position appears to have been caused by the relaxation of the thrust structure following propellant utilization (PU) cutback and a resulting change in thrust of approximately 226,859 N (51,000 lbf). The thrust structure relaxation required the extension of both actuators to reposition the thrust vector through the center of gravity, and a shift in attitude to keep the actuators in the new trim position. This noted shift in the actuators position and attitude errors at the time of PU cutback was more abrupt than on previous flights. This is attributed to the rapid change, less than 2 sec, in thrust and acceleration resulting from the programmed PMRS on AS-205 as opposed to a much slower change in thrust and acceleration experienced on previous flights which employed closed loop PU system operation.

Maximum values of attitude errors, angular rates, and actuator position are summarized for significant events during powered flight in Table 12-II.

Propellant sloshing was observed on data obtained from the LH₂ and LOX PU sensors. The propellant slosh amplitudes and frequencies were comparable to that experienced on previous flights and did not have an appreciable effect on the control system.

The LH₂ slosh amplitudes and frequencies experienced during S-IVB burn are shown in the upper portion of Figure 12-5. The maximum LH₂ slosh amplitude indicated at the PU sensor was 23.8 cm (9.37 in) zero to peak. The LH₂ slosh frequency correlated well with the predicted LH₂ first mode slosh frequency. Previous Saturn IB flights have exhibited an LH₂ slosh frequency near the first mode frequency.

The LOX slosh amplitudes and frequencies during S-IVB powered flight are shown in the lower portion of Figure 12-5. The maximum LOX slosh amplitude observed at the PU sensor was 0.66 cm (0.26 in) zero to peak. The LOX slosh frequency correlated with the predicted LOX first mode slosh frequency with the exception of the time interval between 300 and 350 sec, when LOX sloshing appeared to be driven by the LH₂ sloshing at the LH₂ first mode frequency.

TABLE 12-II MAXIMUM VALUES OF CRITICAL FLIGHT CONTROL PARAMETERS

PARAMETERS	S-IVB/S-IB SEPARATION AND S-IVB IGNITION	GUIDANCE INITIATION	FLIGHT CONTROL COMPUTER GAIN CHANGE	ARTIFICIAL TAU GUIDANCE	CHI BAR GUIDANCE MODE	CHI FREEZE AND J-2 ENGINE CUTOFF
ATTITUDE ERROR (DEG)						
PITCH	1.6	1.8	1.3	1.4	2.0	1.0
YAW	-1.1	-2.8	-1.1	-1.3	-1.2	-1.3
ROLL	1.1	-0.5	0.7	0.7	0.6	0.5
ANGULAR RATE (DEG/SEC)						
PITCH	0.4	1.3	-0.2	-0.3	-0.8	+0.1
YAW	-0.2	1.1	0.0	0.1	+0.1	0.1
ROLL	-0.2	0.2	0.0	0.0	-0.1	+0.1
ACTUATOR POSITION (DEG)						
PITCH	0.9 RET	1.1 RET	0.7 RET	0.7 RET	0.9 RET	(TRIM) 0.8 RET
YAW	0.6 RET	1.0 RET	0.6 RET	0.7 RET	0.7 RET	(TRIM) 0.7 RET

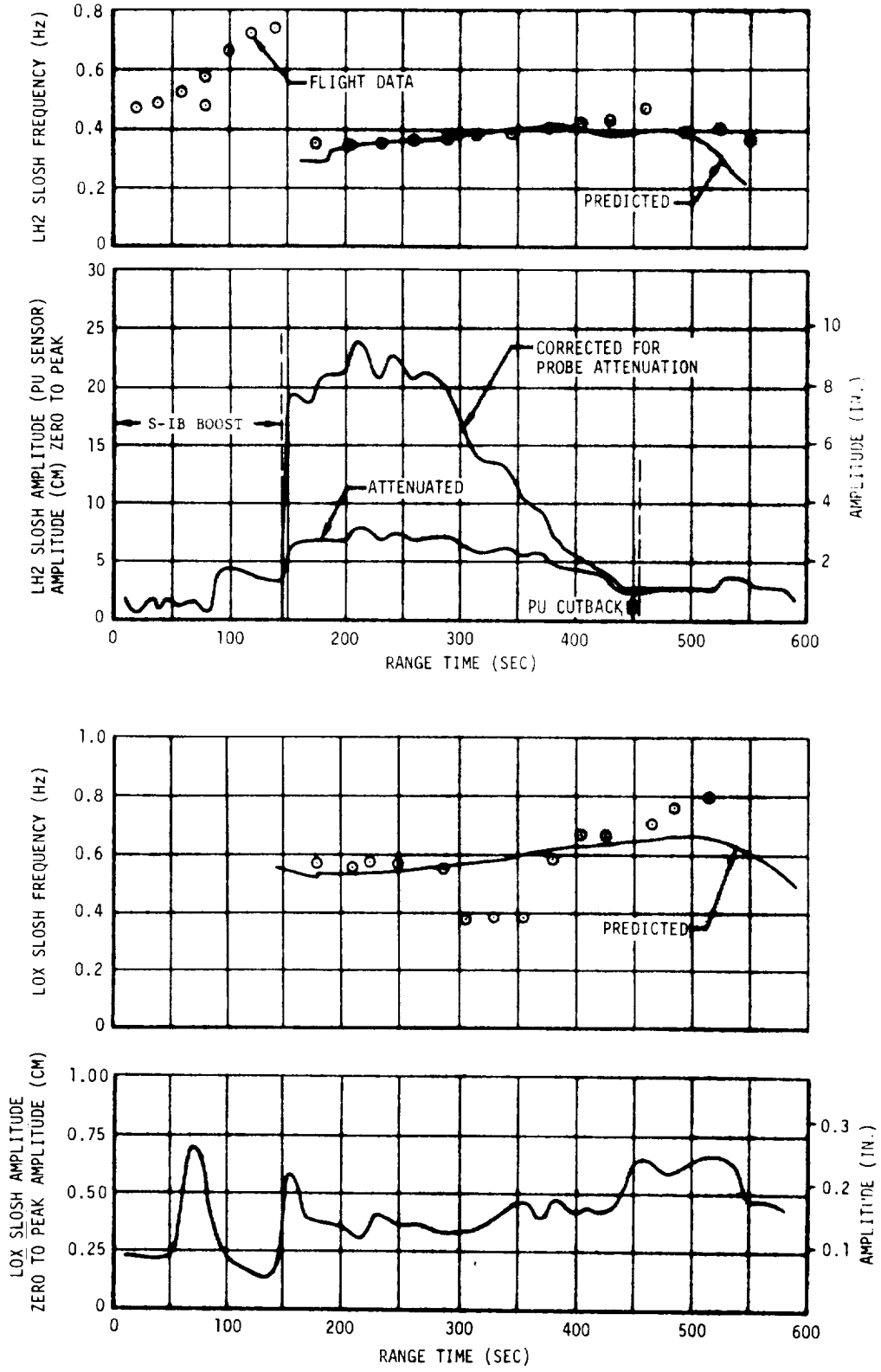


FIGURE 12-5 SLOSHING DURING POWERED FLIGHT

12.3.3 CONTROL DURING ORBITAL COAST

Following S-IVB cutoff and switching to orbital control mode, normal programmed pitch and yaw maneuvers were executed at $T4 + 20$ sec to align the stage with the local horizontal and establish the desired yaw attitude, respectively. Disturbances were noted during the 30 sec propulsive LOX vent, occurring at $T4 + 30.2$ seconds. Attitude control during the interval appeared normal. The control system response to guidance command and stage disturbances during this interval are shown for the pitch axis in Figure 12-6.

Attitude control during the LOX dump (5669 to 6390 sec) appeared normal. APS impulse requirements for attitude control during the LOX dump were 2494.6 N-s (560.8 lbf-sec) for Module 1 and 1174.3 N-s (264.0 lbf-sec) for Module 2. Pitch control system parameters and associated APS engine firings during this interval are shown in Figure 12-7.

Manual control of the S-IVB stage was initiated at approximately 9049 seconds. During a three minute control interface exercise the crew performed various pitch, yaw, and roll maneuvers. Control system attitude commands, corresponding vehicle attitude responses, and APS engine firings during this exercise are shown in Figure 12-8 for the pitch, yaw, and roll planes. The vehicle commands and responses during manual control correlated well with the scheduled timeline and expected vehicle responses. The actual APS propellant usage during manual control, 3.4 kg (7.6 lbm) from Module 1 and 3.4 kg (7.6 lbm) from Module 2, correlated with the predicted usage of 2.4 kg (5.2 lbm) per module.

Attitude control during spacecraft separation appeared normal. The control system response in the pitch axis during this interval is shown in Figure 12-9.

The command to maneuver to retrograde attitude was begun at 11,816 sec and accomplished satisfactorily. During this maneuver, the pitch attitude error and angular velocity averaged approximately -2.6 deg and 0.4 deg/sec, respectively. A yaw attitude error of 2.2 deg (maximum) was issued as the retrograde maneuver began and produced a maximum yaw rate of -0.4 deg/sec.

Control system attitude commands and vehicle attitude responses prior to and following the navigation update performed at 17,460.4 sec are shown in Figure 12-10 for the pitch, yaw, and roll planes. The update effected a 2.6 deg change in the pitch attitude command and a minor change in the yaw attitude command.

- 1 INITIATE GHI FREEZE
- 2 S-IVB ENGINE CUTOFF COMMAND, LH2 TANK VENT OPEN
- 3 FLIGHT CONTROL COMPUTER BURN MODE OFF
- 4 INITIATE MANEUVER TO LOCAL HORIZONTAL
- 5 LOX TANK VENT OPEN COMMAND

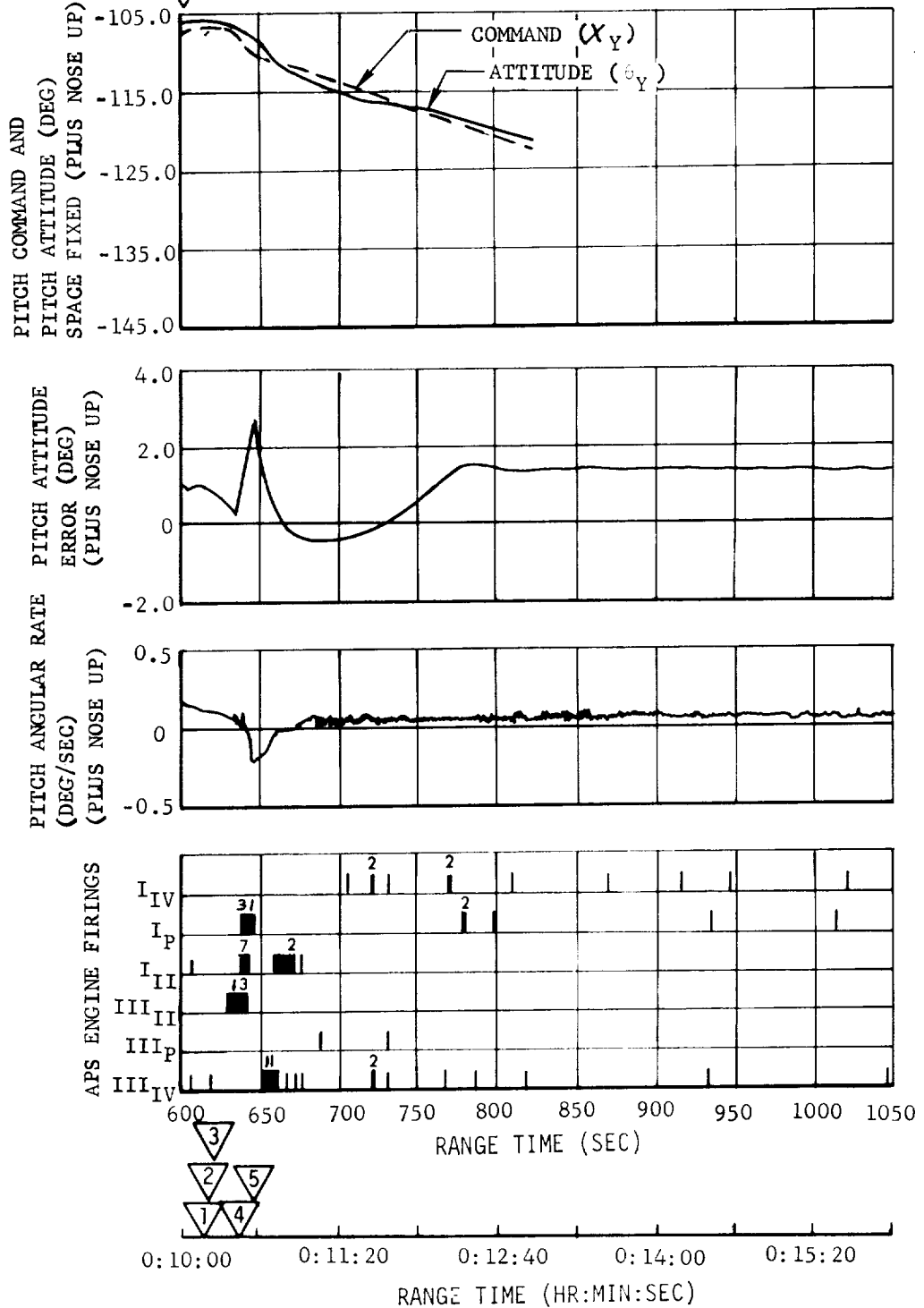


FIGURE 12-6 PITCH ATTITUDE CONTROL DURING S-IVB ALIGNMENT WITH LOCAL HORIZONTAL

- 1 INITIATE LOX DUMP
- 2 TERMINATE LOX DUMP

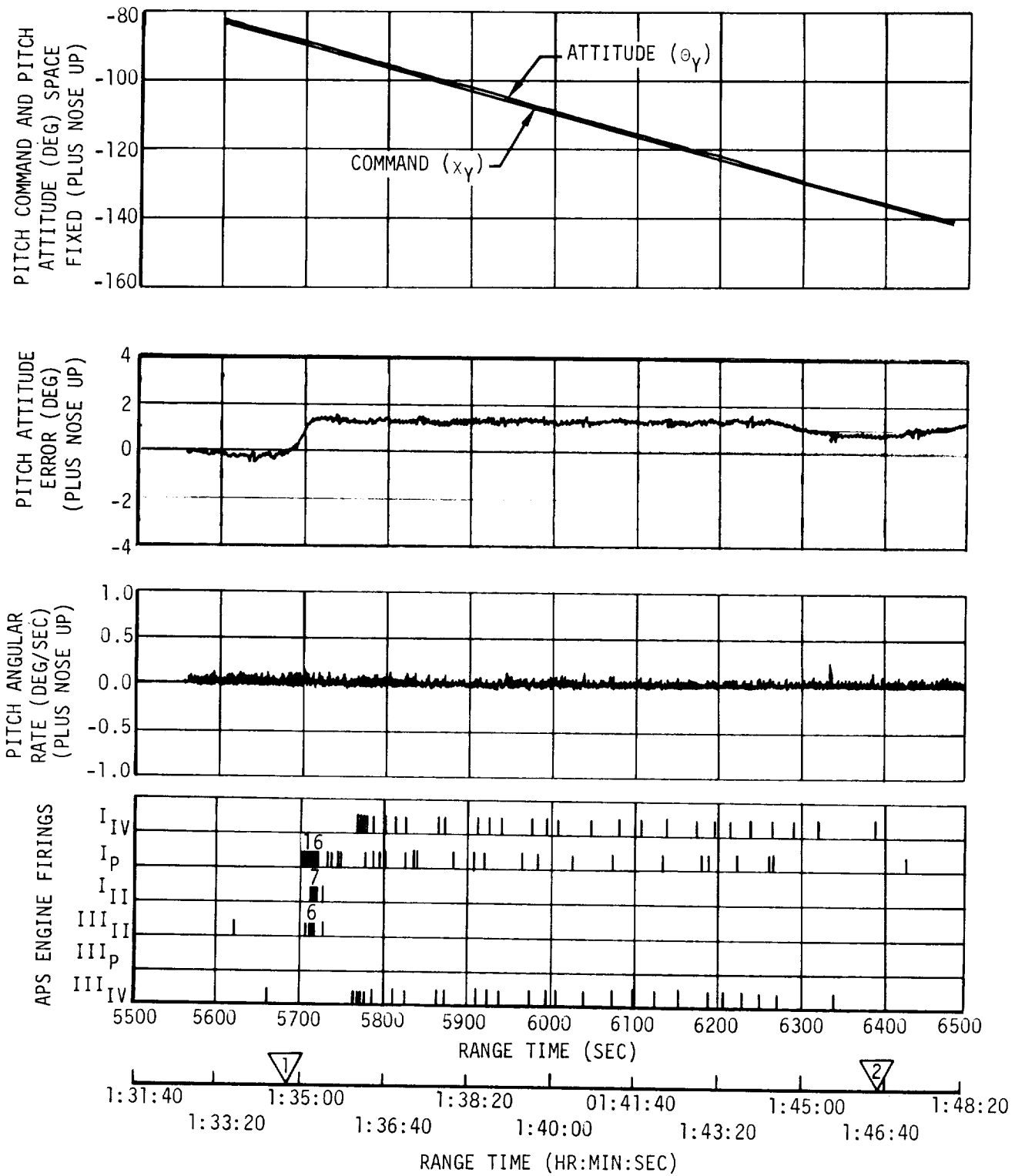
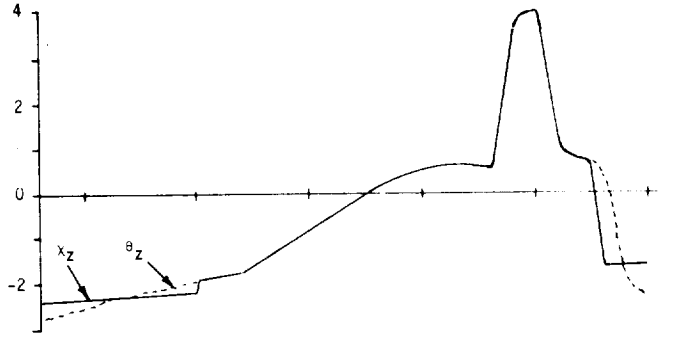
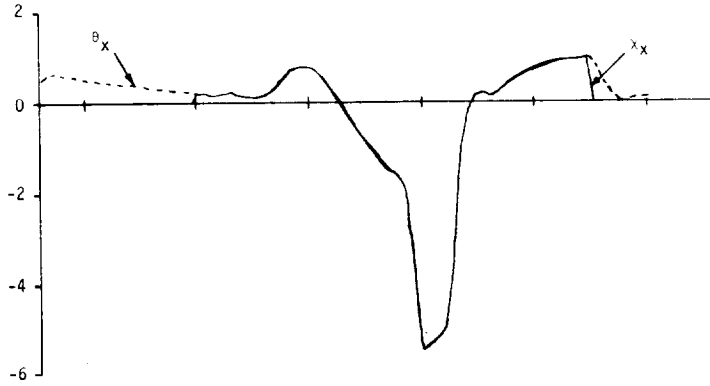


FIGURE 12-7 PITCH ATTITUDE CONTROL DURING LOX DUMP

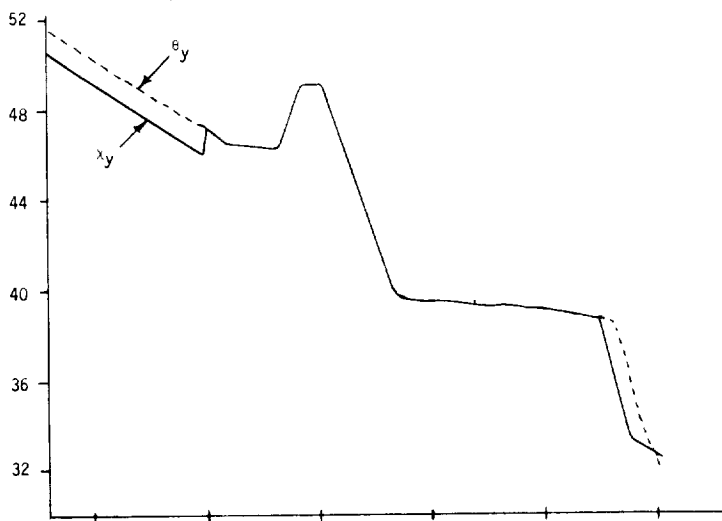
YAW COMMAND (x_z) AND YAW ATTITUDE (θ_z) (DEG)



ROLL COMMAND (x_x) AND ROLL ATTITUDE (θ_x) (DEG)



PITCH COMMAND (x_y) AND PITCH ATTITUDE (θ_y) (DEG)



- ▽ MANUAL TAKE-OVER ($x=\theta$) 9049 SEC
- ▽ 2 BEGIN PITCH 9082 SEC
- ▽ 3 END PITCH 9135 SEC
- ▽ 4 BEGIN ROLL 9142 SEC
- ▽ 5 END ROLL 9171 SEC
- ▽ 6 BEGIN YAW 9181 SEC
- ▽ 7 END YAW 9211 SEC
- ▽ 8 END MANUAL CONTROL 9224 SEC

APS ENGINE FIRINGS

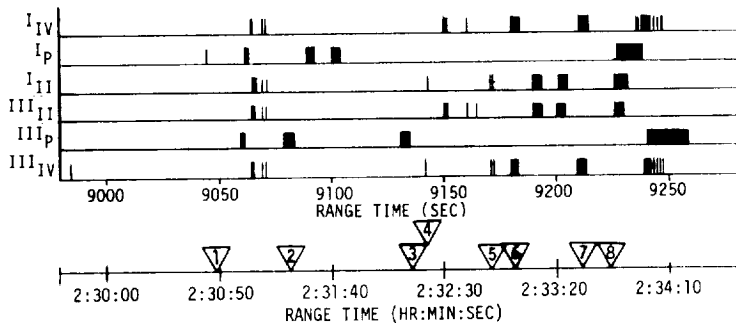


FIGURE 12-8 COMMAND ANGLES AND VEHICLE ATTITUDE DURING MANUAL MANEUVERS

▽ S-IVB/CSM SEPARATION

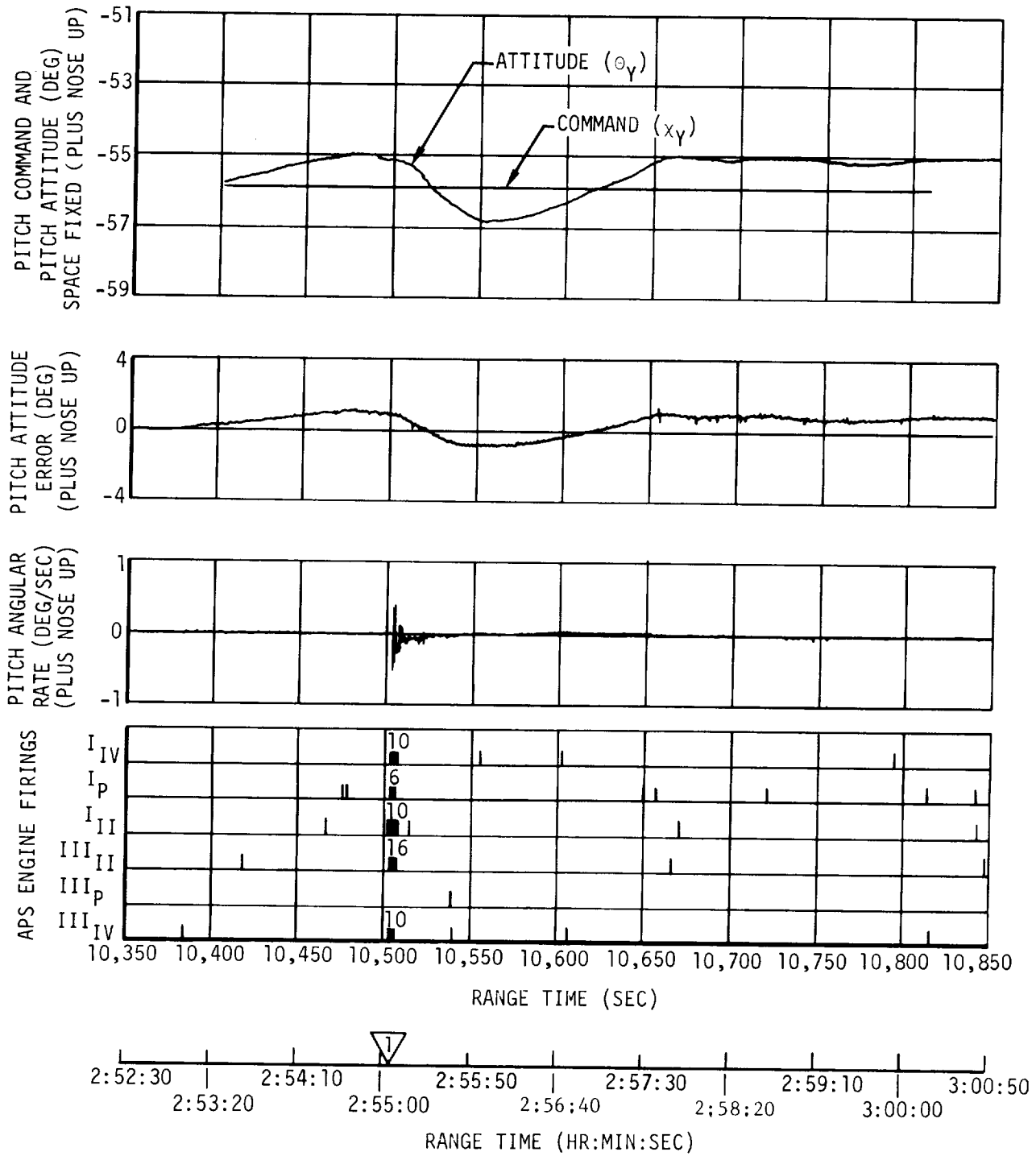
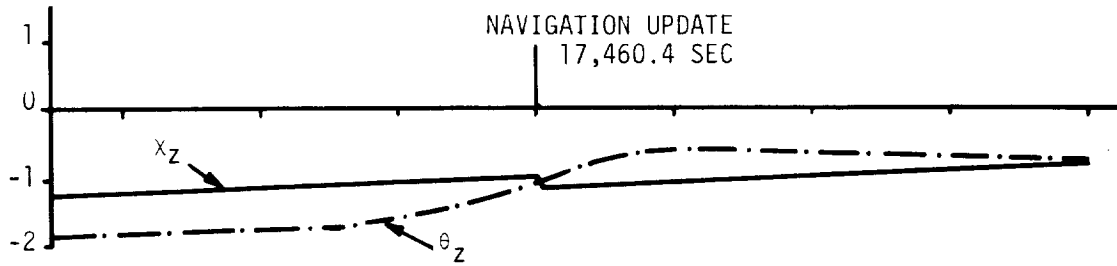
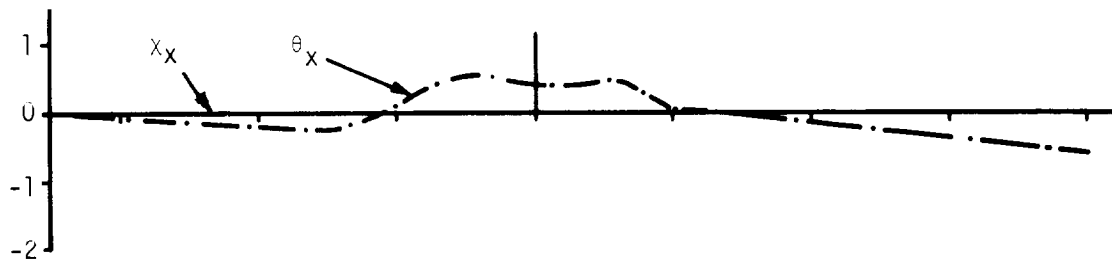


FIGURE 12-9 PITCH ATTITUDE CONTROL DURING S-IVB/CSM SEPARATION

YAW COMMAND (x_z) AND YAW ATTITUDE (θ_z) (DEG)



ROLL COMMAND (x_x) AND ROLL ATTITUDE (θ_x) (DEG)



PITCH COMMAND (x_y) AND PITCH ATTITUDE (θ_y) (DEG)

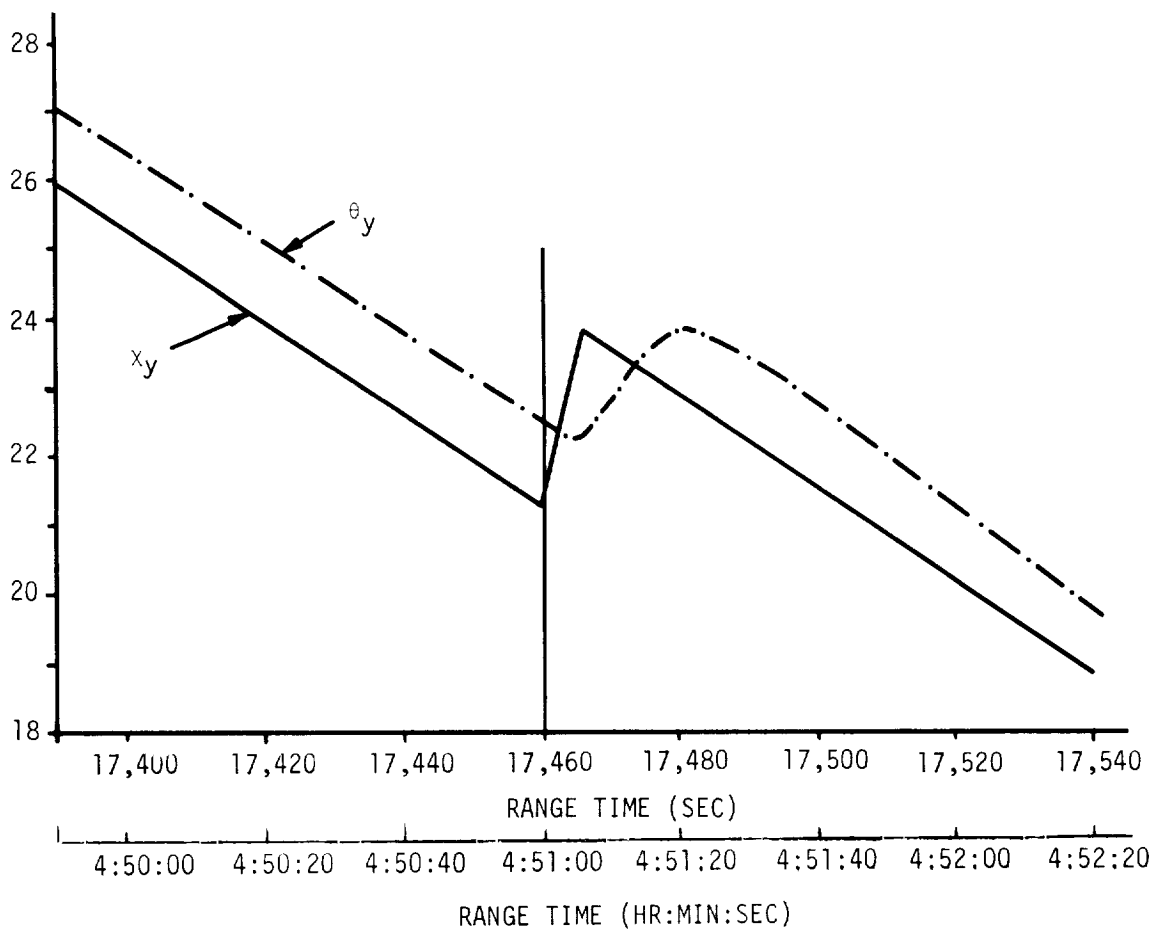


FIGURE 12-10 COMMAND ANGLES AND VEHICLE ATTITUDE DURING NAVIGATION UPDATE

APS propellant requirements for attitude control during this mission correlated closely with the nominal predicted propellant requirements. Some deviations between the actual and nominal predicted usage was noted for Module 2 during the LOX dump. Slightly less APS propellant was required than predicted from this module. This is attributed primarily to a difference in the actual thrust misalignment and that used to determine the mean predicted usage.

A summary of APS impulse requirements for attitude control during significant events is presented in Table 12-III. APS propellant depletion occurred between Guam, revolution 10 (15 hr 30 min) and Canary Island, revolution 11 (16 hr 20 min). Available control system data indicated that attitude control appeared normal prior to the APS propellant depletion. APS propellant depletion occurred on AS-204 at approximately 10 hours. The extended control system lifetime of AS-205 over AS-204 is attributed primarily to a higher AS-205 orbit resulting in lower aerodynamic disturbances than on AS-204.

12.3.4 CONTROL COMPONENT ANALYSIS

Data indicates that all control components performed nominally. The control accelerometer output signals were active in vehicle control from 30 through 110 sec, and power was turned off at 120 seconds. The analyses of the control - EDS rate gyros and control signal processor indicated normal performance. The CSP dual rate switching capability was exercised for the first time during flight, and was satisfactory. The flight control computer performed properly throughout the boost and coast phases of flight. Attitude error and angular velocity signals, as telemetered from the FCC, correlated well with the same signals telemetered from the originating components. All eight actuators performed smoothly during S-IB stage flight, with activity being generally less than on previous flights. The maximum values of gimbal angle deflection, gimbal rate, and differential current to the servo valves were only 13%, 7%, and 13% of the maximum possible values. The performance of the S-IVB actuators was satisfactory.

12.4 LAUNCH VEHICLE NAVIGATION AND GUIDANCE

The overall performance of the navigation and guidance system (ST-124M-3 stabilized platform system, launch vehicle digital computer, and launch vehicle data adapter) was very satisfactory. An analysis of the telemetered guidance data is discussed in subsequent parts of this section.

TABLE 12-III APS IMPULSE SUMMARY

Event	Units	Module 1	Module 2	APS Engine					
				I _{IV}	I _P	I _{II}	III _{II}	III _P	IV _{IV}
Powered Flight: Separation, guidance initiation and ullage rocket jettison + 145 to + 210 seconds	lbf-s	139.4	150.3	51.1	0.0	88.3	59.4	0.0	90.9
	N-s	620.1	668.5	227.3	0.0	392.8	264.2	0.0	404.3
Limit cycle operation for remaining burn time 210 to 617 seconds	lbf-s	251.5	274.5	0.0	0.0	251.5	0.0	0.0	274.5
	N-s	1118.7	1221.0	0.0	0.0	1118.7	0.0	0.0	1221.0
Initial recovery following J-2 cutoff 617 to 636 seconds (includes LH2 venting)	lbf-s	0.0	21.8	0.0	0.0	0.0	19.7	0.0	2.1
	N-s	0.0	96.9	0.0	0.0	0.0	87.6	0.0	9.3
Alignment to local horizontal following J-2 cutoff 636 to 678 seconds (includes LOX and LH2 venting)	lbf-s	391.6	162.0	40.2	252.7	98.7	70.3	5.7	86.0
	N-s	1741.9	720.6	178.8	1124.1	439.0	312.7	25.4	382.5
LOX main engine dump 5669 to 6390 seconds	lbf-s	560.8	264.0	209.9	289.8	61.1	62.9	0.0	201.1
	N-s	2494.6	1174.3	933.7	1289.1	271.8	279.8	0.0	894.5
Manual steering control 9049 to 9225 seconds	lbf-s	1839.5	1511.2	487.4	838.6	513.5	463.8	612.8	434.6
	N-s	8182.5	6722.2	2168.1	3730.3	2284.1	2063.1	2725.9	1933.2
S-IVB/CSM separation 10500 to 10515 seconds	lbf-s	208.9	199.3	84.7	41.7	82.5	101.5	0.0	97.8
	N-s	929.2	886.5	376.7	185.5	367.0	451.5	0.0	435.0
Initiate maneuver to align vehicle retrograde with local horizontal 11816 to 11840 seconds	lbf-s	144.1	299.2	68.3	0	75.8	63.9	170.0	65.3
	N-s	641.0	1330.9	303.8	0	337.2	284.2	756.2	290.5

12.4.1 NAVIGATION AND GUIDANCE SCHEME PERFORMANCE ANALYSIS

The flight program performed as expected. The boost navigation and guidance schemes were executed properly and terminal parameters were well within acceptable limits. All orbital operations were nominal.

The S-IB stage roll maneuver was performed properly. The initial roll attitude of -28.2 deg was removed by 38.5 seconds. The time tilt began at 10.3 sec and was arrested at 134.3 seconds. The pitch profile was executed properly.

The Z accelerometer exhibited zero-changes (changes of 1 count or less) for five successive computation cycles beginning approximately 15 sec after lift-off. The zero-change test properly caused the use of a back-up acceleration value obtained from a prestored acceleration profile instead of the fifth zero-change reading. The Z accelerometer zero-changes were caused by the delaying of downrange (+Z) velocity accumulation due to the uprange surface wind. In a nominal wind environment, the downrange velocity begins to increase from near zero shortly after the initiation of the pitch profile. The zero-change test is enabled approximately 4 sec afterward. However, during AS-205 liftoff, the uprange surface wind caused an uprange acceleration of approximately 0.1 m/sec^2 . The downrange acceleration component balanced this uprange acceleration at approximately 16 sec, 6 sec after pitch profile initiation. The Z velocity became positive at approximately 24.5 sec with an uprange displacement of 19.2 meters. The delay in the accumulation of downrange (+Z) velocity resulted in zero change Z accelerometer readings after the enabling of the zero-change test.

Figure 12-11 shows a sketch of the 95 and 99 percentile steady state surface winds used in design studies. The mean and peak wind velocities at launch obtained from the south pad light pole and the top of the service structure are shown in Table B-I. The wind velocity measured at the 19.5 m (64 ft) level exceeded the 95% wind velocity, but not the 99%. However, this did not result in any close launch support or launch umbilical tower collision problems since the surface wind azimuth was 67 deg (headwind) while the wind restrictions exist for winds along a 160 to 270 deg azimuth. The lift-off geometry for launch complex 34 is shown in Figure 12-12.

The net result of this headwind was a 19 m drift uprange (along negative Z_E axis) as seen in Figure 12-13. By 32 sec, the pitch program had overcome the headwind and the vehicle was headed downrange. The 0.098 m/sec Z velocity error introduced by the selection of the backup value was insignificant as evidenced by the orbital insertion values.

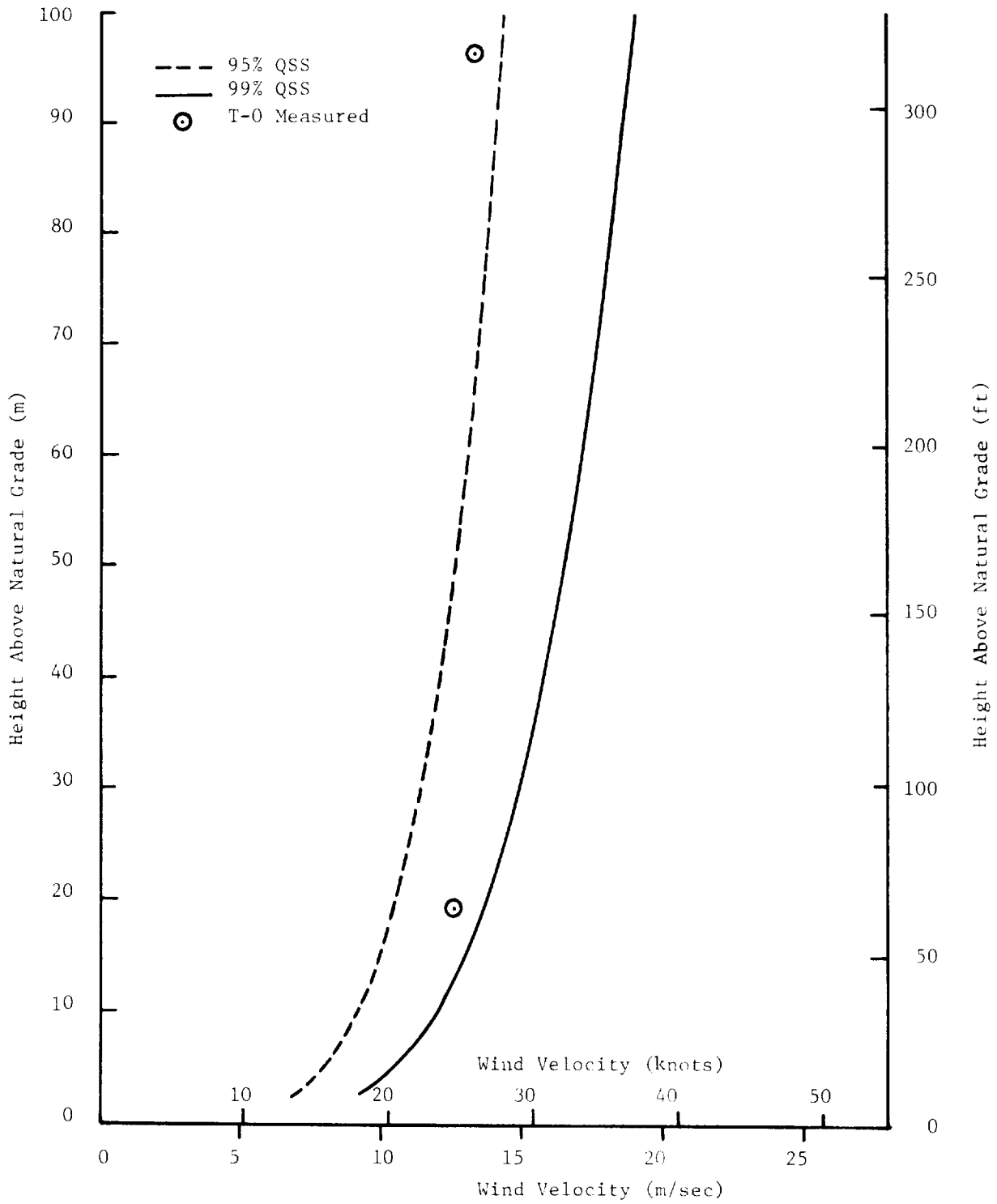


FIGURE 12-11 QUASI-STEADY-STATE SURFACE WIND SPEED ENVELOPE FOR CAPE KENNEDY

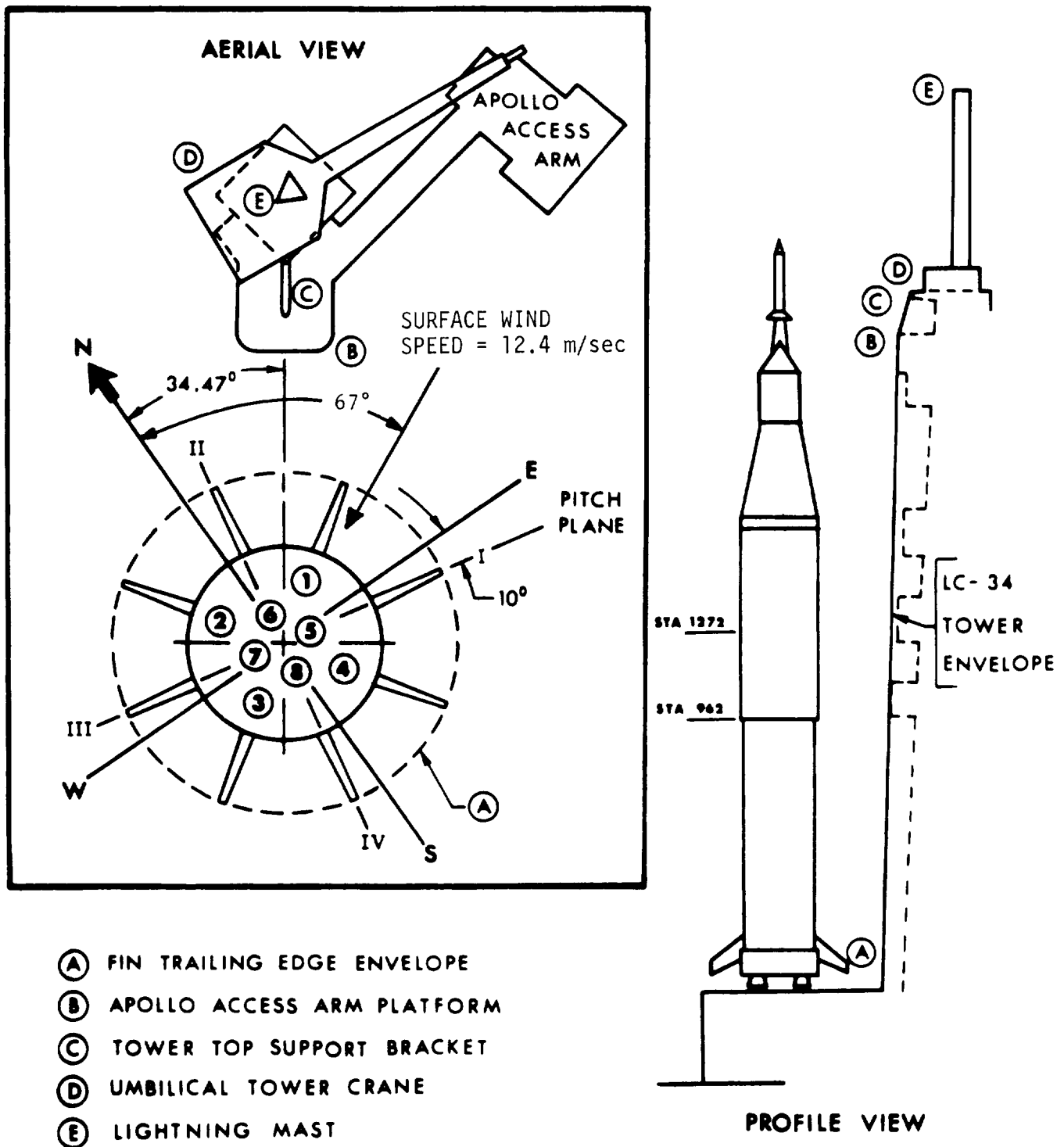


FIGURE 12-12 LIFTOFF GEOMETRY LC-34

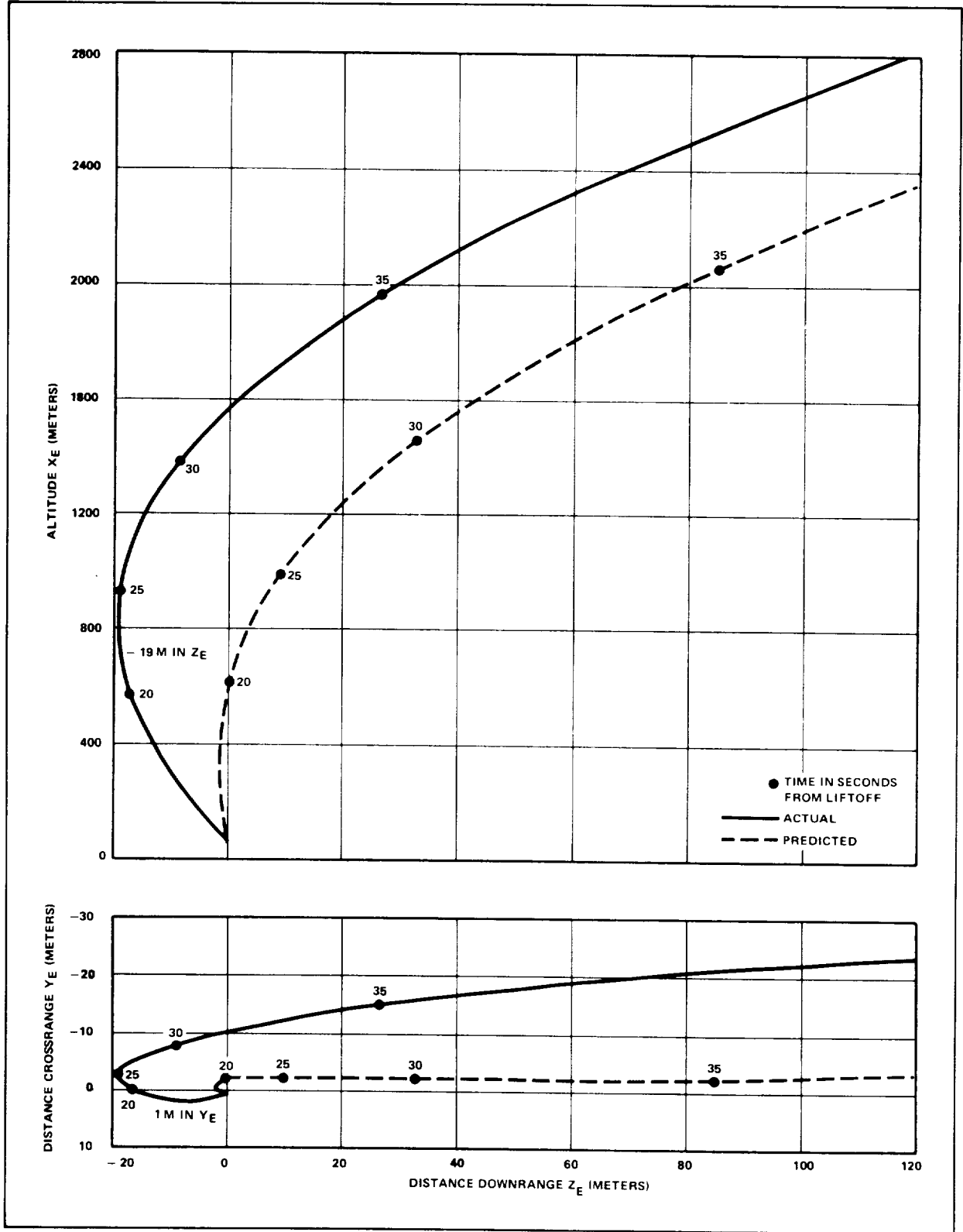


FIGURE 12-13 AS-205 TRAJECTORY PROFILE AND PLAN VIEWS, LIFTOFF THROUGH 35 SECONDS OF FLIGHT

IGM was initiated at 170.9 seconds. The initial changes in the IGM pitch and yaw commands were 10.062 and 2.660 deg, respectively. The IGM commands were as expected. The artificial tau was started at 456.9 sec and completed at 493.1 seconds. The chi bar steering mode was entered at 593.9 seconds. The altitude constraint terms were dropped at this point and the resulting pitch and yaw attitude command changes were -1.447 and -0.180 deg, respectively. Performance of the IGM of the flight program was normal.

Orbital guidance was initiated at 632.2 seconds. Vehicle attitude was held within the control system deadband throughout flight except at the initiation of maneuvers. Determination of telemetry station acquisition, operation of the DCS, telemetering of LVDC data, and compression of LVDC/LVDA data all performed nominally, as expected.

12.4.2 NAVIGATION AND GUIDANCE COMPARISON

12.4.2.1 POWERED FLIGHT COMPARISON

Comparisons between the final post-flight trajectory (OMPT) and the telemetered guidance platform velocities are shown for the powered flight in Figure 12-14. The telemetered range velocity (Z) was adjusted by -0.1 m/sec to compensate for the error made when the Z accelerometer did not pass the zero-change test. The differences indicate very good agreement with the trajectory and are the result of small errors in the data compared, and/or very small guidance hardware errors. Orbital telemetry between 700 and 5500 sec indicated that bias terms associated with each of the guidance accelerometers were well within 3 sigma tolerances.

Platform measured velocities, along with corresponding data from both the post-flight and operational trajectories, are shown for significant powered flight events in Table 12-IV. The differences between telemetered and preflight (operational) velocities are the result of nonstandard flight conditions and performance. The differences between the telemetered and post-flight trajectory velocities are very small and reflect small tracking errors and/or very small guidance hardware errors. The differences are well within the expected accuracy. The comparisons are considered exceptionally good since no precision tracking was available for use in establishing the post-flight trajectory.

Velocity increase due to thrust decay after S-IVB cutoff was the same as for AS-204. The measured velocity vector increase was 6.4 m/sec for AS-204 and AS-205.

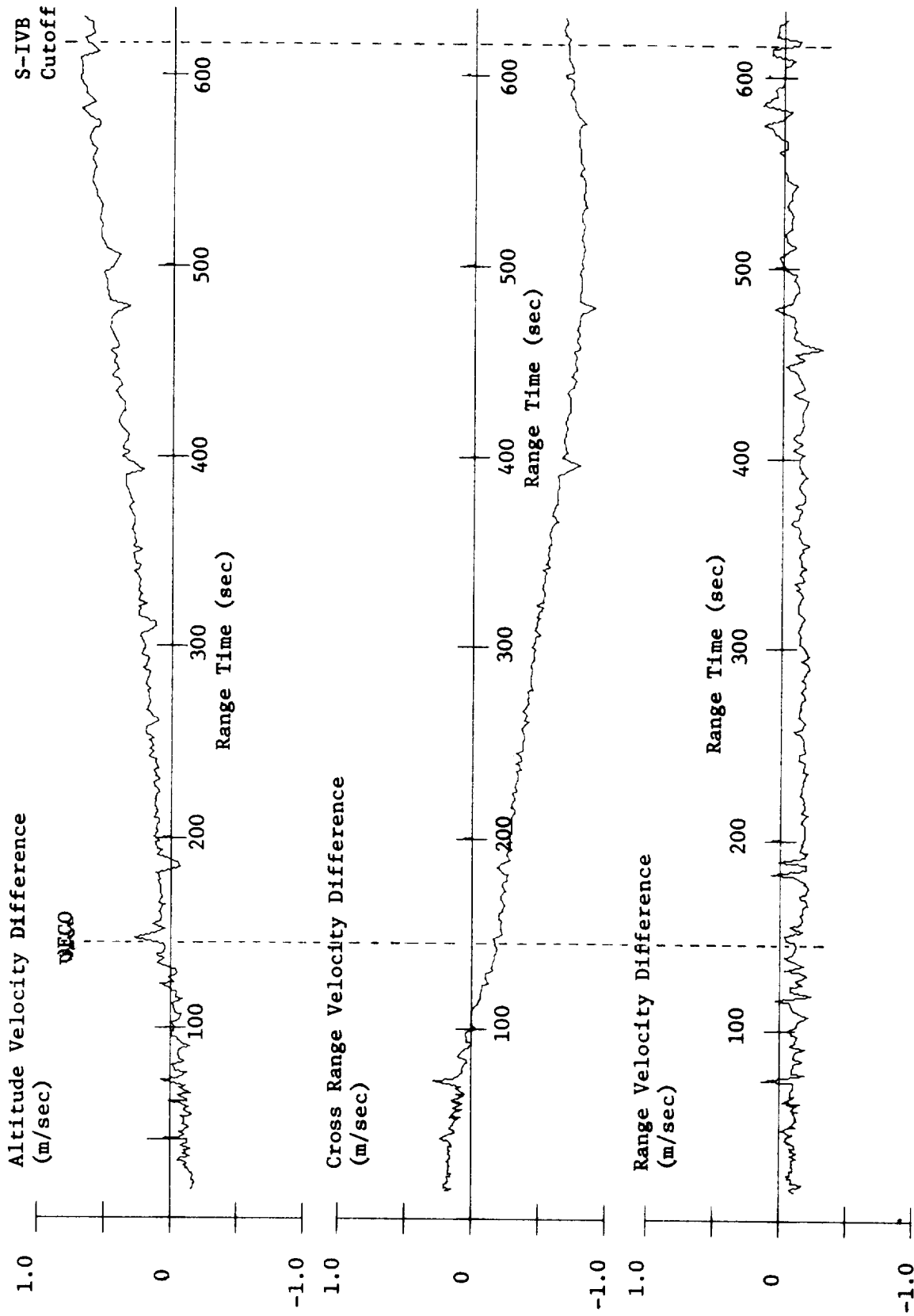


FIGURE 12-14 GUIDANCE PLATFORM VELOCITY DIFFERENCES (TRAJECTORY MINUS MEASURED)

TABLE 12-IV
GUIDANCE INERTIAL PLATFORM VELOCITY COMPARISON

Event	Parameter *	Telemetered	Trajectory	
		LVDC **	Postflight	Preflight
S-IB	\dot{X}_m	2416.15	2416.23	2422.78
IECO	\dot{Y}_m	0.0	-0.21	-3.42
	\dot{Z}_m	1640.00	1639.86	1648.26
S-IB	\dot{X}_m	2458.90	2458.94	2458.84
OECO	\dot{Y}_m	-0.15	-0.36	-3.60
	\dot{Z}_m	1711.60	1711.46	1709.10
IGM	\dot{X}_m	2538.50	2538.54	2538.59
Initiation	\dot{Y}_m	-2.90	-3.16	-4.82
	\dot{Z}_m	1839.80	1839.66	1841.55
S-IVB	\dot{X}_m	3308.96	3309.54	3290.84
Cutoff	\dot{Y}_m	336.41	335.61	336.29
	\dot{Z}_m	7579.93	7580.03	7578.87
Orbital	\dot{X}_m	3306.75	3307.26	3288.99
Insertion	\dot{Y}_m	336.85	336.03	336.65
	\dot{Z}_m	7587.80	7587.88	7585.35

* \dot{X}_m Altitude Velocity (m/sec)
 \dot{Y}_m Cross Range Velocity (m/sec)
 \dot{Z}_m Range Velocity (m/sec)

** Range Velocity (\dot{Z}_m) was adjusted to compensate for error due to accelerometer test failure at 22.968 sec computer time.

Navigation parameters are presented in Table 12-V for S-IB/S-IVB separation, S-IVB cutoff, and orbital insertion (S-IVB cutoff plus 10 sec). Telemetered LVDC values are shown along with post-flight and operational trajectory data. Since guidance is open-loop with only attitude control during S-IB stage flight, the guidance measurements do not necessarily agree with the operational trajectory at stage separation. However, the measured values were unusually close to nominal. After IGM is initiated, the guidance system computes and issues commands to guide the vehicle to the prescribed conditions at S-IVB cutoff to insure the desired orbit. Comparison of the telemetered and predicted radius, velocity vector, and path angle indicates that the guidance system performed well within tolerances. The actual cutoff velocity, as indicated by guidance, was within 0.01 m/sec of the prescribed value. At insertion, the telemetered velocity was 1.4 m/sec greater than predicted. The guidance data are in very good agreement with the post-flight trajectory data. At orbital insertion, the differences (trajectory minus guidance) in radius, total velocity, and path angle were 104 meters, -0.19 m/sec, and 0.00278 deg, respectively.

12.4.2.2 PLATFORM MEASURED VELOCITY CHANGES DURING ORBIT

Figure 12-15 presents the measured and predicted inertial velocity changes due to 30 sec of LOX vent beginning at T4 + 30.2 sec and for LOX dump. The velocity changes shown, both actual and predicted, are the root sum square (RSS) of the incremental velocity outputs of the guidance accelerometers during the respective event times.

"LOX Tank Vent Valve Open" occurred at T4 + 30.17 sec and closed at T4 + 60.17 seconds. A resultant velocity increase of 1.1 m/sec for this event compared well with the predicted value of 1.3 m/sec.

LOX purge began with "Engine Mainstage Control Valve Open On" at 5668.75 sec or T4 + 5051.75 seconds. The slope of the predicted velocity curve was much steeper initially than the measured values. After 131 sec of LOX dump, the predicted value was 5.7 m/sec compared with the measured gain of 3.5 m/sec. The difference between the actual and predicted velocity change remained essentially constant at 2.2 m/sec for about 150 sec or until 5950 seconds. After this time, the measured velocity increased faster than predicted until "Engine Mainstage Control Valve Open Off" at 6388.95 sec when the actual velocity increase was 6.6 m/sec compared to a predicted value of 7.8 m/sec. Although the operational trajectory data remained constant from this point, the telemetered velocity from the accelerometer outputs indicated an additional increase of 0.2 m/sec at 6671 seconds. The additional 0.2 m/sec may be attributed to propulsive venting.

TABLE 12-V
NAVIGATION COMPARISON

Event	Parameter	Symbol	Units	Envelope Tolerance	Guidance Computer	Trajectory	
						Postflight	Predicted
S-1B /S-1VB Separation	Positions:						
	Altitude	X_S	km	+ 2.189 - 2.084	6433.958	6433.951	6434.045
	Cross Range	Y_S	km	+ 3.031 - 3.102	35.901	35.909	35.600
	Range	Z_S	km	+ 5.840 - 4.249	116.390	116.389	115.542
	Radial Distance	R	km	+ 2.140 - 2.018	6435.111	6435.104	6435.180
	Velocities:						
	Altitude	\dot{X}_S	m/s	+ 64.44 - 70.44	990.34	990.44	1003.26
	Cross Range	\dot{Y}_S	m/s	+ 66.17 - 65.97	122.02	121.81	118.63
	Range	\dot{Z}_S	m/s	+ 59.79 - 54.22	2095.05	2094.78	2095.26
	Total Velocity	V_S	m/s	+ 40.5 - 33.7	2320.54	2320.33	2326.09
Path Angle	θ	deg	+ 1.991 - 1.903	26.3157	26.3208	26.5453	
S-1VB Cutoff	Positions:						
	Altitude	X_S	km	+ 25.356 - 28.889	6257.676	6257.785	6258.278
	Cross Range	Y_S	km	+ 4.817 - 4.396	144.810	144.523	144.698
	Range	Z_S	km	+ 84.956 - 77.387	2094.087	2094.096	2092.098
	Radial Distance	R	km	+ 0.602	6600.354	6600.454	6600.292
	Velocities:						
	Altitude	\dot{X}_S	m/s	+ 91.42 - 100.54	-2474.70	-2474.15	-2472.80
	Cross Range	\dot{Y}_S	m/s	+ 3.68 - 3.85	412.40	411.68	412.48
	Range	\dot{Z}_S	m/s	+ 29.82 - 34.02	7365.09	7364.93	7365.73
	Total Velocity	V_S	m/s	+ 1.60	7780.66	7780.30	7780.67
Path Angle	θ	deg	+ 0.026	-0.00336	-0.00038	-0.00667	
Orbital Insertion	Positions:						
	Altitude	X_S	km	NA	6232.473	6232.588	6233.099
	Cross Range	Y_S	km	NA	148.929	148.634	148.817
	Range	Z_S	km	NA	2167.669	2167.673	2165.667
	Radial Distance	R	km	+ 0.602	6600.355	6600.459	6600.287
	Velocities:						
	Altitude	\dot{X}_S	m/s	NA	-2563.50	-2563.02	-2561.23
	Cross Range	\dot{Y}_S	m/s	NA	410.92	410.18	410.93
	Range	\dot{Z}_S	m/s	NA	7343.38	7343.39	7342.68
	Total Velocity	V_S	m/s	+ 1.60	7788.82	7788.63	7787.41
Path Angle	θ	deg	+ 0.026	0.00253	0.00531	-0.00164	

$$\Delta X = X_{t_n} - X_{t_0}$$

$$\Delta V = (\Delta \dot{X}^2 + \Delta \dot{Y}^2 + \Delta \dot{Z}^2)^{1/2}$$

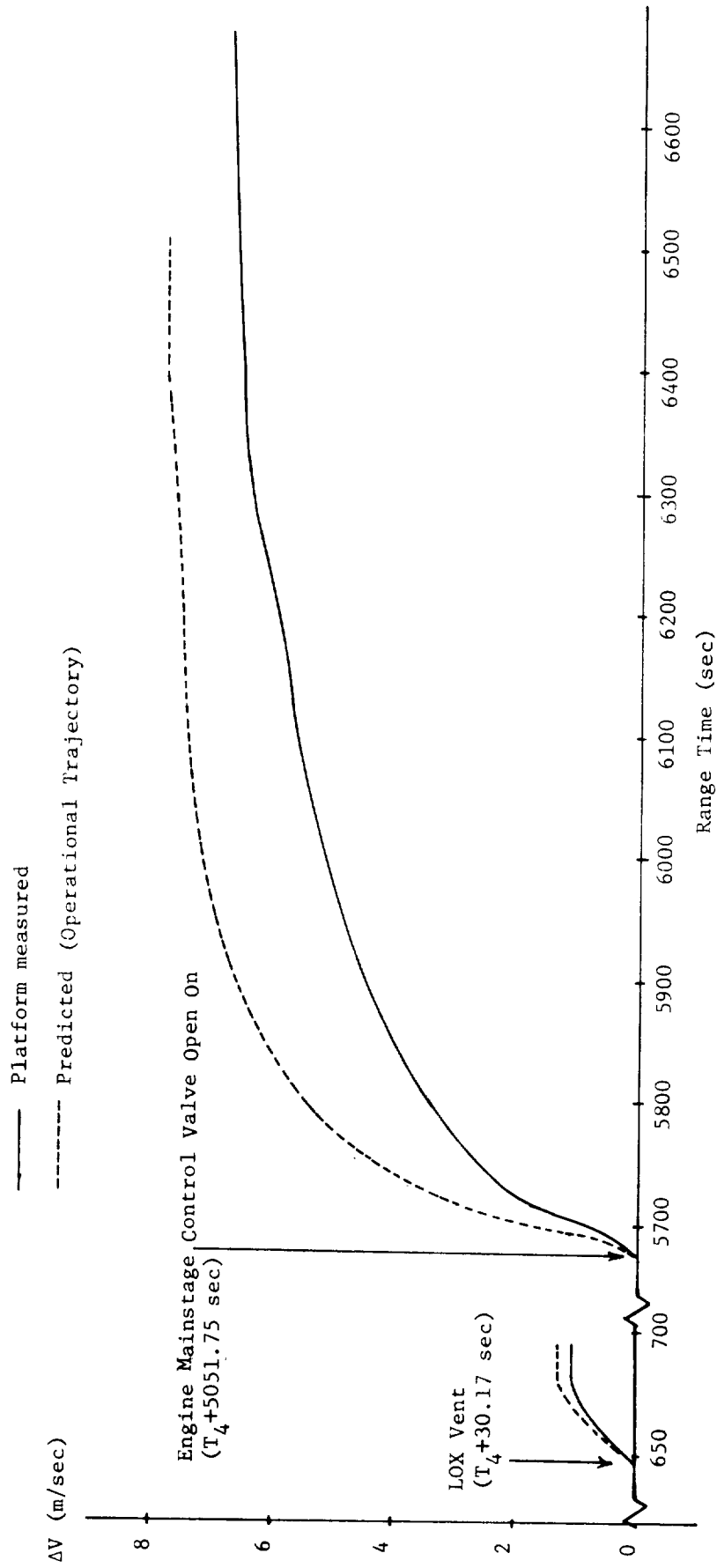


FIGURE 12-15 VELOCITY CHANGE DUE TO PROPULSIVE VENT AND PASSIVATION

12.4.3 GUIDANCE SYSTEM COMPONENT ANALYSIS

12.4.3.1 LVDC/LVDA ANALYSIS

The launch vehicle data adapter (LVDA) and the launch vehicle digital computer (LVDC) performed as predicted for the AS-205 mission. Data received from Guam during the tenth revolution indicated that LVDA error monitor register bit 5 (EMR 5) and its associated error time word (ETW) were occurring constantly at that time. Bit EMR 5 is associated with the transient detector circuitry and indicates in this case that the LVDA input voltage from the batteries dropped below 22.5 volts. The acquisition of Guam during revolution 10 occurred at 15.3 hr after liftoff, a time at which the batteries were nearing depletion. No indication of component malfunction was observed prior to loss of input power which occurred between 57,592 and 58,907 sec (16.0 and 16.4 hr).

12.4.3.2 ST-124M STABILIZED PLATFORM ANALYSIS

The ST-124M-3 stabilized platform assembly and associated equipment performed as designed through 15.5 hr after liftoff. The accelerometer pickup signals indicated normal operation. The gyro pickup and servo amplifier signals indicated that inertial reference was maintained through 16.4 hours. The gyro servo output signals were transmitted on PCM telemetry at 12 samples/sec, and were of little value in determining system performance because of the electrical noise. FM transmission will be recommended for these signals on future vehicles, as was used on past vehicles.

13.0 SEPARATION

13.1 SUMMARY

S-IB/S-IVB separation was accomplished as planned and the sequence executed in the desired time period. The estimated time the S-IVB engine cleared the interstage was approximately 1.0 sec following the separation command.

LV/CSM separation occurred at 10502.40 seconds.

13.2 S-IB/S-IVB SEPARATION

13.2.1 SEPARATION DYNAMICS

Analysis of the AS-205 separation was accomplished by comparing separation data to those of AS-204. The majority of the data comparison was very close. Figure 13-1 shows the longitudinal accelerations for both AS-204 and AS-205. The deviation in longitudinal acceleration indicates that the retro-rocket thrust on AS-205 was slightly higher than that of AS-204. Figure 13-2 presents the angular velocities for both flights, which compared quite favorably. The magnitudes of the yaw and roll rates of AS-204 and AS-205 were close, but with opposite direction. The pitch rate for AS-205 was slightly higher than, and in the reverse direction from, that of AS-204.

The separation events for AS-205 are presented in Table 13-I, compared to AS-204. Since AS-204 and AS-205 separation data compared so favorably, a detailed analysis was not performed to establish the precise clearance distance used and the separation completion time. However, from the evaluation, it was estimated that a detailed analysis would yield a separation completion time of 1.0 sec and a lateral clearance utilization of approximately 12.7 cm (5 inches).

13.3 LV/CSM SEPARATION

The Command Service Module (CSM) was successfully separated from the S-IVB/IU at 10502.40 seconds. The separation relative displacement and attitudes are presented in Figure 13-3. CSM + x translation was commanded 1.09 sec prior to physical separation and continued for 2.25 sec following separation. The largest disturbance occurred in the pitch plane where the CSM pitched upward while the S-IVB/IU pitched slightly downward. However, there were no clearance problems and the CSM cleared the separation plane by 10,513.1 sec, approximately 10.7 sec from physical separation. One of the SLA panels did not fully deploy, but this did not cause any problems. On future Saturn vehicles, the SLA panels will be jettisoned.

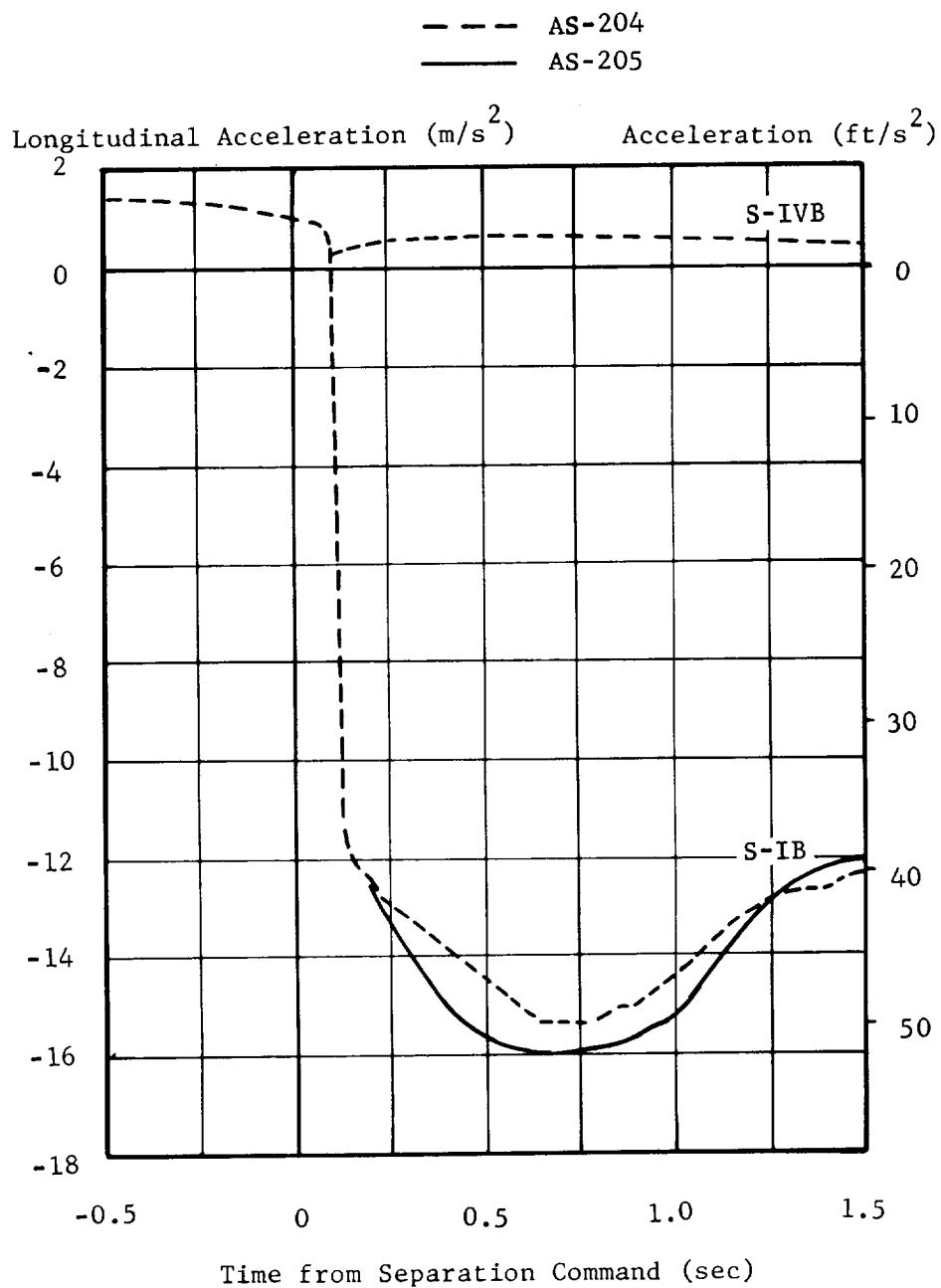


FIGURE 13-1 S-1B/S-1VB LONGITUDINAL ACCELERATION

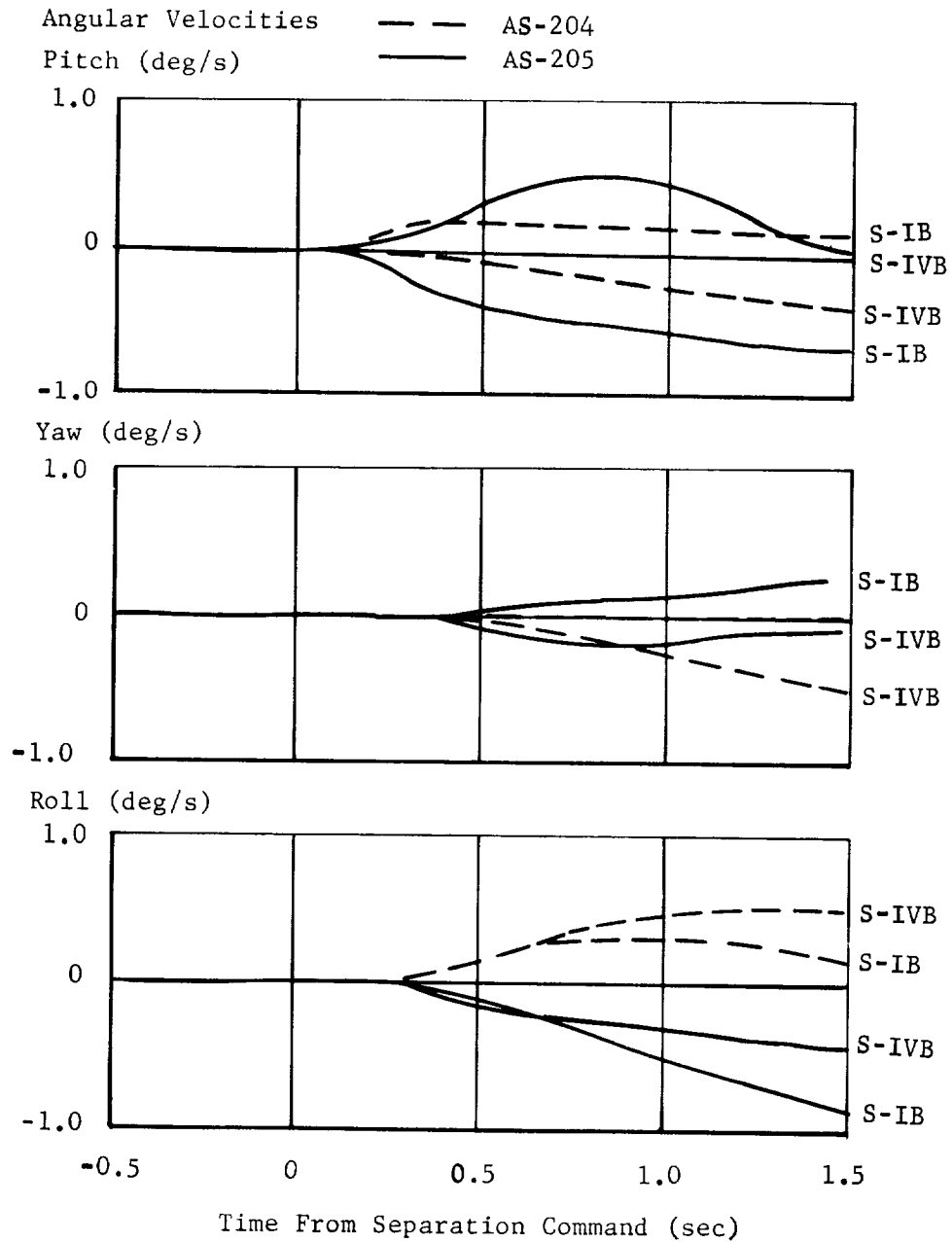


FIGURE 13-2 ANGULAR VELOCITIES DURING S-1B/S-1VB SEPARATION

TABLE 13-I SEPARATION EVENTS

Event	Range Time (sec)		Time from Sep. Command - AS-205		Time from Sep. Command - AS-204	
	Predicted	Actual	Predicted	Actual	Predicted	Actual
Inboard Engine Cutoff Command	140.28	140.64	-4.30	-4.94	-4.30	-4.53
Outboard Engine Cutoff Command	143.28	144.32	-1.30	-1.26	-1.30	-1.25
Ullage Motor Ignition Command	144.38	145.37	-0.20	-0.21	-0.20	-0.20
Separation Command (Retrorocket Ignition Command)	144.58	145.58	0	0	0	0
Retrorocket Ignition		145.63		0.05	0.05	0.076
Separation Complete	144.67	146.58	0.09	1.0*	1.01	0.97
J-2 Engine Start Command	145.98	146.97	1.40	1.39	1.40	1.40

*From AS-204 Separation Analysis

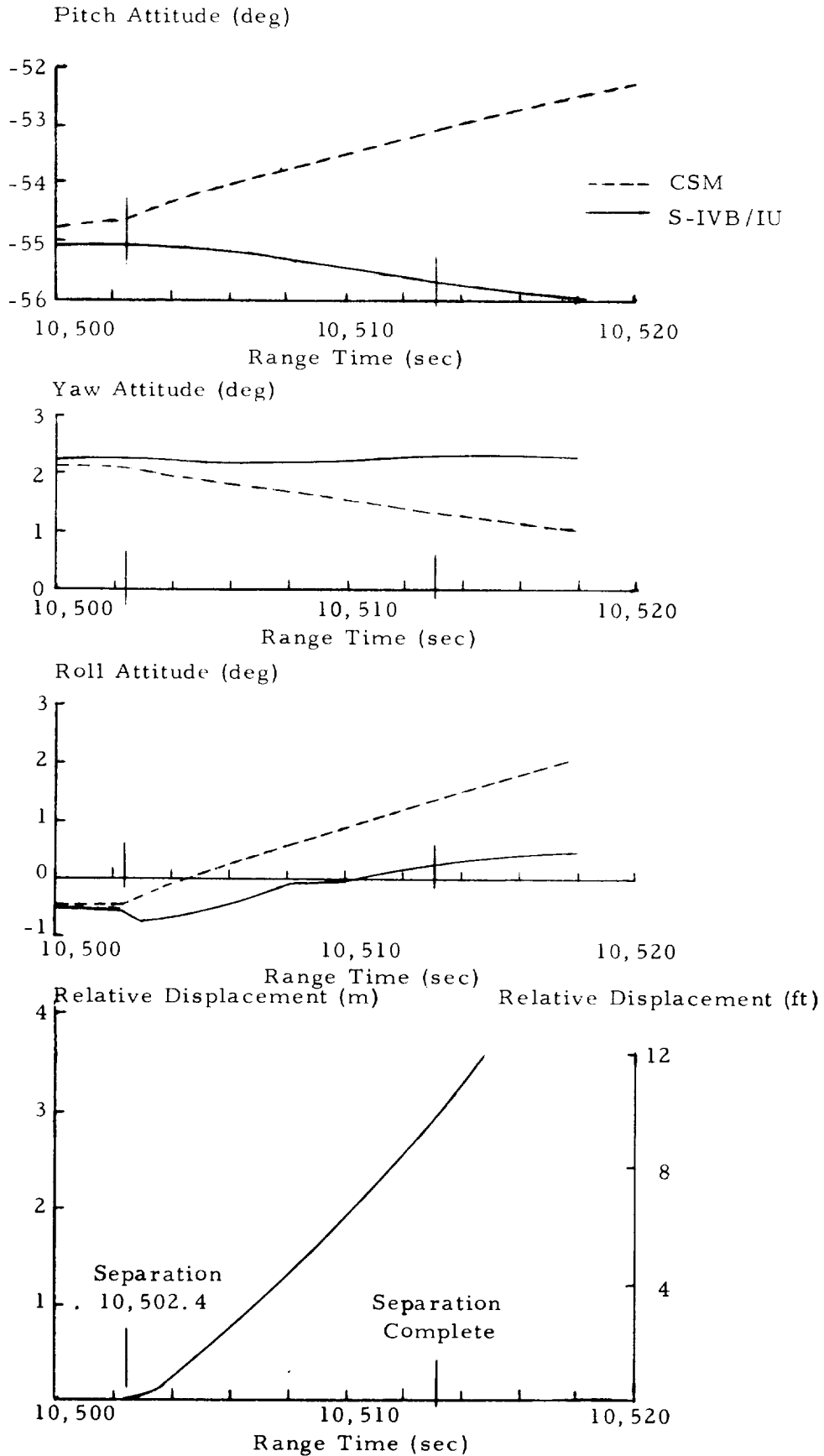


FIGURE 13-3 CSM-S-IVB/IU SEPARATION PARAMETERS

14.0 VEHICLE ELECTRICAL SYSTEMS

14.1 SUMMARY

The electrical systems of the AS-205 launch vehicle operated satisfactorily during the entire flight. Battery performance - including voltages, currents, and temperatures - was satisfactory and remained within predicted tolerances. The master measuring voltage supplies performed satisfactorily. The secure command system and range safety decoder were operable during flight. All Exploding Bridge Wire (EBW) firing units responded correctly. Battery lifetime met mission requirements.

14.2 S-IB STAGE ELECTRICAL SYSTEM

Inflight power for the S-IB stage is supplied by two 28 volt, silveroxide-zinc batteries, designated 1D10 and 1D20. Each battery is rated at 2000 ampere-minutes. The power and distribution system consists of batteries, distributors, plug-type J-Boxes, and interconnecting circuitry. Three master measuring voltage supplies are utilized to furnish a precisely regulated reference voltage to the telemetry system. Each power supply converts 28 vdc to a regulated 5 vdc reference voltage for use in the instrumentation measuring system. Differences in configuration between AS-204 and AS-205 are discussed in Appendix A.

The S-IB-5 stage electrical system performed as expected during the boost phase, and all mission requirements were met. Battery performance-including voltages and currents - was satisfactory and remained within predicted tolerances. The Secure Command System and Range Safety Decoder were operable during flight. All Exploding Bridge Wire (EBW) firing units responded correctly.

All Thrust OK Pressure Switches and EBW units functioned properly. The average charge time for the retro rocket EBW units was 0.73 second. The charge time for the separation EBW units was 0.76 second. The destruct EBW units indicated no charge.

The voltage for 1D10 and 1D20 batteries averaged approximately 28.1 vdc and 28.8 vdc, respectively, from power transfer to separation. Battery voltage drops and current loads correlated with significant vehicle events. The most pronounced power drains were caused at S-IB cutoff by conjoint conax firing and prevalve operation. The current on batteries 1D10 and 1D20 averaged approximately 19.5 amps and 16.3 amps respectively throughout the powered flight. The voltage and current profiles for the batteries are presented in Figure 14-1.

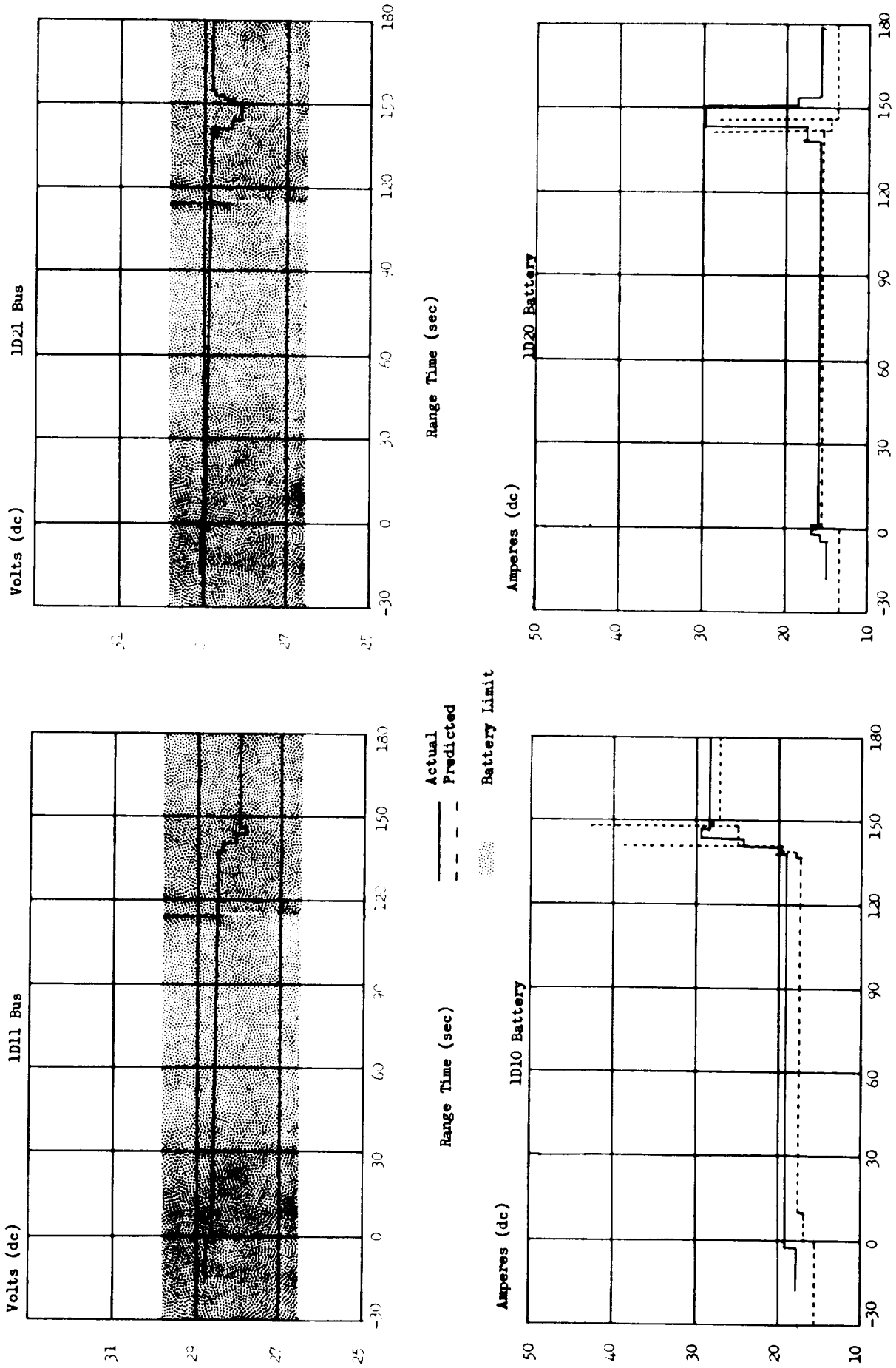


FIGURE 14-1 S-1B BATTERY CURRENT AND VOLTAGE

The Master Measuring Voltage Supplies performed satisfactorily, and remained within the allowable tolerance of 5.000 ± 0.0125 vdc.

The following is a tabulation of events and ampere-minutes delivered by the 1D10 and 1D20 batteries. The total ampere-minutes delivered by each battery from activation to S-IB stage separation was less than 10 percent of the specified minimum battery capacity of 2000 ampere-minutes.

TABLE 14-I S-IB BATTERY PERFORMANCE

Event	Ampere-Minutes Consumed	
	1D10	1D20
Activation Loads	66	58
Standby to Pwr Transfer	72	72
Pwr Transfer to Separation	55	50
Total	193	180

14.3 S-IVB STAGE ELECTRICAL SYSTEM

The AS-205 S-IVB stage electrical power system consisted of four batteries, one LOX and one LH₂ chardown inverter, a static inverter-converter, three 5 vdc excitation modules, and eight 20 vdc excitation modules. Differences in configuration between AS-204 and AS-205 are covered in Appendix A.

The stage electrical system produces and distributes all ac and dc power for flight functions. Four silver-oxide/zinc batteries, two each in the forward and aft skirts, supply primary power. This buses directly to associated distribution assemblies and routes through networks operational equipment and secondary power sources to convert, invert, and regulate for specialized functions. There are four primary (and independent) networks -- one from each battery -- two originating in the forward skirt and two in the aft skirt. 28 vdc is supplied by forward batteries 1 and 2 and aft battery 1; 56 vdc, by aft battery 2.

Forward 1 and 2 batteries were rated at 300 and 4 amp-hours, respectively. Aft 1 and 2 batteries were rated at 58 and 25 amp-hours, respectively. The following tabulation indicates battery power consumption in amp-hours and as a percent of rated capacity:

TABLE 14-II S-IVB BATTERY PERFORMANCE

Battery	Capacity (amp-hours)	Amp-Hours Used at Hr	Consumed at Hr
Fwd 1	300	199.3 at 18 hrs	66% at 18 hrs
Fwd 2	4	4.5 at 7.8 hrs	112.5% at 7.8 hrs
Aft 1	58	58 amp-hrs expended between 15.4 and 17 hrs	
Aft 2	25	22.2 at 18 hrs	88.8% at 18 hrs

The above computations have been calculated from all available data and do not take into account battery heater cycles that may have occurred between the periods of no ground station coverage. Aft Battery No. 1 could not be fully calculated due to lack of data between ground stations. Entire performance was well beyond the mission requirements.

Battery voltage and current profiles for the entire flight are presented in Figures 14-2 and 14-3. The composite average temperature of the batteries from the switch to internal power until S-IVB engine start command was 303°K (86°F). The battery temperature histories indicate normal heat rise during battery loading and proper cycling of the heater circuits to maintain battery temperature. Temperature limits of 366.2°K (199°F) were not approached.

The static inverter-converter operated within design limits throughout the flight. Although, on one measurement, it exhibited a shift in frequency from 401 Hz at 5540 sec to 395 Hz at 5840 sec, this apparent degradation of the frequency was resolved to be an instrumentation problem, since a correlative measurement did not exhibit the frequency shift.

All EBW firing units performed satisfactorily. The ullage rocket ignition EBW units were charged at 140.8 sec; the normal ullage rocket ignition occurred, on command, at 145.37 seconds. The ullage rocket jettison EBW units were charged at 153.6 sec and were discharged at 157.58 seconds. This and other data indicated that all three ullage rockets were jettisoned satisfactorily.

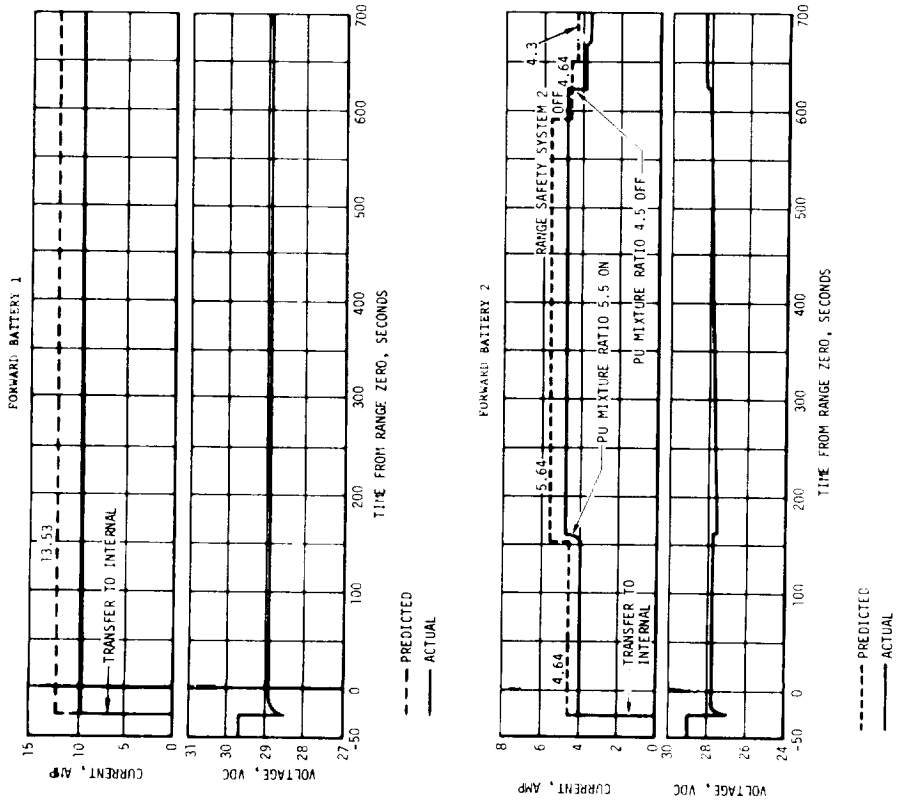
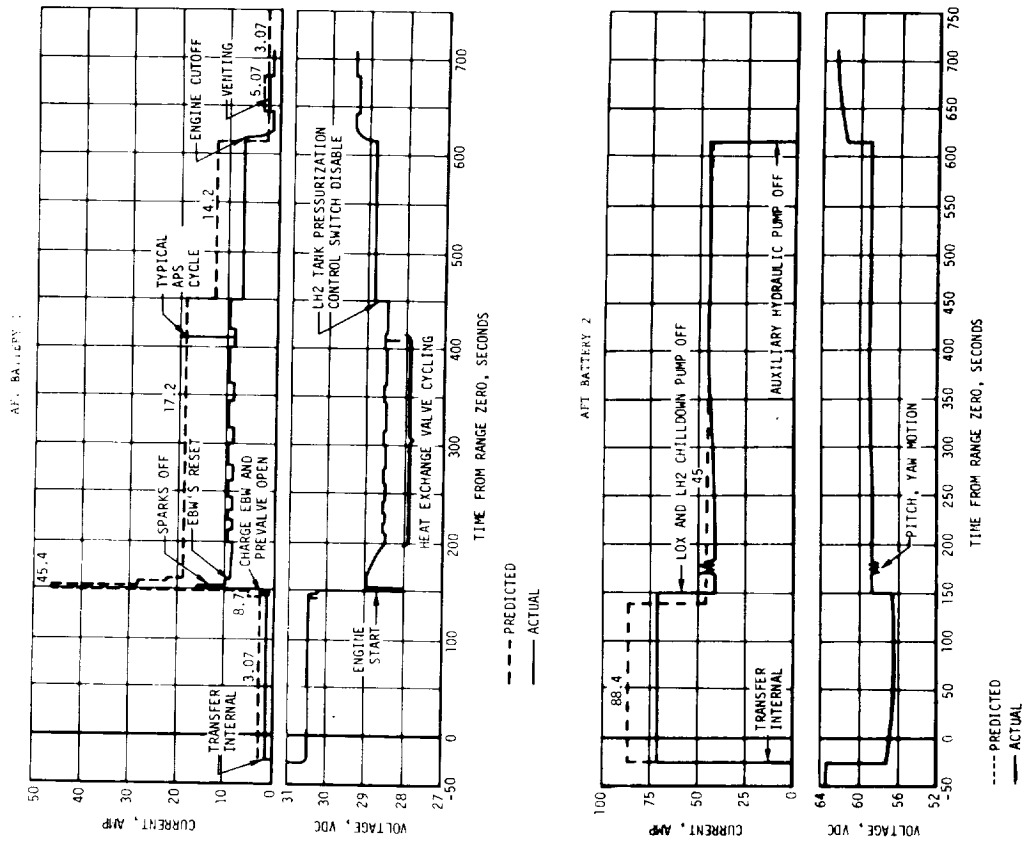


FIGURE 14-2 S-IVB BATTERY CURRENT AND VOLTAGE-LAUNCH PHASE

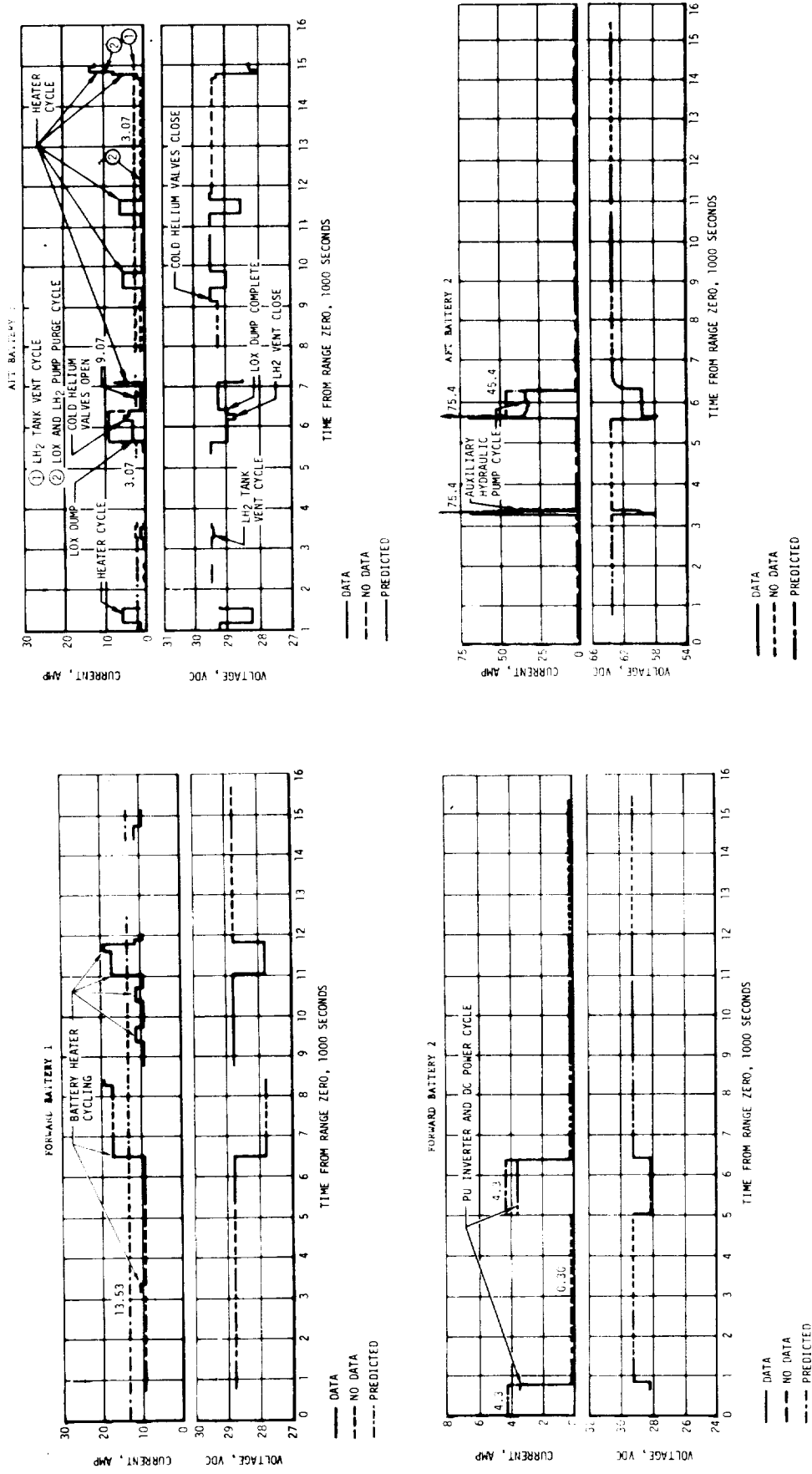


FIGURE 14-3 S-IVB BATTERY CURRENT AND VOLTAGE-ORBIT

The electrical portions of the S-IVB control system responded properly to the commands generated by the sequencer and the Instrument Unit. The S-IVB stage switch selector performed as expected. Telemetry data indicated that both range safety receivers functioned properly during the entire flight. The Electrical Control and Electrical Power Systems operated satisfactorily to provide the necessary control functions and electrical power during the dump experiment.

The range safety system was not required for propellant dispersion during flight. All indications showed that it operated properly and would have satisfactorily terminated an erratic flight.

14.4 INSTRUMENT UNIT ELECTRICAL SYSTEM

The Electrical Subsystem functioned normally from liftoff through at least 14 hours.

The IU electrical system consisted of four batteries (designated 6D10, 6D20, 6D30, 6D40), two power supplies, five types of distributor, a switch selector, and an EDS cutoff-inhibit timer. The four batteries, each rated at 350 ampere-hours, provided the 28 vdc power for the IU. Each battery contained 20 alkaline silver-zinc cells with potassium hydroxide electrolyte. The 6D20 battery was used solely for C-Band transponder operation. The two power supplies converted the unregulated 28 vdc from the batteries to regulated 56 vdc required for stabilized platform electronics and to highly regulated 5 vdc used as excitation and reference voltage for transducers and signal conditioning equipment. The five types of distributor provided power signal distribution, and switching for IU components. The switch selector decoded the flight sequence commands issued by the LVDC/LVDA and activated the proper circuits to execute the commands. No forced reset commands were issued, and no complement commands were necessary. The cutoff-inhibit timer functioned nominally.

The 56-volt power supply voltage remained within the tolerance limits of 56 ± 2.5 vdc for a 1.1 to 8 ampere load. The 5-volt measuring voltage supply remained within the 5 ± 0.005 vdc tolerance for a 1 ampere load. The distributors performed without discrepancy.

Voltages and currents were normal during the flight. The 6D10, 6D20, and 6D30 Battery Currents were near the preflight predictions; however, current on the 6D40 Battery was 2.3 amperes less than predicted.

Battery temperature measurements were not used on this flight. Battery voltages indicate a gradual increase over a period from liftoff to 12.2 hours as

expected. This voltage increase is in proportion to the battery current drain. The maximum observed increase of 1.4 volts occurred on the 6D40 battery.

Table 14-III depicts battery conditions at 19.0 hours of flight. Figures 14-4 and 14-5 are plots of SC 4020 data for battery bus voltages and currents.

TABLE 14-III IU BATTERY CONDITIONS AT 19.0 HOURS OF FLIGHT

Battery	Ampere-Hours Used	Percent Used	Average Current (Amperes)	Battery Life From Liftoff to 26-Volt Point of Decay (Hours)
6D10	374	100.0	24.0	15.6 (1)
6D20	34.2	9.8	1.8	See Note (2)
6D30	385	100.0	20.6	18.7 (1)
6D40	378	100.0	26.4	14.3 (1)

(1) Decay curves were extrapolated to the 26-volt point.

(2) This battery powered only the C-Band Transponders, which operated 162.5 hours until re-entry of the S-IVB/IU.

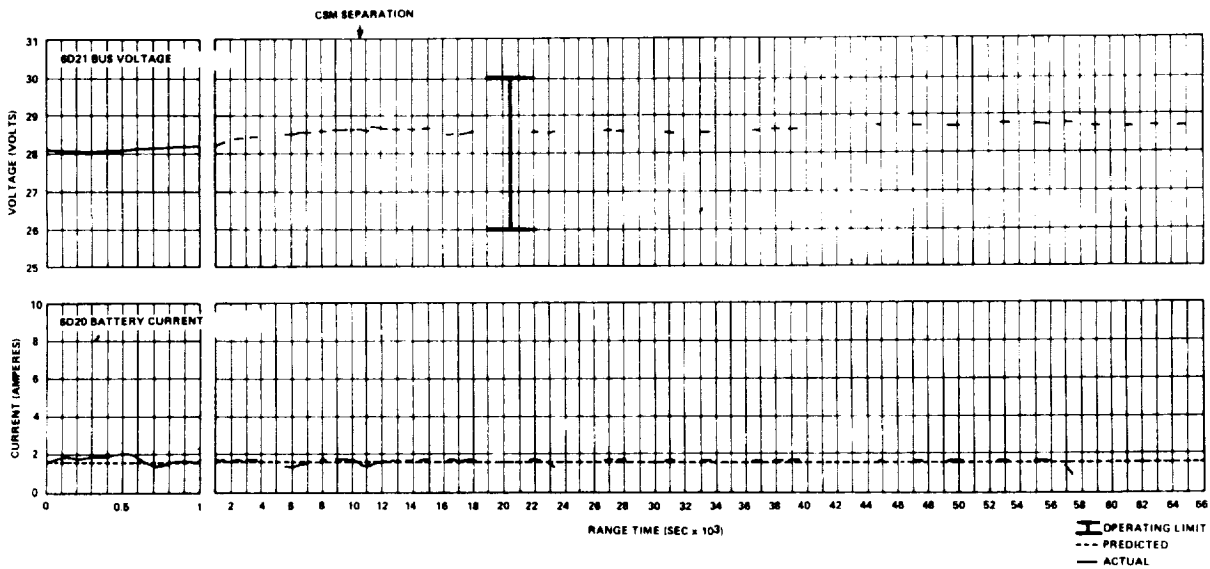
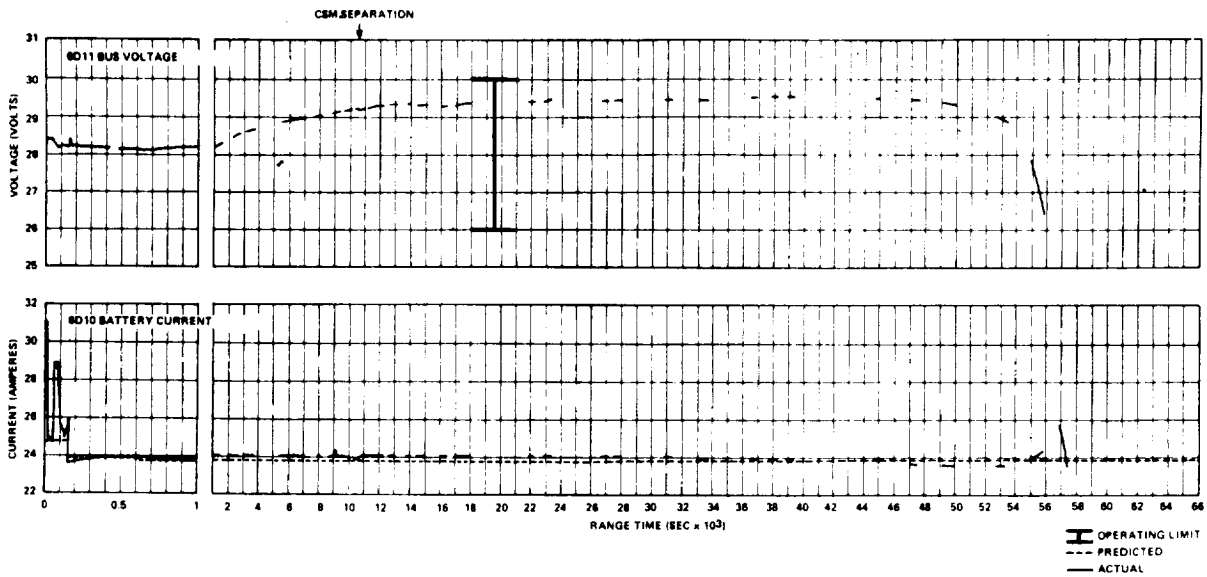


FIGURE 14-4. 6D10 AND 6D20 BATTERY CURRENTS AND VOLTAGES

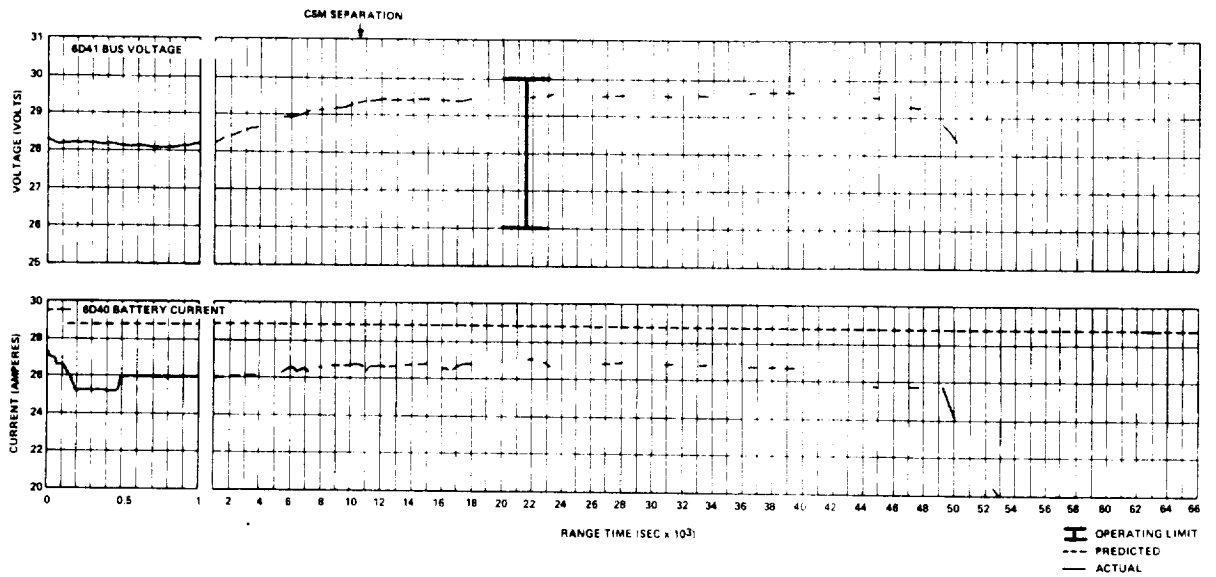
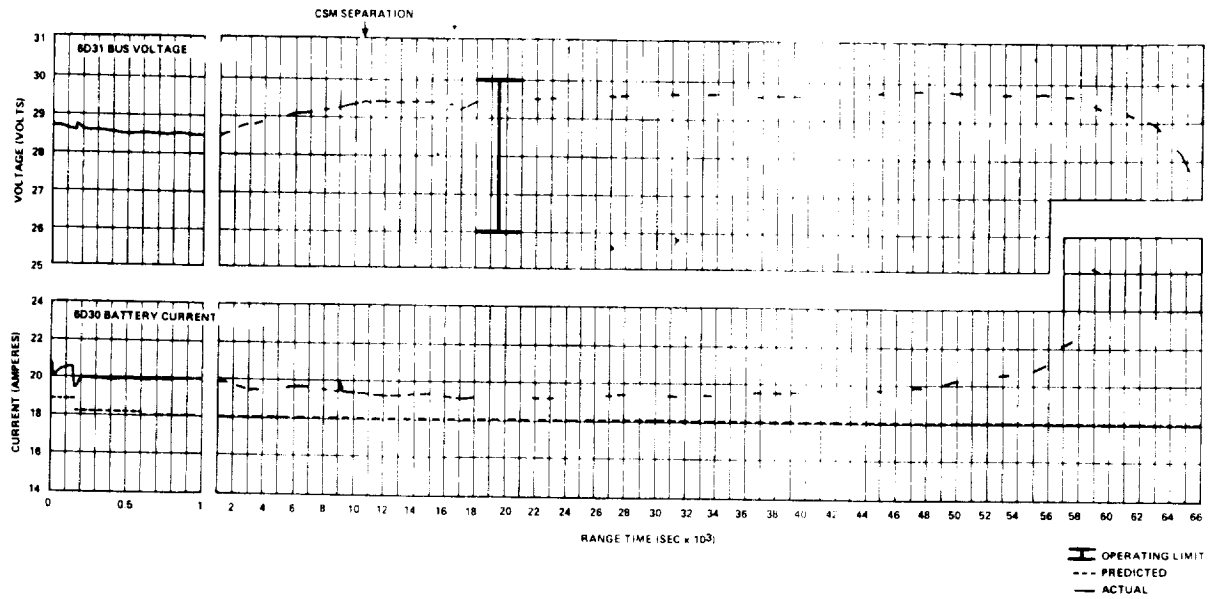


FIGURE 14-5. 6D30 AND 6D40 BATTERY CURRENTS AND VOLTAGES

15.0 RANGE SAFETY AND COMMAND SYSTEMS PERFORMANCE

15.1 SUMMARY

Secure Range Safety Command Destruct Systems (RSCDS) were fully operational and could have performed the destruct function at any time during powered flight except for a 0.83 sec interval at 120.94 sec and a 0.60 sec interval at 122.59 seconds. The Digital Command System (DCS) performed satisfactorily. Two commands from Carnarvon, one from Hawaii, and one from Ascension were not issued in proper form to obtain the desired DCS response.

15.2 COMMAND DESTRUCT SYSTEMS PERFORMANCE

The Command Destruct Receivers (CDR) 1 and 2 of the S-IB stage and CDR 2 of the S-IVB stage lost input signal from 120.94 to 121.77 sec and from 122.59 to 123.19 seconds. A defective relay, K1 in the Monitor Protector Unit of the ground support equipment, did not open instantly as the carrier was blanked for change-over, thus resulting in a fault indication. This fault indication initiated the backup transmitter turn-on sequence, causing the first loss of input signal. Interruption from 122.59 to 123.19 sec was due to blanking while the backup transmitter came on line as the primary transmitter.

No arm/cutoff and no destruct commands were required. With the exception of the times mentioned above, telemetry indicates that the command antenna, receivers/decoders, destruct controllers, and EBW firing units would have performed satisfactorily if needed. EBW firing unit data indicated that the units were in the required state of readiness.

15.3 INSTRUMENT UNIT COMMAND SYSTEM PERFORMANCE

Table 15-I contains a list of commands that were attempted by the Mission Control Center (MCC). The remarks column indicates whether the command was accepted or rejected by the vehicle.

The station command history from MILA on revolution 3 indicated the mode word for the command transmitted at 11,754 sec was transmitted twice. There were no indications that the IU DCS saw the first transmission. The MILA station log and the command verification magnetic tape were not available. Therefore, the command could not be analyzed to determine if the proper address bits were transmitted.

TABLE 15-I DCS COMMAND HISTORY

Sequence Initiate (SEC)	Station	Command	Remarks	Switch Selector Output (SEC)
11, 353	Texas	LH ₂ Vent Open	Accepted	11, 354. 47
11, 754	MILA	LH ₂ Vent Closed On	Accepted	11, 756. 11
11, 754	MILA	LH ₂ Vent Boost Closed On	Accepted	11, 756. 99
11, 762	MILA	LH ₂ Vent Boost Closed Off	Accepted	11, 763. 35
14, 481	Carnarvon	LH ₂ Vent Open	Not Transmitted	
14, 555		LH ₂ Vent Open	Rejected	
14, 641		Terminate	Rejected	
14, 700		LH ₂ Vent Open	Not Transmitted	
14, 745		LH ₂ Vent Open	Accepted	
14, 820		LOX AND LH ₂ Pump Seal Purge Off	Accepted	
15, 007		LH ₂ Vent Closed On	Accepted	
15, 007		LH ₂ Vent Boost Closed On	Accepted	
15, 014		LH ₂ Vent Boost Closed Off	Accepted	
16, 230	Hawaii	Navigation Update	Rejected	
16, 251		Terminate	Accepted	
16, 263		Navigation Update	Accepted	
16, 291		Sector Dump	Accepted	
17, 034	Texas	LH ₂ Vent Open	Accepted	17, 035. 85
17, 340	MILA	LH ₂ Vent Closed On	Accepted	17, 341. 73
17, 340		LH ₂ Vent Boost Closed On	Accepted	17, 342. 63
17, 347		LH ₂ Vent Boost Closed Off	Accepted	17, 348. 57
18, 538	Ascension	LH ₂ Vent Open	Accepted	
18, 683		LH ₂ Vent Closed On	Accepted	
18, 683		LH ₂ Vent Boost Closed On	Accepted	
18, 690		LH ₂ Vent Boost Closed Off	Accepted	
18, 720		LH ₂ Vent Boost Closed Off	Accepted	
23, 111	MILA	LH ₂ Vent Open	Not Transmitted	
23, 172	MILA	Terminate	Not Transmitted	

The mode word for the command transmitted from Carnarvon at 14,745 sec was also transmitted twice. The command history indicated the vehicle did not see the first transmission but accepted the second transmission. The command verification tape was analyzed: the first mode word transmitted contained the proper address bits and should have been accepted by the IU. The command verification tape also showed the carrier was off until 0.4 sec before the first mode word was transmitted. However, the onboard signal strength measurement indicated the up-link was present throughout the pass.

At 14,481 sec, a command was attempted from Carnarvon. However, the ground station command console rejected the command and it was not transmitted. The next two commands attempted from Carnarvon, at 14,555 and 14,641 sec, were not accepted by the vehicle because the wrong carrier (S-Band) was selected.

At 14,700 sec, an attempt was made to retransmit the command. However, another command was being executed to the spacecraft and the command to the IU was rejected. This command was properly transmitted at 14,745 sec and was accepted by the Digital Command System (DCS).

The first navigation update was rejected on the 15th data word because the ground computer failed to capture an Address Verification Pulse (AVP). Review of the AVP and Computer Reset Pulse (CRP) data from the IU showed a 1-sample dropout on the 15th data word AVP which probably kept the ground computer from recognizing the necessary four logical ones within the 60-millisecond waiting period. The CRP was transmitted with no dropout; but after the ground computer failed to recognize the AVP, it did not search for the CRP. The 15th data word was retransmitted, but rejected by the IU because the sequence bit was in error. (The IU was expecting the 16th data word but was receiving the 15th data word.) A terminate command was transmitted, then the navigation update sequence was repeated and accepted.

The ground computer again failed to capture the AVP and CRP after the last data word from Ascension at 18,690 seconds. Review of the IU data indicates this word was accepted by the DCS and both the AVP and CRP were transmitted. When the last data word was retransmitted, it was rejected by the computer since it was expecting another mode word (another command). The command was repeated at 18,720 sec and was accepted.

The last two commands attempted from MILA at 23,111 and 23,172 sec were not transmitted because the ground station carrier was down at this time.

16.0 EMERGENCY DETECTION SYSTEM (EDS)

16.1 SUMMARY

The Emergency Detection System (EDS) was essentially the same as on previous vehicles with one exception. Since this was a manned flight, the manual abort loop was closed. Two minor hardware differences from the AS-202 configuration were incorporated on the AS-205 Emergency Detection System. (1) The rate limit was switched prior to staging and (2) tank pressure displays were flight tested in the spacecraft. The AS-205 EDS functioned properly throughout its period of operation. All abort parameters remained well below abort limits and all Switch Selector events, EDS Timer operations, and associated discretes functioned nominally.

16.2 EDS BUS VOLTAGE

The EDS busses - 6D91, 6D92, and 6D93 - are supplied by the IU batteries 6D10, 6D30, and 6D40, respectively. The EDS buses were energized properly throughout the flight. The IU battery voltages, shown in Section 14, represent the respective EDS bus voltages.

16.3 EDS EVENT TIMES

Tables 16-I and 16-II list the event times associated with the Emergency Detection System. All timed EDS events occurred properly.

16.4 THRUST OK PRESSURE SWITCHES

There was no indication of S-IB engine-out from ignition to inboard engine cutoff and, therefore, no indication of the automatic abort bus having been energized.

The S-IVB engine thrust was indicated to the crew for a manual abort cue. The performance of the thrust sensors and associated logic was nominal.

16.5 EDS RATE GYROS

The angular rate limit settings were five degrees per second in pitch and yaw and twenty degrees per second in roll. The limits were switched by switch selector command prior to staging. During second stage flight, the limit settings were 9.2 degrees per second in pitch and yaw and 20 degrees per second in roll. The maximum rates detected about the pitch, yaw, and roll axes were: + 1.5 deg/sec,

TABLE 16-I EDS/SWITCH SELECTOR EVENTS

Function	Stage	Range Time (SEC)	Time from Base (SEC)		
			Nominal	Actual	Deviation
<u>Start Time Base 1 (T₁)</u>	-	0.358	T ₁ +0.0	0.0	0.0
Multiple Engine Cutoff Enable	S-IB	10.308	T ₁ +10.0	9.950	-0.050
Launch Vehicle Engines EDS Cutoff Enable	IU	40.324	T ₁ +40.0	39.966	-0.034
Excessive Rate (P,Y,R) Auto-Abort Inhibit Enable	IU	132.907	T ₁ +132.6	132.549	-0.051
Excessive Rate (P,Y,R) Auto-Abort Inhibit & Switch Rate Gyros SC Indivation "A"	IU	133.109	T ₁ +132.8	132.751	-0.049
S-IB Two Engines Out Auto-Abort Inhibit Enable	IU	133.326	T ₁ +133.0	132.968	-0.032
S-IB Two Engines Out Auto-Abort Inhibit	IU	133.510	T ₁ +133.2	133.152	-0.048
<u>S-IB Propellant Level Sensor Actuation-Start Time Base 2 (T₂)</u>	S-IB	137.489	T ₂ +0.0	0.0	0.0
Inboard Engines Cutoff	S-IB	140.643	T ₂ +3.2	3.154	-0.046
Auto-Abort Enable Relays Reset	IU	140.860	T ₂ +3.4	3.371	-0.029
<u>Start Time Base 3 (T₃)</u>	S-IB	144.318	T ₃ +0.0	0.0	0.0
S-IB Outboard Engines Cutoff	S-IB	144.318	T ₃ +0.0	0.004	+0.004
S-IB/S-IVB Separation On	S-IB	145.580	T ₃ +1.3	1.262	-0.038

TABLE 16-II EDS DISCRETE EVENTS

Discrete Measurement	Discrete Event	Range Time (SEC)
K17-602	EDS or Manual S-IB or S-IVB Cutoff (Switch Selector)	40.389
K18-602	EDS or Manual S-IB or S-IVB Cutoff (Timer)	41.472
K9-602	EDS S-IB One Engine Out	140.854
K11-602	EDS S-IB Two Engines Out	140.879
K57-603, K58-603	Q-Ball Power Off	141.479

+ 1.1 deg/sec, and +1.75 deg/sec, respectively. No rates were sufficient to have created an overrate condition.

16.6 Q-BALL DIFFERENTIAL PRESSURES

The maximum Q-Ball differential pressure vector sum recorded was 0.31 N/cm² differential (0.45 psid) at 72.8 seconds. The manual abort limit for this parameter was 1.8 N/cm² differential (2.6 psid).

16.7 LAUNCH VEHICLE ATTITUDE REFERENCE MONITORING

The ST-124 Platform functioned properly; therefore, no reference failures were indicated.

17.0 STRUCTURES

17.1 SUMMARY

The postflight predicted longitudinal load and bending moment for the AS-205 vehicle compares favorably with the flight measured accelerometer and strain data. Vehicle loads due to the combined longitudinal load and bending moment were below limit design values and, therefore, the stress levels in key structural members were below their limit design values.

Measured vehicle first and second bending mode data compared favorably with the results from dynamic analysis. Vehicle response amplitudes at these predominate frequencies were low and comparable to previous Saturn IB flights.

17.2 TOTAL VEHICLE LOADS AND MOMENTS

17.2.1 LONGITUDINAL LOADS

Vehicle postflight predicted longitudinal force distributions were computed using the mass characteristics of AS-205 and the applied forces from the flight trajectory data recorded during S-IB stage burn. The longitudinal accelerations obtained from the analysis show agreement with values measured during flight at all time points and reached a maximum of 41.8 m/s^2 at 140.64 sec, the time of IEEO.

Comparisons between the postflight predicted longitudinal force and that derived from the strain measurements at station 23.9 m are presented in Figure 17-1 for the conditions of maximum bending and maximum compression, which occurred at 73.1 and 140.64 sec, respectively.

The longitudinal load at Station 23.9m was 6,006,434 N (1,350,300 lbf) at IEEO and is 8.1% greater than the design loads analysis value of 5,558,164 N (1,249,525 lbf) based on R-P&VE-SL-212-63. This difference is acceptable, since combined longitudinal and bending moment loads are below limit design values, and occurred due to weight increase above Station 23.9m for the AS-205 configuration as compared to the configuration used in the design loads analysis. The AS-201, AS-202, and AS-204 vehicles longitudinal load values were greater than the design loads analysis values by 3%, 6%, and 7.3%, respectively. The AS-203 vehicle values were less than the design loads analysis values.

— T = 73.1 SEC	--- T = 140.64 sec
$a_x = 19.6 \text{ m/s}^2$	$a_x = 41.8 \text{ m/s}^2$
M = 1.379	
Q = 32,267 N/m ²	
$\alpha = 1.5320 \text{ deg}$	
$\beta = 0.8453 \text{ deg}$	

Longitudinal Force (1000 N)

Longitudinal Force (1000 lbf)

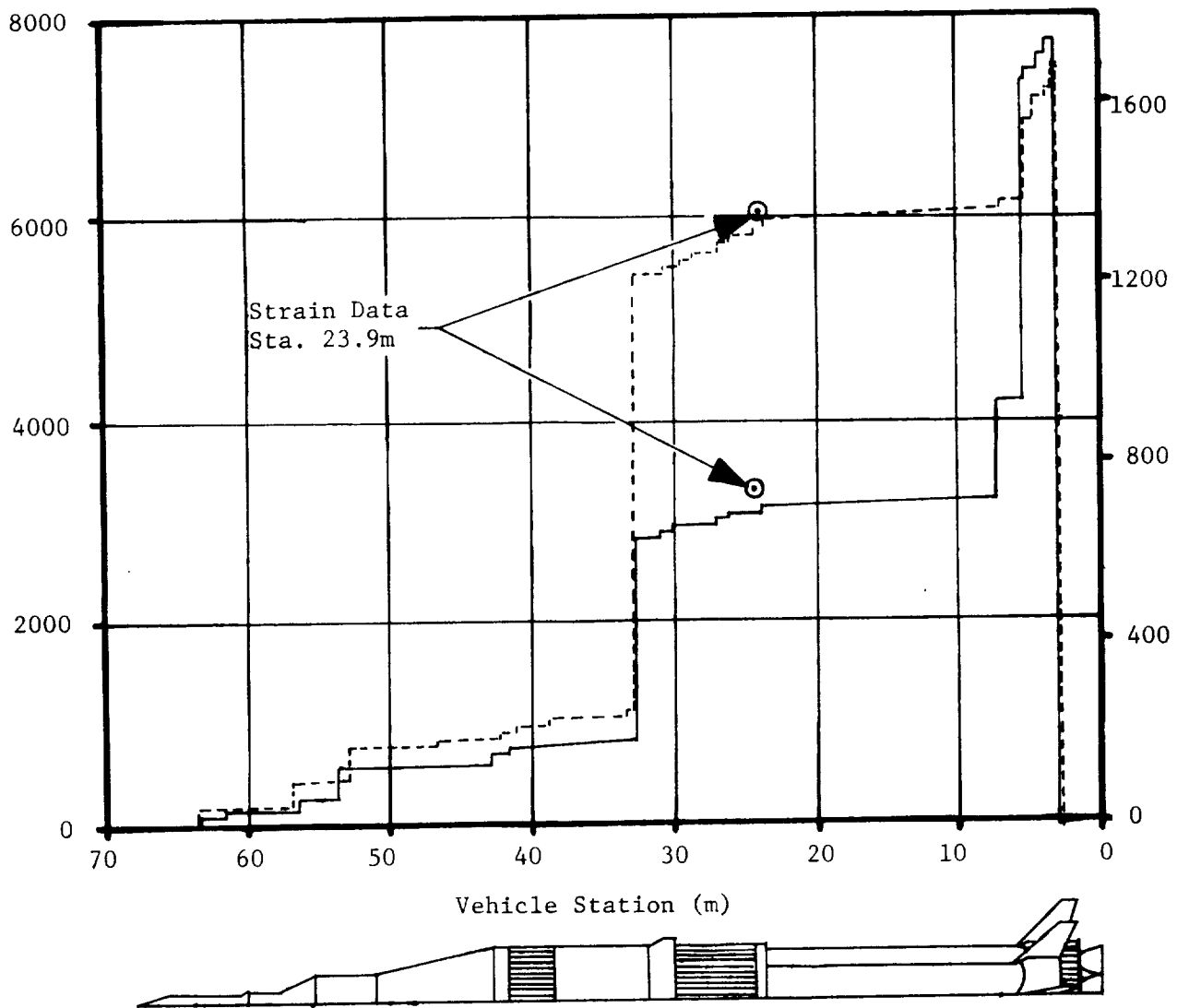


FIGURE 17-1 VEHICLE LONGITUDINAL FORCE DISTRIBUTION

The AS-205 longitudinal load time history at Station 23.9m, obtained from strain data, is compared in Figure 17-2 to the time history band (shaded area) of minimum and maximum load experienced by vehicles AS-202, AS-203, and AS-204.

17.2.2 BENDING MOMENTS

The AS-205 strain measurements at Sta. 23.9m show that the maximum pitch moment of 773,031 N-m (6,841,900 lbf-in) occurred at 74.9 sec and the maximum yaw moment of 524,498 N-m (4,642,200 lbf-in) occurred at 79.3 sec. The maximum resultant moment of 852,584 N-m (7,546,000 lbf-in), occurring at 73.1 sec, is 13% of the vehicle design criteria value of 6,361,000 N-m (56,300,000 lbf-in). The AS-205 measured values do not include the load contribution of the 2.67m (105 in) dia center LOX tank or the 1.78m (70 in) dia fuel tank tension ties. The results from instrumented vehicles have shown the center tank contribution to be about 10% and the tension tie contribution to be negligible.

The postflight predicted bending moment, computed from measured flight parameters at 73.1 sec, is compared to the strain data value in Figure 17-3.

17.2.3 BODY BENDING OSCILLATIONS

The first and second vehicle bending modes, in pitch and yaw, are compared to the mode shapes predicted by dynamic analysis in Figure 17-4. These predominate frequencies were determined from AS-205 flight data by power spectral density analysis and associated with particular modes of vehicle response on the basis of proximity to the predicted frequencies for these modes.

Response amplitudes at these frequencies were low and comparable to previous Saturn IB flights. The greatest amplitude response recorded was 0.102 G_{rms} in the yaw plane at Sta. 22.7m following liftoff. The amplitude time histories are shown in Figure 17-5.

17.3 S-IVB STAGE ANALYSIS

17.3.1 J-2 ENGINE VIBRATIONS

The engine vibration measurements and their maximum composite levels are summarized in Table 17-I. The measured levels during J-2 burn were in reasonable agreement with those measured by Rocketdyne during ground tests. The measured levels were insignificant during S-IB burn and, with the exception of the LOX turbopump, were constant during S-IVB burn. The LOX turbopump level increases with shift to operation at low EMR and is less than levels previously recorded during flight. The time histories of the maximum and minimum composite levels for these measurements are shown in Figure 17-6.

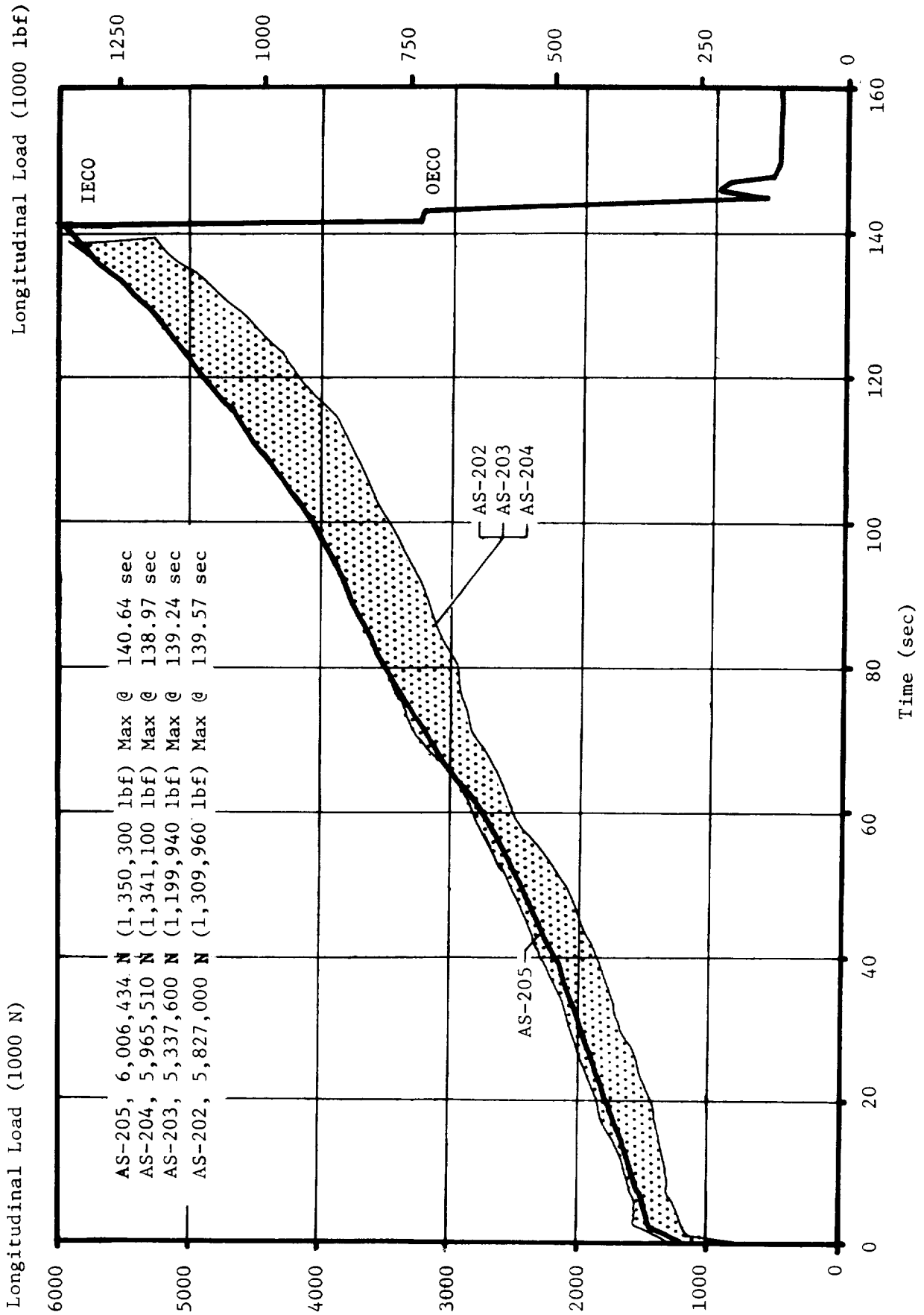


FIGURE 17-2 LONGITUDINAL LOAD (FROM STRAIN DATA AT STATION 23.9m)

T = 73.1 Seconds
 M = 1.379
 Q = 32,267 N/m²
 α = 1.5320 Deg
 β = 0.8453 Deg

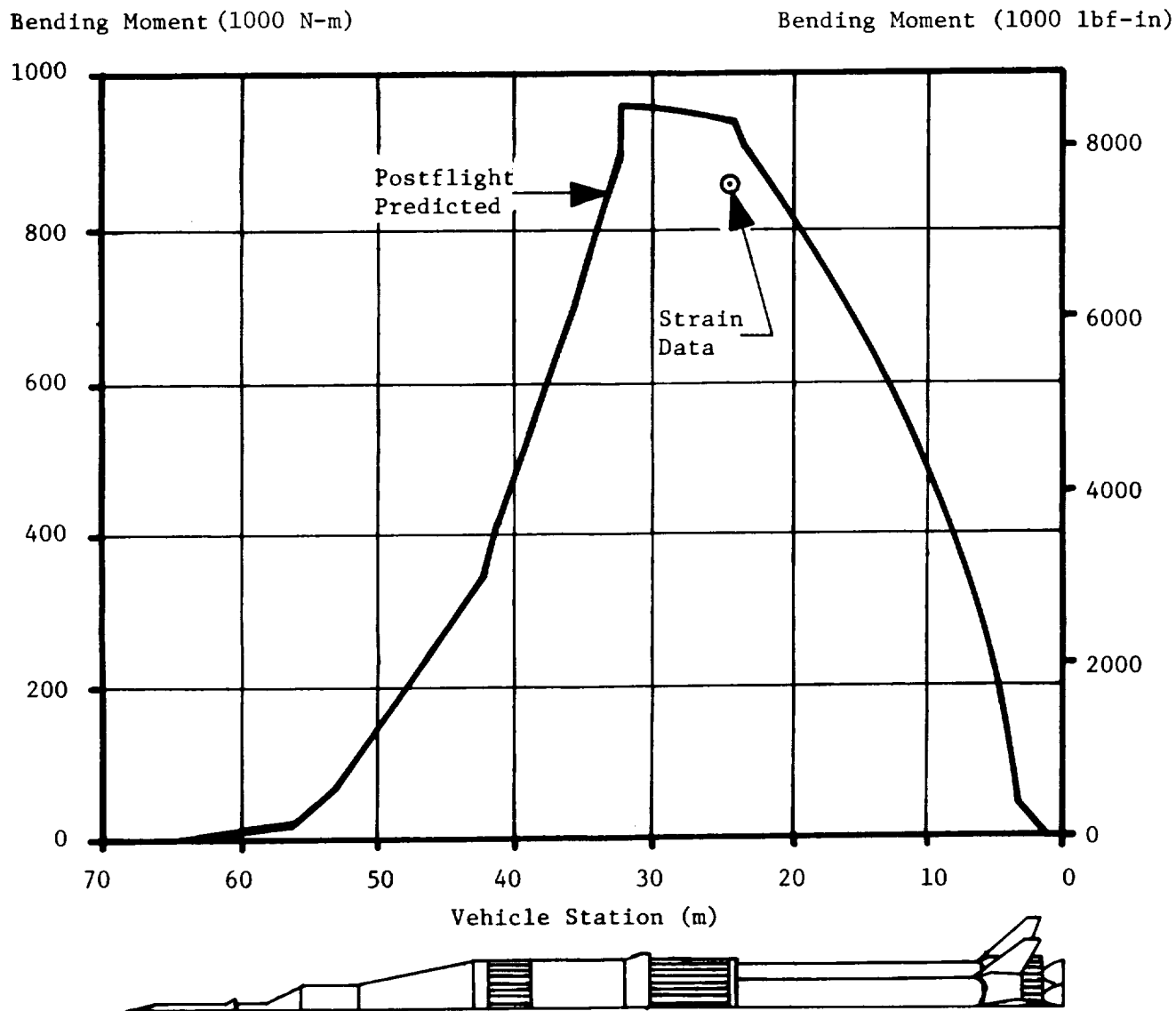


FIGURE 17-3 VEHICLE RESULTANT BENDING MOMENT

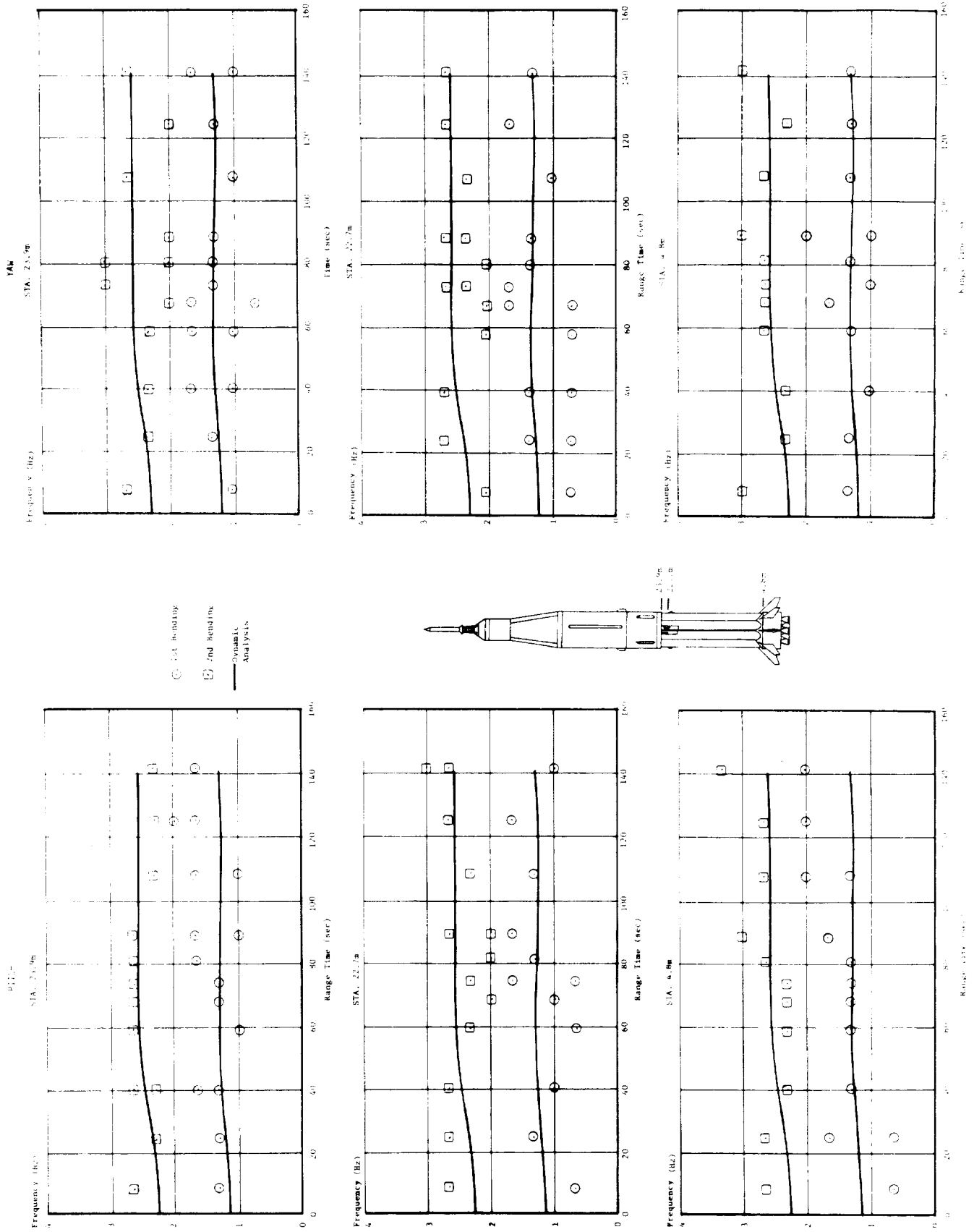
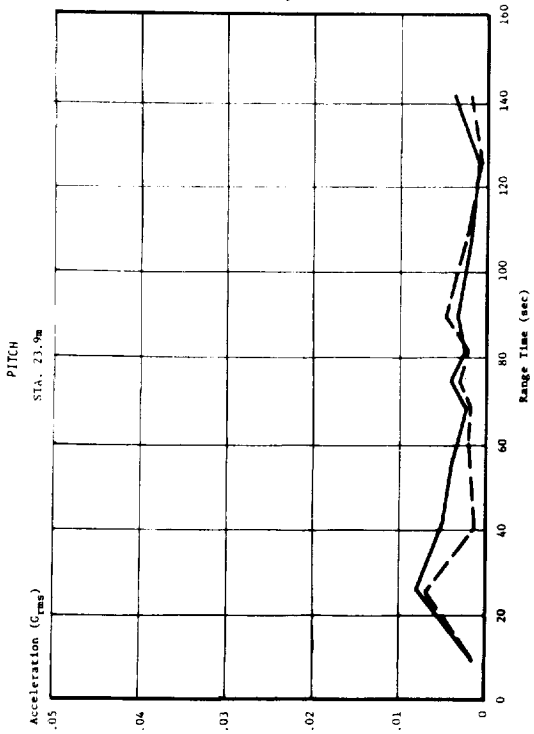


FIGURE 17-4 VEHICLE BENDING MODES



— 1st Bending
- - - 2nd Bending

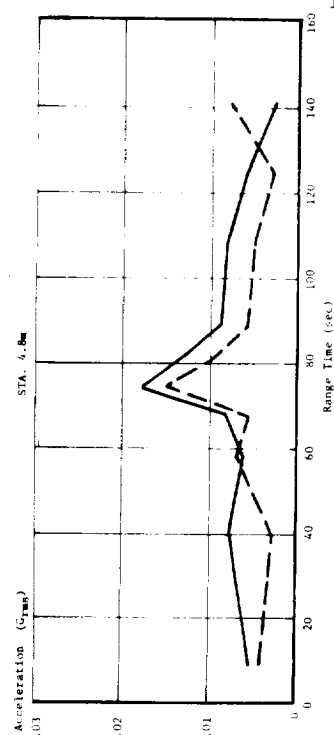
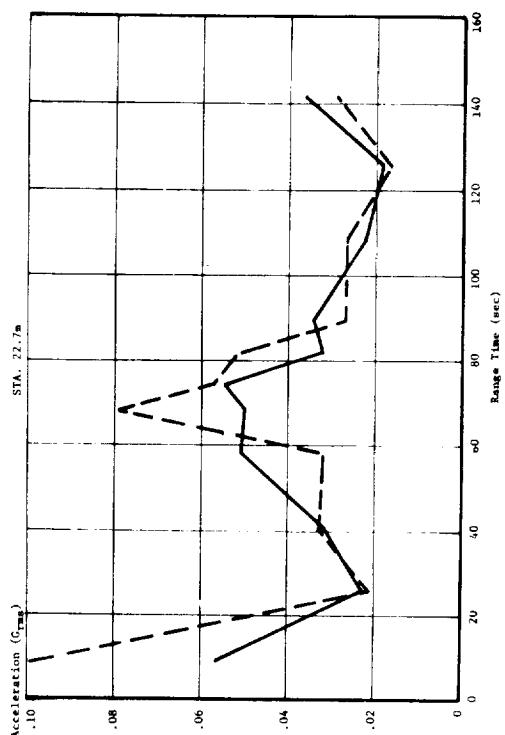
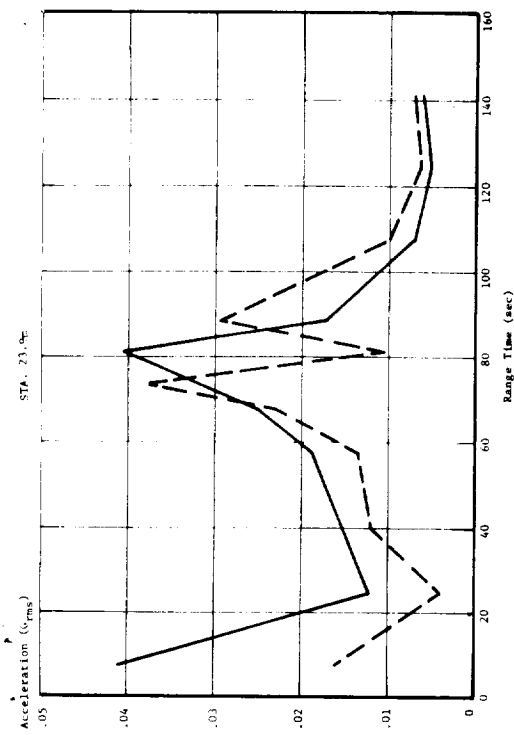
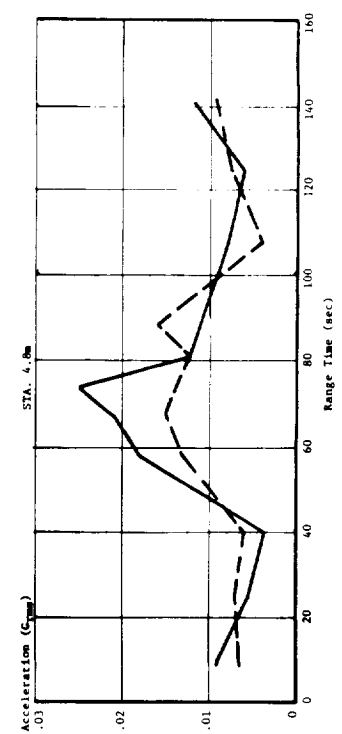
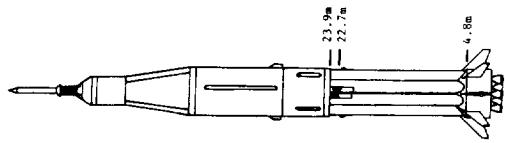
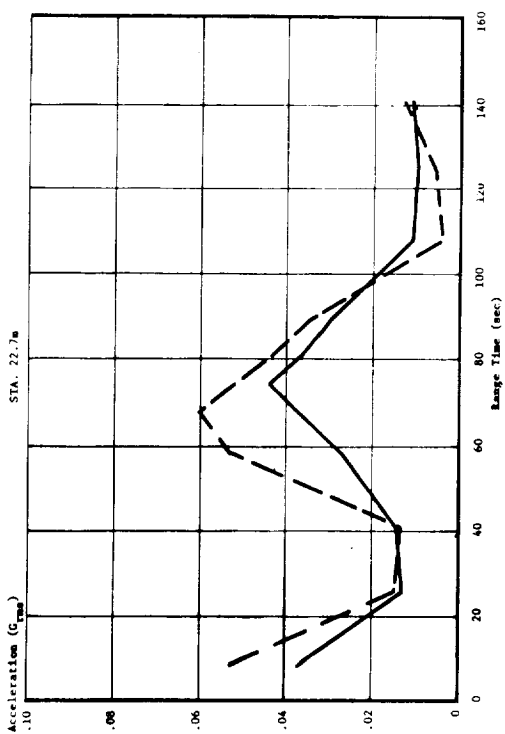


FIGURE 17-5 VEHICLE BENDING AMPLITUDES

TABLE 17-1 S-IVB VIBRATION SUMMARY

	Area Monitored	Max Level (Grms)	Remarks
ENGINE	Main Fuel Valve - Tangential	8	Data invalid between 152.4 and 310.3 sec. Max level measured between 460 sec to cutoff during low EMR. Instrumentation malfunction.
	Main Fuel Valve - Radial	7	
	Fuel ASI Block - Radial	15	
	ASI LOX Valve - Longitudinal	15	
	ASI LOX Valve - Radial	20	
	LOX Turbopump - Lateral	36	
	LH ₂ Turbopump - Lateral	No Data	
	Combustion Chamber Dome-Thrust	8	

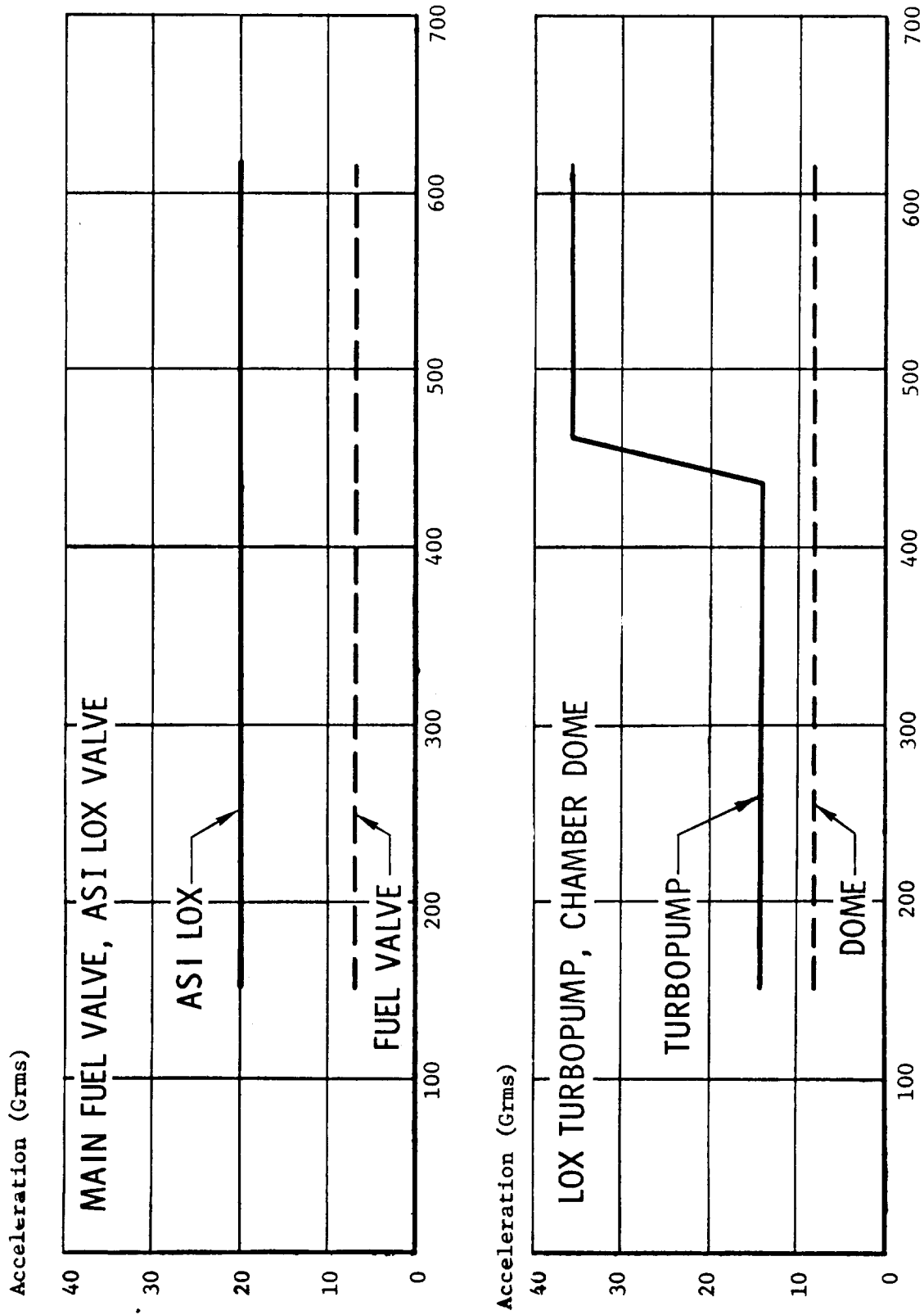


FIGURE 17-6 J-2 ENGINE VIBRATION COMPOSITE LEVELS

18.0 PRESSURE AND THERMAL ENVIRONMENT

18.1 SUMMARY

The mission profile for the AS-205 flight was such that the structural and component thermal environment was well within the design requirement. The S-IB stage heat shield pressure loadings deviated from previous flights after 100 sec (25 km altitude) until outboard engine cutoff. A negative pressure loading was indicated during this entire time, which is contrary to past flights where a peak negative loading occurred at about 25 km altitude and returned to zero at 30 km altitude (120 sec).

The common bulkhead pressures were nominal during loading and flight and at no time approached the expected maximum of 2.4 N/cm (3.5 psi).

The S-IB stage base region experienced a slightly more severe thermal environment than observed previously. The heat shield inner region and flame shield heat loads were 6% and 11%, respectively, more severe than indicated on S-IB-4.

The environmental control system, in the Instrument Unit, maintained acceptable operating conditions for components mounted in the IU and S-IVB forward skirt during preflight and flight operations.

18.2 VEHICLE PRESSURE ENVIRONMENT

18.2.1 S-IB STAGE BASE PRESSURES

The measured loading on the heat shield was in good agreement with previous flights during the most critical loading period. After 100 sec (25 km altitude) the loading on the heat shield deviated from that of previous flights, remaining constant until outboard engine cutoff. During this period, the external pressure was 0.13 N/cm² (0.19 psi) higher than the internal pressure, resulting in a negative loading. Normally this loading has a negative peak which returns to zero. This small negative loading is of no consequence from the structural standpoint. The cause of this negative loading is not known; however, it is possible for the pressure transducer to hang-up and be vibrated loose at outboard engine cutoff, although this cannot be verified. This negative pressure loading could also result from a near-zero engine compartment pressure after 105 sec -- a possibility that cannot be verified because the thrust frame compartment pressure was not measured. Pressure loading on the heat shield is compared with previous flights in Figure 18-1.

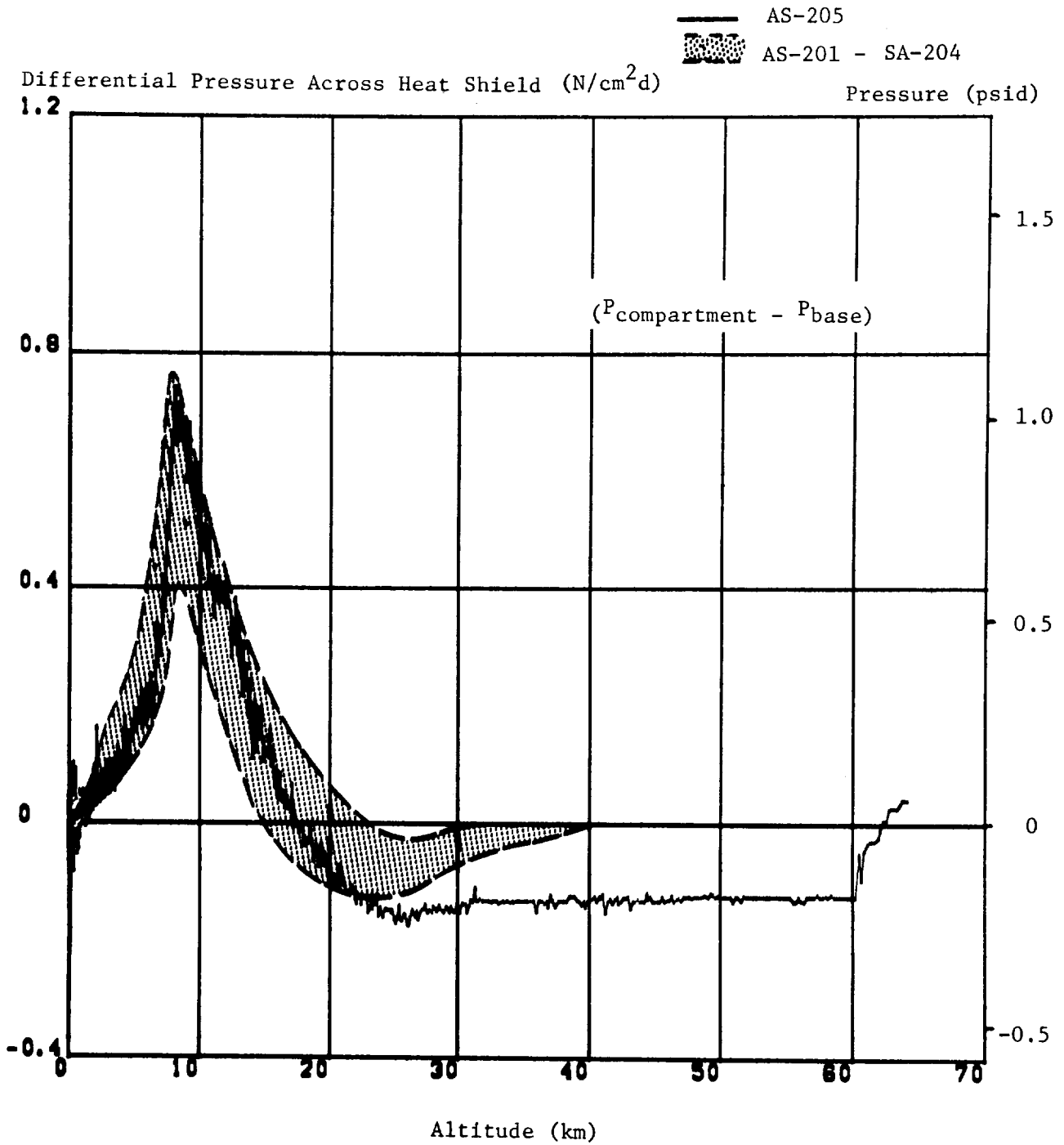


FIGURE 18-1 S-1B STAGE HEAT SHIELD LOADING

Vent holes in the outer wall of the thrust frame compartment were taped shut on AS-205. An analysis of the effect of closing these vents indicated little or no change on the heat shield loading. Based on this analysis, the AS-205 loading should have been similar to previous flights.

Heat shield and flame shield pressures are compared with predicted and with previous flights in Figure 18-2. The AS-205 data is in good agreement with both the prediction and the previous flight data.

18.2.2 S-IVB STAGE INTERNAL PRESSURES

The common bulkhead pressure differential on AS-205 remained below the expected maximum of 2.4 N/cm^2 (3.5 psi) during all loading cycles and throughout flight. The vacuum system operated properly. Bulkhead differential pressure was 1.0 N/cm^2 (1.5 psi) prior to cryogenic loading, dropping to 0.6 N/cm^2 (0.9 psi) following LOX loading. Concurrently with LH₂ loading, the pressure differential dropped to 0.31 N/cm^2 (0.45 psi) and remained there throughout powered flight.

18.3 VEHICLE THERMAL ENVIRONMENT

18.3.1 S-IB STAGE BASE THERMAL ENVIRONMENT

The S-IB stage base thermal environment recorded in the base region on S-IB-5 was slightly more severe than experienced on S-IB-4. The heat shield inner region integrated heat load was approximately 6% more severe than that of S-IB-4, and the flame shield integrated heat load was 11% greater than that of S-IB-4.

Membrane-type calorimeters and gas temperature thermocouples were utilized in establishing the thermal environment of the heat and flame shield. The heat shield inner region total and radiation heating rates are shown in Figure 18-3. The heat shield inner region total heating rates were very similar to those recorded at the same location on S-IB-4. The radiation heating rates, however, showed some inconsistency from those previously recorded. The radiation calorimeter on S-IB-5 did not experience the drop in heat flux above 25 km of altitude that was sensed by similar instrumentation on S-IB-3 and S-IB-4, but the data compared well with the radiant level predicted for the S-IB-5 flight. The predicted thermal environment for AS-205 is presented in Reference 10.

The gas temperatures recorded in the heat shield inner and outer regions are presented in Figure 18-4. The gas temperatures recorded on S-IB-5 were compared with those recorded on S-IB-3 and S-IB-4. The inner region gas

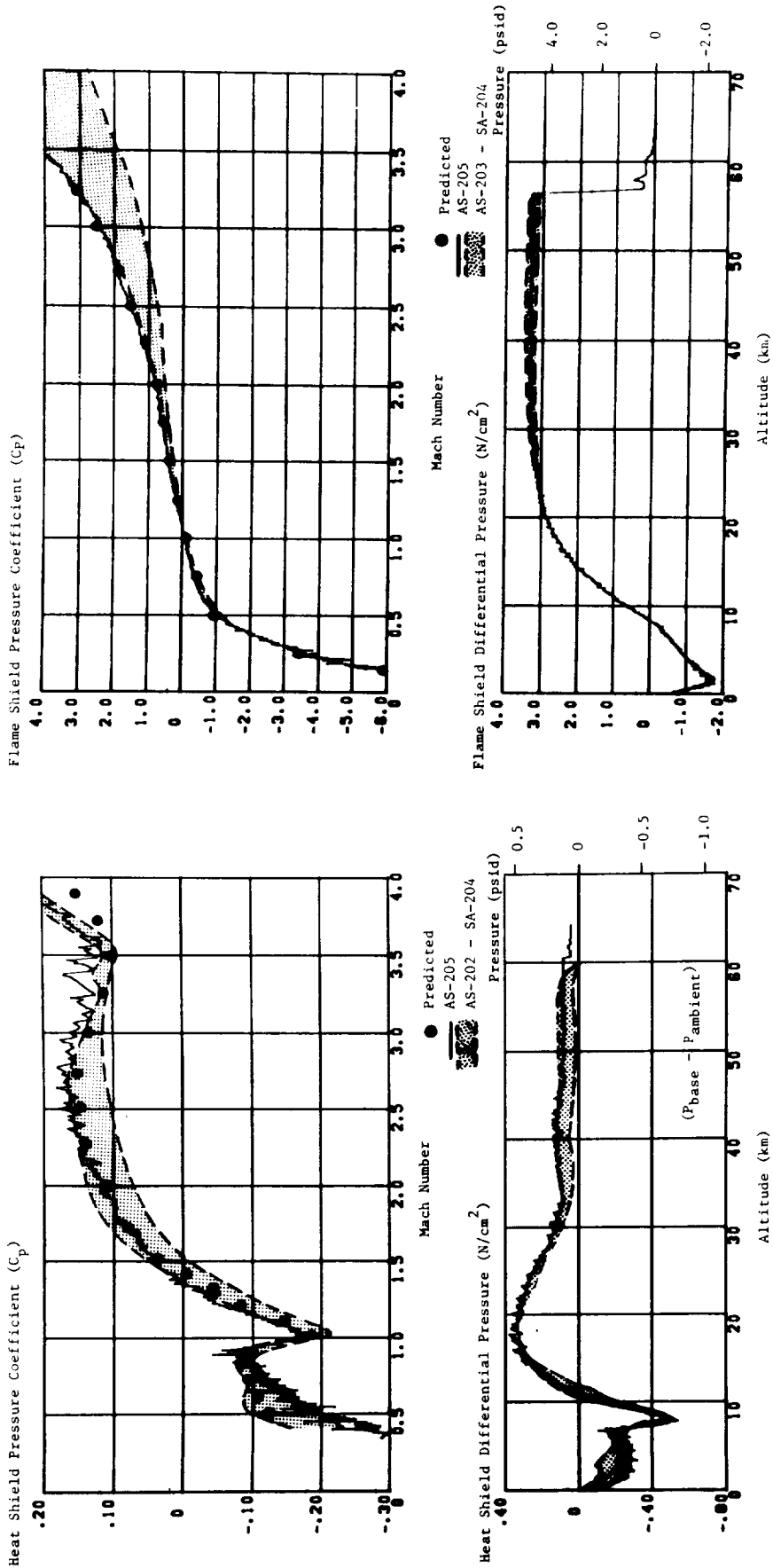


FIGURE 18-2 S-IB STAGE BASE PRESSURES

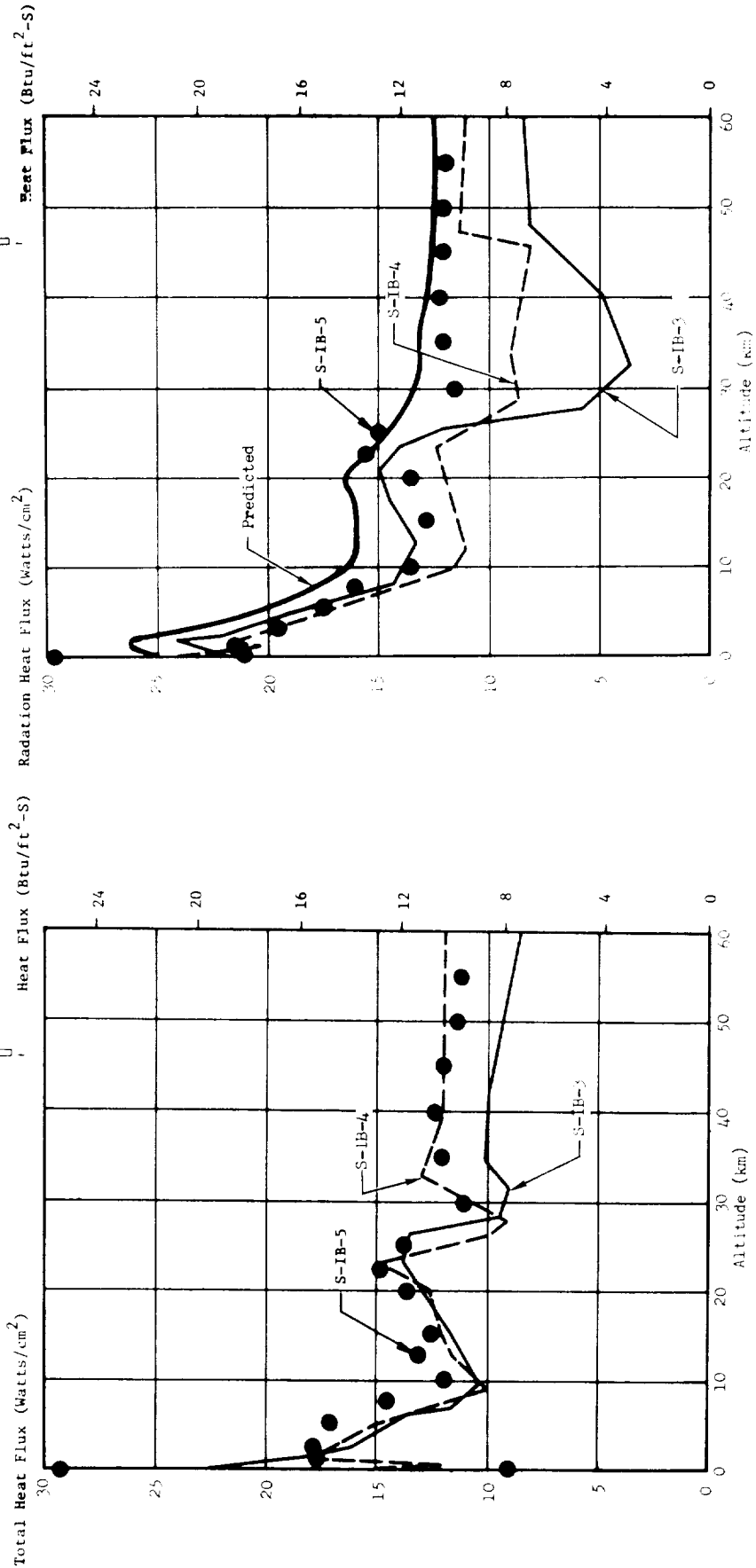
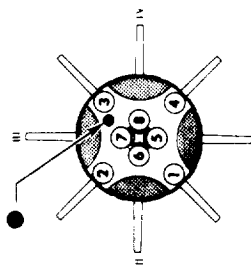
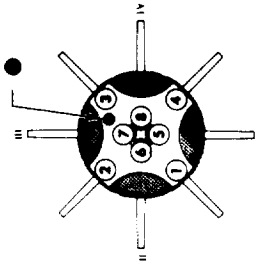


FIGURE 18-3 HEAT SHIELD INNER REGION TOTAL AND RADIATION HEATING RATES

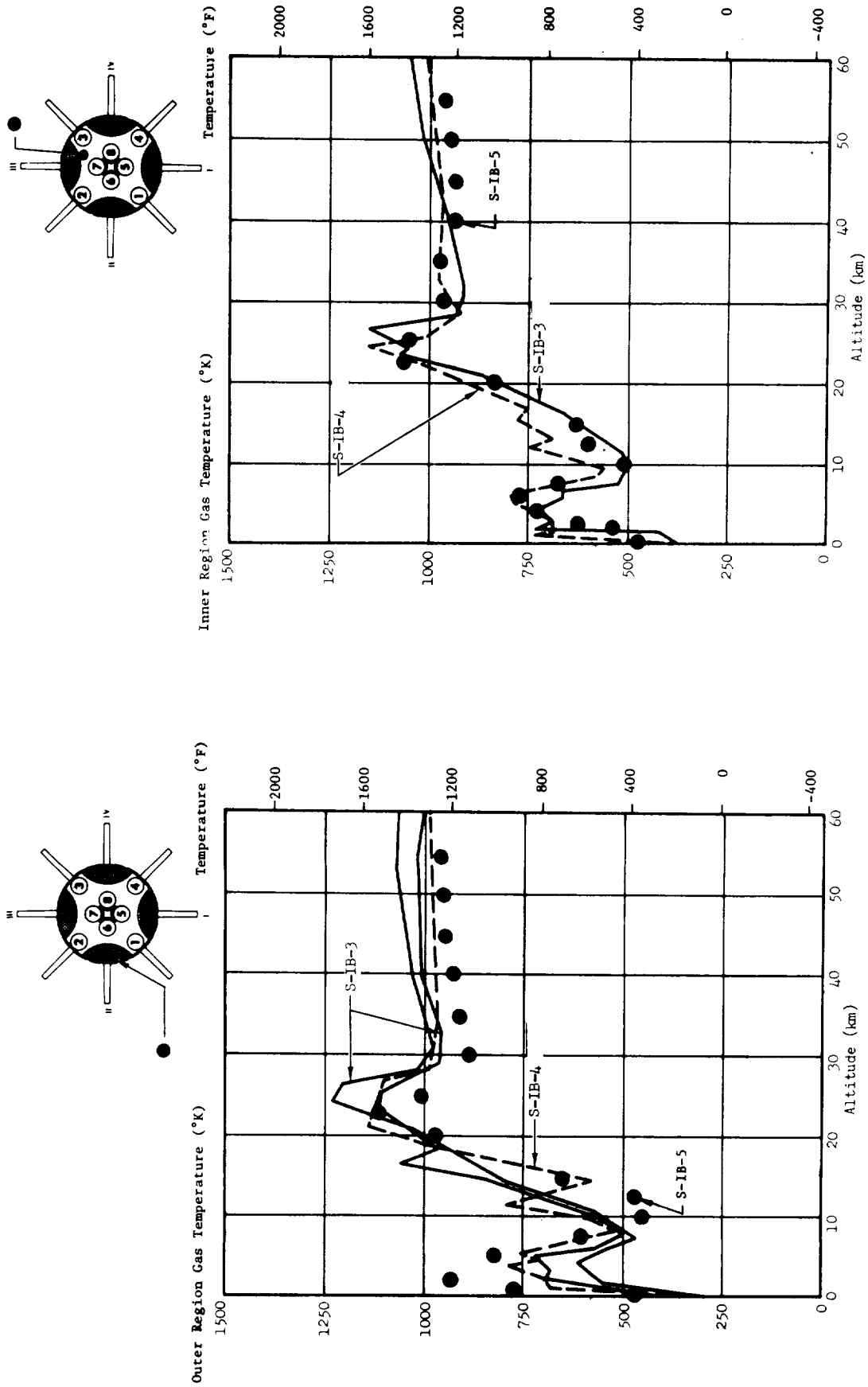


FIGURE 18-4 HEAT SHIELD TEMPERATURES

temperature data were in good agreement with those of previous flights. The outer region temperatures were slightly higher than previously observed during the initial phase of flight but leveled out to a lower value at higher altitudes.

The thermal environment on the S-IB stage flame shield was measured by two calorimeters and one gas temperature thermocouple. The total and radiation heating rates measured on the flame shield are presented in Figure 18-5. The flame shield total heating rates were slightly higher than previously recorded for this configuration; the radiation heating rates were in good agreement with previous data.

The gas temperature thermocouple, positioned on the flame shield, appeared to have malfunctioned, producing excessive data scatter.

Engine compartment temperatures were measured on S-IB-5 to record compartment ambient temperatures around engines 1 through 4, respectively. The engine compartment ambient temperature measured was $273 \pm 15^{\circ}\text{K}$ ($32 \pm 27^{\circ}\text{F}$).

18.3.2 S-IVB STAGE THERMAL ENVIRONMENT

The mission profile of AS-205 was such that the thermal environments for the S-IVB stage components and structure were well within their design environment. The boost and orbital environments resulted in normal structural and components temperatures. The heat input to the propellants was well within expected limits.

18.3.3 INSTRUMENT UNIT TEMPERATURES

Selected Instrument Unit component temperatures are shown in Figures 18-6 through 18-8. The fluctuations indicate internal heat and thermal response to the coolant control temperature and environment. The temperatures generally indicate colder conditions than on previous flights.

18.4 INSTRUMENT UNIT ENVIRONMENTAL CONTROL SYSTEM

The Environmental Control System maintained acceptable operating conditions for components mounted within the Instrument Unit and S-IVB stage forward skirt during preflight and flight operations. The Environmental Control System (ECS) is composed of a Thermal Conditioning Subsystem (TCS) and a Gas Bearing Supply Subsystem (GBS). A Preflight Purge Subsystem provides compartment conditioning prior to launch.

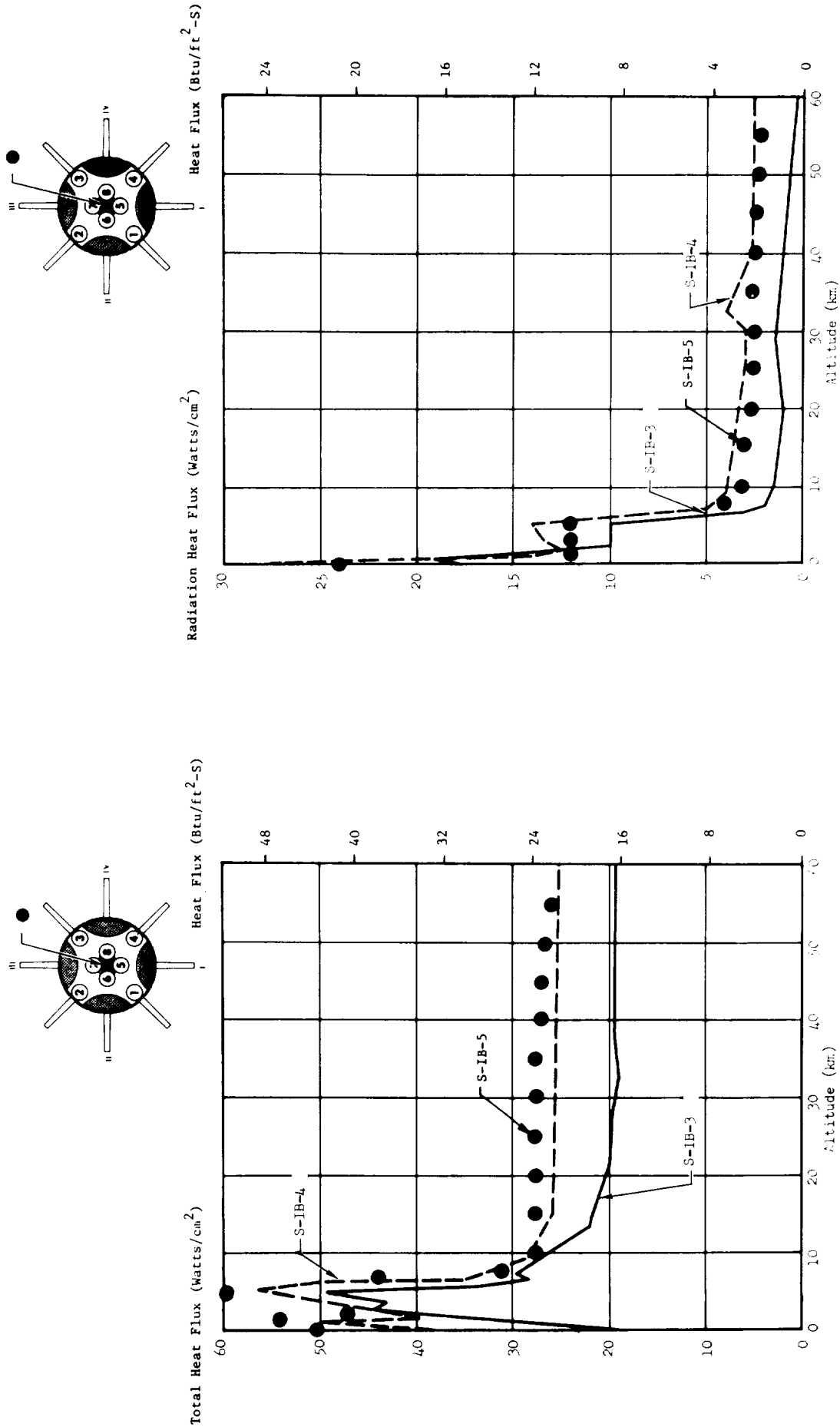


FIGURE 18-5 FLAME SHIELD TOTAL AND RADIATION HEATING RATES

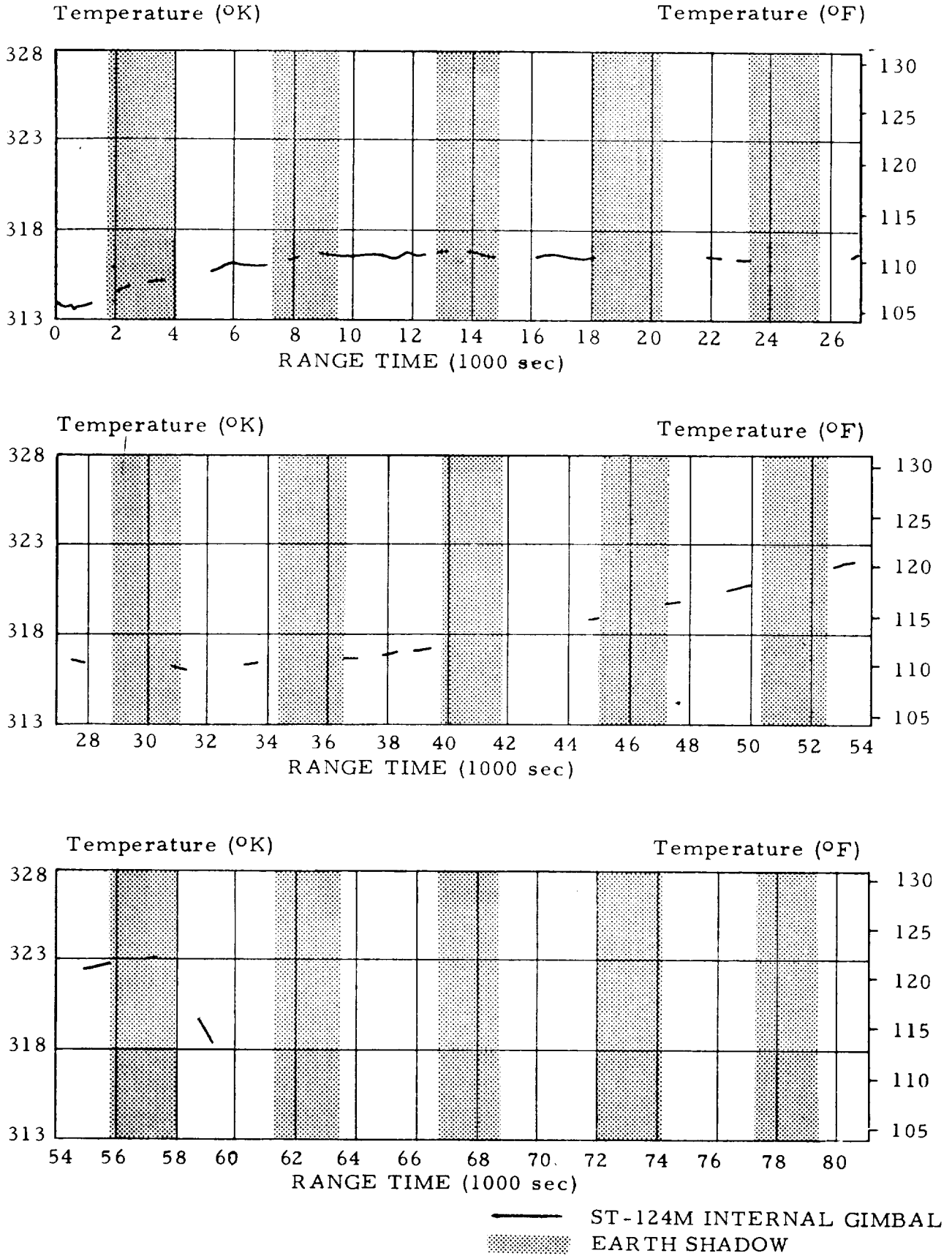


FIGURE 18-6. ST-124M-3 INERTIAL GIMBAL TEMPERATURE

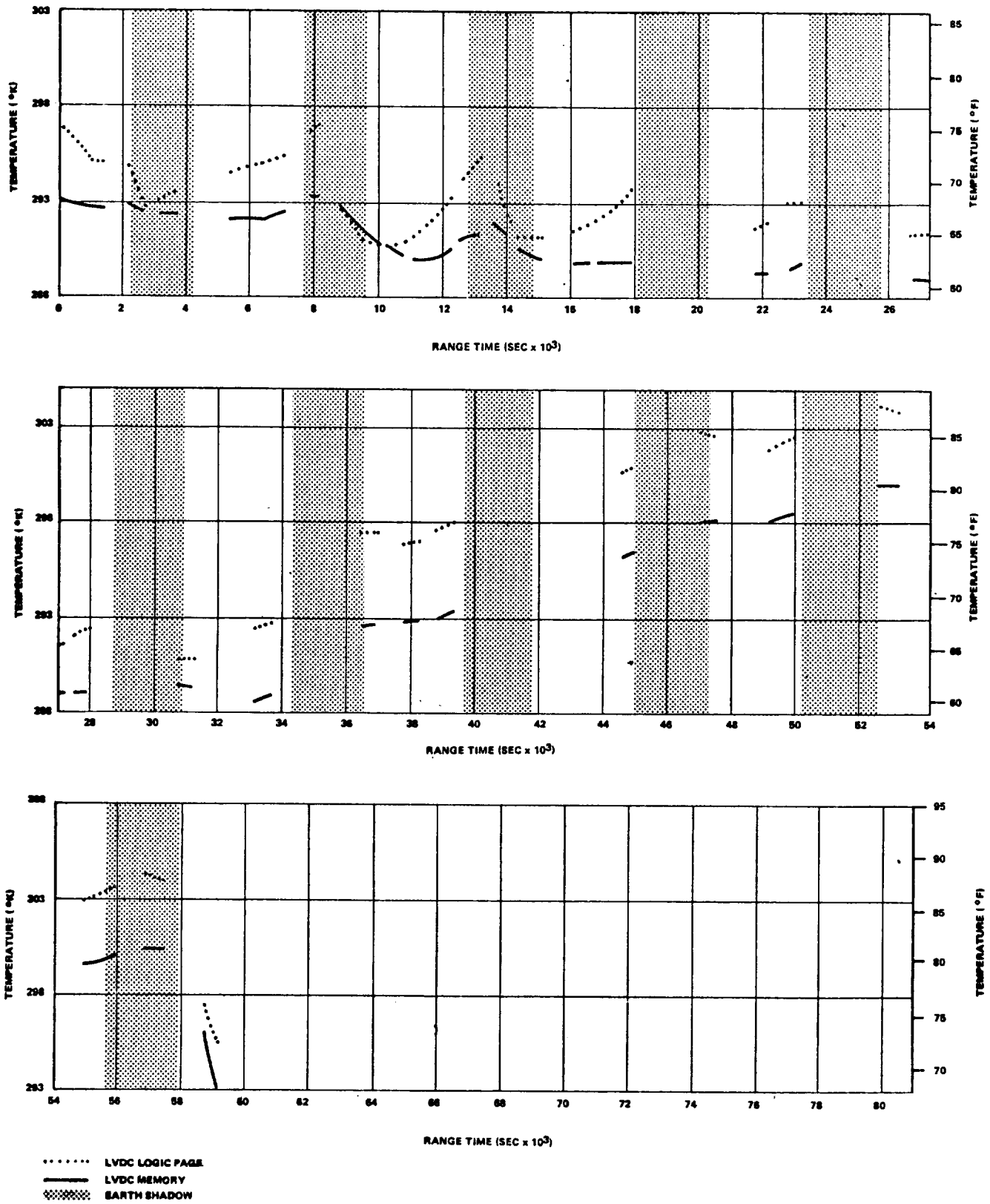


Figure 18-7 LVDC Temperatures

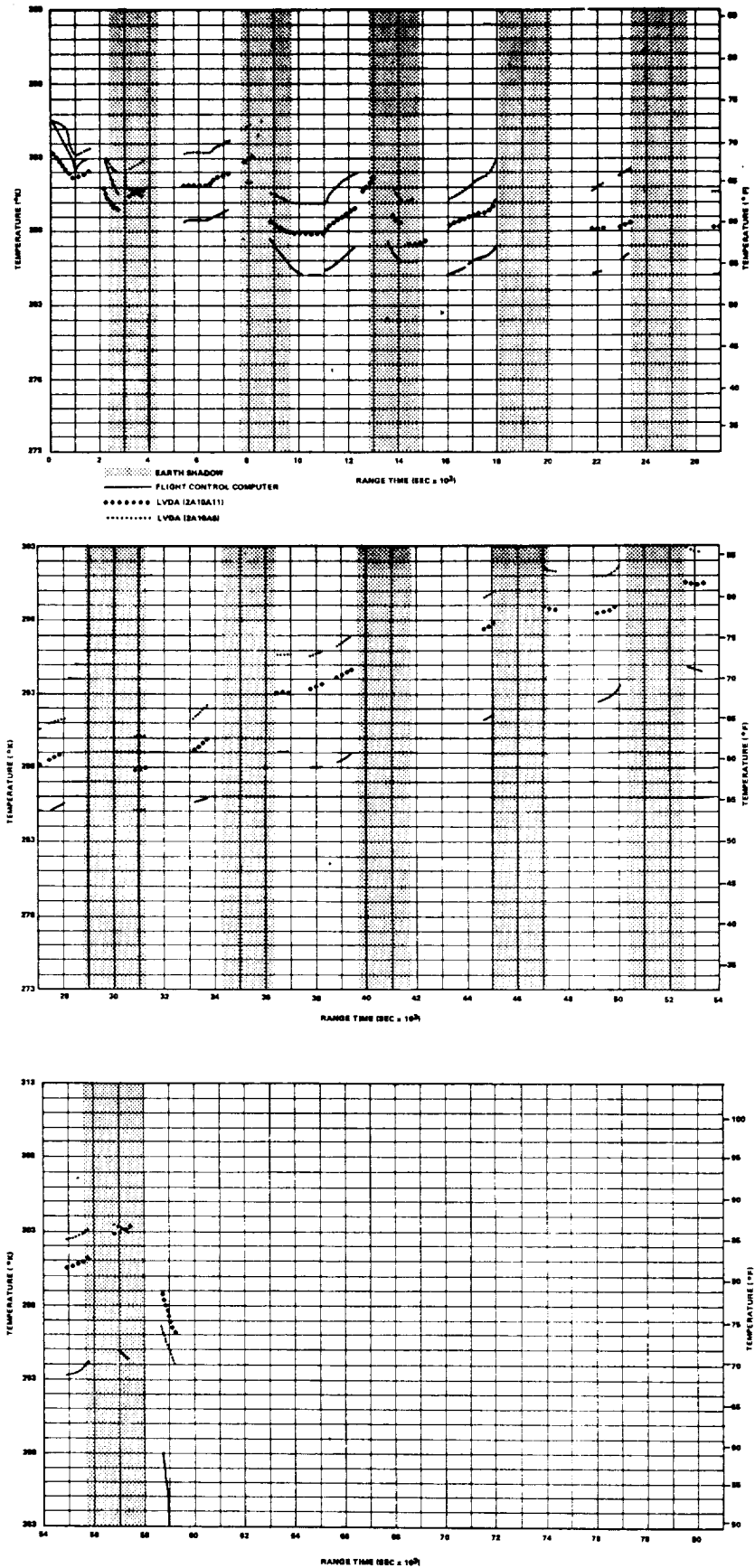


FIGURE 18-8. COMPONENT TEMPERATURES

18.4.1 THERMAL CONDITIONING SUBSYSTEM

The Thermal Conditioning System maintains an acceptable methanol-water coolant temperature of 288°K ($59 + 1^{\circ}\text{F}$) for the IU and S-IVB electrical components during prelaunch and 280.2 to 293°K (45 to 68°F) during flight operations. The system circulates the coolant fluid (60 percent methanol - 40 percent water by weight) through the IU and S-IVB coldplates and through the IU components having integral coolant passages. Each coldplate is capable of dissipating 420 watts. The heat removed from the components with integral coolant passages depends on the heat transfer characteristics of the individual component and the coolant solution flow rates through the components. The flow rates are controlled by fixed orifices.

During prelaunch operations, methanol-water from a ground support cooling unit circulates to and from the preflight heat exchanger through the IU umbilical. The onboard coolant temperature is controlled by the Modulating Flow Control Valve (MFCV), which allows varying amounts of onboard coolant to flow through the preflight heat exchanger. The MFCV position is controlled by the electronic controller assembly/coolant temperature sensor assembly combination.

Inflight heat rejection is achieved in the sublimator, where water supplied under pressure from the water accumulation freezes upon exposure to the vacuum environment and then sublimates. This process removes heat from the on-board coolant.

A TCS pressurization system pressurizes the methanol-water accumulator and water accumulator. The associated pressure regulators maintain methanol-water and water accumulator pressures for coolant pump and sublimator operations, respectively.

Figure 18-9 shows the TCS coolant temperature, flow rate, and pressure, and the TCS manifold inlet pressure. All parameters were within the ranges expected prior to flight; cycling was noted in the methanol-water control temperature as expected until approximately 44,700 sec, when it exceeded the band, reaching a maximum of approximately 296°K (74°F) at about 56,800 seconds. The maximum temperature was extrapolated since it was outside the range of the transducer. No sublimator cooling occurred while the water valve remained closed between 33,388 and 58,000 seconds. Shortly after liftoff, the MFCV began driving as programmed toward full coolant flow into the sublimator, reaching the required full-flow position approximately 17 sec after liftoff. Figure 18-10 shows the sublimator performance during vehicle ascent. The water valve opened at 181 sec and, due to the 286.4°K (55.9°F) coolant control temperature, closed at the first 5-minute sampling before

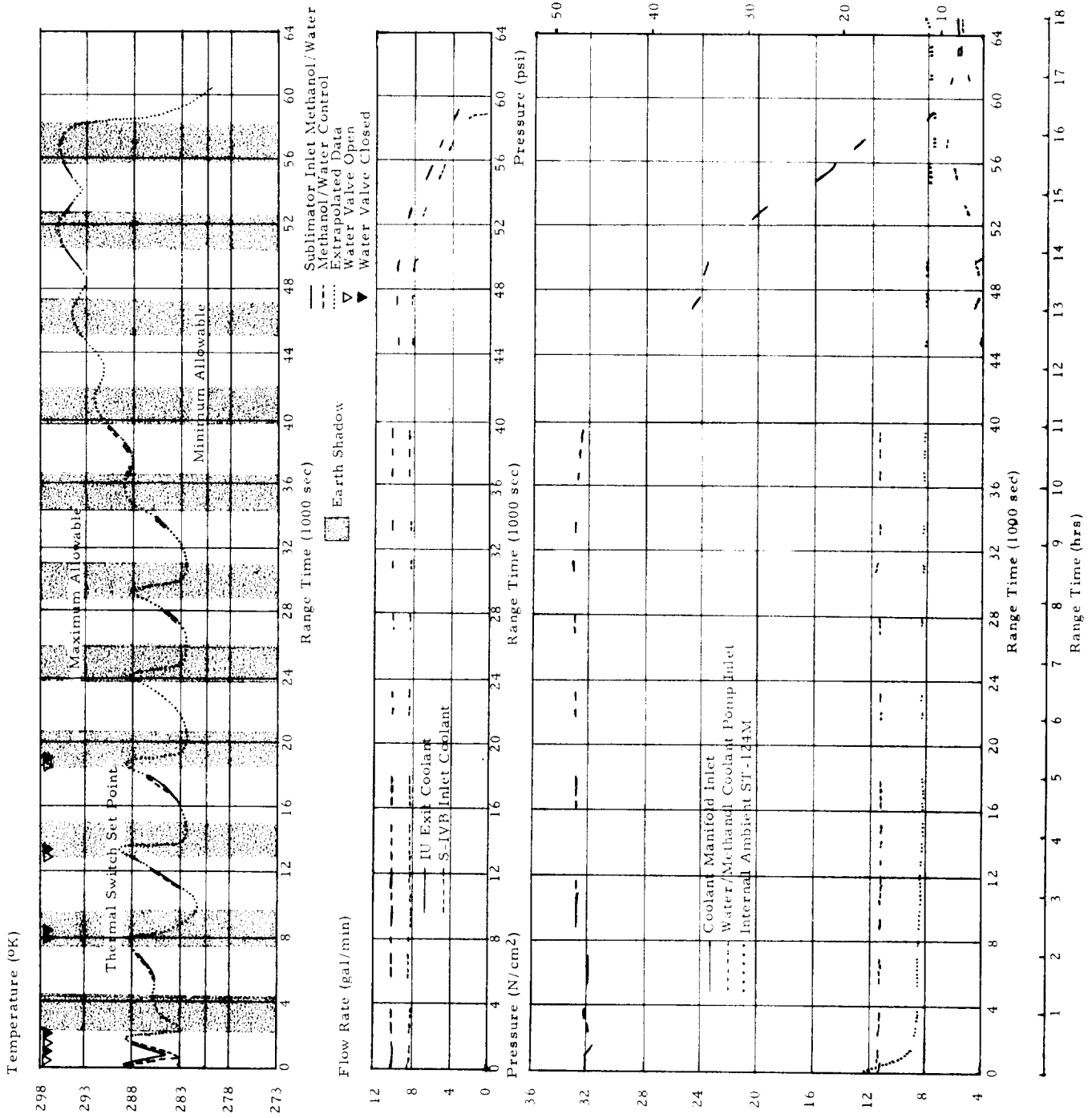


FIGURE 18-9 THERMAL CONDITIONING SYSTEM PERFORMANCE

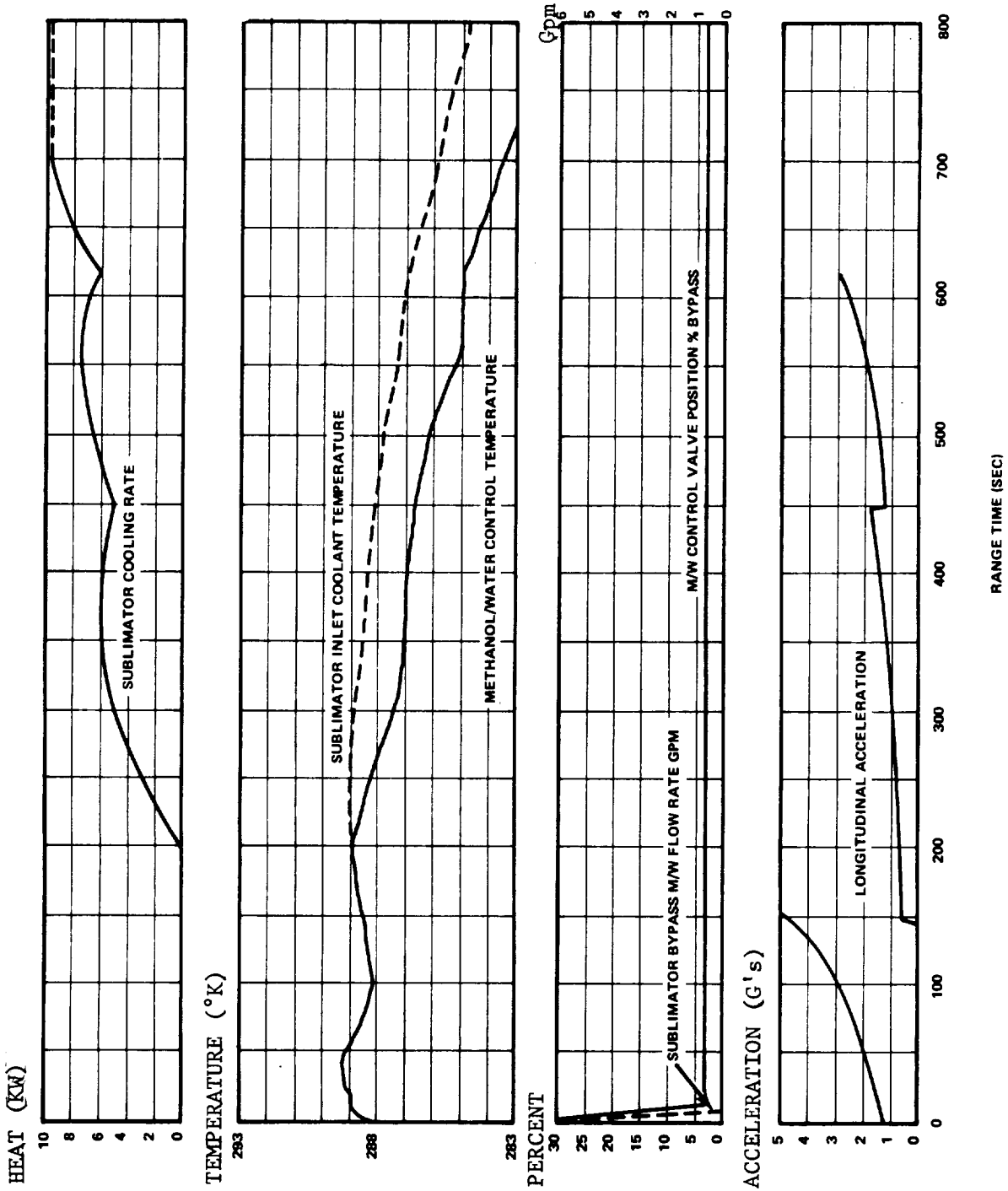


FIGURE 18-10 SUBLIMATOR PERFORMANCE DURING ASCENT

the sublimator was completely filled with water. The irregularly increasing sublimator cooling rate is currently under investigation but appears to be related to the vehicle longitudinal acceleration. This did not impair the sublimator's ability to adequately cool the methanol-water coolant.

A low-level erratic flow, with 0.034 N/cm (0.05 psi) pressure maximums, was observed by the sublimator inlet water flowmeter as the sublimator dried out after the third sublimator cycle. This indicates that a low pressure liquid-to-vapor phase change was occurring in the tube between the water solenoid valve and the water flowmeter. Activity of this nature is characteristic of the normal drying-out of the sublimator and its connecting tubing.

Normal functioning of the TCS is apparent throughout the designed lifetime of the IU and it continued until 33,383 sec, when sampling of the thermal switches was discontinued by computer instruction. The discontinuance of LVDC thermal switch sampling left the water valve in the closed position, terminating the sublimator cooling capability. The effect of this can be seen in the rising TCS M/W control temperatures. The cyclic nature of the rising coolant temperatures shows the effect of sun and shadow periods on the vehicle exterior.

By 59,000 sec, the 6D41 bus voltage decay curve (extrapolated) is near a 5-volt level. This condition should have allowed the water control valve to open. Specifications for this valve require 5 volts or more to keep it closed. The angular momentum due to the rolling motion of the spent S-IVB/IU stage would cause water to be forced into the sublimator, even though GN₂ pressure was gone. Measurements, still reliable at 59,000 sec and showing component and coolant temperature decay at a greater rate than observed during earth shadow conditions, also indicate sublimator cooling at this time.

Pressures and flowrates remained within the ranges recorded during preflight testing for the lifetime of the TCS pressurization system. The GN₂ pressure reached 207 N/cm² (300 psi), the lower limit for reliable regulator performance, at approximately 37,000 seconds. The pump inlet pressure indicated a total loss of GN₂ pressurization by 47,000 seconds. The IU and S-IVB coolant flowrates began decaying at approximately the same time as the total loss of pressurization. During decay of the 6D40 battery, positive coolant circulation was still apparent and was indicating a total system flowrate of 0.000315 m³/s (5 gpm). AS-205 was the last vehicle to use the two 819 cm³ (50 in³) spheres containing 1639 in³ (100 in³) of GN₂; subsequent vehicles will use the larger 2704 cm³ (165 in³) sphere for TCS pressurization.

18.4.2 GAS BEARING SUPPLY SUBSYSTEM

The Gas Bearing Supply System supplies GN₂ at a regulated pressure and temperature to the ST-124M-3 inertial platform assembly for preflight and flight operation. The system performed satisfactorily. Figure 18-11 shows that the ST-124M-3 gas bearing inlet pressure differential drifted above the 10.35 ± 0.345

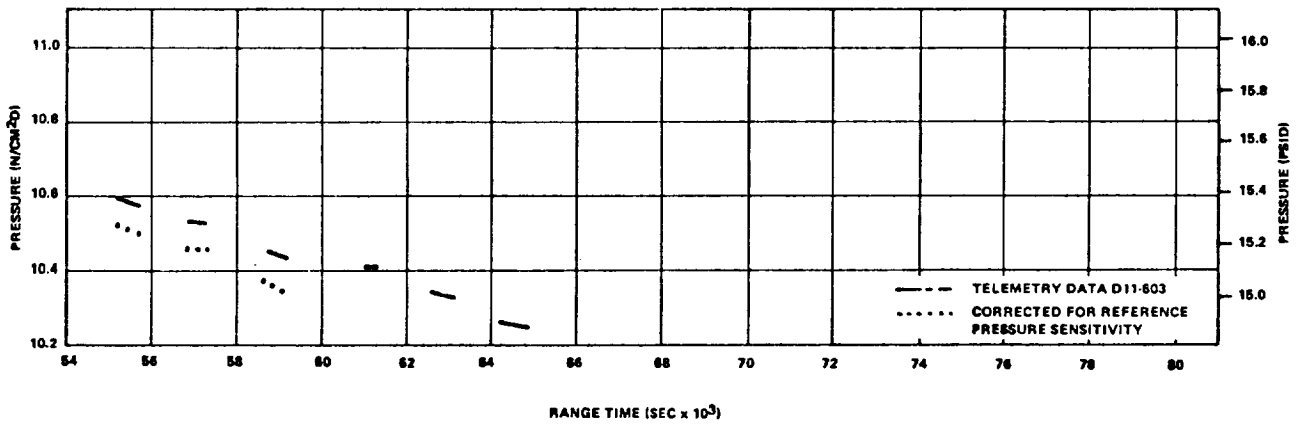
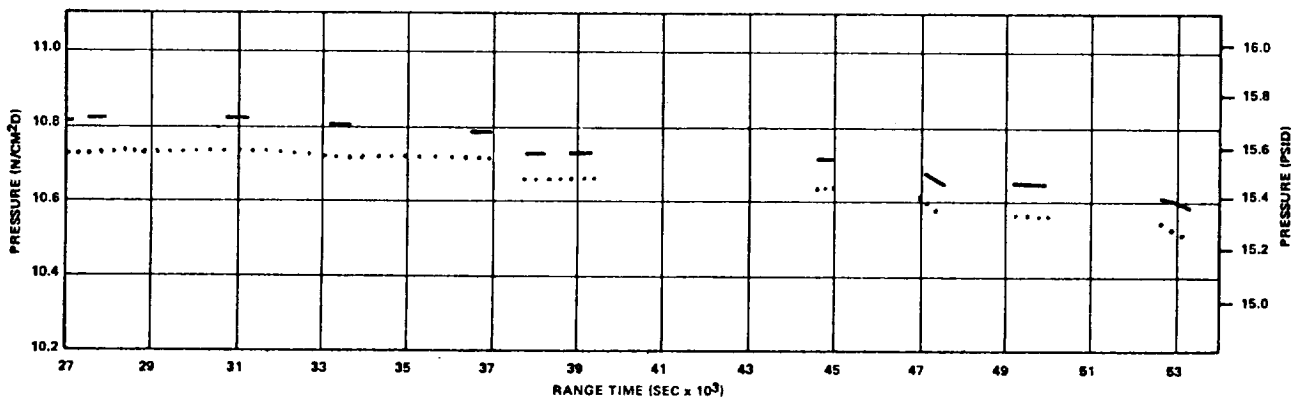
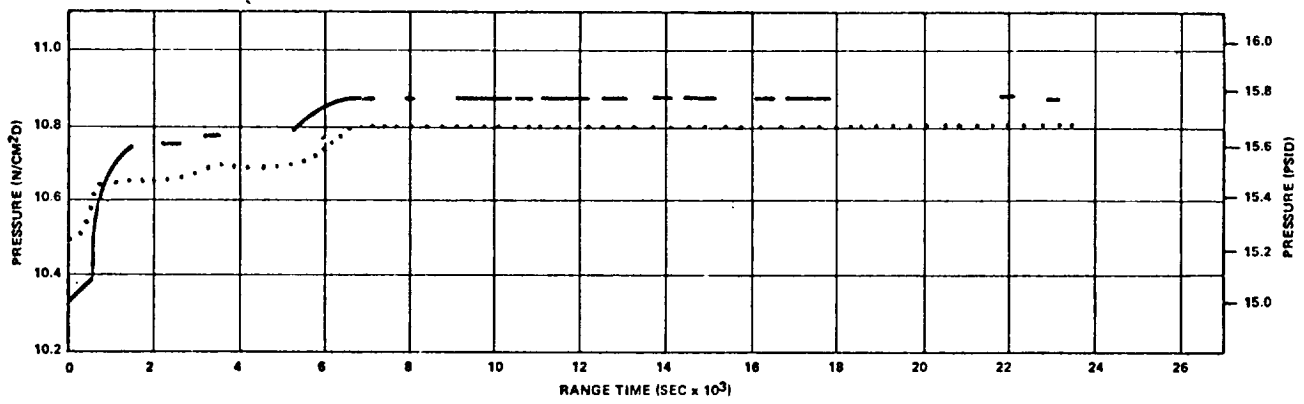


FIGURE 18-11. ST-124M-3 GAS BEARING GN₂ INLET PRESSURE DIFFERENTIAL

$\text{N/cm}^2\text{D}$ (15.0 ± 0.5 psid) specified range. This was primarily due to the reference-pressure-sensitive pressure transducers which allowed the regulator to drift to $10.58 \text{ N/cm}^2\text{D}$ (15.35 psid) instead of the desired $10.35 \text{ N/cm}^2\text{D}$ (15.0 psid) setting at liftoff. The corrected data is between 10.58 and $10.82 \text{ N/cm}^2\text{D}$ (15.35 and 15.79 psid): a 0.24 N/cm^2 (0.35 psi) band. This specification deviation was anticipated prior to flight and assessed as not being detrimental to the platform performance for AS-205 flight. The transducer is being replaced on future vehicles with a transducer which is not reference-pressure-sensitive. The regulator setting procedure is also being modified to ensure proper inflight performance. The GBS GN_2 usage was slightly less than that nominally expected. Approximations indicate a 0.0099 SCMM (0.35 SCFM) usage rate, compared to a 0.008 to 0.014 SCMM (0.3 to 0.5 SCFM) allowable range. Reliable pressure levels, 207 N/cm^2 (300 psi), exceeded dependable measurement lifetime ($59,000$ sec).

19.0 AERODYNAMICS

19.1 SUMMARY

The pressure measurements on this flight indicated a normal aerodynamic environment throughout first stage flight. There were only three aerodynamic pressure measurements used on this vehicle and the data from these compared very well with the AS-204 flight.

The base drag for this flight could not be accurately determined due to insufficient instrumentation in the base region.

The angle-of-attack for this flight was too low to allow an accurate analysis of normal force or center of pressure for this vehicle.

20.0 INSTRUMENTATION

20.1 SUMMARY

Performance of the vehicle instrumentation was satisfactory throughout flight. Of 691 active inflight measurements, only 4 failed -- a reliability of 99.42 percent.

The airborne telemetry systems, including calibrations, performed satisfactorily. All stations except GBI experienced attenuations during maximum flame plume and during separation sequence.

Performance of the RF systems was satisfactory throughout the entire flight of the vehicle, as was coverage of the onboard RF systems by ground tracking and instrumentation stations.

Camera coverage was excellent. Of the 94 engineering sequential cameras, only 4 malfunctioned -- a reliability of 95.74 percent.

20.2 VEHICLE MEASURING ANALYSIS

A total of 717 measurements was programmed for the AS-205 flight. At launch, there were 691 active flight measurements. The S-IB stage had a total of 255 programmed measurements, and all were active at launch. Of these 255 active measurements, 1 was partially successful and 1 failed. A total of 268 measurements was programmed for the S-IVB stage; at launch, 243 were active, of which 3 were partially successful and 3 failed. The IU had a total of 194 measurements. Of these, 1 was waived prior to launch and 3 were partially successful. There were no IU measurement failures. Analysis discloses an overall measuring system reliability of 99.42 percent. Data loss due to the 4 failures had no significant effect on the postflight evaluation. Table 20-I presents a summary of the measurement malfunctions per stage.

20.2.1 S-IB STAGE MEASURING ANALYSIS

The performance of the measurement system onboard the S-IB stage was satisfactory. Analysis of the measurement system indicated that, of 255 flight measurements scheduled for the stage, only 1 failed and 1 was partially successful. The analysis discloses a 99.61 percent measuring reliability.

TABLE 20-1 MEASUREMENT MALFUNCTIONS

STAGE	MEAS. NO.	MEASUREMENT TITLE	REMARKS
WAIVERS PRIOR TO LAUNCH			
IU	D17-601	Press - Coolant Manifold Inlet	Intermittent dropout of the meas. during countdown. Although erratic during countdown, satisfactory data was obtained for the duration of the flight. Due to problems on previous flights, a change (ECP1738-1-2) has been recommended for future vehicles to insert a snubber in the coolant line to protect the sensor.
FAILURES			
S-IB	C600-7	Temp - Flame Shield	Low readings and data dropouts from 35 to 40 sec and from 125 to 140 seconds.
S-IVB	C2044-401	Temp - ASI Combustion Chamber	Indicated a failure 149.1 sec, two sec after engine start command. The sensor circuit opened, causing the channel to exhibit an off-scale-high condition, probably caused by high vibration experienced in the ASI vicinity.
	D0104-403	Press - LH Press Module Inlet	Failed to exhibit valid data subsequently to 350 seconds. The unusual pressure decrease after 350 sec and the off-scale-low indication at cutoff are unexplainable at present. Trend-type info was recovered during the invalid period. During orbit, performance was as expected.
	E0210-4	Vib - LH Turbo Pump - Lat	Failed to indicate valid data from liftoff (off-scale-high to off-scale-low). No usable data was obtained.
PARTIALLY SUCCESSFUL			
S-IB	L500-03	Discrete LOX Level	First discrete probe gave no indication; however, the other probes functioned properly.
S-IVB	C2043-401	Temp - Skin LH ₂ ASI Line	Exhibited invalid data from 415 to 1000 sec and from 1200 to 1300 sec and then performed as expected for duration of the flight.
	E0243-401	Vib - ASI LOX Valve, Rad.	Unusual low frequency (12Hz) oscillations were observed during sampling periods between 152 to 310 sec and data was lost during this time.
	C0001-401	Temp - LH ₂ Turbine Inlet	Failed at 1170 sec by indicating an abrupt off-scale low response. Observations did not indicate recovery from malfunction. Meas. operated satisfactorily during boost and S-IVB burn, which fulfilled its intended purpose.
IU	H44-603 H45-603 H46-603	Output Z Gyro Servo Output X Gyro Servo Output Y Gyro Servo	Data from all three measurements indicate they were very noisy during the entire flight. Investigation revealed the noise was due to reassignment of the measurements from the FM/FM (which had a low pass filter) to the PCM/FM which had no filter.

20.2.2 S-IVB STAGE MEASURING ANALYSIS

The measurement system performance onboard the S-IVB stage was nominal. Of the 268 programmed measurements, 8 add-on vibration measurements were telemetered by the IU and are not CPIF measurements, 12 were used for checkout only, 3 were landline, and 2 were not connected because of stage configuration. The total number of measurements to be evaluated from automatic countdown sequence through the end of mission was 243. Of these 243 measurements, 2 were partially successful, and 2 failed during Phase I (liftoff to S-IVB cutoff plus 10 sec). During Phase II (liftoff to spacecraft separation), 1 measurement was partially successful and the same 2 measurements failed as in Phase I. Both Phase I and Phase II measurement reliabilities were 99.17 percent. One of the 8 measurements telemetered by the IU failed but is excluded from the above assessment.

20.2.3 IU MEASURING ANALYSIS

The IU measuring system inflight performance was nominal. There were 194 flight measurements on the IU. One measurement was waived prior to launch but provided usable data during the flight, and 3 partially successful. Data from these 3 measurements (H44-603, H45-603, and H46-603) indicate that they were very noisy during the entire flight. The investigation revealed that the apparent noise was not extraneous, but was due to telemetering the measured parameters on the PCM/FM system. The PCM/FM system does not contain a low pass filter as does the FM/FM system (on which they were previously assigned) to suppress the high frequency (1 K H_z) data contained in these measurements. An ECP will be written to return these measurements to the FM system. The IU measurement system reliability was 98.45 percent.

20.3 AIRBORNE TELEMETRY SYSTEMS

The AS-205 launch vehicle, because of its operational status, used only 5 airborne telemetry links to transmit the measurements data to ground stations. Table 20-II lists the launch vehicle telemetry links and functions by stage.

Performance of the airborne telemetry system was generally satisfactory. Telemetry calibration data from the IU DP-1 link indicated noise variations larger than normally expected. The cause of the variations is under investigation and has not been fully explained. This problem had no serious impact on the vehicle evaluation.

TABLE 20-II LAUNCH VEHICLE TELEMETRY SYSTEM DESCRIPTION

Link	Frequency (MHz)	Modulation	Stage
GF-1	240.2	FM/FM	S-IB
GP-1	256.2	PCM/FM	S-IB
CF-1	258.5	PCM/FM	S-IVB
DF-1	250.7	FM/FM/FM	IU
DP-1	255.1	PCM/FM	IU

20.3.1 S-IB STAGE

Performance of the two airborne telemetry links GF-1 and GP-1 was satisfactory, and all calibrations and synchronizations functioned as programmed.

20.3.2 S-IVB STAGE

The performance of the Pulse Code Modulation (PCM) System was excellent. All multiplexers were properly synchronized and their outputs properly interlaced, as attested by the reduced data.

The RF System performed without any difficulty in the transmission of airborne data to ground stations located throughout the orbital flight path during the Phase I and Phase II evaluation period. Approximately 0.75 sec of data blackout was observed at 146.7 sec on the data from Bermuda. As a result, the exact S-IVB engine start time was not retrievable.

Subsequent data evaluated after Phase II, at 64,000 sec from Canary Island, indicate the loss of RF transmitter power on the S-IVB CP1 data link. A check of Forward Battery 1 voltage indicated 29 vdc and a load current of 6 amps. Nominal loading of Forward Battery 1, without the battery heaters and with the transmitter operational, was 9.5 amps. This problem is still under investigation.

20.3.3 INSTRUMENT UNIT

The IU onboard telemetry systems consisted of two telemetry links (DF1 and DP1) and their associated components. All data reviewed indicated satisfactory performance of both telemetry systems. Dropouts as viewed in the data appeared to be caused by low signal strength at the ground stations.

20.4 RF SYSTEMS ANALYSIS

The Launch Vehicle RF Systems performance was satisfactory throughout the flight of the vehicle, as was coverage of the onboard RF systems by ground tracking and instrumentation stations.

The S-IB, S-IVB, and Instrument Unit telemetry signals were attenuated by approximately 30 db during maximum flame plume. The stations affected by this signal attenuation were Cape Telemetry 4 and Central Instrumentation Facility (CIF) telemetry. The Grand Bahama Island (GBI) telemetry station was not affected by main engine flame plume. As expected, all stations experienced a reduction in signal during the separation sequence, with Cape Tel 4 experiencing a momentary signal dropout. The RF system coverage is presented in Figure 20-1.

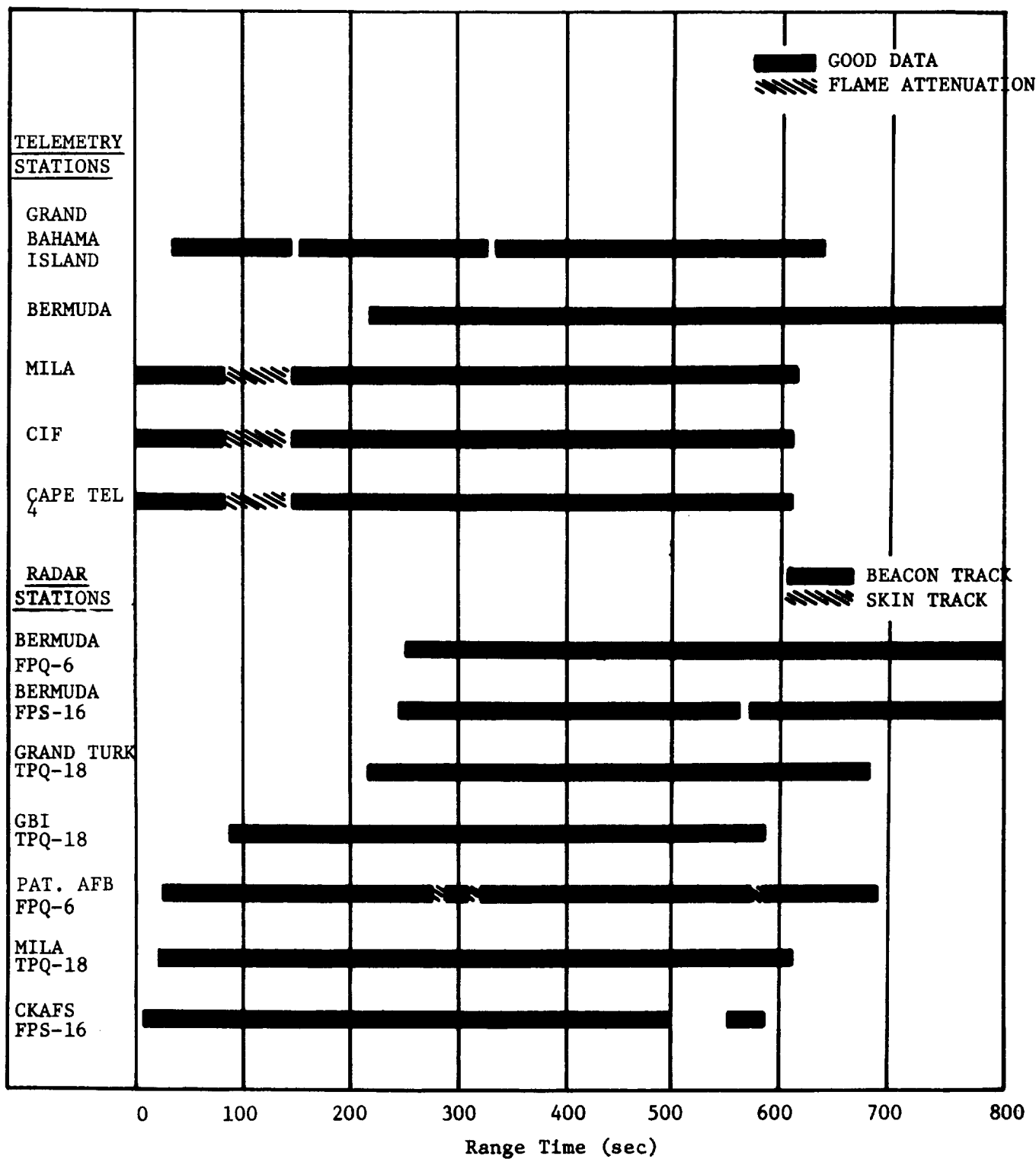


FIGURE 20-1 AS-205 RF SYSTEM COVERAGE

The onboard ODOP tracking system operated satisfactorily; flight measurements indicated proper functioning of the secure command system.

20.4.1 TELEMETRY

The telemetry signal levels from the S-IB stage were at maximum level for the first 85 sec of flight at the Central Instrumentation Facility (CIF) and Tel 4 stations, with a reduction of 12 db at 22 sec due to multipath effects. Cape area stations experienced a maximum flame attenuation of about 30 db at 107 seconds. The Grand Bahama Island (GBI) station began receiving S-IB data at 55 sec and tracked through 390 seconds.

The Cape area telemetry stations experienced similar flame attenuation of the S-IVB signals as on the S-IB stage. CIF and Tel 4 coverage was from lift-off through 615 seconds. The GBI station began S-IVB data reception at 55 sec and received data through approximately 635 seconds. The Bermuda station began receiving S-IVB telemetry at approximately 235 sec and received data through 830 seconds. At 550 sec the CP-1 link showed a marked increase in noise perturbation, which continued until J-2 engine cutoff. This noise was indicated by the same recording system as starting some 15 sec later and continuing until engine cutoff for the DF-1 and DP-1 links. The event of engine cutoff is accentuated by a sharp noise spike followed by a damping of the noise on all three links over the next second.

The Cape area telemetry stations experienced a similar flame attenuation of the IU signals as on the S-IB and S-IVB stages. Cape area telemetry coverage was from liftoff through 615 sec with some minor data drops during the first 30 sec of flight and a dropout at separation sequence lasting approximately 3 seconds. The system performed satisfactorily in orbit. Figure 20-2 presents the orbital telemetry system coverage.

20.4.2 TRACKING

During launch and powered flight, the C-Band radar systems operated satisfactorily. The FPS-16 at Bermuda tracking station lost lock at 576 sec due to an operator error while reading the point of closest approach (PCA) of the vehicle. Bermuda FPQ-6 had no tracking problems. Cape Radar 1.16 had transmitter problems at 500 sec and was off track for 58 seconds. The radar transponder was still operating at the time of splashdown. Splashdown occurred at 162 hr: 27 min during the tracking of the 103rd revolution by Tananarive. Figure 20-3 presents the initial orbital radar coverage by the C-Band System.

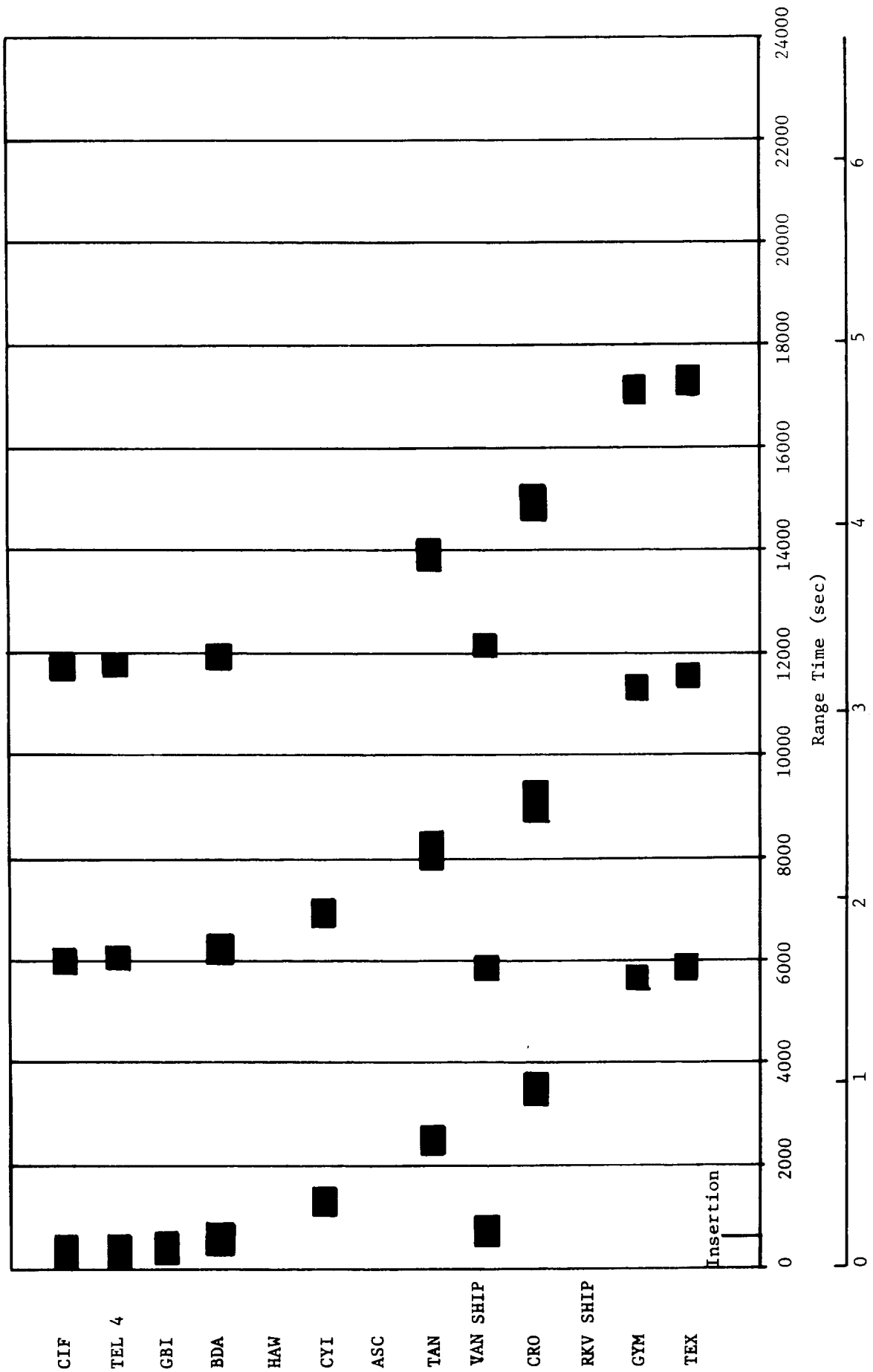


FIGURE 20-2 ORBITAL TELEMETRY COVERAGE

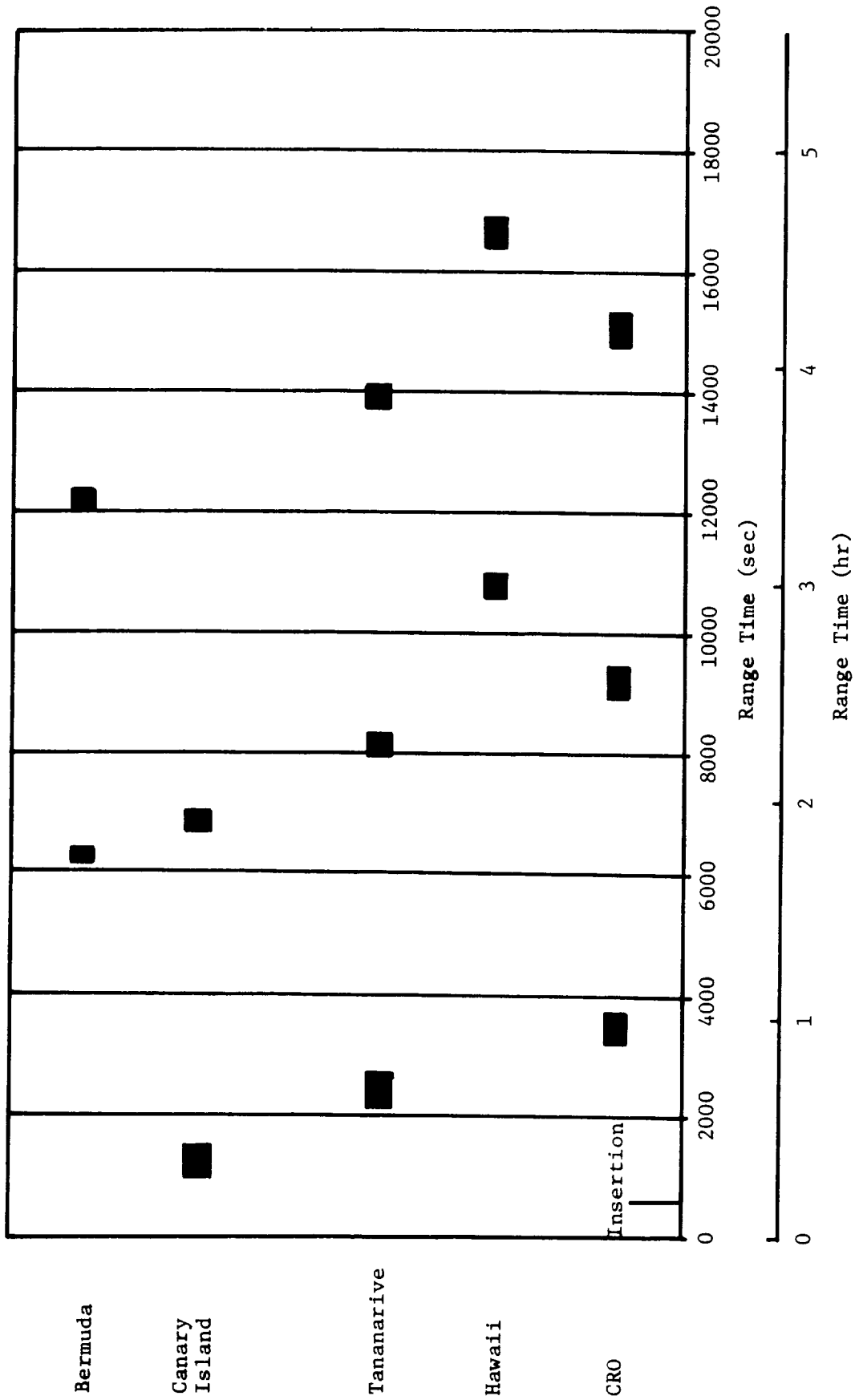


FIGURE 20-3 ORBITAL RADAR COVERAGE

The AGC and lock indicator data indicate that the ODOP system operated satisfactorily throughout the flight. The data revealed that the transponder received a signal well within tolerance and that the transmitter was locked to the received frequency throughout the flight.

20.5 OPTICAL INSTRUMENTATION

The engineering photographic coverage of the launch was excellent. Photographic coverage was provided by 94 sequential cameras, in three major categories: 79 fixed cameras provided coverage during prelaunch operations and liftoff through three vehicle lengths of flight; 14 ground based tracking cameras tracked the vehicle from first acquisition to loss of view or film depletion; and there was 1 airborne tracking camera (ALOTS).

Of the 94 cameras programmed, 28 surveillance/malfunction films did not require processing, 1 ground based tracking camera did not operate, 3 films produced no timing, and the field of view of 2 GSE cameras was obscured by frost and ice at the time of release. With 4 failures in 94 film items, the reliability was 95.74 percent.

21.0 SPACECRAFT

The Apollo 7 space vehicle was launched from Cape Kennedy, Florida, at 1102:45 EDT on October 11, 1968. Following a nominal boost phase, the spacecraft and S-IVB combination was inserted into an orbit of 120.0 by 152.3 nautical miles. Prior to separation of the command and service modules from the S-IVB, the crew manually controlled the spacecraft/S-IVB combination. After separation, a transition and simulated docking exercise was completed. Phasing maneuvers were later executed in preparation for a successful rendezvous with the S-IVB. During the 10.8-day flight, eight planned maneuvers using the service propulsion system were completed, and all major test objectives were satisfied.

Almost without exception, spacecraft systems operated as intended. All temperatures varied within acceptable limits and essentially exhibited predicted behavior. Consumable usage was always maintained at safe levels and permitted introduction of additional flight activities toward the end of the mission. Communications quality was generally good, and live television was transmitted to ground stations on seven occasions. A test of the rendezvous radar system was completed in support of later flights with the lunar module. Manual operation of the spacecraft by the crew was good. Even though they were somewhat hampered by head colds and congestion, the crew satisfactorily performed all flight-plan functions, and the photographic experiments were completed.

A normal deorbit, entry, and landing sequence was completed, with all parachutes operating properly. At approximately 260 hr 09 min 08 sec after launch, the vehicle landed in the Atlantic Ocean southeast of Bermuda, with coordinates of 27° 33' north latitude and 64° 04' west longitude. The crew was retrieved by helicopter, and both the spacecraft and crew were taken aboard the prime recovery ship, USS Essex.

APPENDIX A

CONFIGURATION DIFFERENCES

A.1 SUMMARY

The flight of AS-205 was the fifth in a series of Saturn IB vehicles, the third to carry a command module, and the first to have a manned command module. AS-205 measured approximately 68m (223 ft) in overall length [13m (42 ft) longer than AS-204] and consisted of four major units: S-IB Stage, S-IVB Stage, Instrument Unit and Payload (Figure A-1). All of these major units are essentially the same as on AS-204 (aside from the modifications listed in the following paragraphs) except for the Payload. The Lunar Module and Nose Cone, flown as the AS-204 Payload, were replaced by the Command Service Module (Apollo 7/CSM-101) and the Launch Escape System on AS-205.

A.2 S-IB-5 CONFIGURATION DIFFERENCES

The significant configuration differences between S-IB-5 and S-IB-4 existed in the structural, H-1 engine, flight control, instrumentation, and electrical systems. Listed below are the significant modifications to the S-IB-4 configuration that were incorporated on S-IB-5.

1. Structural System

70-inch LOX Tanks - A load redistribution structure was installed in the 70-inch LOX tank upper skirts as a result of S-IB-3 qualification testing.

2. H-1 Engine System

LOX Drain Line - A new LOX seal cavity drain line was added which provided an in-line fitting to accommodate a 3-element temperature probe.

3. Flight Control System

Hydraulic System - A second source auxiliary pump (Kellogg) was added to pressurize the hydraulic system for preflight test and readiness. This pump is for ground service and is inactive during flight.

4. Instrumentation System

Continuous Liquid Level Probes - These probes and their corresponding adapters were deleted on S-IB-5 and subsequent stages.

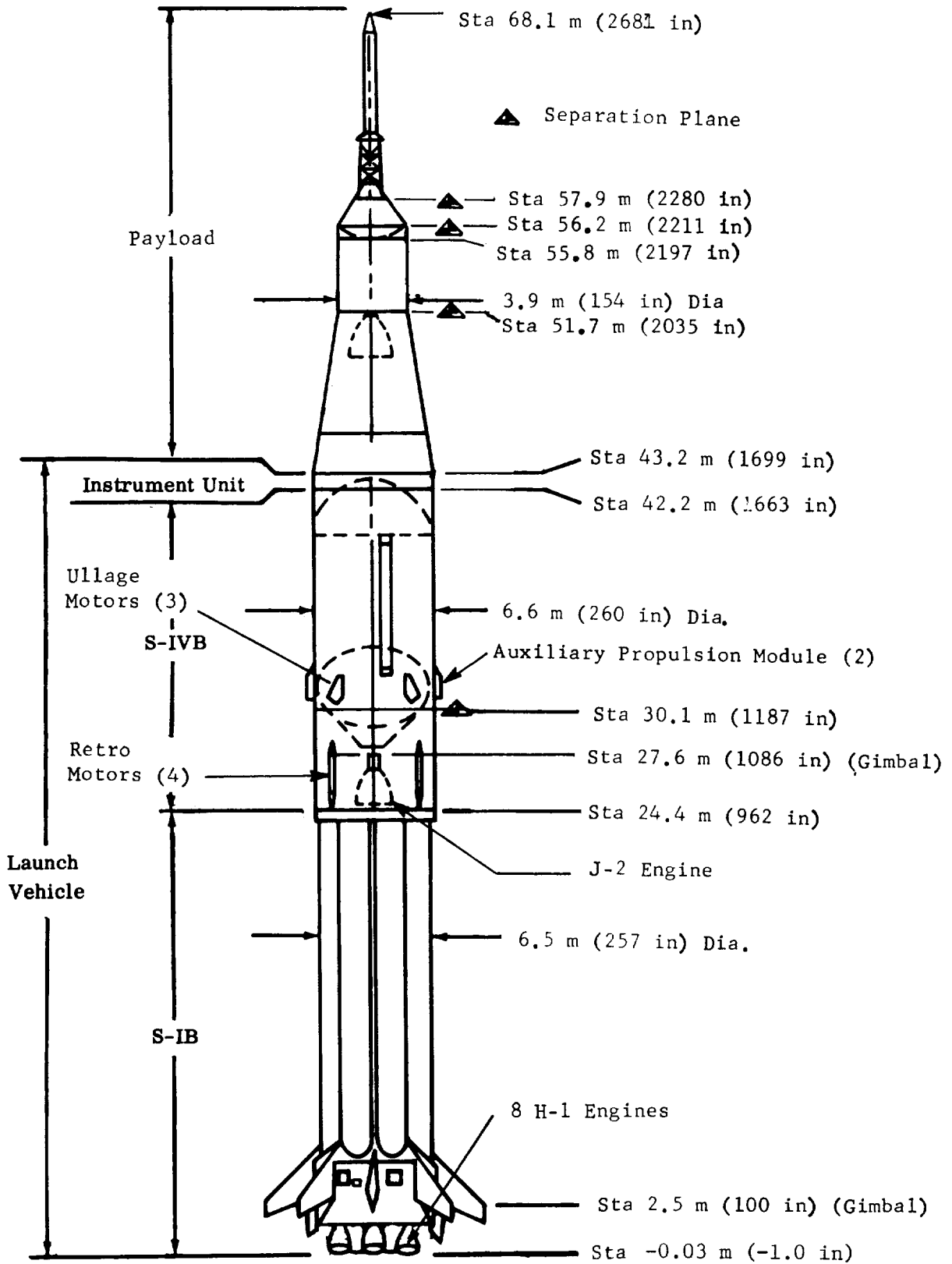


FIGURE A-1 AS-205 CONFIGURATION

LOX Seal Drain Line - The LOX seal drain line temperature interlock system was added to S-IB-5 and subsequent stages as a result of an explosion experienced during a static test of S-IB-11.

Telemetry System - The single sideband/frequency modulation (SS/FM) subsystem and the tape recorder were deleted from S-IB-5. The two-pulse amplitude modulation/frequency modulation (PAM/FM) subsystems were replaced by a single FM subsystem which provided up to 17 Inter-Range Instrumentation Group (IRIG) channels of continuous analog data. The PAM wave train was also deleted.

5. Electrical System

Propulsion Distributors - The initial installation of the propulsion system distributors was modified to a shock-mounted installation. This change was necessary for compliance with the 100 micro-second relay contact chatter limit.

A.3 S-IVB-205 CONFIGURATION DIFFERENCES

The significant configuration differences between S-IVB-205 and S-IVB-204 existed in the structural, J-2 engine, propellant, tank: vent/pressurization, flight control, environmental control, and instrumentation systems. Listed below are the significant modifications to the S-IVB-204 configuration that were incorporated on S-IVB-205.

1. Structural System

Drag-in-Cable Door - The door was added at the S-IVB forward skirt to preclude routing ground cabling through the IU.

Forward Skirt Vent - The vent area was changed from 968 to 1290 cm² (150 to 200 in²).

Insulation - A thermal insulation coating was added to the ullage rocket fairing wake, chilldown return line fairing wake, APS wakes, and retrorocket wakes (all on the S-IB/S-IVB interstage) due to an 8 percent increased thermal load requirement in the AS-205 mission. The external ablative coating insulation patterns on S-IVB-205 covered less area than on S-IVB-204. However, the reduced area was compatible with the maximum AS-205 aerodynamic heating trajectory.

2. J-2 Engine System

ASI Feed System - The propellant feed system for the Augmented Spark Ignition (ASI) was modified to prevent recurrence of engine anomalies experienced on

S-IVB-502. The propellant lines were strengthened by replacing flex lines with rigid lines, single welds with double welds, and by reducing the number of welds. The orifice in the start tank liquid refill line was relocated downstream of the check valve.

ASI and Gas Generator Spark Cables - Shielding was added to reduce generation of radio frequency interference.

Start Tank - The refill orifice was replaced with a blank orifice to preclude recharging during engine operation. A redundant emergency dump valve was added to improve operational safety. The valve has ground-only capability to dump the bottle in case of an aborted launch.

Thrust Chamber - The thrust chamber tube inlets were flared to reduce the pressure drops, thereby increasing the fuel pump stall margin. The purge line size was increased from 0.3175 cm (0.125 in) to 1.27 cm (0.50 in).

Gas Generator Choke Ring - A canted choke ring was incorporated to reduce hot spots.

LH₂ Turbine Exhaust Duct - A coating of Dyna-therm was added to the duct. This permitted evaluation of duct temperature as a function of orbital time.

3. Propellant System

Orbital Safing Kit - The kit permitted automatic passivation of the ambient helium sphere, the cold helium spheres, the LOX tank, and the LH₂ tank. Passivation provided a safe stage condition for spacecraft rendezvous. (Specific modifications are presented in various portions of Appendix A.)

PU System - The propellant utilization (PU) system was changed from closed-loop to open-loop. Capability of preprogramming the system to 5.5:1, 5.0:1, and 4.5:1 mixture ratios was incorporated.

Engine-Pump Purge-Control Module - The module was redesigned to conform to low temperature leakage requirements.

LOX Chillover-Pump Purge Module - This module was removed and replaced by pump-motor-container inlet and outlet orifices, with a check valve at the end of the outlet line. A hand valve was provided to isolate the purge system during pneumatic system checkout.

LOX Pump - Provided capability of venting the leakage overboard from the pump primary-seal during prelaunch and vehicle-boost phase of flight.

LOX and LH₂ Tank Prevalves - Reworking of the prevalves improved response time by enlarging the actuator orifice and prevented cryopumping through the shaft-seal-leak check port.

4. Tank: Vent/Pressurization System

LOX NPV System - The LOX nonpropulsive vent (NPV) subsystem was added to avoid uncertainties of center-of-gravity location and to cancel vent thrust with opposed nozzles. A pneumatically controlled latch-open valve provides for LOX tank nonpropulsive venting, permitting LOX tank safing after stage orbital insertion.

LOX Tank Vent and Relief Valve - The new valve incorporated open poppet piston seat, and gold-plated pilot-bellows.

LH₂ Tank Pressure Switch - The tank pressure switch was changed in order to lower the operating range to 19.3 to 21.4 N/cm² (28 to 31 psi) as a result of the fracture mechanics study. Operating range on AS-204 was 21.4 to 23.4 N/cm² (31 to 34 psi).

LH₂ Tank Vent-and-Relief Valve - The new valve incorporated a re-designed open actuator seal, close piston seal, Creavy-type body seal, and a new crack and reseal pressure range of 21.4 to 23.4 N/cm² (31 to 34 psi). Operating range of the backup relief valve was lowered to 24.1 to 26.2 N/cm² (35 to 38 psi). Both operating range changes are the result of the fracture mechanics study.

LH₂ Tank Safing Subsystem - A LH₂ tank passivation valve with activation control module was added to the LH₂ vent system. The passivation valve latches open to permit tank safing by venting continuously and nonpropulsive after stage orbital insertion.

5. Flight Control System

APS Filters - Two in-line recirculation filters were added, one each to the APS oxidizer system and the APS fuel system.

6. Environmental Control System

Cold Plates - The number of cold plates were reduced from 16 to 5 as a result of changing to the operational telemetry system.

7. Instrumentation System

Data Acquisition Subsystem - The subsystem was reduced to one PCM/FM

system. The subsystem was modified to multiplex and transmit the required high frequency measurements through the IU FM/FM data system (DF1). The following telemetry subsystems were removed: PAM/FM/FM, FM/FM, SS/FM, and the airborne tape recorder. The remote analog submultiplexer and remote digital submultiplexer were added to the PCM/FM system.

A.4 S-IU-205 CONFIGURATION DIFFERENCES

The significant configuration differences between S-IU-205 and S-IU-204 existed in the structural, guidance, flight control, instrumentation, electrical, and thermal conditioning systems. Listed below are the significant modifications to the S-IU-204 configuration that were incorporated on S-IU-205.

1. Structural System

Segment Assembly - Thicker vertical splice plates were implemented at the segment splices to prevent inter-fastener buckling under flight loads.

Antenna Mountings - Two of the nine antennas located on the outside of S-IU-204 were deleted on S-IU-205.

2. Guidance System

LVDC/LVDA - A change was incorporated in the LVDA telemetry processor logic to alleviate the loss and alteration of LVDA/LVDC telemetry data. The resultant functional changes were:

(a) Real time register position 5 was restructured to function as a validity indicator for LVDA and LVDC data.

(b) T-SYNC receiving logic timing was changed to reduce the loss of LVDC data.

ST-124M Stabilized Platform System (SPS) - The following three modifications were incorporated:

(a) Redundant slip rings were added to flight critical circuits.

(b) A wiring change was made to allow the gimbal rotation exercise to be performed more expediently.

(c) Cracked solder joints were reworked by the soft-wire-wrap technique.

3. Flight Control System

Flight Control Computer (FCC)

(a) Attitude Control - AS-205 had the capability of allowing the astronauts to take command of the vehicle during S-IVB burn and coast modes. When the capability was exercised, limiters were switched into the attitude error channels, the gain of the input DC amplifiers in those channels was changed, and normal LVDA input to the FCC was replaced by the Apollo spacecraft input. The limiters were switched so that the astronaut could program a maximum attitude error of 2.5 deg in pitch and yaw, and 3.5 deg in roll. The DC amplifier gain change (3.75 to 10.00) corrected for the different scale factors of the LVDA (0.8 v/deg) and the Apollo spacecraft (0.3 v/deg).

(b) RFI Filter - A newly designed filter was installed.

(c) Control Signal Processor (CSP) - The overrate switch settings were changed on S-IU-205. The S-IU-205 settings were:

Pitch and Yaw	- 5 deg/s	and	+9.2 deg/s
Roll	-20 deg/s	and	+20 deg/s

The S-IU-204 settings were:

Pitch and Yaw	- 3 deg/s	and	+ 5 deg/s
Roll	-21 deg/s	and	+21 deg/s

(d) Stabilization Filters - The stabilization filters for the S-IU-205 FCC were modified because of changes in vehicle bending and torsion data. For the S-IB pitch and yaw attitude error channels, the control gains were modified by changing switch points. The S-IB roll channel shaping networks were changed to reduce high roll attitude errors and possible LVDA saturation and to improve stability margins which were reduced by the updated torsion data. The S-IVB pitch and yaw attitude rate networks were modified to improve marginal stability due to changes in elastic body data.

4. Instrumentation System

Remote Digital Submultiplexer - This unit was replaced with a Remote Digital Multiplexer.

Azusa System - This system was removed with the exception of the antenna.

The following units/assemblies were deleted: tape recorder, slow-speed multiplexer assembly, S1 telemeter assembly, F2 telemeter assembly, S1 RF assembly, and F2 RF assembly.

VSWR Measuring Assembly - A TM Directional Coupler was substituted for this assembly.

5. Electrical System

Batteries - The cell case material was changed from Lustran to Bakelite. One battery (6D20) powered the C-Band Transponder only and the remaining three batteries had their loads redistributed to obtain a proper load balance.

5-Volt Master Measuring Power Supply - The monitor point which was used to adjust the 5-volt supply was moved from the Power Supply to the Measuring Distributor bus. This was necessary to compensate for line drops between the supply and the distributor.

Power Distributor - QAST testing disclosed a loose terminal in one of the Power Distributor bus bars. The Power Distributor was replaced with the 206 logistic spare that was reworked to have all roll swage terminals on the bus bars.

6. Thermal Conditioning System

Coolant Pump - The coolant pump incorporated a sealed current limiter which was required due to insulation resistance degradation experienced during qualification testing.

Coldplates - Pressure caps were used on S-IU-205 to block coolant flow into two vacant coldplates (13 and 24), thereby reducing system heat losses.

Temperature Control - The Environmental Control System (ECS) was modified to provide a new method of in-flight temperature control. Basically, the modification consisted in the addition of two thermal switches in the coolant supply manifold, and a pressure transducer in the water supply line. Temperature control was achieved by controlling the supply of water to the sublimator.

A.5 PAYLOAD

The overall length of the Payload (Apollo Spacecraft) was 16.0m (632 in),

excluding the Launch Escape System. The maximum diameter was 6.6m (260 in). Figure A-2 shows the payload subdivided into the Command Module, Service Module, Lunar Excursion Module Adapter Section, and Launch Escape System. The Launch Escape System, 1016 cm (400 in) long with a maximum diameter of 66 cm (26 in), was jettisoned shortly after S-IVB stage ignition.

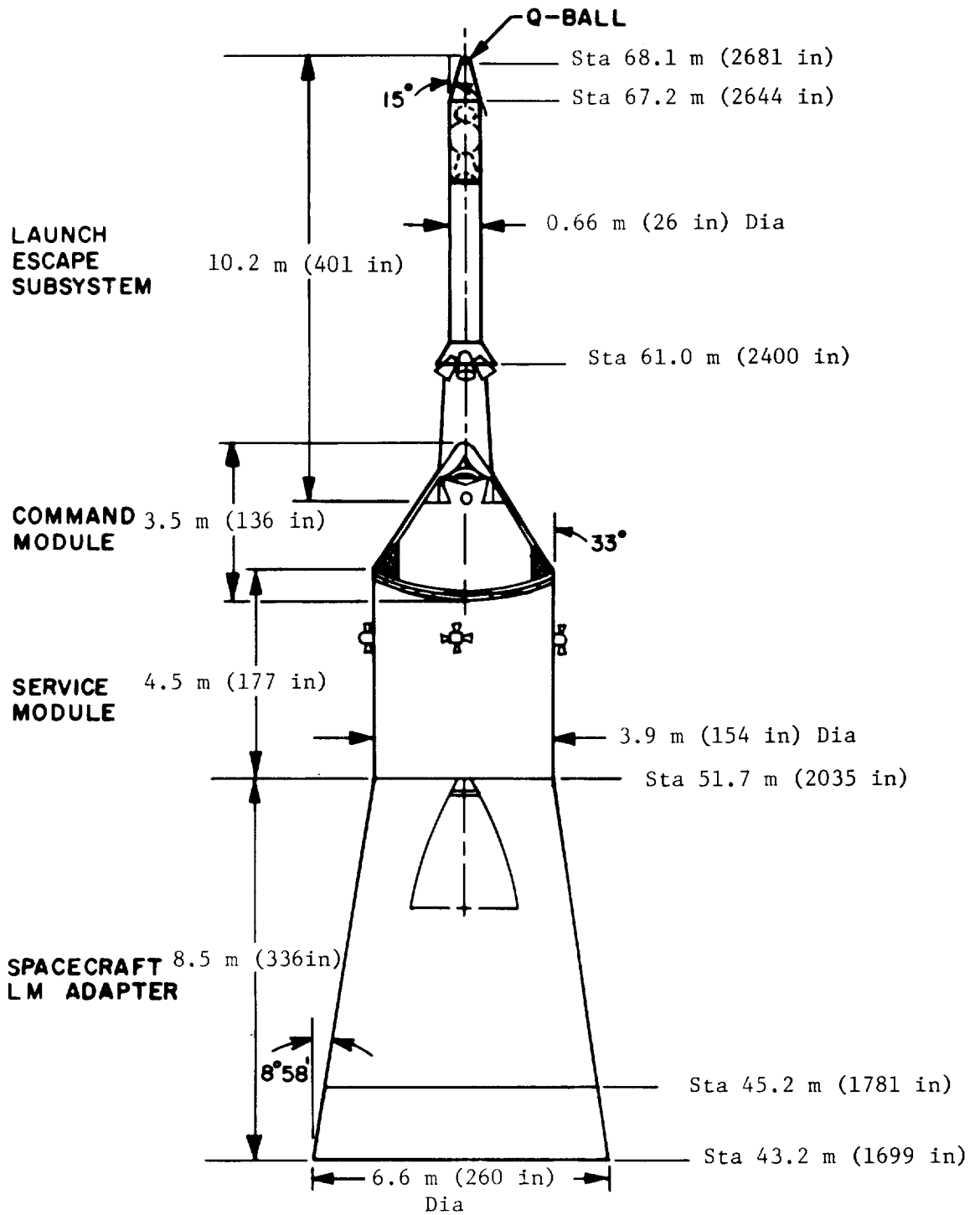


FIGURE A-2 PAYLOAD

APPENDIX B

(U) ATMOSPHERIC SUMMARY

B.1 INTRODUCTION

This appendix presents a summary of the atmospheric environment at the time of launch of AS-205. The format used to present the data in this report is similar to that presented for other Saturn vehicle launches to allow comparisons to be made. Surface and upper air wind and thermodynamic data are presented for this launch with summary tables comparing the atmospheric data with other Saturn vehicle launches (Tables B-III, B-IV, and B-V).

B.2 GENERAL ATMOSPHERIC CONDITIONS AT LAUNCH TIME

A large high pressure system, centered over Nova Scotia, caused high easterly surface winds. The upper winds, above 10 kilometers (30,500 feet), were light from the west.

B.3 SURFACE OBSERVATIONS

At the time of launch, a few scattered cumulonimbus clouds were in the area. Surface wind speeds were the highest observed for any Saturn vehicle launch. A summary of the surface observations is given in Table B-I.

B.4 UPPER AIR MEASUREMENTS

Wind Data

Upper air wind data were obtained from five different measurements, using four different wind measuring systems. All the wind data were used in the final meteorological tape. A summary of the wind data used is shown in Table B-II.

Wind Speed

The wind speeds below 30 kilometers (91,500 feet) were low, with the maximum wind speed of 15.6 m/s (30 knots) at 14.6 km (44,500 feet). Above 30 kilometers (91,500 feet), the wind speeds increased with altitude, reaching a maximum of 41.5 m/s (81 knots) at 56.5 km (172,000 feet). See Figure B-1.

Wind Direction

The wind directions were from the east at the surface, but shifted through north to west with increasing altitude up to 10 km (30,500 feet). Above 10 km (30,500 feet), the wind direction remained generally from the west. See Figure B-2.

TABLE B-I
SURFACE OBSERVATIONS AT AS-205 LAUNCH TIME

Location	Time After T-0 (min)	Pressure N/CM ² (PSIA)	Temperature °C (°F)	Dew Point °C (°F)	Visibility km (Sta. Mi)	SKY COVER		WIND			
						Amount (Tenths)	Type	Height of Base meters (feet)	Mean m/s (knots)	Peak m/s (knots)	Direction degrees
Cape Kennedy Weather Station	T-0	101800 (14.8)	28.3 (82)	21.1 (69)	18.5 (10)	3/10	Cumulonimbus	6400 (2100)			
Pad 34 South Light Pole (19.5m) #	T-0								11.5 (22.4)	12.6 (24.5)	076
Service Structure Top (96.3m) #	T-0								13.3 (25.8)	(13.5) (26.2)	088

#Above natural grade.

TABLE B-II
SYSTEMS USED TO MEASURE UPPER AIR WIND DATA

Type of Data	Release Time		Portion of Data Used			Remarks	
	Z	Time After T-0 (min)	Altitude (m)	Start			End
				Time After T-0 (min)	Altitude (m)		
FPS-16 Jimsphere	1509	6	125	6	7950	32	
FPS-16 Jimsphere	1237	-146	7975	-120	15975	-98	
Rawinsonde	1509	6	16000	66	37500	148	
Arcasonde	1630	87	60250	92	37750	100	
Viper Dart	1903	240	90000	250	60500	252	

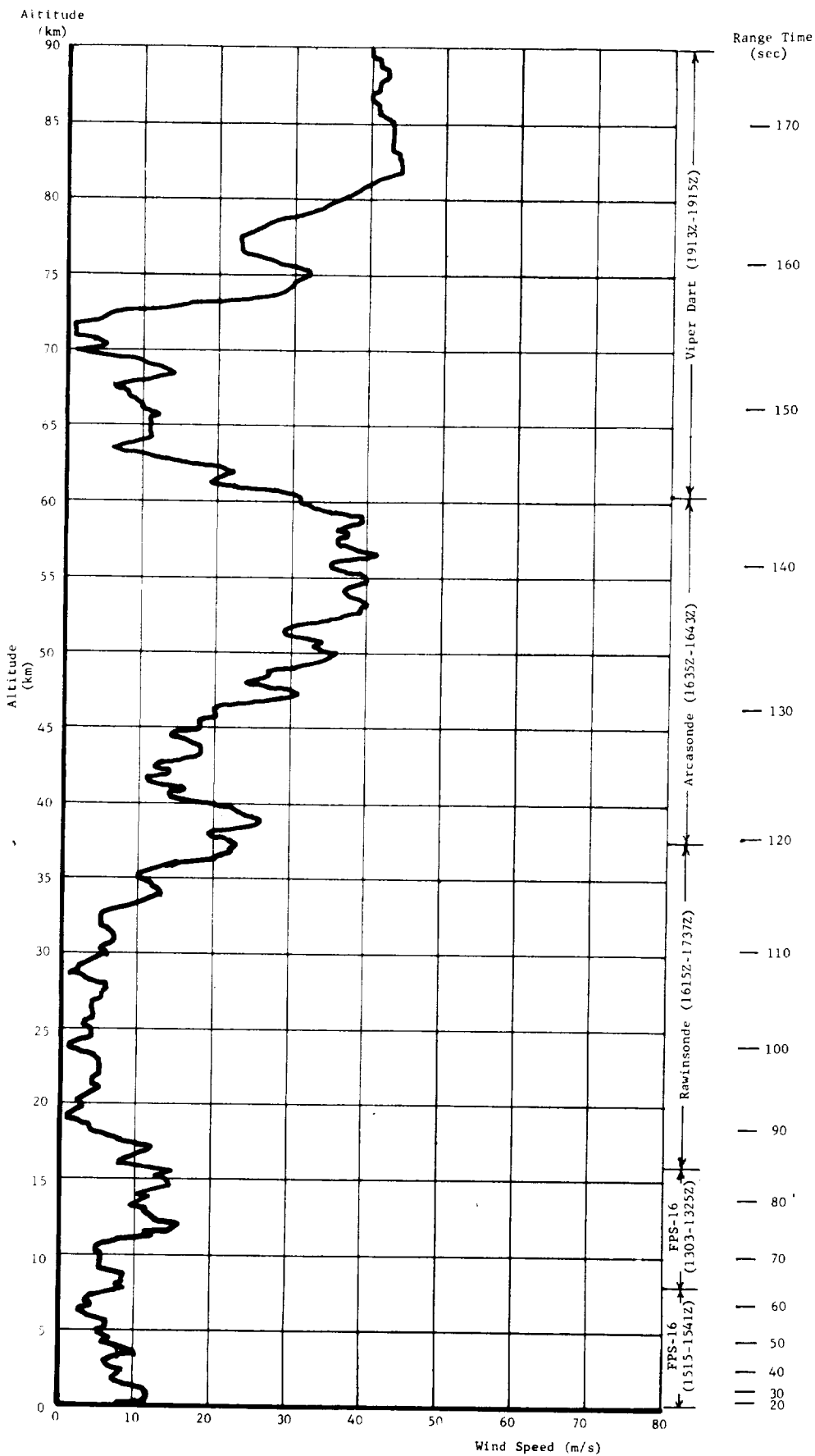


FIGURE B-1 SCALAR WIND SPEED AT LAUNCH TIME OF AS-205

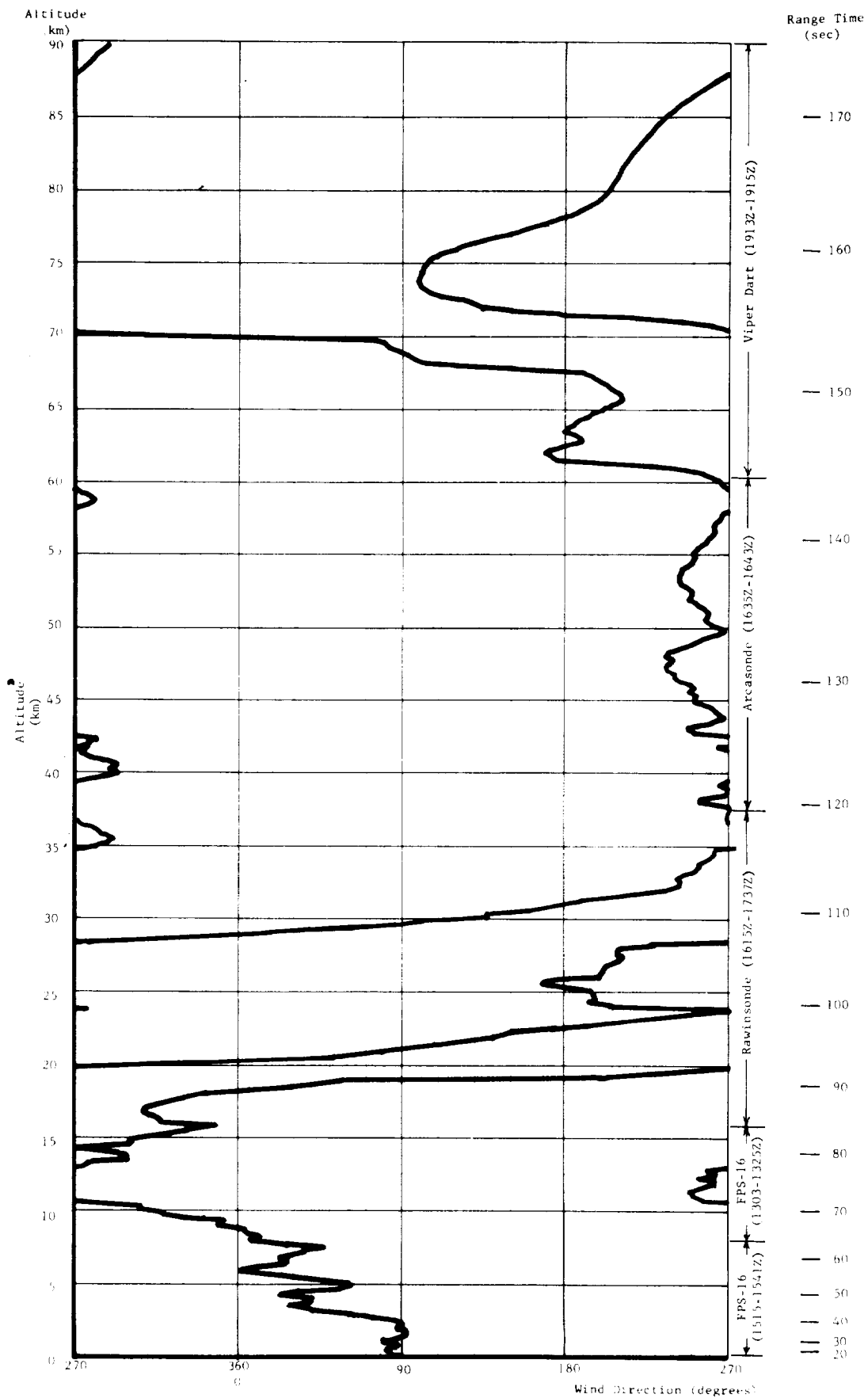


FIGURE B-2 WIND DIRECTION AT LAUNCH TIME OF AS-205

Pitch Wind Component

In the lower levels below 10 km (30,500 feet), the pitch component winds were head-winds. Above 10 km (30,500 feet), the winds were tailwinds, reaching a maximum value of 15.8 m/s (31 knots) at 12.1 km (36,900 feet). At higher altitudes, the winds were tailwinds, with a maximum of 40.4 m/s (78 knots) at 56.5 km (172,000 feet). See Figure B-3.

Yaw Wind Component

The yaw wind component speeds were less than ± 20 m/s (38 knots) up to 60 km (183,000 feet). The peak in the high dynamic pressure region was a wind from the left of +15.7 m/s (31 knots) at 15.6 km (47,500 feet). See Figures B-4 and B-5.

B.5 THERMODYNAMIC DATA

Comparisons of the thermodynamic data taken at launch time with the Patrick Reference Atmosphere (1963) for temperature, density, pressure, and optical index of refraction are shown in Figures B-6 and B-7.

Temperature

The temperature deviated only slightly from the Patrick Reference Atmosphere (1963) (less than 3 percent) up to 48 km (146,000 feet).

Density

There were only slight deviations (less than 2 percent) of the density from the Patrick Reference Atmosphere below 24 km (73,000 feet). Above 24 km (73,000 feet) the deviations of the density increased with altitude, to a maximum of 7% at 46 km (140,000 feet). At 35.5 km (108,000 feet) a jump of 3% occurred in the density deviation values, caused by a similar discontinuity in the pressure values when merging the rawinsonde and arcasonde data.

Pressure

The pressure deviations from the Patrick Reference Atmosphere (1963) reached a maximum of 3.1% at 25 km (75,400 feet). At 35.5 km (108,000 feet), a 3% jump occurred in the data as a result of merging the rawinsonde and arcasonde data.

Optical Index of Refraction

The optical index of refraction at the surface had a deviation of $-10.1 (n-1) \times 10^{-6}$ units from the Patrick Reference Atmosphere (1963). Above the surface, the deviations decreased with altitude.

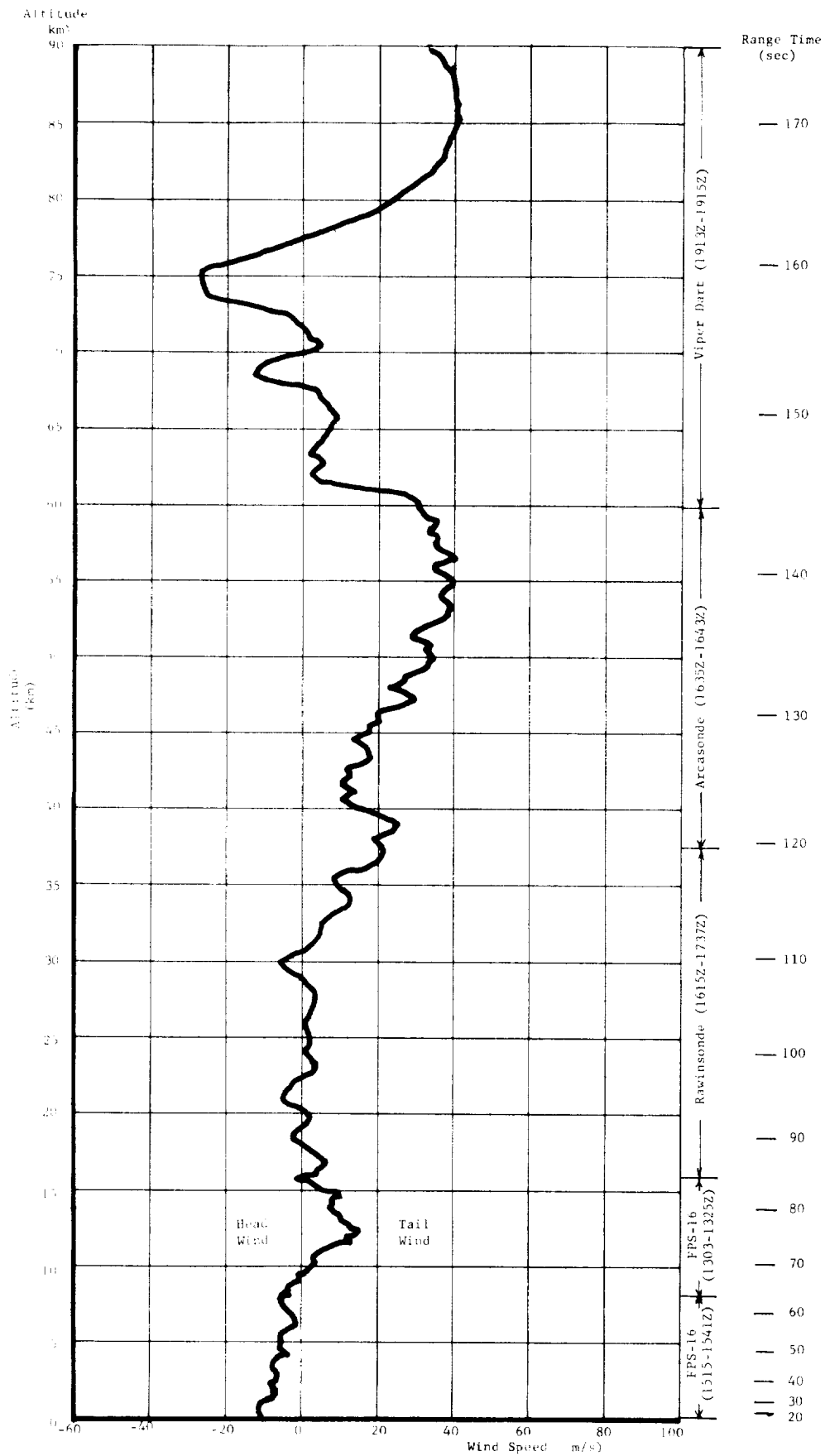


FIGURE B-3 PITCH WIND SPEED COMPONENT (W_X) AT LAUNCH TIME OF AS-205

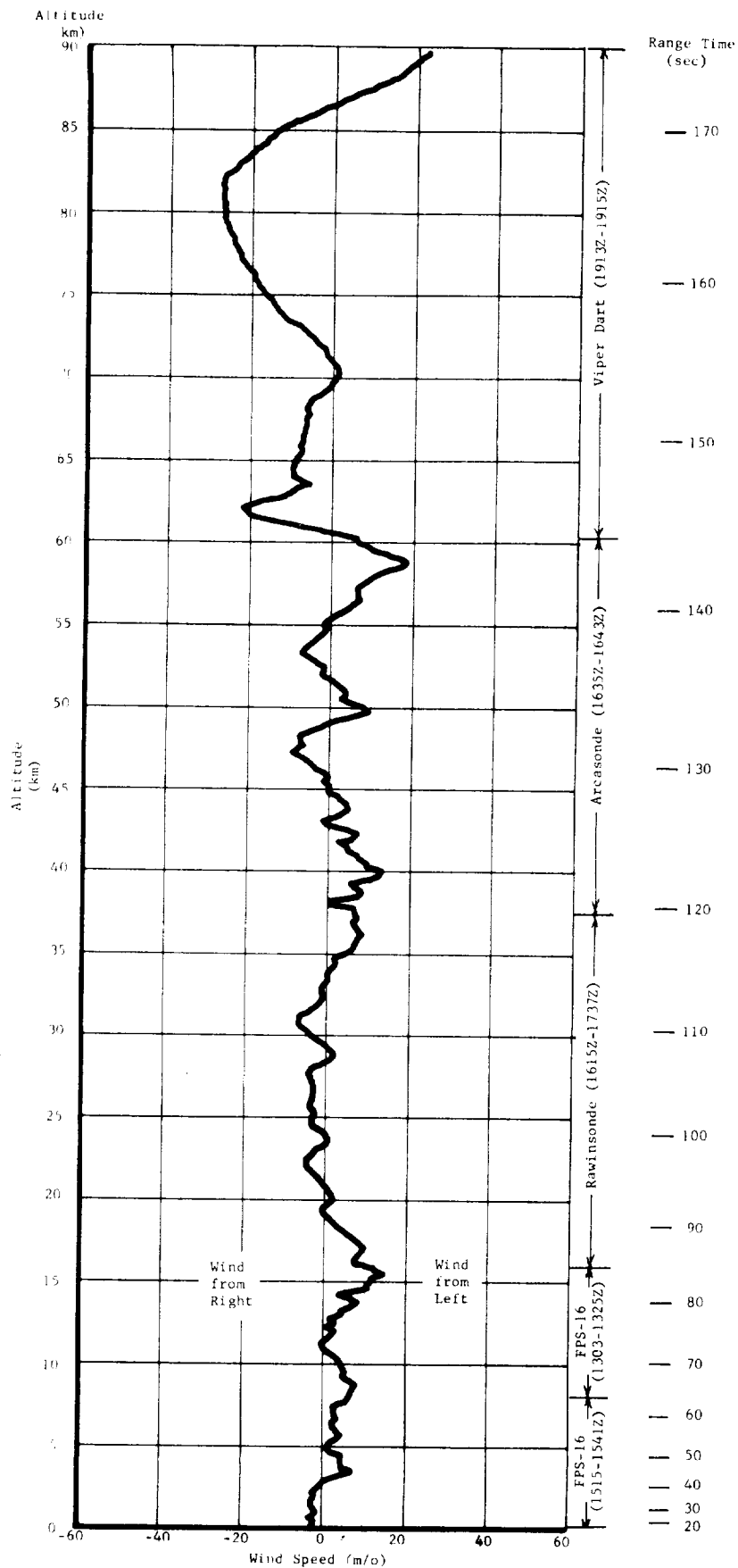


FIGURE B-4 YAW WIND SPEED COMPONENT AT LAUNCH TIME OF AS-205

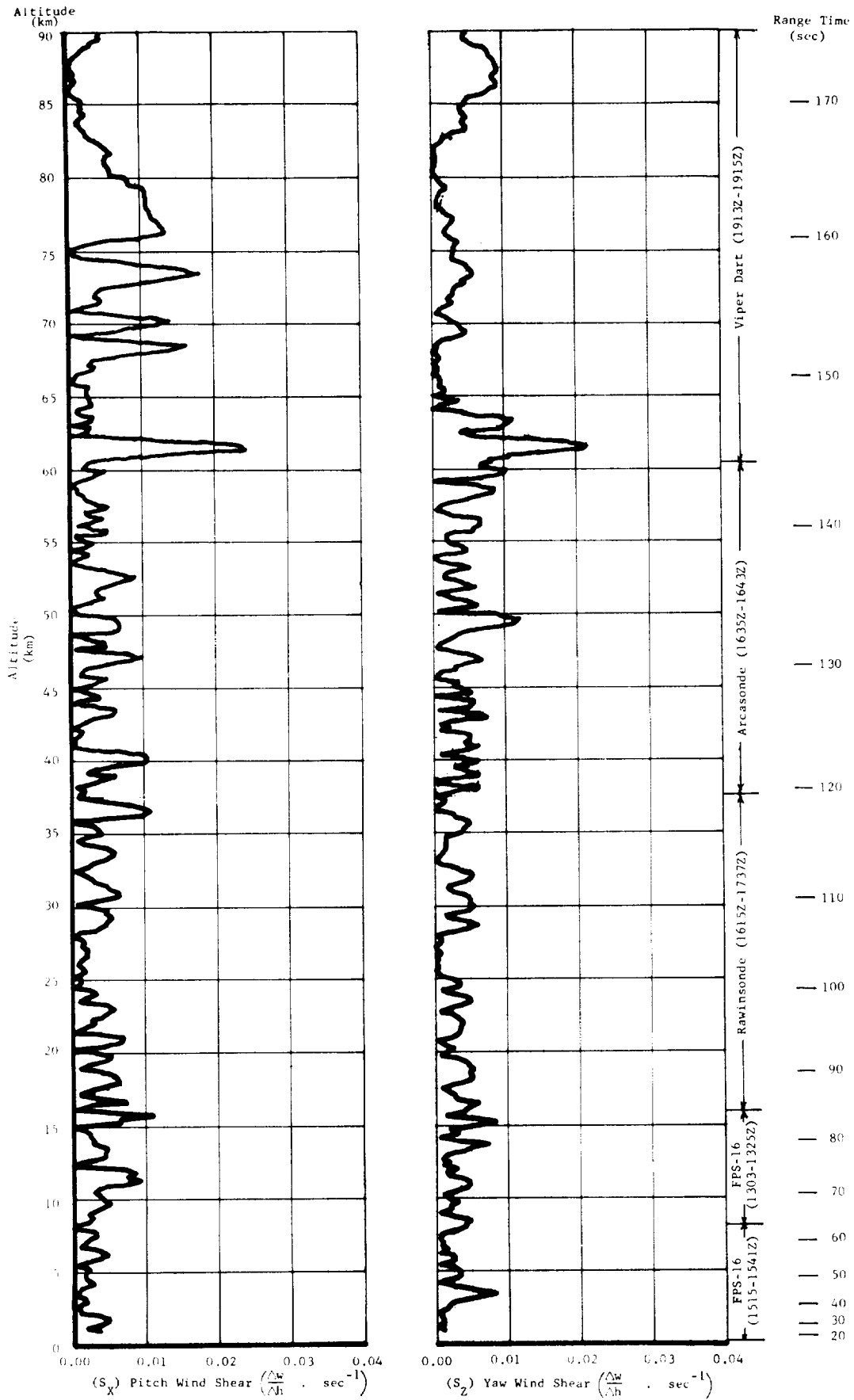


FIGURE B-5 PITCH (S_x) AND YAW (S_y) COMPONENT WIND SHEARS AT TIME OF LAUNCH OF AS-205

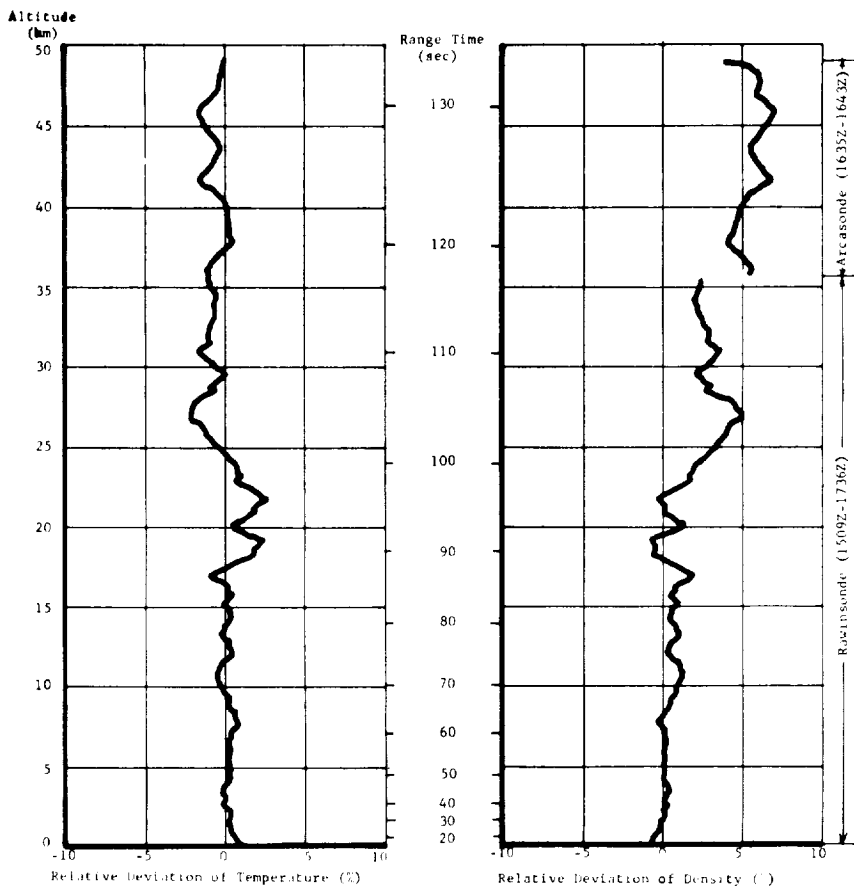


FIGURE B-6 RELATIVE DEVIATION OF TEMPERATURE AND DENSITY FROM PAFB (63) REFERENCE ATMOSPHERE, AS-205

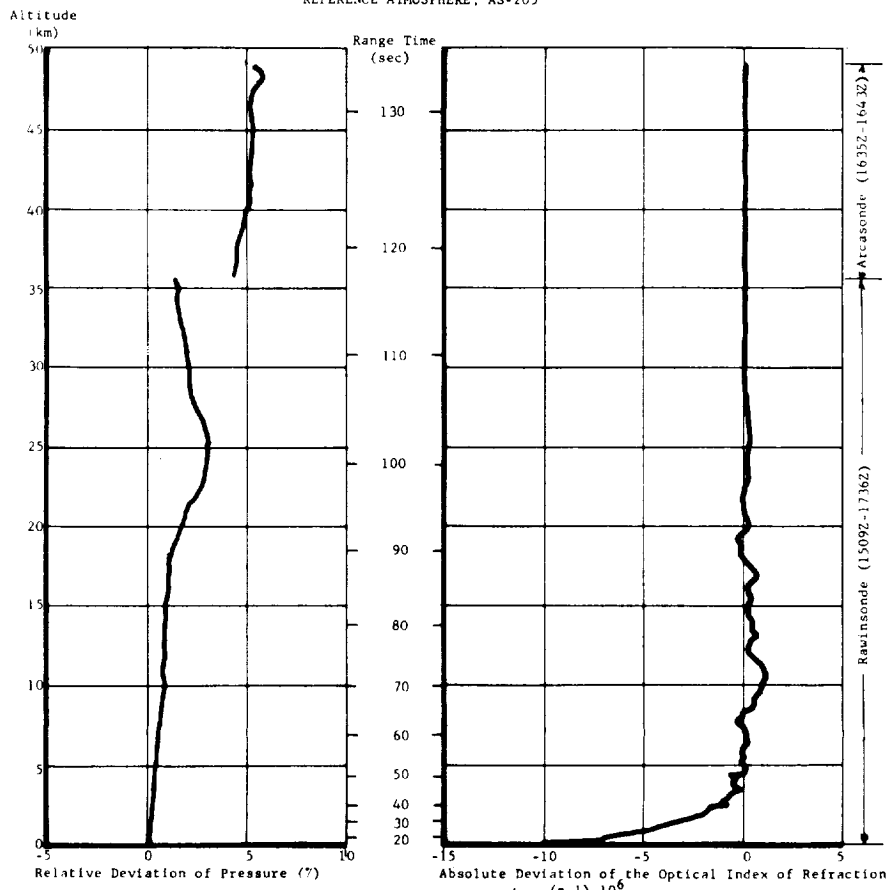


FIGURE B-7 RELATIVE DEVIATION OF PRESSURE AND ABSOLUTE DEVIATION OF THE INDEX OF REFRACTION FROM THE PAFB (63) REFERENCE ATMOSPHERE, AS-205

TABLE B-IIIa

MAXIMUM WIND SPEED IN HIGH DYNAMIC PRESSURE REGION
FOR SATURN 1 THROUGH SATURN 10 VEHICLES

Vehicle Number	Maximum Wind			Maximum Wind Components			
	Speed m/s (knots)	Dir (Deg)	Alt km (ft)	Pitch (W_x) m/s (knots)	Alt km (ft)	Yaw (W_z) m/s (knots)	Alt km (ft)
SA-1	47.0 (91.4)	242	12.25 (40,200)	36.8 (71.5)	13.00 (42,600)	-29.2 (-55.8)	12.25 (40,200)
SA-2	33.6 (65.3)	216	13.50 (44,300)	31.8 (61.8)	13.50 (44,300)	-13.3 (-25.9)	12.25 (40,200)
SA-3	31.3 (60.8)	269	13.75 (45,100)	30.7 (59.7)	13.75 (45,100)	11.2 (21.8)	12.00 (39,400)
SA-4	51.8 (100.7)	253	13.00 (42,600)	46.2 (89.8)	13.00 (42,600)	-23.4 (-45.5)	13.00 (42,600)
SA-5	42.1 (81.8)	268	10.75 (35,300)	41.1 (79.9)	10.75 (35,300)	-11.5 (-22.4)	11.25 (36,900)
SA-6	15.0 (29.2)	96	12.50 (41,000)	-14.8 (-28.8)	12.50 (41,000)	12.2 (23.7)	17.00 (55,800)
SA-7	17.3 (33.6)	47	11.75 (38,500)	-11.1 (-21.6)	12.75 (41,800)	14.8 (28.8)	12.00 (39,400)
SA-9	34.3 (66.7)	243	13.00 (42,600)	27.5 (53.5)	10.75 (35,300)	23.6 (45.9)	13.25 (43,500)
SA-8	16.0 (31.1)	351	15.25 (50,000)	12.0 (23.3)	11.00 (36,100)	14.6 (28.4)	15.25 (50,000)
SA-10	15.0 (29.2)	306	14.75 (48,400)	12.9 (25.1)	14.75 (48,400)	10.8 (21.0)	15.45 (50,700)

TABLE B-IIIb

MAXIMUM WIND SPEED IN HIGH DYNAMIC PRESSURE REGION FOR
APOLLO-SATURN 201 THROUGH APOLLO-SATURN 205 VEHICLES

Vehicle Number	Maximum Wind			Maximum Wind Components			
	Speed m/s (knots)	Dir (Deg)	Alt km (ft)	Pitch (W_x) m/s (knots)	Alt km (ft)	Yaw (W_z) m/s (knots)	Alt km (ft)
AS-201	70.0 (136.1)	250	13.75 (45,100)	57.3 (111.4)	13.75 (45,100)	-43.3 (-84.2)	13.25 (43,500)
AS-203	18.0 (35.0)	312	13.00 (42,600)	11.1 (21.6)	12.50 (41,000)	16.6 (32.3)	13.25 (43,500)
AS-202	16.0 (31.1)	231	12.00 (39,400)	10.7 (20.8)	12.50 (41,000)	-15.4 (-29.9)	10.25 (33,600)
AS-204	35.0 (68.0)	288	12.00 (39,400)	32.7 (63.6)	15.25 (50,000)	20.6 (40.0)	12.00 (39,400)
AS-205	15.6 (30.3)	309	14.60 (44,500)	15.8 (30.7)	12.08 (36,800)	15.7 (30.5)	15.78 (47,500)

TABLE B-IIIc

MAXIMUM WIND SPEED IN HIGH DYNAMIC PRESSURE REGION FOR
APOLLO-SATURN 501 AND 502 VEHICLES

Vehicle Number	Maximum Wind			Maximum Wind Components			
	Speed m/s (knots)	Dir (Deg)	Alt km (ft)	Pitch (W_x) m/s (knots)	Alt km (ft)	Yaw (W_z) m/s (knots)	Alt km (ft)
AS-501	26.0 (50.5)	273	11.50 (37,700)	24.3 (47.2)	11.50 (37,700)	12.9 (25.1)	9.00 (29,500)
AS-502	27.1 (52.7)	255	12.00 (42,600)	27.1 (52.7)	12.00 (42,600)	12.9 (25.1)	15.75 (51,700)

TABLE B-IVa

EXTREME WIND SHEAR VALUES IN THE HIGH DYNAMIC PRESSURE REGION
FOR SATURN 1 THROUGH SATURN 10 VEHICLES

($\Delta h = 1000$ m)

Vehicle Number	Pitch Plane		Yaw Plane	
	Shear (sec^{-1})	Altitude km (ft)	Shear (sec^{-1})	Altitude km (ft)
SA-1	0.0145	14.75 (48,400)	0.0168	16.00 (52,500)
SA-2	0.0144	15.00 (49,200)	0.0083	16.00 (52,500)
SA-3	0.0105	13.75 (45,100)	0.0157	13.25 (43,500)
SA-4	0.0155	13.00 (42,600)	0.0144	11.00 (36,100)
SA-5	0.0162	17.00 (55,800)	0.0086	10.00 (32,800)
SA-6	0.0121	12.25 (40,200)	0.0113	12.50 (41,000)
SA-7	0.0078	14.25 (46,800)	0.0068	11.25 (36,900)
SA-9	0.0096	10.50 (34,500)	0.0184	10.75 (35,300)
SA-8	0.0065	10.00 (32,800)	0.0073	17.00 (55,800)
SA-10	0.0130	14.75 (48,400)	0.0090	15.00 (49,200)

TABLE B-IVb

EXTREME WIND SHEAR VALUES IN THE HIGH DYNAMIC PRESSURE REGION
FOR APOLLO-SATURN 201 THROUGH APOLLO-SATURN 205 VEHICLES

($\Delta h = 1000$ m)

Vehicle Number	Pitch Plane		Yaw Plane	
	Shear (sec ⁻¹)	Altitude km (ft)	Shear (sec ⁻¹)	Altitude km (ft)
AS-201	0.0206	16.00 (52,500)	0.0205	12.00 (39,400)
AS-203	0.0104	14.75 (48,400)	0.0079	14.25 (46,800)
AS-202	0.0083	13.50 (44,300)	0.0054	13.25 (43,500)
AS-204	0.0118	16.75 (55,000)	0.0116	14.00 (45,900)
AS-205	0.0113	15.78 (48,100)	0.0085	15.25 (46,500)

TABLE B-IVc

EXTREME WIND SHEAR VALUES IN THE HIGH DYNAMIC PRESSURE REGION
FOR APOLLO-SATURN 501 AND 502 VEHICLES

($\Delta h = 1000$ m)

Vehicle Number	Pitch Plane		Yaw Plane	
	Shear (sec ⁻¹)	Altitude km (ft)	Shear (sec ⁻¹)	Altitude km (ft)
AS-501	0.0066	10.00 (32,800)	0.0067	10.00 (32,800)
AS-502	0.0125	14.90 (48,900)	0.0084	13.28 (43,500)

TABLE B-Va
 SELECTED ATMOSPHERIC OBSERVATIONS FOR SATURN 1 THROUGH 10 VEHICLE LAUNCHES
 AT KENNEDY SPACE CENTER, FLORIDA

Vehicle Number	Vehicle Data			Surface Data					Inflight Conditions			
	Date	Time (EST) Nearest Minute	Launch Complex	Pressure N/cm ²	Temperature °C	Relative Humidity Percent	Wind* Speed m/s	Wind* Direction Degrees	Clouds	Maximum Altitude m	Wind Speed m/s	Direction Degrees
SA-1	27 Oct 61	1006	34	10.222	26.2	64	6.4	65	8/10 cumulus	12.25	47.0	242
SA-2	25 Apr 62	0900	34	10.205	24.6	59	3.5	180	1/10 cumulus, 3/10 cirrostratus	13.50	33.6	261
SA-3	16 Nov 62	1245	34	10.193	23.9	54	4.0	250	2/10 cumulus, 4/10 cirrus	13.75	31.3	269
SA-4	28 Mar 63	1512	34	10.176	23.9	71	6.0	40	1/10 stratocumulus, 1/10 cirrus	13.00	51.8	253
SA-5	29 Jan 64	1125	37B	10.278	17.8	59	9.0	38	4/10 stratocumulus, 2/10 cirrus	10.75	42.1	268
SA-6	28 May 64	1207	37B	10.142	28.7	64	7.0	150	1/10 cumulus, 1/10 cirrus	12.50	15.0	96
SA-7	18 Sep 64	1123	37B	10.173	29.5	55	5.0	70	1/10 cumulus, 5/10 altocumulus, 1/10 cirrus	11.75	17.3	47
SA-9	16 Feb 65	0937	37B	10.244	23.3	74	6.0	125	1/10 stratocumulus	13.00	34.3	243
SA-8	25 May 65	0235	37B	10.186	22.8	93	4.4	140	1/10 cumulus	15.25	16.0	351
SA-10	30 Jul 65	0800	37B	10.163	24.7	86	10.7	185	1/10 cumulonimbus, 2/10 altostratus, 5/10 cirrus	14.75	15.0	306

* Instantaneous readings from charts at T-0 from anemometers on poles at 19.5 m (59.4 ft) on launch complex 34, 20.7 m (63.1 ft) on launch complex 37B. Heights of anemometers are above natural grade.

TABLE B-Vb

SELECTED ATMOSPHERIC OBSERVATIONS FOR APOLLO-SATURN 201 THROUGH APOLLO-SATURN 205 VEHICLE LAUNCHES
AT KENNEDY SPACE CENTER, FLORIDA

Vehicle Number	Vehicle Data		Surface Data					Inflight Conditions				
	Date	Time (EST) Nearest Minute	Launch Complex	Pressure N/cm ²	Temperature °C	Relative Humidity Percent	Wind* Speed m/s	Wind* Direction Degrees	Clouds	Maximum Altitude m	Wind in 8-16 km Layer Speed m/s	Direction Degrees
AS-201	26 Feb 66	1112	34	10.217	16.1	48	6.5	330	clear	13.75	70.0	250
AS-203	5 Jul 66	0953	37B	10.173	30.2	70	6.3	242	8/10 cumulus, 1/10 cirrus	13.00	18.0	312
AS-202	25 Aug 66	1216	34	10.166	30.2	69	4.1	160	1/10 cumulus, 1/10 altocumulus, 1/10 cirrus	12.00	16.0	231
AS-204	23 Jan 68	1748	37B	10.186	16.1	93	4.2	45	3/10 cumulus	12.00	35.0	288
AS-205	11 Oct 68	1003	34	10.180	28.3	65	11.5	90	3/10 cumulonimbus	15.60	14.6	309

* Instantaneous readings from charts at T-0 from anemometers on poles at 19.5 m (59.4 ft) on launch complex 34, 20.7 m (63.1 ft) on launch complex 37B. Heights of anemometers are above natural grade.

TABLE B-Vc

SELECTED ATMOSPHERIC OBSERVATIONS FOR APOLLO-SATURN 501 THROUGH 502 VEHICLE LAUNCHES
AT KENNEDY SPACE CENTER, FLORIDA

Vehicle Number	Vehicle Data		Surface Data					Inflight Conditions				
	Date	Time (EST) Nearest Minute	Launch Complex	Pressure N/cm ²	Temperature °C	Relative Humidity Percent	Wind* Speed m/s	Wind* Direction Degrees	Clouds	Maximum Altitude m	Wind in 8-16 km Layer Speed m/s	Direction Degrees
AS-501	9 Nov 67	0700	39A	10.261	17.6	55	8.0	70	1/10 cumulus	11.50	26.0	273
AS-502	4 Apr 68	0600	39A	10.200	20.9	83	5.4	132	5/10 stratocumulus	13.00	27.1	255

* Instantaneous readings from charts at T-0 from anemometers on poles on launch pad at 18.3 m (60.0 ft) on launch complex 39A. Heights of anemometers are above natural grade.

REFERENCES

1. NASA Operational Trajectory Data Report, "AS-205/CSM-101 Launch Vehicle Operational Trajectory" (Revision 1), dated September 10, 1968.
2. CCSD TB-P&VE-68-284, "S-IB Stage Criteria for AS-205 Final Flight Prediction", dated April 23, 1968.
3. R-P&VE-VAW-68-116, "AS-205 Mass Characteristics, Guidance Cutoff", dated September 18, 1968.
4. SE 008-001-1, "Project Apollo Coordinate System Standards", dated June 1965.
5. Memorandum not numbered, "J-2 Engine Technical Program Review", dated June 1, 1966.
6. CCSD SDES-69-400, "S-IB-5 Stage Flight Evaluation Report", dated January 15, 1969.
7. MDC SM-46990, "Saturn S-IVB-205 Stage Flight Evaluation Report", dated December 1968.
8. IBM No. 68-K11-0011 (MSFC No. I-4-408-15), "S-IU-205 Final Flight Evaluation Report for Apollo 7 Mission (Volume I)", dated December 18, 1968.
9. CCSD TB-AP-68-156, "Statistical Evaluation of Saturn I and Saturn IB Engine Mechanical Misalignment Data", dated September 9, 1968.
10. CCSD TN-AP-68-321, "SA-205 Launch Vehicle Thermal Environment", dated April 17, 1968.
11. MPR-SAT-FE-66-8 (Confidential), "Results of the First Saturn IB Launch Vehicle Test Flight AS-201", dated May 6, 1966.
12. MPR-SAT-FE-66-12 (Confidential), "Results of the Second Saturn IB Launch Vehicle Test Flight AS-203", dated September 22, 1966.
13. MPR-SAT-FE-66-13, "Results of the Third Saturn IB Launch Vehicle Test Flight AS-202", dated October 25, 1966.
14. MPR-SAT-FE-68-2, "Results of the Fourth Saturn IB Launch Vehicle Test Flight AS-204", dated April 5, 1968.
15. CCSD TR-P&VE-68-65, "Final S-IB-5 Propulsion System Flight Performance Predictions for Launch Month August Through December", dated June 15, 1968.

APPROVAL

MPR-SAT-FE-68-4

RESULTS OF THE FIFTH SATURN IB LAUNCH VEHICLE TEST FLIGHT
AS-205

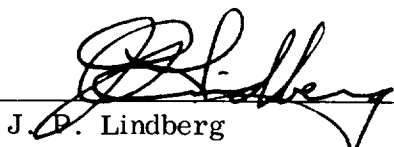
By Saturn IB Flight Evaluation Working Group

The information in this report has been reviewed for security classification. Review of any information concerning Department of Defense or Atomic Energy Commission programs has been made by the MSFC Security Classification Officer. The highest classification has been determined to be Unclassified.



Stanley L. Fragge
Security Classification Officer

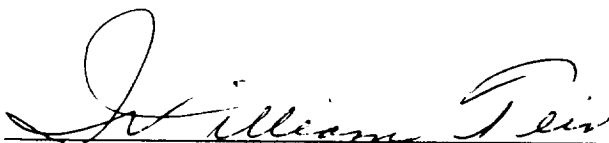
This report has been reviewed and approved for technical accuracy.



J. P. Lindberg
Chairman, Saturn Flight Evaluation Working Group



Hermann K. Weidner
Director, Research and Development Operations



William Teir
Saturn I/IB Program Manager

REPORT DISTRIBUTION DATE 1-28-69

OFFICE OF THE DIRECTOR

DR. W. VON BRAUN DIR
DR. F. REFS DEP-T

EXECUTIVE STAFF

MR. H. MAUS E-DIR
MR. R. ABBOTT E-P
MR. T. SMITH E-S

MANAGEMENT SERVICES OFFICE

MR. D. AKENS MS-H
MR. I. REMER MS-I
MS-IL
MS-IP
MS-D
MR. W. GARRETT

PATENT COUNSEL

MR. L. WOFFORD PAT

INDUSTRIAL OPERATIONS

GEN. F. O'CONNOR I-DIR
DR. W. MRAZEK I-DIR

ENGINE PROGRAM OFFICE

MR. W. BROWN I-E-MGR
MR. T. FERRELL I-E-J
MR. L. WEAR I-E-J
MR. T. SMITH I-E-H
MR. R. THORNTON I-E-H

MICHoud ASSEMBLY FACILITY

DR. G. CONSTAN I-MICH-MGR
MR. R. KOWR I-MICH-OP
MR. M. MARCHESE I-MICH-OR

MISSISSIPPI TEST FACILITY

MR. J. BALCH I-MT-MGR
MR. H. AUTER I-MT-MGR

MISSION OPERATIONS OFFICE

DR. F. SPEER I-MO-MGR
MRS. V. NORMAN I-MO-OL
MR. G. EMANUEL I-MO-RC

SATURN/APOLLO APPLICATION PROGRAM OFFICE

MR. R. RIEMER I-S/AA

SATURN I/IB PROGRAM OFFICE

COL. W. TEIR I-I/IB-MGR
MR. H. JOHNSON I-I/IB-C
MR. W. HUFF I-I/IB-F
MR. D. GERMANY I-I/IB-F
MR. J. SISSON I-I/IB-E
MR. J. FIKES I-I/IB-T
LT. COL. J. KMINEK I-I/IB-F
MR. J. JORDAN I-I/IB-F
MR. N. RALEY I-I/IB-F
MR. A. THOMPSON I-I/IB-SI/IB
MR. T. KINSER I-I/IB-SI/IB
MR. J. ALTER I-I/IB-SI/IB
MR. C. MEYERS I-I/IB-SI/IB
MR. W. SIMMONS I-I/IB-U
MR. P. DUNLAP I-I/IB-G

SATURN V PROGRAM OFFICE

COL. L. JAMES I-V-MGR
MR. J. MOODY I-V-Q
MR. J. MC CULLOCH I-V-SIVR
MR. A. HIGGINS I-V-SIVR
MR. J. GALEY I-V-IU

RESEARCH AND DEVELOPMENT OPERATIONS

MR. H. WEIDNER R-DIR

ADVANCED SYSTEMS OFFICE

MR. F. WILLIAMS R-AS-DIR

AERO-ASTRODYNAMICS LABORATORY

DR. E. GEISSLER R-AERO-DIR
MR. D. JEAN R-AERO-DIR
MR. C. HAGOOD R-AERO-P
MR. R. JACKSON R-AERO-P
MR. G. MC KAY R-AERO-P
MR. R. CUMMINGS R-AERO-T
MR. W. VAUGHAN R-AERO-Y
MR. D. SMITH R-AERO-YT
MR. G. DANIELS R-AERO-YT
MR. W. DAHM R-AERO-A
MR. D. HOLDERER R-AERO-A
MR. H. DUMN R-AERO-ADV
MR. H. WILSON R-AERO-AT
MR. I. JONES R-AERO-AT
MR. T. REFD R-AERO-AU
MR. S. GUEST R-AERO-AU
MR. J. LINDBERG R-AERO-F
MR. R. MC ANNALLY R-AERO-FP
MR. R. TEASLEY R-AERO-FP
MR. E. DEATON JR R-AERO-FF
MR. R. RENSON R-AERO-FT
MR. R. COULTER R-AERO-FT
MR. M. HARDAGE R-AERO-FM
MR. J. CRAFTS R-AERO-FM
MR. H. HORN R-AERO-D
MR. R. RYAN R-AERO-DD
MR. C. BAKER R-AERO-G

ASTRONICS LABORATORY

DR. W. HAEUSSERMANN R-ASTR-DIR
MR. D. HORERG R-ASTR-DIR
MR. J. MACK R-ASTR-S
MR. F. HAMMERS R-ASTR-S
MR. J. WOLFE R-ASTR-S
MR. F. DIGESU R-ASTR-A
MR. F. MOORE R-ASTR-N
MR. P. NICAISE R-ASTR-NGI
MR. J. LOMINICK R-ASTR-NFM
MR. C. MANDEL R-ASTR-G
MR. G. FERRELL R-ASTR-GDA
MR. J. POWELL R-ASTR-I
MR. W. THRELKELD R-ASTR-ITP
MR. J. AVFERY R-ASTR-IM
MR. J. KERR R-ASTR-IRD
MR. H. FICHTNER R-ASTR-E
MR. H. ROBINSON R-ASTR-FSA
MR. J. STROUD R-ASTR-EA
MR. J. VANN R-ASTR-EA
MR. H. HOSENTHIEN R-ASTR-F
MR. D. JUSTICE R-ASTR-FA
MR. W. CLARKE R-ASTR-FD
MR. J. BLACKSTONE R-ASTR-FT
MR. J. TAYLOR R-ASTR-R
MR. J. BOEHM R-ASTR-H

(8)

(2)

(2)

(33)

(4)

(2)

COMPUTATION LABORATORY

DR. H. HOELZER R-COMP-DIR
 MR. C. PRINCE R-COMP-DIR
 MR. W. FORTENRERRY R-COMP-A
 MR. P. COCHRAN R-COMP-RR
 MR. C. HOUSTON R-COMP-RRM

EXPERIMENTS OFFICE

DR. W. JOHNSON R-EO-DIR

MANUFACTURING ENGINEERING LABORATORY

MR. M. SIFBEL R-ME-DIR
 MR. H. WUENSCHER R-ME-DIR
 MR. J. ORR R-ME-M
 MR. W. FRANKLIN R-ME-T

PROPULSION & VEHICLE ENGINEERING LAB.

MR. K. HEIMBURG R-PRVE-DIR
 MR. F. HELLEBRAND R-PRVE-DIR
 MR. H. PALAORO R-PRVE-DIR
 MR. W. MARSHALL R-PRVE-X
 MR. K. RÖTHE R-PRVE-XSR
 MR. R. GRINER R-PRVE-XSJ
 MR. C. ROONE R-PRVE-XSK
 MR. E. GÖRNER R-PRVE-A
 MR. A. STFIN R-PRVE-AP
 MR. J. KINGSBURY R-PRVE-M
 MR. R. HUNT R-PRVE-S
 MR. J. FURMAN R-PRVE-SJ
 MR. N. SHOWERS R-PRVE-SL
 MR. E. BEAM R-PRVE-SLA
 MR. P. FREDERICK R-PRVE-SS
 MR. J. KEY R-PRVE-SSV
 MR. J. BLUMRICH R-PRVE-SA
 MR. C. GFREN R-PRVE-SVM
 MR. J. THOMSON R-PRVE-PA
 MR. C. WOOD R-PRVE-PT
 MR. W. MC ANELLY R-PRVE-PTD
 MR. H. FUHRMANN R-PRVE-PM
 MR. W. CORB R-PRVE-PPE (2)
 MR. R. GARCIA R-PRVE-PPE
 MR. J. ABFRG R-PRVE-V (2)
 MR. W. SCHULZE R-PRVE-V
 MR. R. MARMANN R-PRVE-VAW
 MR. R. SCOTT R-PRVE-VAW (2)
 MR. R. DEVENISH R-PRVE-VNP (2)
 MR. H. SELLS R-PRVE-VOO

QUALITY AND RELIABILITY ASSURANCE LAB.

MR. D. GRAU R-QHAL-DIR
 MR. R. CHANDLER R-QHAL-DIR
 MR. F. KLAUSS R-QHAL-J
 MR. S. PECK R-QHAL-F
 MR. SMITH R-QHAL-R
 MR. A. WITTMANN R-QHAL-T
 MR. W. BRIEN R-QHAL-Q
 MR. R. HENRITZE R-QHAL-A
 MR. C. BROOKS R-QHAL-P (3)
 MR. J. LANDERS R-QHAL-PC
 MR. H. RUSHING R-QHAL-PI

SPACE SCIENCES LABORATORY

DR. E. STUHLINGER R-SSL-DIR
 MR. G. HELLER R-SSL-T

SYSTEMS ENGINEERING OFFICE

MR. L. RICHARD R-SF-DIR
 MR. F. MAY R-SF-S

TEST LABORATORY

MR. T. EDWARDS R-TEST-M
 MR. W. GRAFTON R-TEST-C
 DR. W. SIEBER R-TEST-I
 MR. D. DRISCOLL R-TEST-S
 MR. K. REILMANN R-TEST-SE

EXTERNAL

NASA HEADQUARTERS

DR. A. EGGERS JR E
 DR. W. LESHER U
 DR. J. CONDON KR
 DR. G. MUELLER M
 CAPT. R. FREITAG MC
 MAJ. GEN. S. PHILLIPS MA
 MR. R. WAGNER MAS/BELLCOM (3)
 MR. A. ACKERMAN MAS/BELLCOM
 MR. L. DAY MAT (8)
 MR. C. KING JR MAT
 CAPT. J. HOLCOMB MAO
 MR. G. WHITE MAR
 MR. S. DI MAGGIO MAR
 MR. W. WILLOUGHBY JR MAR
 MR. W. SCHNEIDER ML
 MR. J. DISHER MLD
 MR. D. RUMGARDNER MLT
 MAJ. GEN. J. STEVENSON MO (2)
 DR. J. NAUGLE S (10)
 MR. V. JOHNSON SV
 DR. M. ADAMS R
 DR. A. TISCHLER RP
 MR. W. UNDERWOOD RVA

AMES RESEARCH CENTER

DR. H. ALLEN DIR

FLIGHT RESEARCH CENTER

MR. P. BIKLE DIR

GODDARD SPACE FLIGHT CENTER

MR. H. LA GOW CODE 300

JET PROPULSION LABORATORY

MR. H. LEVY CCMTA (4)
 MR. I. NEWLAN REPORTS GROUP

KENNEDY SPACE CENTER

DR. K. DEBUS CD
 DR. A. KNOTHE EX-SCI
 MR. A. SMITH AP-LVO
 MR. R. RODY AP-PQA
 MR. R. PETRONE LO (3)
 DR. H. GRUENE LV
 MR. M. EDWARDS LV-INS
 MR. D. MC MATH LV-INS-1
 MR. J. FITZGERALD LV-INS-2
 MR. L. FANNIN LV-MEC
 MR. A. PICKETT LV-TOM-1 (2)
 MR. A. O'HARA LV-TOM-2 (2)
 MR. I. RIGELL LV-FNG
 MR. J. MIZELL LV-PLN-12
 MR. J. GOSSETT LL-PLV-2
 COL. G. PRESTON DE
 MR. G. WILLIAMS DE
 MR. J. DE VAULT DE-FEM
 MR. J. DARBY DF-FEM-4
 MR. T. POPPEL DE-MSD
 MR. K. SENDLER IN (4)
 DR. R. BRUNS IN-DAT
 MR. W. JELEN IN-DAT-1
 MR. D. COLLINS IN-QAL
 MR. M. BRITT IN-TEC
 MRS. L. RUSSELL IS-CAS-42
 MR. R. SPARKS NAA-ZK64
 MR. T. LEF I-K-L

LANGLEY RESEARCH CENTER

MR. E. CORTWRIGHT DIR

LEWIS RESEARCH CENTER

DR. A. SILVERSTEIN DIR
MR. E. JONASH MGR CENTAUR PROJ
MR. R. WASHKO

MANNED SPACECRAFT CENTER

DR. R. GILRUTH AA
MR. J. HAMILTON RL
MR. G. LOW PA
MR. D. ARABIAN PT (2)
MR. J. LOBB JR PT4 (3)
MR. C. GRANT JR BM1 (2)
MR. J. MC ANULTY FM13 (3)
MR. M. QUINN JR FS

WALLOPS STATION

MR. R. KRIEGER DIR

WESTERN SUPPORT OFFICE

MR. R. KAMM DIR

U.S. ATOMIC ENERGY COMMISSION

MR. C. CRAIG TID UC RAD, LAR,
TECH LIBRARY

CENTRAL INTELLIGENCE AGENCY

OCR/DD/PUBLICATION (5)

NATIONAL SECURITY AGENCY

DIR C3/TDL

SCIENTIFIC & TECH. INFORMATION FACILITY

NASA REPRESENTATIVE S-AK/RKT (25)

DEPARTMENT OF DEFENSE

DIR OF GUIDED MISSILES OFFICE OF SEC.
TECHNICAL LIBRARY ASST SEC FOR R&F

ARMED SERVICES TECHNICAL INF. AGENCY

COMMANDER TIPCR (5)

U.S. AIR FORCE

CHIEF OF STAFF DCS/D AFDRD
CHIEF OF STAFF DCS/D AFDRD-EX
COMMANDER-IN-CHIEF STRATEGIC AIR COM.
COMMANDER ARNOLD F.D.C. (2)
COMMANDER EDWARDS F.T.C.
COMMANDER HOLLOWAN M.D.C.
EYLLG-1 AFETR PATRICK AFB
MR. H. VONGIERKE 6570TH AMD AFSC
SYSTEMS ENG. GROUP SEPIR RTD WPAFB
FOREIGN TECHNOLOGY DIV FTD TDRDP

U.S. ARMY

RSIC AMSM-RBLD REDSTONE ARSENAL (3)
COMMANDING GENERAL WHITE SANDS P.G. (3)

U.S. NAVY

CHIEF OF RESEARCH DEPT. OF NAVY
DIRECTOR RESEARCH LAB,
BUREAU OF WEAPONS AD3
BUREAU OF WEAPONS RES1
BUREAU OF WEAPONS REW3
BUREAU OF WEAPONS SP
COMMANDER NAMTC PT. MUGU

CONTRACTORS

BELLCOMM INC.

MISS SCOTT LIBRARIAN

THE BENDIX CORPORATION

MR. F. REUTTER NAV & CONTROL DIV.

THE BOEING COMPANY

MR. R. NELSON DEPT 5-1010 (3)
MR. S. JOHNSON DEPT 5-5300
MR. T. KORNELL DEPT 5-7990
MR. J. SCOTT DEPT 5-9630
MR. K. HAGENAU DEPT 5-9633
MR. M. WITHEE DEPT 5-9633 (2)

CHRYSLER CORP. SPACE DIV.

MR. H. RADER DEPT 4800 (3)
MR. G. MARTIN DEPT 4820 (2)
MR. J. FLETCHER DEPT 4831 (2)
MR. L. SMITH DEPT 2712 (6)

GRUMMAN AIRCRAFT ENGINEERING CORP.

MR. J. JOHANSEN NASA RES OFFICE

INTERNATIONAL BUSINESS MACHINE

MR. R. POUPARD DEPT 229 (2)
MR. H. WEAVER DEPT F-03 (13)
MR. D. REAZER DEPT K-11

MARTIN COMPANY SPACE SYSTEMS DIV.

MR. W. SOMMERS

MC DONNELL DOUGLAS CORP.

MR. R. MOHR (40)
MR. G. SCHAR (4)

NORTH AMERICAN ROCKWELL ROCKETDYNE DIV.

MR. T. JOHNSON DEPT 596 (5)
MR. G. SOPP DEPT 596

NORTH AMERICAN AVIATION SAI SYSTEMS DIV.

MR. R. BURKES BC-05 (4)
MR. W. PARKER BC-05

RADIO CORPORATION OF AMERICA

DATA SYSTEMS DIVISION